DISSERTATION

INHIBITION OF THE HOST 5'-3' RNA DECAY PATHWAY IS A NOVEL MECHANISM BY WHICH FLAVIVIRUSES INFLUENCE CELLULAR GENE EXPRESSION

Submitted by

Stephanie L. Moon

Department of Microbiology, Immunology and Pathology

In partial fulfillment of the degree requirements

For the Degree of Doctor of Philosophy

Colorado State University

Fort Collins, Colorado

Spring 2014

Doctoral Committee:

Advisor: Jeffrey Wilusz
Co-Advisor: Carol Wilusz

Alan Schenkel
Norman Curthoys

ABSTRACT

INHIBITION OF THE HOST 5'-3' RNA DECAY PATHWAY IS A NOVEL MECHANISM BY WHICH FLAVIVIRUSES INFLUENCE CELLULAR GENE EXPRESSION

Host gene expression is an intricate process that requires many levels of regulation to allow the cell to react properly to a given stimulus or maintain homeostasis. One mechanism by which RNA viruses perturb host gene expression and potentially favor the allocation of host cell resources for viral proliferation is through interfering with cellular post-transcriptional processes. Furthermore, because viral RNAs must persist in the host cell cytoplasm to allow translation of viral proteins and ultimately viral replication, the same post-transcriptional processes that regulate host messenger RNAs (mRNAs) likely act on viral RNAs as well. The general RNA decay machinery in the cell serves as an important regulatory step for proper gene expression at the post-transcriptional level. Many RNA viruses have evolved unique mechanisms for dealing with the cellular RNA decay machinery to preserve their transcripts and ensure a productive infection. Viruses in the *Flaviviridae* contain positive-sense, single-stranded RNA genomes that are not polyadenylated. Therefore, these viral RNAs are likely recognized by the host cell as deadenylated, incongruous mRNAs and are likely substrates for the general cellular RNA decay machinery. Remarkably, members of the *Flavivirus* genus including the dengue viruses (DENV) and West Nile virus (WNV) produce an abundant non-coding subgenomic RNA (sfRNA) during infection that is generated through incomplete degradation of the viral genome by the host 5'-3' exoribonuclease 1 (XRN1). We demonstrate that human and mosquito XRN1 stalls on highly structured, conserved elements in the 3' untranslated region of flaviviral RNAs, resulting in sfRNA formation. Furthermore, we determined that these sfRNAs act as competitive, reversible inhibitors of XRN1. Infected cells display several signs of sfRNA-dependent XRN1

dysfunction, including the accumulation of uncapped transcripts and an overall stabilization of host mRNAs. Additionally, sfRNA acts as a weak inhibitor of the host cell RNA interference (RNAi) pathway. We propose that sfRNA likely acts as a sponge for Argonaute-2 (AGO2) and DICER, and have determined that siRNA-mediated decay is suppressed in an sfRNA-dependent fashion in flavivirus-infected human cells. This suppression of the RNAi pathway appears to alter host gene expression to a limited extent, and may be especially important for viral replication in the mosquito vector. Other members of the *Flaviviridae*, including hepatitis C virus (HCV) and bovine viral diarrhea virus (BVDV) do not form an sfRNA from their 3' untranslated regions, but they do contain highly structured 5' untranslated regions. Herein we show that aside from acting as internal ribosome entry sites, the 5' UTRs of HCV and BVDV also stall and inhibit XRN1. Therefore, members of the *Flavivirus*, *Pestivirus*, and *Hepacivirus* genera appear to inhibit a major mRNA decay pathway by suppressing XRN1 activity via highly structured viral RNAs. Consequences of XRN1 suppression during viral infection include the stabilization and upregulation of short-lived transcripts including those encoding oncogenes, angiogenic factors, and pro-inflammatory factors. Furthermore, we present evidence that WNV sfRNA may dysregulate the coordination between mRNA stability and transcription. Therefore, the suppression of XRN1 may potentially act as an important mechanism by which diverse viruses in the *Flaviviridae* induce pathogenesis by dysregulating cellular gene expression.

ACKNOWLEDGEMENTS

I would first like to thank all of our collaborators that contributed to the following work: Dr. Alexander Khromykh at The University of Queensland; Drs. Yutaro Kumagai and Shizuo Akira at Osaka University; Drs. Bin Tian, Mainul Hoque, and Liu Liang at Rutgers New Jersey Medical School; Dr. Shelton Bradrick at Duke University; Drs. Jeffrey Kieft and Erich Chapman at University of Colorado Denver, and Dr. Doug Brackney and Benjamin Dodd at Colorado State University. Furthermore, Drs. Hana van Campen, Irma Sanchez-Vargas, Aaron Phillips, and Richard Bowen provided virus stocks for these studies for which I am very thankful. I would also like to thank our funding sources: the Regional Center of Excellence/NIH, a USDA Animal Biosecurity Training Program Fellowship, and a Sigma Xi grant-in-aid of research award.

John Anderson provided invaluable assistance and support in the laboratory and he performed and optimized several *in vitro* RNA decay assays presented herein for which I am grateful. I would also like to thank Mike Barnhart for his assistance and support. Dr. Alan Schenkel was very helpful in allowing me to use his microscope throughout my time here and giving advice and encouragement. I must thank Mary Dozier and Wahida Khan for assisting with BVDV and HCV experiments, and other members of the Wilusz labs that provided assistance to me over the years, particularly Dr. Jerome Lee and Fumi Sagawa. I am also grateful for the advice given to me from my graduate committee. Thanks to Dr. Carol Wilusz for her helpful advice and ideas on experimental approaches. I am sincerely very grateful to have been able to join Dr. Jeffrey Wilusz's lab and work on this project. Thanks Dr. Wilusz for your enthusiasm, support, and optimism and for giving me so many opportunities. Finally, I would like to thank friends and family for their support and encouragement. Ben- thank you for all of your support- for sharing ideas, technical advice, and encouragement.

TABLE OF CONTENTS

LIST OF FIGURES

INTRODUCTION

The molecular mechanisms by which viruses interact with their hosts coupled with how the host responds to infection form the basis for virus-induced pathology. Viruses with RNA genomes lack the genetic space necessary to encode all protein factors required for viral replication and gene expression, and therefore rely on the host cell for many aspects of viral propagation. Viral mRNAs must access the cellular translation machinery in the cytoplasm for gene expression. Furthermore, because viral mRNAs mimic cellular mRNAs, they are likely to interact with cytoplasmic RNA-binding proteins and mRNA decay factors. One important but under-studied aspect of host-virus interactions is how viral transcripts evade or suppress the cellular RNA decay machinery. We have identified a unique mechanism by which all members of the *Flaviviridae* family appear to suppress a major aspect of cellular RNA decay. We posit that major changes in host gene expression occur as a consequence of this inhibition of RNA decay by members of the *Flaviviridae*. Furthermore, pathways by which virus-induced changes in mRNA stability could contribute to pathology as a result of mis-regulated gene expression will be discussed herein. This introduction seeks to contextualize the following studies and is separated into two major sections. Section I will give an overview of the molecular aspects of flavivirus propagation and viral pathogenesis. Section II will discuss the major pathways by which cellular mRNAs are degraded and will provide background on how RNA viruses are known to interact with the RNA decay machinery.

Section I: Introduction to the *Flaviviridae* family

The following studies are focused on a particular group of viruses that as a whole are endemic around the globe and affect humans and animals. The *Flaviviridae* family includes three genera: the *Flaviviruses*, *Hepaciviruses*, and *Pestiviruses* (Quan et al. 2013; Stapleton et

al. 2011). Colloquially, all members of the *Flaviviridae* family (and the *Flavivirus* genus) are referred to as 'flaviviruses'. The overall goal of this section is to provide the reader with a literature review on the known mechanisms of flaviviral propagation and the innate immune response to flavivirus infections. We hypothesize that one mechanism by which diverse flaviviruses cause disease is by the suppression of normal cellular RNA decay pathways that are essential for the coordinated regulation of gene expression in the cell. Therefore, the known mechanisms by which these viruses propagate and cause disease will be important to provide background for the following studies presented herein.

The *Flavivirus* genus includes many vector-borne viruses transmitted by mosquitoes or ticks to mammalian or avian hosts (Burke and Monath 2001). Members of this genus, Yellow Fever virus (YFV), DENV, WNV, and Japanese encephalitis virus (JEV) cause significant morbidity and mortality worldwide. The dengue viruses are four closely related flaviviruses that are known as dengue virus type 1-4, and the following studies utilized dengue virus type 2 (DENV-2). Dengue viruses are the cause of the most common vector-transmitted disease globally (Centers for Disease Control and Prevention (CDC) 2012) and JEV is the most common cause of mosquito-borne pathogen-induced encephalitis worldwide (Sips et al. 2012). Of particiular importance in discussing the threat of arthropod-borne flaviviruses to human and animal health is the fact that these viruses can rapidly spread to new geographic regions. For example, WNV was introduced into North America in 1999 and is now endemic in the United States (Jia et al. 1999). Alarmingly, DENV is now likely circulating in the southern United States (CDC 2010; Shin et al. 2013). Vaccines against some flaviviruses and some mosquito control approaches have been effective in mitigating disease in certain populations, although we still lack effective vaccines and vector control strategies for many of these viruses (Heinz and Stiasny 2012; Gubler 2011). Therefore there is a profound need to develop effective anti-viral treatments and/or vaccines to combat these viruses, particularly with the threat of further geographic expansion of mosquito-borne flaviviruses.

Members of the *Hepacivirus* genus currently include HCV and the GB viruses (GBV; named after the surgeon with the initials G.B. that GB viruses were initially derived from). This taxon is expanding, as several HCV and GBV genome-like RNA sequences have been detected in samples from dogs, rodents, bats and horses (Kapoor et al. 2013; Drexler et al. 2013; Chandriani et al. 2013; Burbelo et al. 2012; Kapoor et al. 2011; Epstein et al. 2010). Intriguingly, a recent survey of serum samples collected from 58 species of bats identified several new GB- and HCV- like viral RNA sequences, indicating that bats may be a major reservoir for these viral pathogens (Quan et al. 2013). Furthermore, these recent studies have revealed that the GB viruses have likely diverged significantly from the hepaciviruses and should be classified in their own taxonomic group, the *Pegiviruses* (Stapleton et al. 2011; Quan et al. 2013). Importantly, HCV is the most common blood-borne pathogen in the United States and is a leading cause of hepatocellular carcinoma (HCC) and liver disease worldwide (Wise et al. 2010; Armstrong et al. 2006). Although the incidence of HCV is decreasing in the U.S., the overall incidence and costs associated with chronic disease associated with HCV infection are predicted to continue to rise (Razavi et al. 2013). Risk factors for acquiring HCV include infection with human immunodeficiency virus (HIV-1), use of injected drugs, receipt of an organ transplant or blood transfusions before 1992, and being born during the period from 1945-1965 (Smith et al. 2012). There are no vaccines available to protect against HCV, but several anti-viral drugs are in use or in development (Scheel and Rice 2013). However, identifying patients infected with HCV and providing adequate therapy to infected individuals around the globe remain significant challenges (Scheel and Rice 2013). Therefore, further research into the mechanisms of viral propagation and host response to infection is vital for the discovery and application of novel diagnostics, treatments and vaccines.

The pestiviruses include several pathogens of livestock, including BVDV, Border Disease virus (BDV) and Classic Swine Fever virus (CSFV; also known as hog cholera virus; Becher et al. 2003). Pestiviruses generally infect animals in the order Artiodactyla (the even-

toed ungulates) (Peterhans et al. 2010). The economic burden of BVDV infections worldwide in the dairy and beef industries is substantial (Lanyon et al. 2014). For example, Heuer et al. (2007) found that in New Zealand, BVDV infection of cattle was associated with decreased milk production, increased time to conception, increased abortions, and loss of calves due to persistent infection or abortion. The resulting cost due to BVDV infection was thus estimated to be 73 dollars (US) per cow per year (Heuer et al. 2007). Commercially available vaccines against BVDV and CSFV have been used to limit disease prevalence in livestock, but one major limitation to this strategy to eradicate disease is the ability of these viruses to be transmitted vertically from mother to offspring *in utero* (Newcomer and Givens 2013). Several anti-viral compounds including nucleoside analogs that target the activity of the pestiviral RNA-dependent RNA polymerase (RdRp) have been efficacious in laboratory settings (Hoover and Striker 2008; Dukhan et al. 2005; Angusti et al. 2008; Newcomber and Givens 2013). However, these viruses are known to mutate frequently and are likely to evolve to resist anti-viral agents, particularly if applied individually (Newcomer and Givens 2013). Therefore, the eradication of BVDV will likely require the development and use of effective vaccines, diagnostics, and novel therapeutics targeting several viral and/or host factors.

Overview of the flaviviral 'life' cycle

All members of the *Flaviviridae* are enveloped, contain single stranded positive-sense RNA genomes, and replicate exclusively in the cytoplasm of host cells. The replication cycle of flaviviruses can be broken into eight important steps (Figure 1). First, the virus enters the cell by receptor-mediated endocytosis mediated by the viral envelope glycoproteins (Box 1, Figure 1) (Smit et al. 2011) and a slew of cellular factors including the glycosaminoglycans (Chen et al. 1997; Hilgard and Stockert 2000; Mandl et al. 2001; Germi et al. 2002). These low-affinity interactions are thought to concentrate the virus in certain regions of the cell surface to permit

entry by more specific viral receptors that remain unidentified (Lecoin et al. 2014). Once viral particles adhere to the cell surface they are permitted entry into the cell via clathrin-mediated endocytosis (Chu et al. 2006; Acosta et al. 2008; Suksanpaisan et al. 2009; Yang et al. 2013).

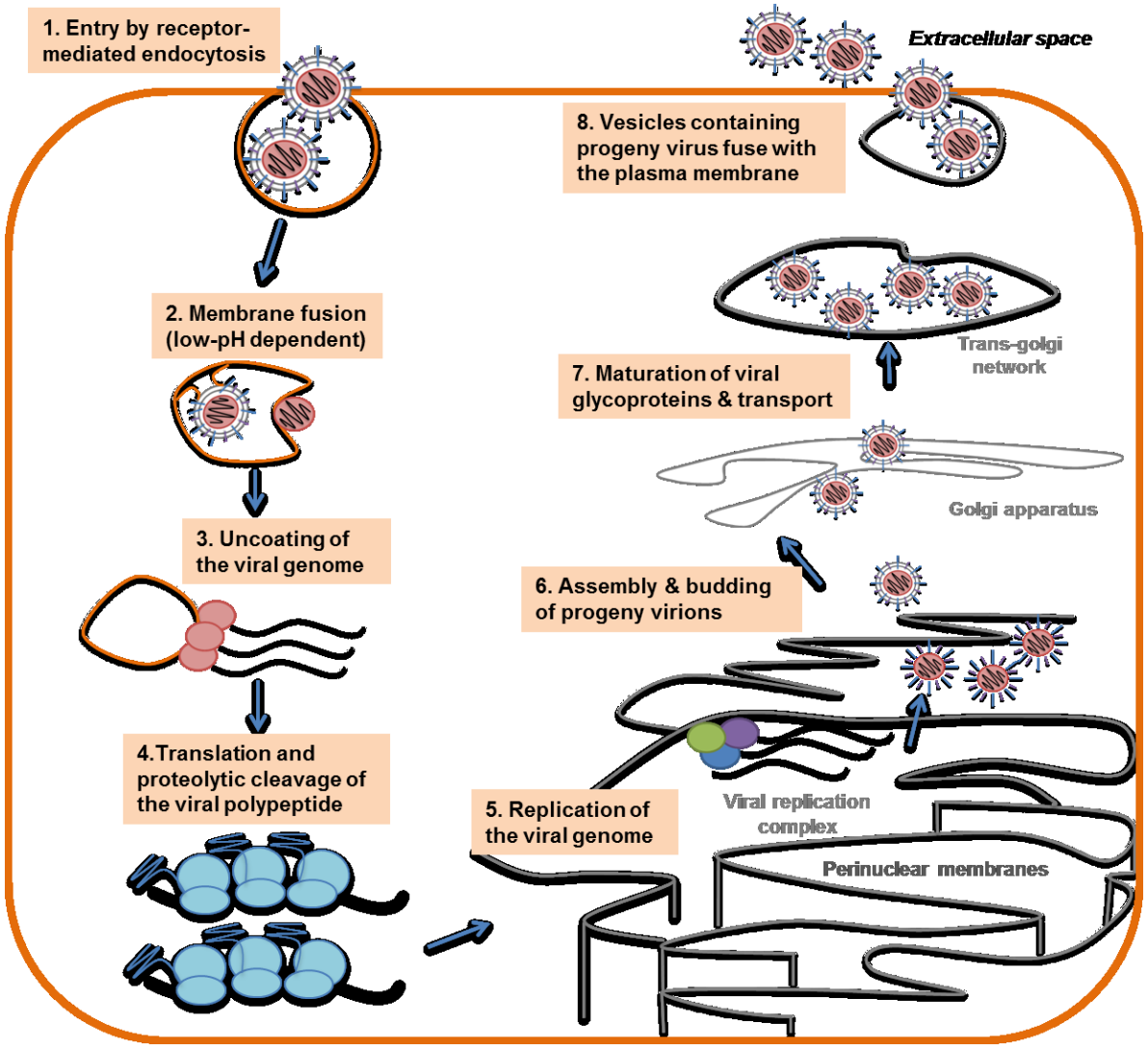

Figure 1. Flaviviruses, hepaciviruses, and pestiviruses replicate exclusively in the cytoplasm. The eight major steps in the replication cycle are highlighted in orange boxes.

Unlike the flaviviruses, hepaciviruses and pestiviruses encode at least two envelope proteins that likely mediate entry into the cell and subsequent fusion of the viral and cellular membranes (Kim and Chang 2013; Lindenbach and Rice 2001). Hepatitis C virus appears to enter cells by interacting with several receptors including CD81, occludin, scavenger receptor

type B class 1, and claudin 1 (Ploss et al. 2009; Evans et al. 2007; Scarselli et al. 2002). Interestingly, the expression of human CD81 and human occludin alone was sufficient to permit HCV infection in a mouse model (Dorner et al. 2011). The CD46 protein may act as a common receptor for the pestivirus E2 protein (Hulst and Moormann 1997; Flores et al. 1996; Maurer et al. 2004); although the pestivirus E(rns) protein may mediate non-specific interactions between the virus and glycosaminoglycans on the surface of the cell (Iqbal et at 2000). Like the flaviviruses, HCV and BVDV appear to enter the cell by clathrin-mediated endocytosis (Grummer et al. 2004; Mathapati et al. 2009; Blanchard et al. 2006; van der Schaar et al. 2008). Therefore, flavivirus entry into the cell appears to require several steps: initial association of the virus with low-affinity receptors (e.g. glycosaminoglycans), recognition of virus-specific receptors, and initiation of clathrin-mediated endocytosis.

Following receptor-mediated entry into the cell, pH-dependent fusion of viral and cellular membranes takes place in pre-lysosomal endocytic vesicles (Box 2, Figure 1) (Gollins and Porterfield 1985; Tscherne et al. 2006; Chu and Ng 2004; van der Schaar et al. 2008; Pierson and Kielian 2013). Interestingly, the flavivirus E protein appears to undergo an irreversible conformational change in the low pH environment of pre-lysosomal vesicles that facilitates membrane fusion (Stiasny et al. 2002; Modis et al. 2003; Li et al. 2008; Yu et al. 2008). However, the mechanisms by which envelope proteins mediate hepacivirus and pestivirus membrane fusion are slightly different (Lindenbach and Rice 2001). Studies of HCV and BVDV cell entry have revealed that low pH alone is not sufficient for membrane fusion and HCV and BVDV maintain their infectivity after exposure to low pH (Depner et al. 1992; Krey et al. 2005; Tscherne et al. 2006). These studies indicate that either an additional factor is required for HCV and BVDV fusion (aside from low pH alone) or that conformational changes of the envelope proteins of the virions at low pH are reversible (Tscherne et al. 2006). Ultimately, fusion of the viral and endocytic membrane causes extrusion of the viral core protein in complex with the RNA genome into the cytoplasmic membrane (Lindenbach and Rice 2001).

The next stage of the flavivirus replication cycle is the uncoating of the viral genome, or the dissociation of the core protein from the viral RNA (Box 3, Figure 1). Importantly, this occurs in the cytoplasm of infected cells where the viral RNA can be translated to produce non-structural and structural proteins for replication and nascent virion production (Box 4, Figure 1) (Lindenbach and Rice 2001). Therefore, these viral RNAs are likely exposed to constitutively expressed cellular ribonucleases that function in normal host mRNA turnover and/or quality control functions (and will be discussed in Section II of this Introduction). All flaviviruses encode a single polyprotein that is co- and post-translationally cleaved by cellular and viral proteases to generate distinct proteins as discussed in further detail below. Because viral translation is required for subsequent genome replication to take place (Brinton 2013), the flaviviral RNA must remain intact and protected from nucleases to permit viral propagation.

Replication of flavivirus genomes then takes place in induced membranous compartments that are derived from the endoplasmic reticulum (ER) as depicted in Box 5, Figure 1 (Ng 1987; Egger et al. 2002; Weiskircher et al. 2009; Romero-Brey et al. 2012; Miorin et al. 2013; Kaufusi et al. 2014). The resulting compartmentalization of the cell is thought to serve three important functions: (1) to segregate the distinct processes of translation, viral particle assembly, and RNA replication for proper virion production, (2) to concentrate cellular factors necessary for viral RNA replication and construction of nascent virions, and (3) to shield newly made viral genomic RNAs and viral proteins from cellular ribonucleases and proteases (Paul and Bartenschlager 2013). Replication of flavivirus RNAs in these membranous compartments is thought to require the activity of all seven viral non-structural (NS) proteins (Brinton 2013). The four membrane associated proteins NS2A, NS2B, NS4A, and NS4B are thought to anchor the flaviviral protein-RNA replication complexes to induced membranous compartments for localized genome replication (Mackenzie et al. 1998; Westaway et al. 2002; Miller et al. 2006; Miller et al. 2007; Kaufusi et al. 2014). Recent studies have implicated the activity of NS4B in the formation of these ER-derived membranous sites of viral RNA replication

in flavivirus (Kaufusi et al. 2014), pestivirus (Weiskircher et al. 2009), and hepacivirus (Egger et al. 2002; Gouttenoire et al. 2010; Paul et al. 2011) infected cells.

Upon the formation of replication complexes in these membranous compartments, viral RNA replication ensues (Box 5, Figure 1). The *Flaviviral* RNA-dependent RNA polymerase NS5 (or the hepaciviral or pestiviral NS5B) synthesizes nascent viral RNAs. Interestingly, the flavivirus NS3 protein possesses a helicase activity and a triphosphatase activity that is responsible for dephosphorylation of the 5' ends of newly transcribed viral RNAs (Luo et al. 2008; Wang et al. 2009). This permits the addition of a methylated 5' cap on flaviviral RNAs (discussed in more detail in the next below) (Issur et al. 2009; Yap et al. 2010). The NS5 and NS5B proteins are anchored to the ER-derived membranes via hydrophobic trans-membrane domains to cause the localized, protected replication of viral RNAs (Gu and Rice 2013; Caillet-Saguy et al. 2014). Newly transcribed viral RNAs are excreted from these membranous replication complexes into the cytoplasm, and can then either be packaged into nascent virions, undergo translation or serve as templates for further genome replication (Brinton 2013; Miorin et al. 2013).

For viral assembly, nascent viral RNA genomes form a complex with the basic core or capsid proteins and these ribonucleoproteins (RNPs) assemble with viral structural proteins to form immature virions (Box 6, Figure 1). Similar to the flavivirus capsid protein, the HCV and BVDV core proteins are enriched in basic amino acid residues to facilitate their tight association during viral RNA packaging in the ER (Lindenbach and Rice 2001). These newly constructed viral particles then bud through ER-associated membranes to create mature enveloped viruses.

Finally, fully formed, immature viral particles are trafficked through the trans-Golgi network in large vesicles (Box 7, Figure 1). Flavivirus particles undergo furin-mediated proteolytic cleavage of the structural prM protein to liberate the pr peptide from the mature M protein. The maturation of M on nascent viral particles is important for subsequent infections to be initiated (Guirakhoo et al. 1992; Elshuber et al. 2003; Junjhon et al. 2010; Zhang et al. 2003).

Although other viral proteins are proteolytically processed during or shortly after translation, delaying the cleavage of the pr peptide from M until viruses are in the trans-Golgi network likely protects the virus from undergoing pre-mature fusion with cellular membranes (Yu et al. 2008; Li et al. 2008). The flavivirus pr peptide therefore protects the viral E protein from undergoing irreversible conformational changes in the low pH of the trans-Golgi network (Yu et al. 2008; Li et al. 2008). Interestingly, pestiviruses and hepaciviruses appear to actively modulate the pH in these vesicular compartments via the p7 protein, which is known to oligomerize to form pore-like structures in membranes that selectively allow cations (e.g. protons) to cross the membrane (Griffin et al. 2003; Pavlovic et al. 2003; Premkumar et al. 2004; Wozniak et al. 2010). The p7 protein was shown to be essential for HCV propagation in a non-human primate model of infection (Sakai et al. 2003), and further studies demonstrated that p7 is required for HCV and BVDV assembly and egress from the cell (Harada et al. 2000; Jones et al. 2007). Finally, virus-laden vesicles ultimately fuse with the cellular membrane for release of the virions into the extracellular environment (Box 8, Figure 1). To summarize, flaviviruses, hepaciviruses, and pestiviruses undergo 'life' cycles exclusively in the cytoplasm of the cell and require both host and viral factors for successful propagation.

Overview of flavivirus genome structure and gene expression strategy

Flaviviral genomic RNAs are approximately 10-12 kilobases in length and contain a single open reading frame flanked by 5' and 3' untranslated regions. In general, viral structural proteins are encoded at the 5' end and non-structural proteins at the 3' end of the open reading frame. Viruses of all three genera use a similar gene expression strategy, in which the viral RNA is translated into one long polypeptide that is proteolytically cleaved by viral or cellular proteases to generate distinct gene products. The genome structure, organization and gene expression strategy of flaviviruses will be discussed below.

Conserved elements in the flavivirus genomic RNA

The flavivirus genome is ~11 kb in length and contains a 5' 7-methylguanosine cap but no poly(A) tail (Thurner et al. 2004; Brinton and Dispoto 1988; Chambers et al. 1990). Like many mammalian cells (Furuichi et al. 1975; Werner et al. 2011; Smietanski et al. 2014), the 5' caps of flavivirus RNAs contain an additional 2' O ribose methylation (Daffis et al. 2010; Zust et al. 2011; Szretter et al. 2012). The flavivirus NS5 protein mediates the methylation of the 5' cap via a guanine N7 methyltransferase activity and a nucleoside 2' O-ribose methyltransferase activity (Issur et al. 2009; Yap et al. 2010; Caillet-Saguy et al. 2014). This cap structure is required for cap-dependent translation of the flavivirus genome.

The 5' and 3' untranslated regions (~100 nt and 400-700 nt, respectively) have conserved sequence and structural elements that facilitate viral RNA replication, genome packaging, and translation (Lindenbach and Rice 2001). In general, the overall sequence composition of the 3' and 5' UTRs are not especially well conserved among all flaviviruses, but several structural motifs and short sequence elements that facilitate viral translation and replication are conserved (Thurner et al. 2004; Brinton and Dispoto 1988; Brinton et al. 1986). The short conserved sequence elements in the 5' and 3' UTRs are thought permit viral genome cyclization through long range RNA-RNA interactions, resulting in the formation of a complex tertiary structure necessary for genome replication (Hahn et al. 1987; Khromykh et al. 2001; Alvarez et al. 2005; Polacek et al. 2009; Friebe and Harris 2010). The specific RNA-RNA interactions between the viral RNA 5' and 3' UTRs are thought to position the viral RdRp appropriately for viral transcription initiation (Filomatori et al. 2006; Filomatori et al. 2011). The conserved structural motifs present in the 5' UTRs and 3' UTRs of flavivirus genomes will be discussed in more detail below and are diagrammed in Figure 2.

The 5' UTRs of flaviviral RNAs are ~100 nucleotides long and contain a conserved stem-loop structure (SLA) of ~70 nucleotides in length (Figure 2A; Liu et al. 2009(a)). This stem-loop is thought to function as a promoter for negative strand viral RNA synthesis in conjunction with a

short conserved U-rich region adjacent to SLA (Liu et al. 2009(a); Lodeiro et al. 2009). Two additional stem-loops are conserved in flavivirus RNAs downstream from SLA, stem-loop B (SLB) and a hairpin in the capsid-coading region of the open reading frame (cHP; Figure 2A). The SLB moiety contains a conserved sequence motif that mediates genome cyclization (Liu et al. 2009(a)). Finally, cHP is thought to be important for viral RNA replication and translation initiation (Liu et al. 2009(a); Clyde and Harris 2006; Clyde et al. 2008). Unlike the hepaciviruses and pestiviruses, the 5' UTR of the flavivirus RNA does not harbor an IRES element. The flaviviral 5' UTR therefore contains essential sequence and structural elements for viral RNA synthesis and cap-dependent translation initiation.

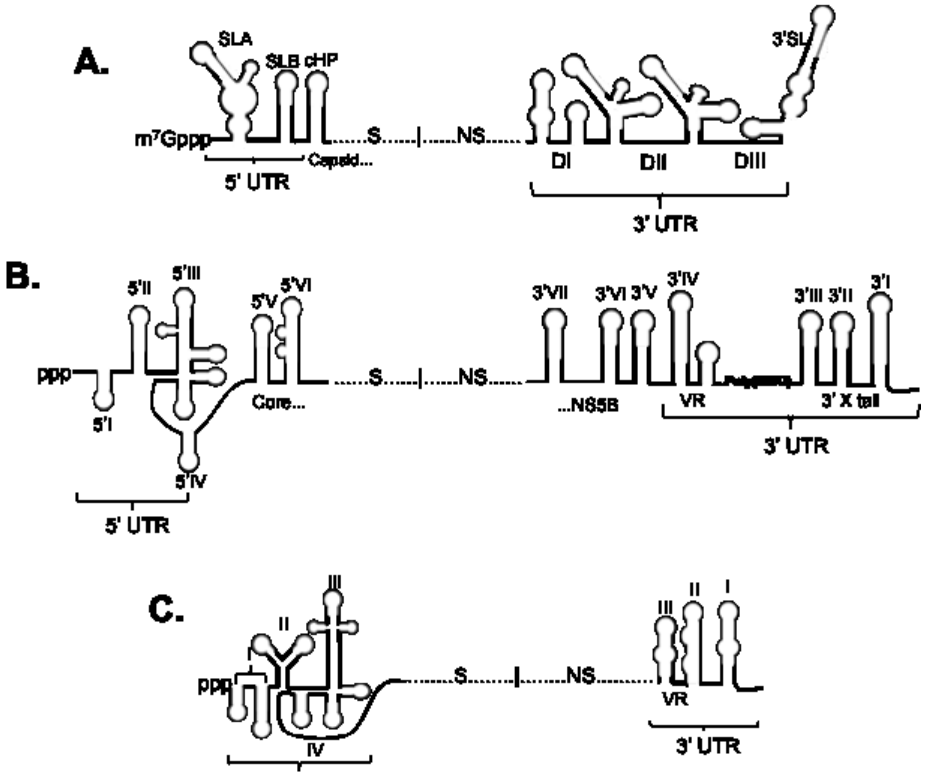

Figure 2. Conserved structural elements in flaviviral RNAs. (A) The conserved structures in the 5' capped RNA of dengue viruses (representative of the *Flavivirus* genus) with 5' and 3' UTRs flanked by structural (S) and non-structural (NS) protein-coding regions. The three conserved stem-loops, SLA, SLB, and cHP (capsid-coding region hairpin) are indicated. (B) Conserved structures in the triphosphorylated HCV RNA (a representative of the *Hepacivirus* genus). The 5' UTR contains four conserved structural domains numbered as 5'I-IV and two additional conserved stem-loops are present in the core-coding region (5'V and 5'VI). The seven conserved stem-loops at the 3' end of the viral RNA (3'I-VII) are found in the non-structural protein coding region and the 3' UTR. The 3' UTR contains a variable region (VR), a poly(U/UC) tract, and a 3' X

tail. (C) The conserved structural motifs in the triphosphorylated BVDV RNA (a representative of the *Pestivirus* genus). As in the HCV RNA, the BVDV 5' UTR contains four major structural elements labeled I-IV. The 3' UTR contains three stem-loops (I-III), two of which are in the variable region (VR). Adapted from Liu et al. (2009(a)).

The 3' UTRs of most flaviviruses encompass three conserved domains containing unique conserved structural and sequence elements (Figure 2A; Liu et al. 2009(a)). Domain I is adjacent to the open reading frame and is variable in sequence, but contains at least two conserved stem-loop structures (Liu et al. 2009(a); Ward et al. 2011). Directly 3' to Domain I, Domain II has two dumbbell structures, each containing conserved sequence motifs (Liu et al. 2009(a); Ward et al. 2011). Domain III encompasses the 3' end of the viral RNA and contains two conserved sequence elements that are complementary to regions in the 5' UTR (facilitating genome cyclization) plus a large stem-loop (3'SL) at the RNA terminus (Liu et al. 2009(a); Rauscher et al. 1997; Romero et al. 2006).

All flaviviruses tested to date generate distinct subgenomic RNAs (sfRNAs) of ~500 nt in length that contain the majority of the viral 3' UTR (Urosevic et al. 1997; Lin et al. 2004; Pijlman et al. 2008). Intriguingly, higher-ordered pseudoknot-like structures formed from interactions between the conserved stem-loops and dumbbell motifs in Domains I and II in the 3' UTR are implicated in sfRNA formation (Pijlman et al. 2008; Funk et al. 2010; Silva et al. 2010; Chapman et al. 2014). These viral RNAs are particularly interesting because they appear to be formed as a result of incomplete digestion of the viral genome by the major cellular exoribonuclease XRN1 (Pijlman et al. 2008; Silva et al. 2010). We have therefore focused our studies on the interactions between the cellular RNA decay machinery and flaviviruses by studying the formation and function of sfRNA, the subject of this dissertation.

Hepacivirus and pestivirus genome structure

Although there are many similarities in the genome organization of the flaviviruses and viruses in the other two genera in the *Flaviviridae* family, the 3' and 5' UTRs of hepacivirus and pestivirus RNAs are more similar to one another than they are to flavivirus RNAs. Hepatitis C virus (the proto-typical hepacivirus) has a ~9.6 kb genome and pestivirus genomes are ~12.3 kb in length (Lindenbach and Rice 2001). Viruses in both genera have highly structured 5' UTRs and several conserved sequence and structural elements in their 3' UTRs that are diagrammed in Figure 2B (Bukh et al. 1992; Lindenbach and Rice 2001; Liu et al. 2009(a)). Two pieces of evidence indicate that hepacivirus and pestivirus genomes likely possess a 5' triphosphate in lieu of a methylated cap structure: (1) they are translated by a cap-independent mechanism, and (2) their RNA dependent RNA polymerases do not harbor methyltransferase activities (Li et al. 2013(a); Lindenbach and Rice 2001; Caillet-Saguy et al. 2014; Le et al. 1996; Wang et al. 1993). Both viruses use internal ribosome entry sites (IRES) that have similar structural elements to undergo cap-independent translation (Le et al. 1996; Wang et al. 1993; Pestova et al. 1998).

Similar to what is observed in flaviviruses, hepacivirus and pestiviruses genomes may circularize for efficient viral RNA replication and/or translation. In HCV, genome cyclization is thought to occur via long-range RNA-RNA interactions and/or by interactions between the cellular RNA binding proteins (RBPs) including poly(C) binding protein 2 (PCBP2) and a group of normally nuclear NFAR proteins with the viral 5' and 3' UTRs (Wang et al. 2011; Romero-Lopez and Berzal-Herranz 2009; Isken et al. 2007). Studies in BVDV replication revealed that these NFAR proteins likely form a complex on the viral 3' UTR and bridge the interaction with the viral 5' UTR to promote viral translation and/or replication (Isken et al. 2003; Isken et al. 2007). Therefore, in contrast to what is known about flavivirus genome cyclization, it appears that hepaciviruses and pestiviruses rely on cellular RBPs to mediate these long range RNA-RNA interactions.

In further contrast to the flavivirus genome structure, the 5' UTRs of hepacivirus and pestivirus RNAs contain structural motifs that facilitate cap-independent translation. These viral 5' UTRs have four distinct conserved structural domains that are numbered I-IV from the 5' end of the genome as depicted in Figure 2B and C (Liu et al. 2009(a); Brown et al. 1992; Fletcher and Jackson 2002). Additionally, there are four predicted conserved stem-loops in the open reading frame of HCV in the region encoding the core protein adjacent to the IRES element as depicted in Figure 2B (Vassilaki et al. 2008). In contrast, pestivirus genomic RNAs appear to contain only two highly conserved, short (~20-30 nt) stem-loops in the NS4A- and NS5B-coding regions of the open reading frame, quite distant from the IRES element (and therefore not depicted in Figure 2) (Thurner et al. 2004).

Interestingly, stem-loops I and II in the HCV and BVDV genomes were shown to be essential for viral RNA replication (Yu et al. 2000; Kim et al. 2002). The pestivirus and hepacivirus IRES elements encompass Domains II, III and IV, all of which were shown to be required for viral translation (Liu et al. 2009(a); Lukavsky 2009; Fletcher and Jackson 2002). The eukaryotic initiation factor 3 (eIF3) and 40S ribosomal subunits were shown to specifically interact with these IRES elements to facilitate translation (Pestova et al. 1998; Sizova et al. 1998; Kieft et al. 2001). Interestingly, the IRES elements contain a complex pseudoknot-like structure in Domain IV that positions the 40S ribosomal subunit appropriately for translation initiation (Fletcher and Jackson 2002; Berry et al. 2010; Moes and Wirth 2007). Two of the stem-loops in the HCV ORF (5'V and 5'VI in Figure 2B) were shown to be important for viral translation and replication in both cell culture and non-human primate models of infection (McMullan et al. 2007). Therefore, the 5' UTRs of hepacivirus and pestivirus RNAs contain several highly conserved structural elements that are primarily thought to facilitate cap-independent translation and mediate viral RNA synthesis.

Not only does the HCV 5' UTR harbor the essential structural elements necessary for viral replication and translation, but it uniquely contains two conserved binding sites for a host

microRNA, miR-122 (Jopling et al. 2005). A region containing the first 50 nucleotides in the HCV 5' UTR has two sites complementary to 2^{nd} – 8^{th} or 2^{nd}-7^{th} nucleotides of miR-122 (Jopling et al. 2008). This cellular microRNA is highly specific to human hepatocytes, and was shown to be essential for HCV propagation in tissue culture cells and in a non-human primate model of infection (Jopling et al. 2005; Jopling et al. 2008; Lanford et al. 2010). Furthermore, miR-122 was shown to bind the HCV genome in complex with Argonaute-2 (AGO2) to promote efficient viral replication, possibly by enhancing viral translation and/or by stabilizing the viral RNA (Jopling et al. 2005; Jangra et al. 2010; Li et al. 2013(b); Conrad et al. 2013). Recent evidence indicates that miR-122 may mask the 5' terminus of the HCV genome from exonucleolytic decay, potentially stabilizing the RNA as a replacement for the 5' methylguanosine cap that these viruses lack (Machlin et al. 2011; Li et al. 2013(b)). It will be interesting to determine whether or not pestiviruses commandeer microRNAs to similarly facilitate viral propagation. However, in contrast to HCV, the BVDV 5' UTR contains a conserved stem-loop at the exact 5' terminus (Yu et al. 2000) that could potentially serve a similar function in protecting the 5' end of the viral RNA from exonucleolytic decay (Figure 2C). Therefore, although the exact mechanism by which miR-122 enhances HCV replication and/or translation has yet to be fully elucidated, this viral RNA-miRNA interaction is important for mediating viral propagation.

The 3' untranslated regions of hepaciviruses and pestiviruses share several sequence and structural elements (Thurner et al. 2004). Both viral 3' UTRs contain a variable region adjacent to the open reading frame, an AU- or UC-rich region, and a conserved region at the 3' terminus (Figure 1B and C). The HCV 3' UTR variable region is ~50 nt long and is adjacent to a conserved poly(U/UC) stretch of ~30-80 nt in length, and the ~100 nt highly conserved sequence element called the X-tail is at the 3' terminus of the viral RNA (Kolykhalov et al. 1996; Tanaka et al. 1996; Yamada et al. 1996; Tsuchihara et al. 1997; Thurner et al. 2004). Similarly, the 5' end of the pestivirus 3' UTR is known to contain a short region of variable sequence and length (~50-120 nt), an AU-rich region (of variable location and size), and a ~100 nt highly

conserved region at the 3' terminus (Deng and Brock 1993; Becher et al. 1998; Yu et al. 1999; Vilcek et al. 1999). The hepacivirus variable region is not absolutely required for viral replication, but deletion of this region was shown to significantly reduce viral RNA replication in one study (Friebe and Bartenschlager 2002). The pestivirus variable region contains several conserved stem-loop structures and was also shown to be required for efficient BVDV replication in addition to translation termination (Isken et al. 2004). Interestingly, the conserved U-rich regions in hepacivirus and pestivirus 3' UTRs are quite important for viral propagation. The HCV poly(U/UC) tract was shown to be required for viral replication (Friebe and Bartenschlager 2002; Yi and Lemon 2003; You and Rice 2008) and for mediating viral translation (Song et al. 2006; Bradrick et al. 2006). Similarly, all pestivirus 3' UTR sequences compared in one study (including BDV, BVDV, and CSFV) harbor conserved AU-rich regions, although these sequence motifs are variable in location and size in the viral RNA (Vilcek et al. 1999). The X-tail, or the 3' terminus of the HCV 3' UTR harbors three highly conserved stem-loops (SL I, II, and III) that are also required for HCV replication (Yi and Lemon 2003; Friebe and Bartenschlager 2002). Stem-loop II was shown to interact with a cruciform RNA structure in the NS5B coding region in a long-range RNA-RNA interaction that appears to be required for viral replication (You and Rice 2002; You et al. 2004; Friebe et al. 2005; You and Rice 2008). The 3' conserved region of the pestivirus RNA has a short conserved sequence element (ACAGCACUUUA) in addition to a conserved stem-loop at the 3' terminus of the RNA that is required for efficient viral replication (Deng and Brock 1993; Isken et al. 2004). It is important to note that hepaciviruses and pestiviruses do not generate sfRNA-like subgenomic RNAs from their 3' UTRs. However, as described above, the structural and sequence elements in these 3' UTRs are important for viral replication.

Flavivirus gene expression strategy

Flaviviruses use an elegant post-translational processing scheme to generate multiple distinct protein products from a single translated polyprotein precursor. A schematic of the organization and pre-/post-translational processing of the flaviviral polyprotein is provided in Figure 3. As described above, the structural proteins are generally encoded at the 5' end of the viral open reading frame (ORF) and the non-structural proteins are grouped at the 3' end of the viral ORF. A brief description of the flavivirus, hepacivirus, and pestivirus genome organization and post-translational processing of the viral polyprotein is provided below.

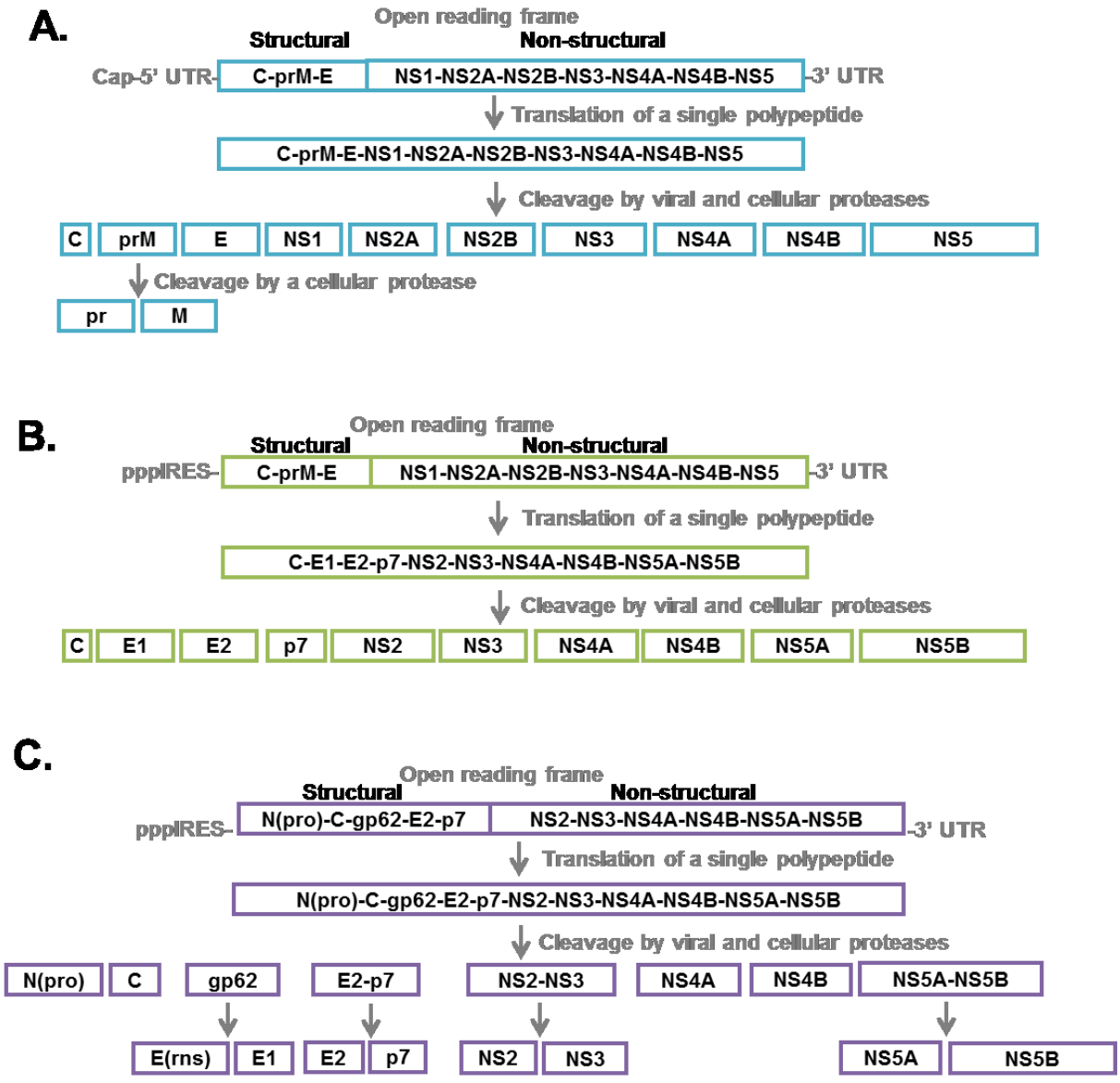

Figure 3. Post- and co-translational processing of gene products in viruses of the *Flaviviridae* family. (A) Flaviviruses have 5' methylguanosine caps and 5' and 3' untranslated regions flanking a single open reading frame that is processed by cellular and viral proteases to generate distinct protein products. Three structural proteins and seven non-structural proteins are made. (B) The hepacivirus genome contains a 5' triphosphate instead of a methylated cap, and is translated via an internal ribosome entry site (IRES) that makes up the 5' untranslated region. Four structural and six non-structural proteins are generated. (C) Pestiviruses generate up to five structural and seven non-structure proteins through cap-independent translation via an IRES element and genomes are also likely 5' triphosphorylated (Linderbach and Rice 2001).

As diagrammed in Figure 3A, the flavivirus RNA encodes three structural proteins, C (capsid), M (membrane; the precursor protein is prM), and E (envelope) and seven non-structural proteins, NS1, NS2A, NS2B, NS3, NS4A, NS4B, and NS5 (Lindenbach and Rice 2001; Chambers et al. 1990). As the viral polyprotein is translated, the C protein first undergoes several proteolytic processing events by both cellular and viral proteases (Boege et al. 1983; Trent 1977; Lindenbach and Rice 2001). Next, the prM protein is generated by distinct proteolytic cleavage events mediated by both cellular and viral proteases. Interestingly, the prM protein undergoes proteolysis by the cellular protease furin long after translation is terminated, when nascent virions are trafficked through trans-Golgi network (Yamshchikov and Compans 1994; Stadler et al. 1997). The final structural protein, E, is generated by cellular signal peptidase cleavage of the viral polyprotein (Markoff et al. 1994). In contrast, the flaviviral non-structural proteins are mostly liberated from the polyprotein by the protease activity of the viral NS3 protein (Yamshchikov et al. 1997). Importantly, as discussed above, the sequential proteolytic cleavage of viral proteins is essential for proper viral gene expression (Lindenbach and Rice 2001; Lee et al. 2000).

The hepaciviruses and pestiviruses also generate a single polyprotein that is co-and post-translationally processed by cellular and viral proteases to generate distinct protein products (Figure 3B and C). As occurs in flaviviruses, the three structural proteins core (C), E1 and E2 of HCV encoded at the 5' end of the viral open reading frame (ORF) are proteolytically cleaved by cellular signal peptidases (Lindenbach and Rice 2001). The E2 envelope protein

then undergoes a second proteolytic cleavage event by a signal peptidase to liberate the non-structural p7 peptide on the surface of the ER membrane (Lin et al. 1994). Seven non-structural proteins are encoded in the rest of the ORF: a small polypeptide cleaved from the E2 protein (p7), NS2, NS3, NS4A, NS4B, NS5A, and NS5B. As is observed in flavivirus polyprotein maturation, viral proteases are mostly responsible for processing the HCV non-structural proteins. The NS2-NS3 polypeptide acts as an autoprotease, and the liberated NS3 protein retains protease activity when directly interacting with NS4A, which acts as a co-factor for this process (Bartenschlager et al. 1994; Lin et al. 1994; Failla et al. 1994; Tanji et al. 1994).

The pestiviruses are slightly more complex in that they harbor four structural proteins and seven non-structural proteins (Figure 3C). Uniquely, the pestiviruses encode a non-structural protein, N(pro), at the 5' terminus of the single open reading frame. The N(pro) protein acts as an autoprotease, liberating itself from the adjacent C protein during translation (Stark et al. 1993; Wiskerchen et al. 1991; Lindenbach and Rice 2001). The four structural proteins that are next translated are the core (C) protein and three envelope proteins E(rns), E1, and E2; these are mostly processed by cellular proteases (Lindenbach and Rice 2001). The other non-structural proteins located at the 3' end of the pestivirus genome from 5' to 3' are NS2, NS3, NS4A, NS4B, NS5A, and NS5B. In contrast to the hepaciviruses, NS2-NS3 and NS5A-NS5B are generated through an initial proteolytic cleavage event, and can then be liberated to form distinct protein products or remain covalently linked (Lindenbach and Rice 2001). Interestingly, not all pestivirus isolates generate NS2 and NS3 from cleavage of the NS2-NS3 precursor. Furthermore, all non-cytopathic BVDV isolates tested to date generate the unprocessed NS2-NS3 precursor only, but cytopathic BVDV (and CSFV) both generate distinct NS2 and NS3 products (Donis and Dubovi 1987; Greiser-Wilke et al. 1992; Meyers and Thiel 1996). There is some evidence that insertion of host RNA sequences into the pestivirus RNA directly contributes to proteolytic processing of the NS2-NS3 precursor. Therefore, pestiviruses are

unique in that they normally maintain the NS2-NS3 and NS5A-NS5B as single protein products, and cleavage of NS2-NS3 is strongly associated with pathogenicity.

To summarize, all members of the *Flaviviridae* use both cellular and viral proteases to generate distinct gene products from a single translated polyprotein. Furthermore, the genome organization of these viruses is generally conserved, in which structural and non-structural proteins are grouped together. Because flaviviral gene expression relies on translation of a single viral mRNA, it is very important for these viruses to evade cellular nucleases to permit viral propagation. Furthermore, because RNA-RNA recombination events can influence the pathogenicity of pestivirus infections by facilitating the formation of distinct NS2 and NS3 proteins, the ability of cellular exonucleases to degrade viral RNAs before they can recombine could ultimately influence viral pathogenesis.

General host anti-flaviviral innate immune mechanisms

A general discussion of the immune mechanisms that are important for anti-flaviviral host response is relevant to this discussion, as aberrant or over-active immune responses (e.g. inflammation) are known to play important roles in mediating the pathology of flavivirus infections (Paton and Greiser-Wilke 2004; Guidotti and Chisari 2006; King et al. 2007; Rossini et al. 2013; Yacoub et al. 2013). The rates at which viral and cellular mRNAs are degraded in the cell could theoretically influence the innate immune response to viral infection in two ways. First, flaviviral RNAs are known to activate host innate immune pathways by triggering cytosolic pathogen recognition receptors (PRRs). Therefore, viral RNAs that are resistant to degradation would theoretically be available for a longer period of time to stimulate PRRs. Second, the expression of pro-inflammatory factors is often heavily regulated at the post-transcriptional level, and virus-induced changes in post-transcriptional gene regulatory mechanisms could therefore alter the immune response to infection (Anderson 2009; Hao and Baltimore 2009). This

discussion will be focused on intrinsic innate anti-flaviviral immune mechanisms including the activation of cellular nucleases that are induced as a result of the cellular recognition of viral RNAs.

Flaviviral RNAs contain several specific motifs, considered pathogen associated molecular patterns (PAMPs) that can stimulate PRRs. Importantly, all flaviviruses generate double stranded RNA (dsRNA) replication intermediates in the cytoplasmic membranous compartments of the host cell that appear to be immunogenic (Errett et al. 2013). Furthermore, higher-order RNA structures present in flaviviral RNAs can also be recognized as PAMPs (Pichlmair et al. 2009). The 5' terminal triphosphate of hepacivirus or pestivirus RNAs stimulate PRRs, and uniquely, a ~36 nt highly conserved poly(U/UC) tract in the HCV 3' UTR also appears to be immunogenic (Sumpter et al. 2005; Schnell et al. 2012). The PRRs that sense these viral RNA motifs include the interferon-induced proteins with tetratricopeptide repeats (IFITs), retinoic acid-inducible gene-I (RIG-I) like receptors (RLRs), Toll-like receptors (TLRs) the NOD, LRR and pyrin domain containing 3 (NLRP3) inflammasome, oligoadenylate synthase (OAS) and the interferon-induced protein kinase R (Samuel et al. 2006; Gilfoy and Mason 2007; Li et al. 2011(a); Kaushik et al. 2012; Schnell et al. 2012; Suthar et al. 2013). In general, the outcome of PRR stimulation is the activation of intracellular signaling cascades that ultimately induce transcription of pro-inflammatory cytokines, chemokines, and/or interferon α or β (the type I interferons; IFN) which can exert anti-viral and/or pro-inflammatory effects (Jensen and Thomsen 2012). IFNβ is ultimately secreted from the cell and binds to the IFNα and IFNβ receptor complex 1 (IFNAR1) located on the same cell or a neighboring cell (Suthar et al. 2013). The activation of IFNAR1 ultimately results in activation of a complex containing interferon regulatory factor 9 (IRF9), the signal transducer and activator of transcription 1 (STAT1) and STAT2 (Horvath 2004). These transcription factors then enter the nucleus and induce the expression of distinct interferon stimulated genes (ISGs) and interferon α (Horvath 2004;

Tenoever et al. 2007). The recognition of flavivirus RNAs by IFITs, RLRs, TLRs, and OAS, and the outcome of PRR stimulation will be discussed further below.

IFIT proteins in flavivirus infections

Viral transcripts that contain non-methylated cap structures (e.g. hepaciviruses and pestiviruses) are recognized by down-stream effectors of the type I interferon pathway called IFITs (Daffis et al. 2010; Hyde et al. 2014). Because mammalian IFIT1 (also known as P56) has been shown to suppress translation initiation by sequestering subunits of the eiF3 complex, inhibition of viral translation was thought to be the mechanism by which IFIT1-mediated virus restriction occurred (Guo et al. 2000; Hui et al. 2005; Daffis et al. 2010). Indeed, one study demonstrated that IFIT1 likely suppressed IRES-mediated translation of HCV through this mechanism (Wang et al. 2003). However, it was later demonstrated that susceptibility of flaviviruses to IFIT-mediated restriction largely depended on the presence or absence of the 2' O-methyl group on the 5' cap of viral RNAs. Although members of the *Flavivirus* genus normally have 5' methylated cap structures that resemble cellular mRNAs, mutant RNA viruses (including WNV) that were incapable of adding the 2' O-methyl group to the 5' cap were shown to be much more sensitive to IFIT-mediated restriction (Daffis et al. 2010; Szretter et al. 2012). Furthermore, it was recently demonstrated that IFIT1 binds directly to 5' triphosphorylated RNAs, limiting their ability to be translated by sequestering these RNAs away from the translation machinery (Pichlmair et al. 2011). Therefore, triphosphorylated RNAs generated in HCV and BVDV infections are likely recognized directly by IFIT proteins that are induced as a result of the type I interferon response to abrogate viral translation.

The RIG-I like receptors in flavivirus infections

The RIG-I like receptors are present in most mammalian cells where they serve as the major sensors of viral RNAs and essential activators of the type I interferon response (Kato et al. 2005; Jensen and Thomsen 2012). These proteins include RIG-1 and melanoma differentiation antigen 5 (MDA5). Both RIG-I and MDA5 also contain caspase recruitment domains essential for signal transduction (Yoneyama et al. 2004; Jensen and Thomsen 2012). MDA5 appears to have some specificity for RNAs longer than 2,000 nucleotides in length, and RIG-I can recognize shorter RNAs (Kato et al. 2005; Triantafilou et al. 2012; Feng et al. 2012). Furthermore, MDA5 is stimulated by higher-order RNA structures that contain both single stranded and double stranded regions (Pichlmair et al. 2009). Importantly, the stimulation of RIG-I by triphosphorylated viral RNAs containing dsRNA-like panhandle structures can occur immediately following viral infection upon disassociation of the viral RNA from the capsid protein (Weber et al. 2013). In addition to dsRNA recognition, both RIG-I and MDA5 may also recognize foreign mRNA 5' cap structures. Viral RNAs with 5' triphosphates (e.g. Hepatitis C virus) can activate RIG-I (Saito et al. 2008; Kato et al. 2008) and a recent study demonstrated that MDA5 may recognize viral RNAs lacking the 2' O methyl group normally present on viral and cellular mRNAs (Zust et al. 2011). Upon stimulation, RLRs undergo a conformational change leading to oligomerization and re-localize to cellular membranes where they bind the cellular mitochondrial antiviral signaling (MAVS) protein, also known as IPS-1 (Loo and Gale 2011; Suthar et al. 2013; Horner 2014). This complex then causes interferon regulatory factor 3 (IRF3) and/or nuclear factor κ B (NFκB) to re-localize to the nucleus and promote the transcription of interferon β and other genes to induce a type I interferon response (Loo and Gale 2011; Suthar et al. 2013).

Flaviviruses including WNV, DENV, JEV, and HCV are known to trigger type I IFN responses as a result of RIG-I and/or MDA5 stimulation (Li et al. 2011(a); Sumpter et al. 2005; Kato et al. 2006; Loo et al. 2008; Fredericksen et al. 2008; Kawai and Akira 2008; Suthar et al. 2010; Schnell et al. 2012). The pestiviruses also trigger RIG-I and MDA5-mediated signaling

pathways, leading to enhanced production of pro-inflammatory cytokines (including IL-1β, IL-6, and TNFα) and type I IFN (Smirnova et al. 2012; Dong et al. 2013). Both cytopathic and non-cytopathic BVDV strains are capable of stimulating type I IFN gene expression in animal and cell culture models of infection (Rossi and Kiesel 1980; Smirnova et al. 2008; Palomares et al. 2013).

Several studies have demonstrated that RLR-mediated signaling is essential for an effective immune response to flaviviral infection. Mice deficient in MDA5 or RIG-I had decreased survival upon WNV infection, and WNV infections in animals lacking both MDA5 and RIG-I or the essential downstream signaling molecule IPS-1 were invariably fatal (Errett et al. 2013). Furthermore, WNV RNA accumulated to significantly greater levels in mouse embryonic fibroblasts lacking both MDA5 and RIG-I in association with dramatic reductions in IFNβ, IFNα2a, IL-6, and other RLR-stimulated genes (Errett et al. 2013). However, WNV infection of mice lacking the signaling protein IPS-1 displayed enhanced inflammation and early virus entry into the CNS (Suthar et al. 2010). Specifically, RLR signaling was shown to be important for promoting the survival of CD8+ T cells during WNV infection and facilitating the expansion of these cells in the CNS to limit viral spread (Suthar et al. 2012). RLRs are therefore important for coordinating adaptive and immune responses in flavivirus infections (Suthar et al. 2010). Furthermore, defects in IFN stimulated gene expression in non-cytopathic BVDV infection of fetuses can contribute to the establishment of a persistent pestivirus infection (Adler et al. 1997; Charleston et al. 2001). Therefore, diverse flaviviruses activate RLR signaling and these pathways are likely important for survival, mitigating neuropathology, and eradicating the virus from the host.

Toll-like receptors in flavivirus infections

Several endosome-associated Toll-like receptors (TLR3, TLR7, and TLR8) also recognize foreign RNAs and signal through two proteins, myeloid differentiation 88 (MYD88) and TIR domain-containing adaptor inducing IFNβ (TRIF), ultimately leading to NFκB-, IRF3-, or interferon regulatory factor 7 (IRF7)-mediated transcription of pro-inflammatory chemokines, cytokines, and interferon stimulated genes (Akira et al. 2006; Li et al. 2011(a); Suthar et al. 2013). DENV has been shown to activate TLR3 following acidification of the endosomal compartment and viral uncoating, leading to the induction of IFN and activation of the transcription factors NFκB, AP-1, and IRF3 (Lee et al. 2012(a); Green et al. 2014). HCV also induces IFN expression through TLR3-mediated sensing of viral dsRNAs (Wang et al. 2009; Eksioglu et al. 2011; Li et al. 2012). Stimulation of TLR3 during HCV infection induces activation and translocation of both NFκB and IRF3 into the nucleus, leading to the transcription of cytokines and chemokines including CCL5, CXCL10, and CCL4 (Li and Lemon 2013). The *Pestivirus* BVDV is similarly known to induce the expression of TLR3 and TLR7 during infection of monocytes, regardless of whether the strain used is cytopathic or non-cytopathic (Lee et al. 2008). TLR3 and/or TLR7 are likely activated in general in various flavivirus infections and probably contribute to the up-regulation of pro-inflammatory immune mediators observed in these systems.

In addition to the RLRs, TLRs are important for stopping the spread of WNV in the central nervous system and may be particularly important for mediating antiviral immunity in neurons (Szretter et al. 2010). Mice lacking the signaling protein MYD88 succumbed to WNV infection more rapidly than wild-type mice and displayed increased WNV titers in the brain (Szretter et al. 2010). Importantly, defects in chemokine induction due to MYD88 depletion likely contributed to reduced recruitment of leukocytes into the CNS upon WNV infection (Szretter et al. 2010). Therefore, TLR-mediated signaling events are likely very important for facilitating anti-viral leukocyte recruitment into the brain for WNV clearance.

Interestingly, the CCCH-type zinc finger nuclease 12A (ZC3H112A or MCPIP1) is induced upon stimulation of Toll-like receptors (TLR) or expression of the pro-inflammatory factors chemokine (C-C motif) ligand 2 (MCP-1) or interleukin-1β (Uehata and Akira 2013; Lin et al. 2013). Several RNA viruses including DENV, JEV, and Influenza virus are restricted by MCPIP1 expression, likely as a result of the decay of viral RNAs and cellular RNAs by MCPIP1 (Liu et al. 2013(a); Lin et al. 2013). Upon resolution of an infection, MCPIP1 expression may mediate the rapid suppression of pro-inflammatory gene expression to reduce tissue damage (Matsushita et al. 2009; Uehata et al. 2013). Of interest, MCPIP1 knockout mice were shown to have severe immune disease characterized by enlarged spleens and lymph nodes, widespread inflammation, and hypergammaglobulinemia (Matsushita et al. 2009). Therefore, MCPIP1 likely serves two roles during viral infection by directly degrading both viral and cellular mRNAs.

The OAS/RNase L pathway

Another important flaviviral dsRNA PRR is 2',5' OAS. The association of OAS with dsRNAs activates OAS to convert adenosine triphosphate to 2',5' oligoadenylate. 2',5' oligoadenylate then induces the dimerization of ribonuclease L (RNase L) monomers, resulting in the formation of a functional endonuclease (Floyd-Smith et al. 1981; Li et al. 2011; Huang et al. 2014). Both OAS and RNase L are constitutively expressed in the cytoplasm and nucleus in monomeric, inactive forms, although they are also transcriptionally up-regulated by type I interferon signaling (Li et al. 2011(a)). Importantly, RNase L cleaves viral and cellular RNAs, including ribosomal RNAs, the U6 small nuclear RNA, and diverse mRNAs (Hovanessian et al. 1979; Cooper et al. 2014). Similarly to MCPIP1, the activation of RNase L is thought to serve as a mechanism by which the cell can limit interferon-mediated gene expression to minimize inflammation following viral clearance (Bisbal and Silverman 2007). Accordingly, RNase L can degrade the transcripts encoding the RNA stability factor tristetraprolin and several interferon

stimulated genes (Li et al. 2000; Khabar et al. 2003; Bisbal and Silverman 2007; Al-Haj et al. 2012). Another important consequence of RNase L activation is the induction of apoptosis, which ultimately results in the death of infected cells to limit viral growth (Castelli et al. 1997; Zhou et al. 1998; Bisbal and Silverman 2007). Therefore, RNase L activity can suppress viral proliferation by actively degrading viral RNAs and also by altering cellular gene expression to induce apoptosis and minimize damaging inflammation.

RNase L is induced during HCV infection and cleaves the viral open reading frame when it encounters UA and UU dinucleotides in single stranded RNA sequences (Han and Barton 2002; Washenberger et al. 2007). Furthermore, the generation of endonucleolytic cleavage products from the HCV RNA can stimulate RLRs to further amplify the innate immune response to infection (Malathi et al. 2007; Malathi et al. 2010). The activation of RNase L also plays an important role in limiting WNV replication (Scherbik et al. 2006). Furthermore, the murine homolog of OAS (Oas1b) is known to be very important for restricting flavivirus infections (Brinton and Perelygin 2003; Courtney et al. 2012). RNase L therefore provides an interesting example of an induced cellular nuclease that can suppress viral propagation and influence viral pathogenicity.

Viral subversion of the type I interferon response

Several flaviviral gene products including subgenomic flavivirus RNA have been implicated in viral inhibition of type I IFN signaling. Two recent studies evaluated the ability of sfRNA in KUNV and JEV infections to counteract the mammalian type I interferon response. It was initially demonstrated that KUNV mutants deficient in sfRNA formation grew to lower titers in certain cell lines, including the non-human primate Vero cell line and mosquito C6/36 cells (Pijlman et al. 2008). However, growth of an sfRNA-deficient KUNV mutant could be partially rescued in mice lacking the type I interferon α/β receptor (IFNAR) and in cell culture when viral growth in wild-type mouse embryonic fibroblasts (MEFs) were compared with that in IRF3-/-

IRF7-/- MEFs (Schuessler et al. 2012). Furthermore, survival dramatically decreased when mice that lacked IRF3, IRF7, or IFNAR were infected with the sfRNA-deficient KUNV, although on average the mice died later than mice infected with wild-type virus (Schuessler et al. 2012). Pathogenicity due to sfRNA deficient KUNV was therefore partially restored when the type I interferon pathway was abrogated, although the mechanism by which this occurs is unknown. Recently, JEV sfRNA was shown to play a role in blocking IRF3 phosphorylation and subsequent nuclear translocation of this important innate immune transcription factor, although the mechanism by which this occurs is also not yet known (Chang et al. 2013). Therefore, sfRNA formation directly or indirectly promotes viral evasion of the type I interferon pathway in mammalian cells.

Many viruses have evolved unique mechanisms for suppressing RNase L activation directly (reviewed in Bisbal and Silverman 2007; Zhang et al. 2013). Of particular relevance to this discussion however is the ability of several viral RNAs to inhibit RNase L direction. A conserved element in the group C enterovirus (e.g. poliovirus) RNA inhibits the endonuclease activity of RNase L by acting as a competitive inhibitor (Han et al. 2007; Townsend et al. 2008). The abundant WNV sfRNA could potentially inhibit RNase L in a similar fashion, as sfRNA-deficient KUNV growth was partially rescued in cells that lacked RNase L (Schuessler et al. 2012). However, the exact mechanism by which sfRNA aids in viral evasion of RNase L-mediated viral restriction remains to be determined.

Flaviviral proteins are also implicated in the evasion of type I interferon responses. The WNV, YFV, and DENV nonstructural protein 4B was shown to block IFN signaling in one study (Munoz-Jordan et al. 2005). Similarly, the NS5 protein of DENV was shown to induce the proteolytic degradation of STAT2, leading to decreased activity of the TLR-mediated innate immune pathway (Ashour et al. 2009; Morrison et al. 2013). The HCV NS5A has also been implicated in the suppression of type I IFN signaling, potentially by blocking STAT1 phosphorylation, to ultimately suppress the formation of the STAT1-STAT2 heterodimer in the

TLR3 pathway (Kumthip et al. 2012). Furthermore, a recent study also demonstrated that HCV may impede TLR-mediated signaling by inducing the expression of a host microRNA, miR-21, that targets the mRNA of MYD88 (Chen et al. 2013(a)). Pestiviruses appear to take a more active approach in shutting down host innate immune responses. The pestivirus N(pro) protease has been shown to trigger the degradation of the signaling molecule IRF3 by the cellular proteasome during CSFV and BVDV infections (Ruggli et al. 2003; Gil et al. 2006; Chen et al. 2007; Seago et al. 2007; Bauhofer et al. 2007; Gottipati et al. 2013). Pestiviruses may also limit the abundance of immunogenic dsRNAs generated during viral infection by expressing a ribonuclease, E(rns). The E(rns) protein has ribonuclease activity and is thought to mediate degradation of intracellular and extracellular dsRNAs generated by BVDV during replication before they can stimulate cellular PRRs to induce a type I interferon response (Meyers et al. 2007; Magkouras et al. 2008; Matzener et al. 2009). Therefore, members of the *Flavivirus* and *Hepacivirus* genera likely impede host innate immune responses by targeting essential components of the cytoplasmic signaling pathways that ultimately trigger transcriptional up-regulation of chemokines and other antiviral immune factors. Because innate immune pathways have been shown to be important clearance of flavivirus infections and can also contribute to immunopathology, the ability of diverse flaviviruses to modulate type I IFN responses in the host can likely dramatically alter the pathogenesis of an infection.

On the role of inflammation in flavivirus-mediated pathology

Although the previous section discussed how innate immunity is important for protecting the host from pathology due to flavivirus infections, excessive inflammation can cause pathogenesis in and of itself. Furthermore, because flaviviruses have evolved mechanisms to escape some innate immune responses, the host innate immune response to infection may fail to clear the virus but still cause damage to the surrounding tissue (i.e. bystander damage). This

section discusses some of the ways that excessive inflammatory responses are known to contribute to flavivirus-induced pathology.

Flaviviruses can cause a range of clinical outcomes, the most serious of which are encephalitis (e.g. JEV or WNV) or hemorrhagic fever (e.g. DENV or YFV). Interestingly, *Flavivirus* infections that generally lead to hemorrhagic fever in humans oftentimes cause encephalitis in mouse models of infection (Burke and Monath 2001). Furthermore, studies have revealed that in some instances up to 21% of patients with Dengue fever also display neurological abnormalities (Domingues et al. 2008; Carod-Artal et al. 2013). It is therefore possible that there are common molecular mechanisms that lead to either hemorrhagic fever or encephalitis (or both). A further discussion on the pathogenesis of *Flavivirus* infections follows below with emphasis on the neuropathogenesis of WNV as a representative *Flavivirus*.

Over-zealous immune responses are considered to be a major contributor to DENV-induced hemorrhagic fever/shock syndrome (Costa et al. 2013, Rothman 2011; Basu and Chaturvedi 2008). Furthermore, the encephalitic flaviviruses JEV and WNV are thought to cause neuropathology by two mechanisms: indirect immune-mediated processes or direct virus-mediated cell death (Ghoshal et al. 2007; Rossini et al. 2013). Inflammation is thought to contribute to WNV-mediated neurologic disease by contributing to the break-down of the blood brain barrier (Wang et al. 2004). Stimulation of TLR3 during WNV infection was shown to induce TNF–α production by infected monocytes, leading to increased entry of WNV and immune cells into the CNS of mice (Wang et al. 2004). TLR3 depletion lead to less neuropathology, inflammation, and viral proliferation and this was correlated with decreased production of the pro-inflammatory factors TNF-α, IL-6, IFN-α, and IL-12 (Wang et al. 2004). Importantly enhanced permeability of the blood brain barrier is a precursor of WNV neuroinvasive disease (Sips et al. 2012; Suthar et al. 2013; Wang et al. 2004). Neuropathogenesis of the related Japanese Encephalitis virus is also enhanced by aberrant expression of pro-inflammatory factors in neural tissues, ultimately leading to immune-mediated cell death in the central

nervous system (Bhattacharyya et al. 2014; Ghoshal et al. 2007; Swarup et al. 2007). Because immunopathology/excessive inflammatory responses are known to play major roles in disease due to various flavivirus infections, it is possible that a common viral factor contributes to this effect in the host by modulating fundamental gene regulatory mechanisms.

In contrast to the neuropathology and/or hemorrhagic syndromes caused by many *Flaviviruses*, Hepatitis C virus causes a very different spectrum of disease, oftentimes due to persistent infections that can last decades. One of the most serious outcomes of HCV infections is hepatocellular carcinoma (HCC). The underlying molecular mechanisms by which HCV causes HCC remain unknown, and whether or not the virus directly (or indirectly) causes HCC has yet to be elucidated (Lemon and McGivern, 2012). However, the onset of cancer in HCV infected patients takes place on average 29 years after infection, and therefore subtle changes in cell homeostasis and gene expression that occur over time as a consequence of infection are thought to contribute to hepatocellular transformation (Kiyosawa 1998). The HCV core protein or non-structural protein 3 have been implicated in HCV-induced carcinogenesis and are known to alter host gene expression in several models of infection, but the exact cause of HCV induced HCC remains unknown (Marusawa 1999; Moriya 1998; Banerjee et al. 2010; Ray et al. 1997; Ray et al. 1998; Bergqvist and Rice 2001; Sakamuro 1995; Thoren et al. 2004). However, pro-inflammatory factors are up-regulated in human patients and cell culture models of HCV infection (Nishitsuji et al. 2013), and there is evidence that excessive production of pro-inflammatory factors during HCV infections can contribute to HCC in human patients (Matsuzaki et al. 2007). Furthermore, it is thought that bystander tissue damage due to chronic inflammation in the infected liver is an important contributing factor to the onset of HCC (Flecken et al. 2012; Brownell and Polyak 2013).

Another mechanism by which HCV-induced carcinogenesis may occur is by dysregulation of oncogenes and angiogenic factors in infected cells, some of which are also induced during the process of inflammation and/or act as transcription factors for pro-

inflammatory gene expression. For example, the AP-1 transcription factor complex is comprised of c-FOS and JUN family members, and is known to play important roles in transcription of pro-inflammatory cytokines, cell proliferation, bone development, and oncogenesis (reviewed in Zenz et al. 2008; Lee et al. 2012(a); Green 2014). Intriguingly, HCV has been shown to benefit from increased abundance of c-FOS (Kang et al. 2011(a)) and c-JUN overexpression can contribute to hepatocellular carcinogenesis (Machida et al. 2010). The oncogene c-myc is also upregulated in HCV patients that have HCC and this protein has been shown to alter cell cycle progression (Higgs et al. 2013). Furthermore, inflammation has long been accepted to contribute to the progression of cancer (Coussens et al. 2002; Romagnani et al. 2004; Benelli et al. 2006; Porta et al. 2009). Importantly, several angiogenic factors known to be involved in both cancer progression and inflammation (Romagnani et al. 2004; Goel and Mercurio 2013) are implicated in HCV-induced HCC. Anti-angiogenic therapies have recently extensively investigated as systemic treatments for HCC although it is interesting to note that hypoxia caused by these agents may lead to metastases (Coulon et al. 2010; Ebos et al. 2009). Secretion of vascular endothelial growth factor A (VEGFA) can induce angiogenesis by activation of endothelial cells and stimulate the production of hepatic growth factor, which in turn causes hepatocyte proliferation (Chiang et al. 2008; Shimizu et al. 2001; LeCouter et al. 2003; Hao et al. 2006). Hypoxia inducible growth factor 1α (HIF1A) has been shown to both enhance HCV propagation and stimulate migration and altered polarity of hepatic cells in a cell culture model of metastasis (Wilson et al. 2012; Mee et al. 2010). Furthermore, HIF1A induces NFκB expression, which in turn promotes CXCL2 expression (Scortegagna et al. 2008). The chemokine CXCL2 (also known as the Gro2 oncogene or macrophage inflammatory protein-2) has been implicated in a variety of cancers (Doll et al. 2010; Kavandi et al. 2012; Dong et al. 2011; Oue et al. 2012), hepatic and extrahepatic tumor metastasis (Kollmar et al. 2008; Kollmar et al. 2006), liver inflammation (Krohn et al. 2009) and has been shown to be upregulated in a *Tupaia belangeri chinensis* hepatocyte culture model of HCV infection (Guitart et al. 2005).

Therefore, the pro-inflammatory response to HCV infection could potentially contribute to the onset of hepatocellular carcinoma.

Intriguingly, pestiviruses can cause persistent infections in their hosts through a unique mechanism that allows the virus to evade adaptive immune responses by infecting their hosts *in utero* early in the gestation period (Peterhans and Schweizer 2010; Hansen et al. 2010). Infected calves can shed BVDV in all excretions/secretions and cytopathic BVDV can cause mild or lethal mucosal disease (the appearance of ulcers in the gastrointestinal tract) in cattle with acute, transient, or persistent infections (Tautz et al. 1998; Fulton et al. 2005). Three important potential outcomes of BVDV infections in cattle are (1) defects in fertility, (2) conception or development of fetuses of infected pregnant heifers, and (3) mucosal disease. Cattle infected with BVDV have decreased conception rates and infection can result in abortion and a variety of congenital defects (Collins et al. 2009). Calves persistently infected with BVDV can develop a lethal mucosal disease, defined as bloody diarrhea and ulcerations in the mucosa including the mouth and intestines (particularly in Peyer's patches; Peterhans et al. 2010; Brownlie et al. 1984). Pregnant heifers that are persistently infected by non-cytopathic BVDV can pass the virus on to the fetus early in the gestational period, leading to a persistent infection in the calf (Hansen et al. 2010). Intriguingly, BVDV infection *in utero* results in the breakdown of self: non-self-recognition leading to immune tolerance; this ultimately inhibits the calf from clearing the virus (Hansen et al. 2010). Furthermore, when a pregnant heifer passes BVDV on to the fetus later in the gestation period, defects in fetal growth including bone and nervous system abnormalities or abortion can result (Hansen et al. 2010). Importantly, these persistently infected calves continue to shed infectious virus throughout their lives, and can die upon super-infection with a cytopathic BVDV (or if the non-cytopathic BVDV mutates into a cytopathic form; Peterhans et al. 2010). In contrast, cytopathic BVDV infections are usually cleared by the host through innate and adaptive immune responses that can protect the animal from future infections (Brackenbury et al. 2003; Ridpath 2013).

Dysregulation of immune responses or inflammation could contribute to the pathogenesis of BVDV. First, there is evidence that cattle infected with BVDV display an anti-viral immune response. Heifers acutely infected with BVDV show a large increase in the abundance of interferon stimulated gene 15 kD (ISG15) which is considered a marker of a robust type I interferon-mediated innate immune response (Hansen et al. 2010). A later study demonstrated that upon infection with a non-cytopathic strain of BVDV, peripheral blood monocytes induce the expression of the chemokines CXCL4 and CXCL12, and several interferon stimulated genes (Weiner et al. 2012). Importantly, fetuses and steers with persistent BVDV infections also have increased expression of innate immune factors and over-exposure to type I interferon may contribute to intrauterine growth restriction in fetuses persistently infected with BVDV (Hansen et al. 2010). Furthermore, the trafficking of BVDV into the central nervous system of the fetuses of infected cattle was shown to coincide with vasculopathy including hypertrophy of endothelial cells and perivascular edema associated with microglial cells that stained positive for BVDV antigen in the surrounding tissues. One type I interferon stimulated gene, ISG15, was shown to be elevated at the protein and mRNA levels in the brains of infected fetuses early in BVDV infection, especially in the vascular endothelial cells of the microvasculature of the developing brain (Bielefeldt-Ohmann et al. 2012). The authors speculate that type I interferon responses early during infection may enhance virus spread to the central nervous system by the extravasation of microglial precursor cells carrying BVDV (Bielefeldt-Ohmann et al. 2012). Lesions consistent with destruction of microvasculature due to excessive type I interferon-induced gene expression were also observed. Therefore, the ability of *Pestiviruses* to stimulate type I interferon responses through the activation of cellular PRRs can potentially contribute to both viral persistence and trafficking to the central nervous system. Importantly, cattle that are persistently infected with BVDV show defects in growth and development including decreased calve weight at cesarean section and malformation of the long bones (Hansen et al. 2010). The exact molecular mechanisms by which these defects in

growth and development occur remain unknown, but dysregulated immune responses likely contribute to disease symptoms observed in BVDV infected cattle.

A role for aberrant post-transcriptional gene regulation in flavivirus-induced pathology

From the moment a virus deposits its RNA genome into the cytoplasm of an infected cell, the virus must evade or suppress constitutively expressed nucleases that normally degrade cellular RNAs to preserve their transcripts and ensure viral gene expression. Therefore, the general cellular RNA decay machinery may act in part as an intrinsic anti-viral mechanism, as viral RNAs may be rapidly destroyed early in an infection if they do not contain the proper stability elements (reviewed in Moon and Wilusz 2013). Understanding how host mRNAs are normally turned over in the cytoplasm provides us with a starting framework for how viral RNAs may be degraded in the cell. Furthermore, changes in post-transcriptional gene regulatory mechanisms due to viral infection could dramatically alter the way the host cell responds to the virus.

As discussed above, pathology induced by flavivirus infections can oftentimes be directly associated with uncontrolled inflammation leading to tissue damage (Ghoshal et al. 2007; Rossini et al. 2013), oncogenesis in HCV infections (Iliopoulos et al. 2009; Stauffer et al. 2012), and developmental defects in BVDV infections (Bielefeldt-Ohmann et al. 2012). Although transcriptional responses are clearly important for inducing a pro-inflammatory response in the host when viral PAMPs are detected by PRRs, the post-transcriptional regulation of cytokines, chemokines, and other pro-inflammatory factors is also likely very important for modulating this response. Many studies on the post-transcriptional regulation of mRNAs containing AU-rich elements (AREs) in their 3' UTRs demonstrate how defects in this important regulatory mechanism can lead to pathology. Importantly, many immune factors contain AREs in their mRNAs (Caput et al. 1986), and AREs were shown to function as cis-acting destabilizing factors

(Shaw and Kamen 1986). Importantly, a later study demonstrated that hundreds of short-lived ARE-containing transcripts are induced upon activation of human T cells, and changes in mRNA decay rates were thought to therefore be an important mechanism by which T cells respond to a given stimulus and become activated (Raghavan et al. 2002). Interestingly, mice lacking tristetraprolin (TTP), an RNA binding protein that destabilizes ARE-containing transcripts, develop an inflammatory autoimmune syndrome (Taylor et al. 1996). Tristetraprolin was later shown to target the ARE-containing mRNA of TNF-α and other pro-inflammatory cytokines induced by TLR stimulation for decay, allowing the cell to rapidly modulate the abundance of this potent pro-inflammatory factor through post-transcriptional mechanisms (Carballo et al. 1998; Lai et al. 1999; Carballo et al. 2000; Kang et al. 2011(b); Van Tubergen et al. 2011; Molle et al. 2013). These studies demonstrate the importance of adequate post-transcriptional regulatory mechanisms to ensure that inflammatory factors can be quickly induced and then degraded to perform an effector function without damaging the surrounding tissue.

Importantly, some viral infections have been demonstrated to dramatically alter the post-transcriptional regulation of certain pro-inflammatory immune factors. The rate of degradation of TNFα mRNA in human monocytes infected with Measles virus was shown to increase substantially in one study, leading to a decrease in the overall abundance of TNF-α mRNA and likely dysregulating the normal response to infection (Leopardi et al. 1992). In contrast, the stability of the transcript encoding chemokine CXCL8 was shown to be substantially increased in several cell lines harboring HCV replicons (Green et al. 2006). Finally, many viruses interact directly with the cellular mRNA decay machinery and therefore likely alter the post-transcriptional regulation of cellular transcripts. Considering the importance of post-transcriptional regulatory mechanisms in modulating the host immune response to infection, The following section aims to describe the major mechanisms by which mRNAs are degraded in the cell to provide a framework for how viral manipulation of cellular post-transcriptional regulatory mechanisms could contribute to pathology.

Section II: Viral interactions with the general mRNA decay machinery

General mRNA decay mechanisms in the cell serve two important functions. They serve as a quality control mechanism to ensure that aberrant transcripts are quickly removed from the translatable pool of mRNAs, and they permit the normal turnover of transcripts. Because viral RNAs must enter the cytoplasm to undergo translation, they are also likely to encounter cellular nucleases that normally degrade cellular mRNAs. Additionally, cellular RNA decay factors may recognize viral RNAs as foreign, as they often lack a nuclear experience (and therefore are not complexed with ribonucleoproteins that normally associate with cellular mRNAs) and can also lack 5' methylated caps and/or poly(A) tails (e.g. hepacivirus RNAs). Furthermore, mRNA decay pathways are likely integral to the rapid host response to viral infection, as transcripts of many immune factors are heavily regulated at the post-transcriptional level. The rate at which a transcript is degraded can dramatically influence gene expression. Indeed, changes in mRNA decay rates can account for up to 50% of all changes in mRNA abundances (Cheadle et al. 2005(a)). By regulating the stability of a transcript in addition to the rate at which the transcript is generated, the cell can fine-tune gene expression and rapidly alter the transcriptome in response to any given stimulus. Otherwise, the cellular response to a stimulus would likely be much slower, as mRNA synthesis, processing (e.g. splicing), and transport of the mRNA from the cytoplasm into the nucleus would have to take place before any changes in gene expression could occur. Intriguingly, several recent studies propose that cytoplasmic mRNA decay is coordinated with mRNA synthesis, and this will be discussed further below. Therefore, viral RNAs may interact with the RNA decay machinery in such a way as to protect their transcripts from decay or to alter the cellular response to infection. The following section will outline the major mechanisms by which cellular mRNAs are degraded to provide context for a discussion on the known interactions between viral RNAs and the mRNA decay machinery.

Deadenylation-dependent decay

The initial step in the degradation of most mRNAs is deadenylation, the removal of the poly(A) tail (Figure 4). Deadenylation is thought to be the rate-limiting step in the degradation of many transcripts in yeast and mammalian cells, and the poly(A) tail is an important stabilizing element for mRNAs (Wilson and Treisman 1988; Muhlrad and Parker 1992; Shyu et al. 1991).

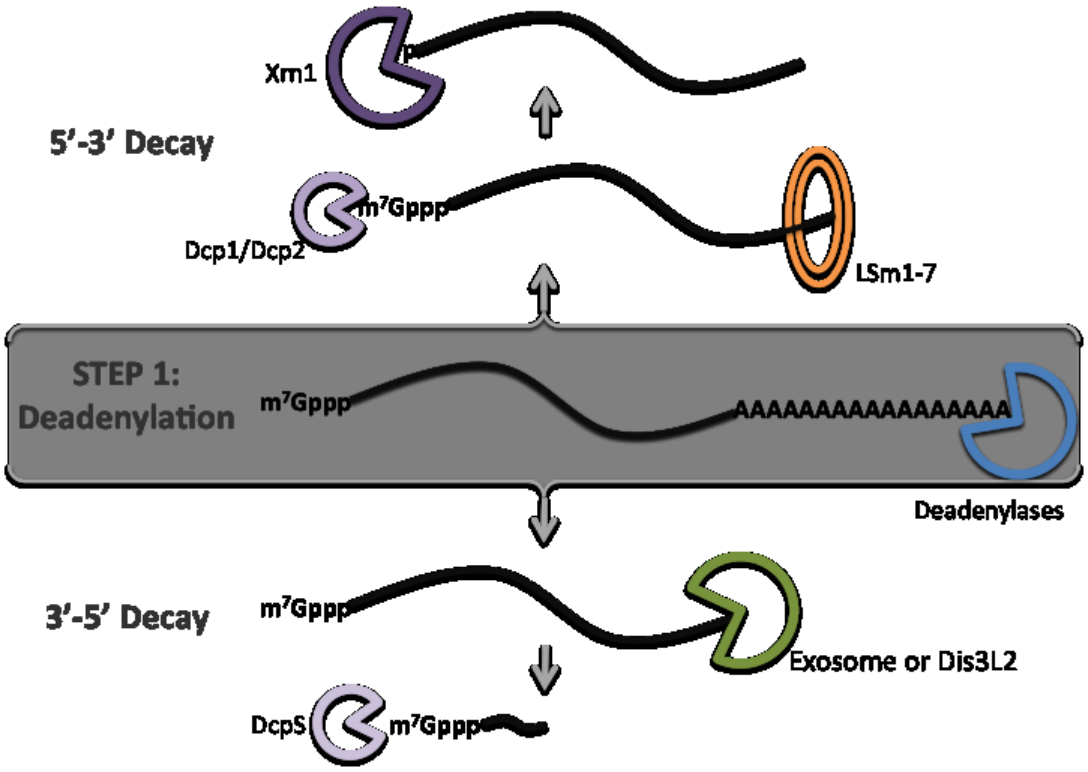

Figure 4. Deadenylation-dependent exonucleolytic decay pathways in the cytoplasm of mammalian cells. Transcripts are first deadenylated by members of the CCR4-NOT complex, the PAN2-PAN3 complex, or PARN. Following removal of the poly(A) tail, the transcript may undergo 3'-5' decay by the exosome complex (bottom) or it may be decapped by DCP1 and DCP2 and degraded in the 5'-3' direction by XRN1 (top).

The ~150-200 nt poly(A) tail of mammalian mRNAs (Brawerman 1974; Brawerman et al. 1972; Nakazato et al. 1973) is removed by deadenylases, proteins that shuttle between nucleus and cytoplasm (Yan 2014; Yamashita et al. 2005). In mammalian cells, the major deadenylases include homologs of the yeast proteins PAN2, CCR4, CAF1, Nocturnin and the poly(A)-specific ribonuclease (PARN) which has no known yeast homolog (Yan 2014; Yamashita et al. 2005). Each of these deadenylases forms a complex or homodimer to be functional. The catalytic

activity of the PAN2 deadenylase requires a protein co-factor, PAN3 (Brown et al. 1996). PAN3 recruits PAN2 to the target mRNA by interacting with the poly(A) binding protein PABP (Mangus et al. 2004; Siddiqui et al. 2007; Uchida et al. 2004). In mammalian cells, the CCR4-NOT protein family is made up of CAF1, Nocturnin, and CCR4 homologs. Interestingly, CAF1 proteins are the major deadenylases in human cells, as knockdown of the two human isoforms of CAF1 resulted in increased poly(A) tail length and delayed deadenylation of cellular transcripts (Schwede et al. 2008). Furthermore, depletion of CAF1 proteins was shown to result in differential abundance of more transcripts than depletion of CCR4 proteins in human cells (Mittal et al. 2011). This study revealed that CCR4 proteins may degrade a set of transcripts that is distinct from that targeted by CAF1 proteins (Mittal et al. 2011). Similarly, PARN was recently shown to regulate the stability and abundance of a discrete set of mRNAs in mouse myoblasts that encode proteins known to be important for mediating cell migration (Lee et al. 2012(b)). Instead of forming a heterogeneous multi-protein complex, PARN must form a homodimer to bind to target mRNAs and exhibit catalytic activity (Yan 2014; Yamashita et al. 2005; Wu et al. 2005). Interestingly, it is possible that several deadenylase complexes work in concert to degrade target transcripts. One study indicated that in mammalian cells, transcripts could be deadenylated through a biphasic process in which the PAN2-PAN3 complex slowly degrades the poly(A) tail until ~100 nt remain, followed by a more rapid removal of the rest of the poly(A) tail by the CCR4-NOT complex (Yamashita et al. 2005). Regardless of which deadenylase specifically acts on the transcript, the end result is a truncated RNA that contains a short oligo(A) tract at the 3' end (Chowdhury et al. 2007).

Upon removal of the poly(A) tail, the majority of mRNAs undergo decapping and 5'-3' decay in eukaryotes (Decker and Parker 1993; Muhlrad et al. 1994; Beelman et al. 1996; Anderson and Parker 1998). This occurs when the short oligoadenylate tract (< 20 nt) remaining at the 3' end of the deadenylated transcript is bound by the LSm1-7 complex (Chowdhury et al. 2007). The LSm1-7 complex is comprised of seven Sm-like proteins and was shown to interact

with the PAT1 homolog PAT1b to promote mRNA decay in yeast (Totaro et al. 2011; Bouveret et al. 2000; Chowdhury et al. 2007; Wu et al. 2014). Mutations or deletion of members of the LSm1-7-PAT1 complex causes increased mRNA stability and the accumulation of capped and oligoadenylated mRNAs in yeast (Tharun et al. 2000). Furthermore, LSm1 protein was shown to be essential for the degradation of a reporter RNA containing an AU-rich element in mammalian cells (Stoecklin et al. 2006). Therefore, the LSm1-7 complex normally recruits the mRNA decapping factors DCP1-DCP2 to promote 5'-3' decay of mRNAs.

Once a transcript is targeted for 5'-3 decay by interacting with the LSm1-7 complex, it undergoes decapping, or the removal of the 7-methylguanosine cap at the 5' end of the mRNA. Decapping factors also form a complex in yeast and mammalian cells to facilitate efficient and specific hydrolysis of the 5' methylated caps from transcripts. The decapping factors DCP1 and DCP2 were first shown to be required for efficient mRNA decapping in yeast (Beelman et al. 1996; Dunckley and Parker 1999). Later, EDC1 and EDC2, two additional protein factors required for decapping, were identified in yeast (Dunckley et al. 2001). These EDC proteins were shown to have the ability to bind RNA, but not decap it directly (Schwartz et al. 2003). It was later determined that DCP2 was the major decapping activity in yeast, and its activity was enhanced by interactions with DCP1, EDC1, and EDC2 (Steiger et al. 2003). In yeast, DCP1 and DCP2 directly interact, likely stabilizing the conformation of the DCP2 protein to facilitate the decapping reaction (She et al. 2008). Importantly, Wang et al. (2002) demonstrated that the yeast homolog of DCP2 was a functional decapping enzyme in mammalian cells. Furthermore, in mammalian cells it appears that rather than directly interacting with one another, DCP1 and DCP2 are bridged by the EDC4 protein (Fenger-Gron et al. 2005). Structural analyses revealed that EDC4 indeed functions as a scaffold for the decapping complex in *Drosophila* and mammalian cells (Braun et al. 2012; Chang et al. 2014). Interestingly, recent studies indicate that additional decapping enzymes (NUDT proteins) exist in mammalian cells (Song et al. 2010; Song et al. 2013). The decapping factor NUDT16 appears to share some mRNA targets with

DCP2 and have some target specificity (Song et al. 2010; Li et al. 2011(b)), but the exact specificities and contributions of DCP2 and NUDT16 to overall mRNA decay in mammalian cells remains to be fully characterized.

Hydrolysis of the 5' methylguanosine cap from the deadenylated transcript exposes the RNA to rapid degradation by the major cytoplasmic exonuclease 1 (XRN1). The highly processive exoribonuclease 1 was first described as an important 5'-3' mRNA decay factor in yeast, as cells lacking XRN1 displayed increased levels of uncapped and deadenylated mRNAs (Hsu and Stevens 1993; Stevens 1980). The cytoplasmic XRN1 protein is highly similar to the major nuclear 5'-3' exoribonuclease 2 (XRN2). The N-terminal regions of XRN1 and XRN2 contain a highly conserved nuclease domain (an alignment of the amino acid sequences of XRN1 homologs is presented in Appendix 2). XRN1 contains five additional conserved regions adjacent to the the nuclease domain: a PAZ/Tudor domain, a KOW domain, a winged helix domain, and an SH3-like domain (Jinek et al. 2011). The PAZ/Tudor domain and the SH3 domain are thought to stabilize the conformation of XRN1 to allow nuclease activity (Jinek et al. 2011; Nagarajan et al. 2013). The winged-helix domain is thought to have several functions. It exists in close proximity to the nuclease domain and was postulated to shield the entry site during nucleolytic decay, it may mediate protein-protein interactions, and it also contains a positively charged region that likely interacts with RNA strands to further stabilize the RNA-protein complex (Jinek et al. 2011). In contrast, the amino acid sequence of the C-terminal region of XRN1 is not well conserved and is also quite unstructured (Jones et al. 2012; Nagarajan et al. 2013). However, the C-terminus of *Drosophila* and human XRN1 harbors a proline-rich region that mediates the interaction between XRN1 and decapping factors (Braun et al. 2012; Chang et al. 2014). Interestingly, the nuclear XRN2 protein does not contain these conserved protein domains, and instead associates with protein partners that stabilize the nuclease domain (Stevens and Poole 1995; Xue et al. 2000; Nagarajan et al. 2013; Xiang et al. 2009; Miki et al. 2014). In this manner, the activity of the yeast XRN2 homolog Rat1 is activated

by the Rai1 protein (Xiang et al. 2009). A recent study identified a unique XRN2-binding domain in the PAXT-1 protein in *Caenorhabditis elegans* that is also present in the human CDKN2AIP (cyclin-dependent kinase inhibitor 2 A interacting protein) and NKRF (NF kappa B repressing factor) (Miki et al. 2014).

Recently, the crystal structure of the N-terminus of *Drosophila* XRN1 (pacman) in complex with an RNA substrate was solved (Jinek et al. 2011). This structure revealed that XRN1 likely sterically blocks the insertion of RNAs with 5' methylguanosine caps or triphosphorylated ends in favor of smaller 5' monophosphorylated RNAs to permit specific decay of uncapped transcripts (Jinek et al. 2011). The nuclear XRN2 protein likely has similar specificity to monophosphorylated transcripts, as the nuclease domain is very similar to that of XRN1 (Nagarajan et al. 2013). In cell-free assays, yeast XRN1 has been shown to stall on stable stem-loop structures and poly(G) tracts. However, yeast XRN1 can degrade highly structured ribosomal RNAs (rRNAs); indeed it is routinely used to deplete rRNAs from total RNA pools to purify mRNAs. Furthermore, *Drosophila* XRN1 can effectively degrade RNA duplexes in vitro if there is a $\geq$5 nt single stranded region at the 5' end to allow the RNA to enter the active site (Jinek et al. 2011). Therefore, viral RNAs that resist XRN1-mediated decay (e.g. the 3' UTRs of flavivirus RNAs) likely contain unique structural or sequence elements that have not been previously characterized.

Both XRN1 and XRN2 serve important roles in degrading mRNAs (or pre-mRNAs in the nucleus in the case of XRN2) and non-coding RNAs that have a 5' monophosphate as a result of decapping or endonucleolytic cleavage (Hsu and Stevens 1993; Muhlrad et al. 1994; Lejeune et al. 2003). Furthermore, XRN2 trims the 5' ends of ribosomal RNA precursors during rRNA maturation (Stevens et al. 1991; Henry et al. 1994; Geerlings et al. 2000). Although XRN1 is primarily localized to the cytoplasm, recent evidence indicates that it can translocate to the nucleus to influence transcription in yeast (Sun et al. 2013(b); Haimovich et al. 2013), and this will be discussed in more detail below. The yeast XRN2 homolog serves an important function

in mediating transcription termination, and was recently shown to influence the phosphorylation state of the C-terminal domain of RNA polymerase II (Kim et al. 2004; Jimeno-Gonzalez et al. 2014). Therefore, these 5'-3' exoribonucleases are important for regulating gene expression by mediating transcription and post-transcriptional processes.

Intriguingly, XRN-deficient organisms exhibit defects in several important biological processes (reviewed in Nagarajan et al. 2013 and Jones et al. 2012). Yeast deficient in a functional XRN1 enzyme exhibit defects in cell growth, proliferation, and sporulation (Larimer and Stevens 1990; Tishkoff et al. 1991; Kim and Kim 2002). More complex organisms (including fruit flies) show developmental defects and reduced fertility in the absence of a functional XRN1 protein (Newbury and Woollard 2004; Grima et al. 2008; Lin et al. 2008; Zabolotskaya et al. 2008). Defects in XRN2 activity have been shown to reduce cell survival and sporulation in yeast and reduce fertility and survival in plants (Amberg et al. 1992; Kenna et al. 1993; Gy et al. 2007). Therefore, the 5'-3' exoribonucleases are important for many essential aspects of organismic growth and development.

How are the seemingly distinct processes of deadenylation, decapping, and 5'-3' decay coordinated? Intriguingly, many of these mRNA decay factors contain disordered domains that likely facilitate the assembly of these large multi-protein complexes (Jonas and Izaurralde 2013).The LSm1-7 complex physically interacts with the decapping complex component DCP1 in yeast (Tharun et al. 2000) and was later shown to co-localize with decapping factors DCP1, DCP2, and the 5'-3' exoribonuclease XRN1 in discrete cytoplasmic foci in mammalian cells (Ingelfinger et al. 2002). Importantly, XRN1 has been shown to interact with EDC4 in mammalian and *Drosophila* cells, coordinating decapping and 5'-3' decay (Braun et al. 2012; Chang et al. 2014). Furthermore, another scaffolding protein, PAT1b, was shown to physically associate with the CCR4-NOT deadenylation complex, the DCP1-DCP2 decapping factors, and LSm1 protein in human cells (Ozgur et al. 2010). A recent study also demonstrated that XRN1 activity can be modulated by the decapping scavenger DCS1 in yeast (Sinturel et al. 2012;

described below), indicating that coordination between 3'-5' and 5'-3' decay may allow fine-tuning of mRNA decay and cellular gene expression. Therefore, physical interactions between distinct RNA decay factors mediated by scaffolding proteins likely facilitate the coordination of these unique events.

Alternatively, the deadenylated transcript may undergo 3'-5' decay by the cytoplasmic exosome complex comprised of 10 subunits (Januszyk and Lima 2014) or the newly described Dis3L2 (Malecki et al. 2013; Lubas et al. 2013). The Dis3L2 exonuclease appears to specifically degrade deadenylated RNAs or pre-miRNAs that were oligouridylated by TUTases (Malecki et al. 2013; Lubas et al. 2013). In contrast, the interaction of various co-factors in yeast with the exosome has been demonstrated to impact the RNA substrates degraded by the exosome (Januszyk and Lima 2014). Following 3'-5' decay of deadenylated transcripts, the scavenger decapping enzyme DCPS then hydrolyses the m7GpppG 5' cap. Interestingly, DCPS (also known as DCS1) has been shown to physically associate with members of the exosome complex in mammalian cells, and it can mediate decapping of RNAs less than 10 nucleotides in length, although it is more efficient at hydrolyzing free cap moieties (Wang and Kiledjian 2001; Liu et al. 2002).

Although deadenylation-mediated decay is an important mechanism by which many cellular mRNAs are degraded in the cell, some mRNAs are degraded via endonucleolytic decay pathways. Three such pathways that serve quality control functions in the cell will be discussed below. Furthermore, small RNAs also mediate degradation of some transcripts, and these pathways serve important functions in regulating both normal gene expression and serving as an important anti-viral immune mechanism. Importantly, factors that participate in deadenylation-mediated decay pathways are also essential for endonucleolytic and small RNA-mediated decay pathways, including XRN1 and the exosome complex.

Quality control mRNA decay pathways

Several deadenylation-independent quality control pathways exist that begin with the endonucleolytic cleavage of aberrant transcripts and end with exonucleolytic decay of the 3' and 5' mRNA fragments by XRN1 or the exosome. Nonsense-mediated decay (NMD), no-go decay, and non-stop decay are three such quality control pathways that are particularly relevant in the context of viral infection. Transcripts that contain multiple termination codons and long 3' untranslated regions are targets for NMD, and a major trigger for NMD is the absence of the exon junction complex on unspliced RNAs. Importantly, viral RNAs often have one or more of these characteristics.

Cellular RNAs can be targeted for NMD due to mistakes made during pre-mRNA splicing, transposon-containing RNAs, and transcripts that contain mutations from inaccurate transcription are all subject to NMD (Maquat and Gong 2009). When a transcript is targeted for NMD, UPF1 assembles with other translation factors and upon ribosome stalling upstream of the premature termination codon, UPF1 is phosphorylated and recruits SMG6, SMG5, and SMG7 (Maquat and Gong, 2009; Eberle et al. 2009; Loh et al. 2013). UPF1 causes translational repression and eventual decay of the target transcript through SMG6-dependent endonucleolytic cleavage and/or by SMG5- SMG7-mediated recruitment of exonucleolytic decay factors (e.g. XRN1) and/or deadenylases (Yamashita et al. 2005; Eberle et al. 2009; Franks et al. 2010; Loh et al. 2013).

Transcripts that do not contain termination codons (e.g. due to premature polyadenylation or mutation) undergo non-stop decay. This process is triggered when the translating ribosome becomes vacant as the ribosome falls off the poly(A) tail of the transcript in the absence of proper termination (van Hoof et al. 2002; Vasudevan et al. 2002; Frischmeyer et al. 2002). The Ski7 protein then recruits the cytoplasmic exosome complex to the mRNA (Vasudevan et al. 2002; van Hoof et al. 2002; Klauer and van Hoof 2012). Finally, aside from improper translation termination, stalling of the ribosome on mRNAs can also trigger a quality

control pathway called no-go decay (Harigaya and Parker 2010). The ribosome can stall on stable stem-loop structures in the open reading frame of an RNA, allowing Dom34p and Hbs1p to bind to the ribosome, triggering endonucleolytic cleavage of the RNA (Doma and Parker 2006; Harigaya and Parker 2010). Importantly, the resulting fragments are degraded by XRN1 and the exosome complex (Harigaya and Parker 2010).

MicroRNA mediated decay

MicroRNAs (miRNAs) are ~22 nt RNAs that are derived from endogenous precursor RNAs that form long hairpin structures and in mammals are post-transcriptionally cleaved by Drosha in the nucleus to form a pre-miRNA and exported to the cytoplasm where the mature miRNA duplex is formed by DICER (Bartel 2004). This duplex miRNA is then loaded onto AGO2 and a helicase activity facilitates the unwinding of the duplex to allow the guide strand to bind its target mRNA (Bartel 2004). Interestingly, the stability of the AGO2 protein is enhanced upon miRNA binding (Smibert et al. 2013; Martinez and Gregory 2013).

MicroRNAs contain a 2-7 nt seed sequence that guides AGO2 to target mRNAs by Watson-Crick base pairing with the target (Bartel 2009). Target sites are mostly found in the 3' UTR, possibly because the translation machinery would disrupt RNA induced silencing complex (RISC) associated with the target mRNA during translation elongation (Bartel 2009). Transcripts targeted by microRNAs may be translationally repressed and/or degraded by a deadenylation-dependent mechanism (Huntzinger et al. 2013). Several mammalian proteins have been identified that mediate the interaction of AGO2 with target transcripts and cause the RISC to localize to distinct cytoplasmic granules in the cell (processing bodies; Eystathioy et al. 2003): TNRC6A (also called TNRC6A) and the related TNRC6B and TNRC6C proteins (Baillat and Shiekhattar 2009; Takimoto et al. 2009). TNRC6A/TNRC6 proteins recruit the CCR4-NOT complex (Fabian et al. 2011; Chekulaeva et al. 2011) and the PAN2-PAN3 complex (Christie et

al. 2013) to AGO2-bound target mRNAs to facilitate both translational repression and deadenylation-dependent decay (Huntzinger et al. 2013; Takimoto et al. 2009; Chen et al. 2009). Following deadenylation, transcripts then undergo DCP1-DCP2-mediated decapping and 5'-3' decay by XRN1 (Rehwinkel et al. 2005; Chen et al. 2009). Therefore, miRNA-mediated decay is an important mechanism by which transcripts are targeted for decay pathway in mammalian cells.

Small interfering RNA mediated decay

Small interfering RNAs (siRNAs) are 21-27 nt RNAs generated from dsRNAs, such as viral replication intermediates that accumulate in infected cells (Ma et al. 2008). Unlike miRNAs, siRNA-mediated decay of target transcripts does not induce deadenylation, but rather results in endonucleolytic cleavage of the mRNA by AGO2 followed by exonucleolytic decay of the resulting mRNA fragments by XRN1 and the exosome complex (Orban and Izaurralde 2005). Recent work has demonstrated that mammalian cells have a functional anti-viral RNAi response (Maillard et al. 2013; Li et al. 2013(c)), although there is some debate about whether this is significant (Cullen et al. 2013). Although most somatic mammalian cells rely on PRRs and the induction of a type I IFN responses that oftentimes result in the expression of induced nucleases to combat RNA virus infections, the current literature supports the hypothesis that mammalian cells are capable of generating siRNAs from viral dsRNAs that may have anti-viral activity (Li et al. 2013(c)). The ability of a mammalian cell to process dsRNAs into siRNAs depends on DICER activity, and it was recently shown that an N-terminal truncated isoform of DICER that is preferentially expressed in mouse oocytes can dice dsRNAs into siRNAs but the isoform that is expressed in differentiated cells does not have this activity (Flemr et al. 2013). Human DICER can cleave dsRNAs with perfect complementarity but this process is less efficient than pre-miRNA cleavage because the N-terminus of the protein serves as an autoinhibitor of DICER

activity (Ma et al. 2008). However, siRNA-mediated gene silencing in human cells is effective and therefore human cells contain the necessary dicing and slicing activities for RNAi to take place (Caplen et al. 2001). Although RNAi may not be a major anti-viral mechanism in human cells, it is very important for anti-viral immunity in mosquito cells which express two unique DICER proteins that function in either the miRNA or siRNA pathway (Blair 2011; Sanchez-Vargas et al. 2009; Campbell et al. 2008). Therefore, arthropod-borne viruses could benefit greatly from impaired RNA interference pathways to facilitate efficient viral transmission to the next host.

Coordination between mRNA synthesis and decay

Changes in mRNA stability and synthesis rates are important for the regulation of cellular gene expression. Studies using an *in vitro* model of T cell activation demonstrated that up to 50% of changes in polyadenylated mRNA abundance may be due to changes in mRNA stability, as nuclear run on experiments demonstrated that altered transcription rates do not account for all observed changes in mRNA abundance (Cheadle et al. 2005(a); Cheadle et al. 2005(b)). A more recent study of gene expression in mouse myoblasts demonstrated that coordination between mRNA decay and synthesis may buffer gene expression, as many stabilized transcripts were also less abundant (Lee et al. 2012b). This may allow the cell to fine-tune gene expression through coordination of mRNA synthesis and decay.

How could the disparate processes of cytoplasmic mRNA decay and transcription be coordinated? Intriguingly, protein factors that mediate transcription may pass between the nucleus and the cytoplasm to link these two processes. For example, the RNA polymerase II Rpb4/7 complex was shown to shuttle from the nucleus to the cytoplasm and influence the stability of mRNAs in yeast (Goler-Baron et al. 2008). The Rpb4/7 complex was later shown to associate with cytoplasmic mRNA decay factors in *Saccharomyces cerevisiae*, and depletion of

decapping activators Pat1 and Dhh1 conferred a similar decrease in yeast life span comparable to Rpb4-deficient cells (Duan et al. 2013). The nuclear Rpb4 protein was shown to shuttle out of the nucleus into the cytoplasm upon shifting cultures of the pathogenic fungus *Cryptococcus neoformans* to 37^{o}C, and Rpb4-deficient organisms had defects in deadenylation (Bloom et al. 2013). Intriguingly, Rpb4/7 may also coordinate mRNA synthesis and decay with translation in yeast (Harel-Sharvit et al. 2010). Therefore, protein factors that facilitate transcription can also alter mRNA decay.

Factors required for mRNA decay in the cytoplasm may also enter the nucleus to potentially influence transcription. The CCR4-NOT complex can be observed in the cytoplasm in processing bodies, associated with ribosomes, or in the nucleus in yeast (Collart et al. 2013; Collart 2003). CCR4-NOT has also been shown to interact with the mRNA export machinery, indicating that it could couple the processes of mRNA decay and export to coordinate post-transcriptional gene regulatory mechanisms in yeast (Kerr et al. 2011). Yeast deficient in the Ccr4-NOT complex were shown to have decreased rates of both mRNA decay and mRNA synthesis (Sun et al. 2012). The 5'-3' exoribonuclease XRN1 was also recently shown to shuttle between the cytoplasm and the nucleus in yeast and could therefore influence mRNA synthesis (Haimovich et al. 2013; Sun et al. 2013b). Several studies have demonstrated that yeast cells lacking XRN1 have lower or unchanged mRNA abundances and increased mRNA half-lives (He et al. 2003; Haimovich et al. 2013; Sun et al. 2013; Medina et al. 2014) and although *Drosophila* expressing a mutant XRN1 homolog allele displayed phenotypic changes, very few mRNAs were differentially expressed compared to wild-type organisms (Jones et al. 2013). However, changes in mRNA stability in these flies were not assessed. In general, these studies support the hypothesis that gene expression is buffered such that stabilization of a transcript may cause decreased transcription (or vice versa) to allow coordination between early and late stages of gene expression. Therefore, interactions between viruses and the mRNA decay machinery

could alter both the degradation and synthesis of mRNAs, and potentially cause dramatic changes in cellular gene expression.

Sites of mRNA decay in the cytoplasm

Another important aspect of cellular gene expression that contributes to the stability of messenger RNAs and the likelihood that they will be translated is the subcellular localization of transcripts in large ribonucleoprotein complexes (e.g. P-bodies or stress granules) that are dynamically regulated in the cytoplasm. In general, transcripts exist in RNP complexes that facilitate export from the nucleus, translation, and ultimately degradation (Wilusz and Wilusz 2010). Processing bodies often contain many mRNA decay factors including XRN1, DCP1a, and AGO2 (Sheth and Parker 2003). Using an MS2 reporter construct containing a poly(G) tract resistant to yeast XRN1-mediated decay, Sheth and Parker (2003) showed that 5'-3' mRNA decay intermediates accumulate in P-bodies, supporting the hypothesis that 5'-3' decay can take place in these discrete RNP granules. It was later shown in both yeast and mammalian systems that RNAs may be stored in P-bodies and eventually exit these distinct cytoplasmic foci and associate with polysomes to undergo translation (Brengues et al. 2005; Bhattacharyya et al. 2006). Interestingly, treating human or yeast cells with cyclohexamide to inhibit translation elongation results in P-body dispersal, indicating that P-body formation may be seeded by mRNAs that have undergone translation and are targeted for decay (Sheth and Parker 2003; Cougot et al. 2004). Transcripts targeted for miRNA-mediated decay are guided to P-bodies in human cells (Bhattacharyya et al. 2006). Processing bodies therefore may function as discrete pseudo-organelles where the fate of an mRNA is decided (Buchan and Parker 2009).

Yeast and mammalian cells also form stress granules (SG), which are induced upon inhibition of translation initiation by a variety of stressors (Buchan and Parker 2009; Kedersha et al. 1999). Puromycin treatment, which causes mRNA-ribosome complexes to disassemble,

causes formation of SG in mammalian and yeast systems (Buchan and Parker 2009; Kedersha et al. 2000; Buchan et al. 2008). Stress granules and P-bodies likely interact and mRNPs may be shuttled between them (Buchan and Parker 2009). Indeed, stress granule assembly in yeast depends on P-body formation and may be seeded by mRNP complexes assembled in P-bodies (Buchan et al. 2008). Therefore the subcellular localization and mRNP context is likely a major contributing factor for the regulation of cellular gene expression.

In summary, eukaryotic cells harbor several constitutively expressed nucleases that can potentially act on viral RNAs during an infection. These pathways normally allow for the post-transcriptional regulation of cellular mRNAs and likely play important roles in mediating the proper host response to infection by facilitating the rapid induction and degradation of normally short-lived pro-inflammatory immune mediators. Therefore, viruses could benefit from altering cellular RNA decay processes by influencing host gene expression and potentially protecting their transcripts from decay. The following section will discuss some of the known interactions between viruses and the cytoplasmic mRNA decay machinery.

Viral evasion of deadenylation

Several pieces of evidence indicate that polyadenylated viral RNAs are susceptible to deadenylation-dependent decay, and many viruses appear to have evolved mechanisms for resisting deadenylation. Viral RNAs are known to evade deadenylation-dependant decay by either interacting with cellular RNA binding proteins or by forming stable structures that essentially hide the poly(A) tail from deadenylases.

The arthropod-borne viruses in the *Togaviridae* family possess positive sense, single stranded RNA genomes that have 5’ methylated caps and poly(A) tails, and in this sense they mimic cellular transcripts. Intriguingly, Sindbis virus (SINV; a representative member of the *Alphavirus* genus in the *Togaviridae* family) encodes a conserved U-rich sequence element in

the 3' UTR of the viral RNA that is essential for inhibiting deadenylation-dependent decay (Garneau et al. 2008). The cellular RNA stability factor ELAVL1 (also known as HuR) was shown to bind with high affinity to this U-rich region of alphavirus RNAs, thus inhibiting deadenylation and promoting viral RNA stability in both mosquito and mammalian systems (Garneau et al. 2008; Sokoloski et al. 2010). The interaction between HuR and SINV RNAs was shown to be very important for viral proliferation, as cells deficient in HuR protein supported less viral growth than normal cells, and viruses lacking the U-rich HuR binding site replicated to lower levels than wild-type viruses (Sokoloski et al. 2010). Interestingly, HuR is normally present in the nucleus of mammalian cells. However, alphavirus infections specifically induce the re-localization of HuR from the nucleus to the cytoplasm (Sokoloski et al. 2010; Dickson et al. 2012). Therefore, alphaviruses cause the selective re-localization of the RNA stability factor HuR to protect their transcripts from deadenylation-dependent decay, and this is essential for optimal viral propagation in mammalian and mosquito cells.

Suppressing the deadenylation-dependent decay of viral transcripts can not only enhance viral propagation in general, but could also permit the fine-tuning of viral gene expression. Rabies virus (a member of the *Rhabdoviridae* family) contains a negative sense RNA genome from which five capped and polyadenylated transcripts (encoding the N, P, M, G, and L proteins) are synthesized by the viral polymerase in the cytoplasm (Schnell et al. 2010). The abundance of each viral transcript is dictated by its position in the RNA genome such that sequences closest to the 3' end of the negative sense viral RNA genome are transcribed more frequently than those at the 5' end of the genome (Schnell et al. 2010). However, it was recently demonstrated that the viral glycoprotein (G) mRNA was present in greater abundance in human cells infected with rabies virus than would be expected as a result of the accepted mode of viral transcription (Palusa et al. 2012). In an analogous mechanism to alphaviruses, the 3' UTR of the G mRNA was shown to interact specifically with the cellular poly(C) binding protein 2 (PCBP2) in infected cells (Palusa et al. 2012). Importantly, this interaction was shown to

suppress deadenylation of the G transcript in cell extract systems, and the 72 nt element in the G mRNA 3' UTR was shown to act as a stability element in reporter assays (Palusa et al. 2012). Therefore, rabies virus G mRNA likely binds specifically to the cellular PCBP2 to permit differential viral gene expression.

Deadenylation can also be suppressed by unique structural elements that bind and sequester the 3' poly(A) tail of a transcript, essentially hiding the adenylate tract from deadenylases in the nucleus. The highly abundant polyadenylated nuclear (PAN) RNA generated by Kaposi's sarcoma-associated herpesvirus (a DNA virus in the *Herpesviridae* family) possesses an RNA stability element near the 3' end of the RNA that associates with the poly(A) tail to form a triple helix structure (Mitton-Fry et al. 2010). This triple helix structure was shown to suppress deadenylation of an RNA reporter in vitro (Mitton-Fry et al. 2010). Importantly, many other viruses and even host non-coding RNAs were later shown to contain similar RNA stability elements that likely protect these transcripts from deadenylation (Tycowski et al. 2012; Brown et al. 2012).

Viral evasion of 5'-3' decay

Many viral RNAs, including flavivirus RNAs, do not contain poly(A) tails. It is not known whether or not these RNAs are recognized as deadenylation-mediated decay intermediates or are degraded through a deadenylation-independent mRNA decay pathway. However, there is some evidence that transcripts can be decapped without first being deadenylated. The yeast mRNA EDC1 can be deadenylated without first being decapped (Muhlrad and Parker 2005). Therefore, some viral RNAs might undergo 5'-3' decay even though they lack a poly(A) tail. Several pieces of evidence indicate that flaviviral RNAs can be degraded by 5'-3' and 3'-5' exonucleases without first being deadenylated. First, replication-competent HCV RNAs transfected into Huh7.5 human liver cells had increased stability when XRN1 was depleted, and

accordingly XRN1 depletion resulted in enhanced HCV replication (Li et al. 2013(b)). Second, as described in Section I of the Introduction, subgenomic flavivirus RNAs generated from all viruses in the *Flavivirus* genus tested to date are formed due to incomplete 5'-3' decay of the viral genome by XRN1 (Pijlman et al. 2008; Silva et al. 2010). Furthermore, the exosome may potentially also act on flavivirus RNAs, as one study demonstrated that YFV sfRNA was truncated from the 3' end and therefore may be resistant to further 3'-5' decay as well (Silva et al. 2010). Two major mechanisms by which viruses evade or likely shut down 5'-3' decay by XRN1 are discussed below.

Some viruses may simply shield the 5' termini of their RNAs from XRN1 through several distinct mechanisms. First, many viruses (including the alphaviruses and members of the *Flavivirus* genus) have 5' methylguanosine caps added co-transcriptionally by viral proteins. The 5' methylated caps likely serve two important functions: proteiction from degradation by XRN1, and evasion of IFIT-mediated innate immune responses as discussed above Section I. Viruses that do not undergo capping during transcription use other mechanisms to 'cap' their RNAs, likely serving to protect them from 5'-3' decay. First, these viral RNAs may acquire a 5' methylated cap by stealing them from cellular RNAs (cap-snatching). The negative- or ambi-sense RNA viruses including members of the *Bunyaviridae*, *Arenaviridae*, and the *Orthomyxoviridae* cap-snatch, likely to protect their transcripts from 5'-3' decay and also undergo cap-dependent translation (Raju et al. 1990; Mir et al. 2008; Hopkins et al. 2013). Second, the RNAs of hepaciviruses and pestiviruses appear to contain 5' triphosphates that are likely sterically hindered from entering the active site of XRN1, and as discussed above these viruses undergo cap-independent translation via IRES elements (Jinek et al. 2011). Finally, some viral RNAs can even be 'capped' by a covalently linked viral protein. The genomic RNAs of viruses in the *Picornaviridae* family (e.g. poliovirus) are 'capped' by VPg (virus protein, genome-linked), which is required for viral RNA synthesis but not viral RNA translation (Nomoto et al. 1977(a); Nomoto et al. 1977(b); Racaniello 2001). Therefore, the 5' methylated cap

structure, triphosphate group, or VPg serve as *cis*-acting stability factors that blocks decay by XRN1. However, viral RNAs could become susceptible to XRN1-mediated decay if they are decapped or subjected to endonucleolytic cleavage events that reveal a terminal 5' monophosphate group.

Finally, picornaviruses cause the RNA decay factors XRN1, the PAN3 deadenylase, DCP1 and DCP2 to undergo proteolytic degradation through cellular or viral protease-dependent mechanisms (Dougherty et al. 2011). Picornavirus RNAs may also be targeted for decay by the AUF1, as this cellular protein relocalizes from the nucleus to the cytoplasm and binds the 5' UTRs of poliovirus and human rhinovirus RNAs (Cathcart et al. 2013). These viruses avoid being degraded upon binding this destabilizing factor by proteolytically cleaving AUF1 during infection (Rozovics et al. 2012). Coxsackievirus B3 also causes redistribution of AUF1 into the cytoplasm and cleavage, and this also appears to require the activity of viral proteins (Wong et al. 2013). Therefore, these viruses use an aggressive mechanism to combat cellular exonucleolytic decay in addition to simply shielding their RNAs from XRN1.

Viral evasion of quality control mRNA decay pathways

Although there is a dearth of research into the role of constitutive quality control mRNA decay pathways in degrading viral RNAs, there are several reasons why viral RNAs may be targeted for decay in this manner. First, as discussed above most viral RdRps lack proof-reading activity, and therefore some viral transcripts likely contain aberrantly placed termination codons (or lack them altogether). Second, many viral RNAs do not have a nuclear experience and contain multiple open reading frames, and are therefore likely to undergo NMD. Indeed, although retroviral transcripts do have a nuclear experience, they are unspliced and susceptible to NMD (Hogg and Goff, 2010). Third, many viral RNAs contain stable structural elements that could potentially cause ribosome stalling during translation elongation and trigger no-go decay.

However, viruses have likely evolved mechanisms to avoid degradation by these pathways. For example, a structured RNA element in the avian Rous sarcoma virus was shown to be essential for protecting the transcript from NMD (Withers and Beemon 2011). It is likely that other viruses also suppress or evade these important quality control pathways in the cell. Finally, suppression of exoribonucleases (e.g. XRN1) could cause a reduction in the efficicacy of these quality control pathways.

Unconventional miRNA-viral RNA interactions

Diverse viruses are known to generate unconventional miRNAs from their RNAs during infection, and can be positively or negatively regulated by host cellular miRNAs. Intriguingly, Shapiro et al. (2012) showed that SINV infection causes relocalization of the microprocessor Drosha from the nucleus to the cytoplasm, allowing miRNAs to be generated from viral RNAs. Therefore cellular miRNAs could serve an anti-viral function in mammalian cells (Shapiro et al. 2012). Furthermore, miRNA target sites can be introduced into RNA viruses to restrict their replication to specific cell types. Influenza A virus that encodes a miR-192 binding site can replicate and be transmitted by ferrets (which don't express miR-192) but is attenuated in mice, which express miR-192 in respiratory tract epithelial cells (Langlois et al. 2013). This implies that the tissue expression of certain host miRNAs could modulate where a virus may successfully propagate.

Conversely, HCV is known to steal a specific host miRNA to promote viral RNA replication; indeed HCV requires the host microRNA-122 to propagate effectively in human liver cells (Jopling et al. 2005). Although the exact function of miR-122 in enhancement of HCV replication remains unknown, recent studies have shown that miR-122 may serve to protect the HCV genome from degradation by shielding the terminus of the viral RNA from decay factors (Machlin et al. 2011; Shimakami et al. 2012; Mortimer and Doudna 2013; Li et al. 2013(b)).

Finally, several herpesviruses deplete specific cellular miRNAs via highly abundant non-coding viral RNAs. Herpesvirus saimiri (HVS) and murine cytomegalovirus (mCMV) both generate unique virus-derived RNAs that sponge up cellular miRNAs and cause their degradation (Buck et al. 2010; Cazalla et al. 2010; Libri et al. 2012). The mCMV transcript m169 is predicted to contain an open reading frame, is polyadenylated and capped, and contains a miR-27 binding site in its 3' UTR (Libri et al. 2012). Upon expression of m169 during mCMV infection or when expressed via an adenovirus vector, miR-27a and miR-27b are rapidly and specifically depleted (Libri et al. 2012; Marcinowski et al. 2012).). HVS also selectively targets miR-27 for degradation via U-rich non-coding viral RNA called HSUR1 (Cazalla et al. 2012). Although the exact function of miR-27 in the context of herpesvirus infection remains unknown, it is possible that miR-27 negatively regulates the abundance of host cellular transcripts that would otherwise be beneficial to these disparate herpesviruses.

Poxviruses also appear to have evolved a unique mechanism by which many cellular miRNAs can be degraded during an infection. The poxvirus poly(A) polymerase induces cellular miRNA degradation by polyadenylating these small RNAs, targeting them for decay (Backes et al. 2012). Interestingly, the 3' ends of virus-derived siRNAs generated during Vaccinia virus infection of *Drosophila* cells are 2'-O methylated, and this motif blocks the addition of a poly(A) tail and subsequent decay of these small RNAs. Therefore, diverse viral RNAs are susceptible to miRNA-mediated decay in cells and many use unique mechanisms by which they successfully interact with this RNA decay pathway.

Dispersal of processing bodies during flavivirus infections

Several recent studies have shown that XRN1 may be involved in degradation of the HCV genome and the subcellular localization of XRN1 is altered during HCV infection. XRN1 is usually localized to processing bodies, discrete cytoplasmic foci that may be localized sites of

mRNA decay. Processing body composition is altered during HCV infection (Perez-Vilaro et al. 2012). Intriguingly, XRN1, miR-122, and AGO2 have been shown to be localized in ring-like structures with the HCV core protein in lipid droplets (Ariumi et al. 2011; Berezhna et al. 2011). XRN1 is similarly re-localized to viral replication complexes in West Nile virus infected cells (Chahar et al. 2013). Furthermore, as observed in DENV and WNV infections, processing bodies are dispersed during HCV and poliovirus infections (Emara and Brinton 2007; Dougherty et al. 2011; Pager et al. 2013). Furthermore, a slew of RNA decay factors including XRN1, LSM1, TNRC6A, and DDX6 were shown to re-localize to viral replication complexes and increase viral replication in HeLa cells infected with WNV (Chahar et al. 2013).

Interestingly, DDX6 and CAPRIN1 are known to bind to the DENV 3' UTR but the functional importance of many of these interactions remains to be characterized (Ward et al. 2011; Roby et al. 2014). Furthermore, a recent study showed that the JEV C protein interacts directly with Caprin 1 (Katoh et al. 2013). However, CAPRIN1 and the G3BP1 proteins are known to interact with cellular factors present in stress granules (Solomon et al. 2007; Ward et al. 2011; Matsuki et al. 2013). The sequestration of these and other stress granule-associated proteins (e.g. TIA-1 and TIAR) in flavivirus replication complexes may therefore be an underlying mechanism for the observed defects in stress granule formation in flavivirus infections (Emara and Brinton 2007; Ward et al. 2011; Matsuki et al. 2013).

Pathogenic consequences of viral interactions with the cellular RNA decay machinery

The regulation of cellular gene expression relies on a complex interplay between RNA synthesis, degradation, and translation as described above. Because changes in mRNA stability can influence the steady-state level of an mRNA, the ability of a virus to manipulate or inactivate mRNA decay factors could have multiple complex profound effects on host cellular gene expression. In addition to the constitutively expressed mRNA decay factors that regulate host

gene expression, cells may express a variety of virus-induced nucleases that are part of the anti-viral innate immune response to infection. Furthermore, many different viruses have been shown to influence the formation of mRNP granules, which likely also contributes to changes in cellular gene expression (Beckham and Parker 2008; Lloyd 2013). The mechanisms that underlie the innate immune response to viral infection leading to induced nuclease expression and how viruses interfere with the constitutive mRNA decay machinery are therefore important to understand in order to determine how cellular gene expression is changed during infection and how this contributes to pathogenesis. Viral RNAs can sponge host RNA stability factors, suppress host exoribonucleases, and disperse cytoplasmic RNA granules, all of which likely contribute to virus-induced pathology (Moon and Wilusz 2013).

Considering the importance of post-transcriptional mechanisms in controlling cellular gene expression, perturbation of the cellular RNA decay machinery likely causes dramatic changes in how the cell responds to infection or cell biology in general. The following discussion will focus on how pathology may be induced by three viral mechanisms: sponging/sequestration of host miRNAs or RNA binding proteins by viral RNAs, the production of viral nucleases that degrade cellular mRNAs, and the proteolytic degradation of host mRNA decay factors (depicted in Figure 5). For a more detailed review on this topic, please see Moon and Wilusz (2013).

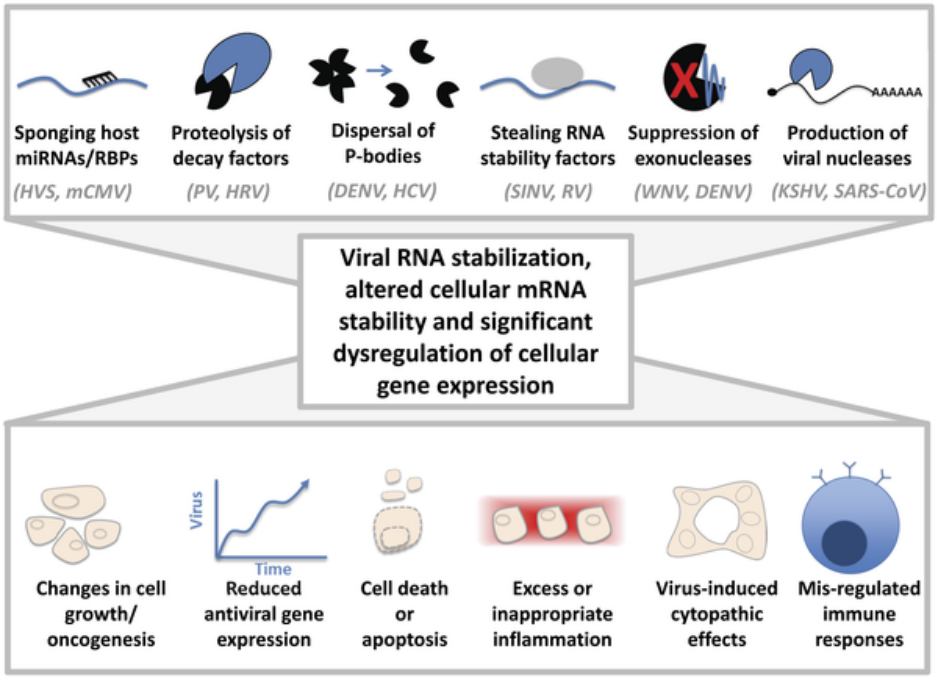

Figure 5. **Mechanisms that viruses use to evade or suppress general host RNA decay factors and how this may contribute to virus-induced pathogenesis.** HVS: Herpesvirus saimiri, mCMV: murine Cytomegalovirus, PV: Poliovirus, HRV: Human rhinovirus, DENV: the dengue viruses, HCV: hepatitis C virus, SINV: Sindbis virus, RV: Rabies virus, WNV: West Nile virus, KSHV: Kaposi Sarcoma-associated herpesvirus, SARS-CoV: Severe Acute Respiratory Syndrome coronavirus.Taken from: Moon SL, Wilusz J (2013) Cytoplasmic Viruses: Rage against the (Cellular RNA Decay) Machine. PLoS Pathog 9(12): e1003762.

Sponging/stealing host miRNAs and RNA-binding proteins

Recent studies have demonstrated that viral RNAs can serve as sponges for cellular miRNAs and RBPs, consequently altering cellular gene expression. The seven HVS non-coding U-rich RNAs were discovered by northern blots targeting RNA products of the viral genome associated with T cell transformation (Cazalla et al. 2010; Lee et al. 1988). These HVS non-coding RNAs (ncRNAs) are also associated with T cell activation and may increase the growth rate of transformed T cells (Cazalla et al. 2010). As discussed above, several of these HVS RNAs and an RNA generated by mCMV appear to selectively bind and degrade the host microRNA miR-27 (Buck et al. 2010; Cazalla et al. 2010; Libri et al. 2012). Could the sponging of miR-27 alter host gene expression and potentially cause pathology during infection with these lymphotropic viruses? Interestingly, the transcription factors RUNX1 and FOXO1, have been

identified as miR-27 targets, all of which are known to function in development and/or cell proliferation (Ben-Ami et al. 2009; Guttilla et al. 2009; Crist et al. 2009). The RUNX1 transcription factor is essential for the development of lymphoid cells and differentiation of all hematopoietic cell lineages, and mutations in the RUNX1 gene are associated with leukemia (Kuo et al. 2009, Ichikawa et al. 2004; Schnittger et al. 2011; Kuo et al. 2009; Grossmann et al. 2011). The FOXO1 protein has been shown to play a role in apoptosis, cell cycle progression, proliferation, and muscle cell differentiation (Guttilla et al. 2009; Crist et al. 2009). Therefore, the sponging and degradation of miR-27 by diverse herpesviruses could contribute to virus-induced oncogenesis or cause pathogenesis by aiding viral propagation. In support of this idea, mutant mCMV unable to target miR-27 were attenuated in a mouse model of infection and significantly fewer viruses were detected in lungs, spleen, and salivary glands compared to wild-type virus infections (Marcinowski et al. 2012). Therefore, viral interferance with normal miRNA-mediated decay processes can contribute to pathology.

We recently demonstrated that the sequestration of HuR by Sindbis virus RNA leads to changes in mRNA stability, polyadenylation, and splicing (Barnhart et al. 2013). Not only is HuR required for robust viral proliferation as the RNAs are stabilized by their interaction with HuR (Sokoloski et al. 2010), but the sponging of HuR in the cytoplasm of infected cells may also contribute indirectly to virus-induced pathology by altering host gene expression. The HuR protein is known to interact with a wide array of cellular transcripts in different cell types and stabilizes mRNAs (Lebedeva et al. 2011; Mukherjee et al. 2011; Peng et al. 1998). HuR associates with both intronic and exonic regions of transcripts in HeLa cells and can mediate alternative splicing (Lebedeva et al. 2011; Mukherjee et al. 2011). Furthermore, Mukherjee et al. (2011) showed that transcripts that bound to HuR in intronic sequences were also more stable, indicating that HuR couples pre-mRNA processing events with stabilization of the mature transcript, possibly by loading onto the mRNA in the nucleus. Mammalian Hu proteins regulate alternative splicing, as they bind U-rich transcripts and block the polyadenylation machinery

from recognizing upstream alternative polyadenylation signals (Zhu et al. 2007). Intriguingly, global analyses of HuR and AGO2 associated transcripts showed that HuR may compete with AGO2 to relieve miRNA-mediated gene silencing (Mukherjee et al. 2011), and it was later determined that HuR can cause the miRISC to dissociate from target transcripts (Kundu et al. 2012).

Many studies have sought to characterize the RNAs that HuR associates with in a variety of cell types using several different experimental approaches. An analysis by St Laurent et al. (2012) of 4 published datasets containing all detected HuR interacting RNAs (St Laurent et al. 2012; Kishore et al. 2011; Mukherjee et al. 2011; Lebedeva et al. 2011) determined that 1,156 RNAs were represented in all 4 datasets that were compared, and 3,508 RNAs were represented in 3 out of 4 datasets. These results indicate that HuR contributes to the post-transcriptional regulation of many cellular transcripts, and sequestration of HuR on viral RNAs could have dramatic consequences for the cellular response to viral infection. Indeed, it may be that the sponging of HuR in the cytoplasm on viral RNAs could be one mechanism by which alphaviruses shut down host gene expression during infection. Surprisingly, HuR was shown to play a role in the post-translational regulation of the pro-inflammatory factor NFkB (Rhee et al. 2010). This study showed that depletion of HuR by siRNA treatment in human embryonic vascular endothelial cells reduced monocyte binding, induction of ICAM-1 and VCAM-1 expression, and NFkB phosphorylation upon two different pro-inflammatory stimuli (Rhee et al. 2010). The authors determined that rather than altering mRNA stability, HuR regulated the phosphorylation state of the constitutively expressed inhibitors of NFkB, IκBα and IKKα/β, leading to NFkB activation and subsequent increased transcription of pro-inflammatory factors including VCAM-1 (Rhee et al. 2010). However, HuR is also known to be important for mediating proper immune responses by stabilizing AU-rich element containing transcripts (Fan and Steitz 1998). In a cell culture model of T cell activation, HuR was shown to relocalize from the nucleus into the cytoplasm where it stabilizes the short-lived transcripts of potent pro-

inflammatory cytokines, including TNF-α and interferon-γ (Wang et al. 2006). Therefore there are a variety of interesting defects in post-transcriptional regulatory mechanisms that may arise due to the sponging of HuR on high affinity binding sites in alphavirus RNAs that could contribute to virus evasion of immune mechanisms or potentially immunopathogenesis.

Inactivation of cellular RNA decay factors

As described above, poliovirus causes the rapid depletion of XRN1, DCP1, DCP2 and a PAN deadenylase through the activity of a viral protease or by targeting these proteins for decay by the proteasome (Dougherty et al. 2011). Because the 5'-3' decay pathway is important for turnover of cellular mRNAs, reducing the abundance of XRN1 and the decapping enzymes likely has major effects on host gene expression. XRN1 is important for proper organismic development and growth (Grima et al. 2008; Till et al. 1998; Jones et al. 2013; Szankasi et al. 1996; Larimer and Stevens 1990; Larimer et al. 1992). Furthermore, mutations in XRN1 have been associated with osteosarcoma in humans (Zhang et al. 2002; Kruzelock et al. 1997). Therefore the selective depletion of cellular decay factors could contribute to virus-induced defects in development, growth, and/or cell differentiation.

Picornaviruses are also known to induce the proteolytic decay of AUF1. Interestingly, AUF1 has been shown to participate in the degradation of AU-rich element containing mRNAs including those encoding cytokines and oncogenes (Laroia et al. 1999). It would therefore be interesting to determine if changes in the post-transcriptional regulation of ARE-containing transcripts results from the degradation of AUF1 by these positive-sense RNA viruses, and if this could play a role in virus-induced pathology.

Subgenomic flavivirus RNAs are generated by XRN1 and contribute to pathogenesis

Disparate viruses are known to interact with the cellular RNA decay machinery and as a result likely cause dramatic changes in cellular gene expression that could ultimately contribute to pathology. Although there is ample evidence that flavivirus-mediated pathology can derive from changes in host cellular gene expression (as discussed above in Section I), the exact mechanisms by which this occurs remain to be fully characterized. Because some viral RNAs interact with cellular RNA binding proteins (e.g. the SINV 3' UTR) and microRNAs (e.g. mCMV RNAs) that likely contribute to changes in cellular gene expression during infection, we wondered if the flaviviruses might influence post-transcriptional regulatory processes in a similar manner. As discussed above, all members of the *Flavivirus* genus tested to date generate subgenomic RNAs that may be generated by incomplete 5'-3' decay of the viral genome by XRN1 (Pijlman et al. 2008; Silva et al. 2010). Intriguingly, these sfRNAs are required for viral pathogenesis (Pijlman et al. 2008; Liu et al. 2014). Therefore, sfRNA serves as an important point of interaction between the cellular RNA decay machinery and viral gene products.

What is known about how sfRNA is formed in the cell? Two pieces of evidence inducate that sfRNAs are generated as XRN1 stalls on conserved elements in the flavivirus 3' UTR upon processive 5'-3' decay of viral RNAs. First, depletion of XRN1 using siRNAs reduced the abundance of Kunjin virus sfRNA in infected human cells, and second, it was later shown that YFV sfRNA could be generated by incubating a reporter RNA containing the viral 3' UTR with recombinant yeast XRN1 (Pijlman et al. 2008; Silva et al. 2010). However, the XRN1 homologs in yeast and in trypanosomes known to stall on G-tracts and long, highly stable G-C stem-loops in reporter RNAs, but mammalian XRN1 has not been previously documented to stall on such sequence or structural elements (Muhlrad et al. 1994; Li et al. 2006). Mutational analyses of several conserved pseudoknot motifs revealed that they are important for formation of sfRNAs from the YFV and KUNV 3' UTRs (Funk et al. 2010; Silva et al. 2010). However, the exact

mechanism by which these viral RNAs stall XRN1, and whether or not other sequence or structural determinants were necessary for sfRNA formation remains to be determined.

What is the role of sfRNA during viral infection? Intriguingly, these non-coding viral RNAs were shown to be essential for virus-induced pathology in WNV and DENV-2 infections (Pijlman et al. 2008; Liu et al. 2014). Mutant flaviviruses deficient in sfRNA formation display defects in viral growth in certain cell lines; therefore these viral RNAs likely aid viral propagation (Pijlman et al. 2008; Silva et al. 2010). Furthermore, several studies have demonstrated that sfRNA formation is important for viral evasion of innate immune responses in mammalian and insect cells, and DENV sfRNA was recently shown to trigger apoptosis (Schnettler et al. 2012; Schuessler et al. 2012; Chang et al. 2013; Liu et al. 2014; Roby et al. 2014). However, although the pathogenicity and growth of KUNV was partially restored when innate immune modulators were depleted, these observations do not directly implicate sfRNA accumulation in the suppression or evasion of innate immune pathways in mammals. Alternatively, altered cellular gene expression that occurs as a result of sfRNA accumulation could enhance viral growth and/or indirectly suppress innate immune pathways. Furthermore, sfRNA may play a role in allowing arthropod-borne flaviviruses to evade the anti-viral RNA interference response, as sfRNA has been shown to moderately suppress RNA interference activity in mosquito and non-human primate cells (Schnettler et al. 2012). Arthropods rely on this small RNA-mediated decay pathway for antiviral immunity, and many viruses are known to suppress RNAi to enhance their propagation (Nayak et al. 2010; van Mierlo et al. 2012; Blair 2011). Considering that many RNA viruses successfully interface with the cellular RNA decay machinery by suppressing or evading decay factors, flaviviruses likely also interfere with RNA decay in the cell to suppress these activities. The following studies aimed to determine if sfRNA formation might allow flaviviruses to evade or otherwise successfully interact with the normal RNA decay machinery, thereby contributing to the dys-regulation of cellular gene expression.

RATIONALE

As discussed above, viruses in the *Flaviviridae* replicate exclusively in the cytoplasm of the host cell (Lindenbach and Rice 2001). Importantly, the cytoplasm of eukaryotic cells contains constitutively expressed ribonucleases (e.g. XRN1) that participate in quality control pathways, normal turnover of cellular transcripts and in targeting invading viral transcripts for destruction. Flaviviral RNAs interact with cellular RNA decay enzymes (e.g. XRN1, RNAse L) and other factors known to play important roles in post-transcriptional processes (e.g. HuR, PCBP2, miR-122) but little is known regarding how these interactions might promote viral RNA stabilization and/or interfere with normal cellular gene expression, leading to virus induced pathology. Furthermore, although the importance of sfRNA to viral pathogenesis is clear (Pijlman et al. 2008; Liu et al. 2014), the mechanism by which sfRNA benefits the virus and/or impairs the host response is unknown.

Hypotheses

The studies described herein test the following hypotheses:

(1) In addition to being a key factor in generating sfRNA, the major host exoribonuclease XRN1 is functionally inhibited by sfRNA, contributing to pathogenic changes in cellular gene expression during flavivirus infections.

(2) Other members of the *Flaviviridae* (namely HCV and BVDV) generate XRN1 inhibitory RNAs through a similar mechanism via highly structured RNA elements present in their 5' UTRs, and these also contribute to virus-induced changes in cellular gene expression.

(3) The subgenomic flavivirus RNA suppresses RNAi by associating with the cellular nuclease AGO2.

MATERIALS AND METHODS

Cell culture

All mammalian cells were cultured at 37°C and mosquito cells were grown at 28°C. All cells were maintained in 5% CO_2 and media was routinely supplemented with 1% streptomycin and penicillin (Fisher Scientific-Hyclone). Human embryonic kidney 293T cells were maintained in Dulbecco's Modified Eagle's medium (DMEM; Mediatech) with 10% fetal bovine serum (FBS; Atlas Biologicals) and were a gift of the laboratory of Dr. Chaoping Chen at Colorado State University. Madin-Darby bovine kidney (MDBK) cells (*Bos taurus*) from ATCC (CCL-22) were cultured in Modified Eagle's medium (MEM; Corning) with 10% donor equine serum (Hyclone) to prevent potential contamination with non-cytopathic BVDV that could be present in FBS stocks (Xia et al. 2011). The *Macaca mulatta* kidney epithelial cell line (LLC-MK2; a gift from the CSU Arthropod-borne Infectious Diseases Laboratories) and the baby hamster kidney cell line BHK-21 (ATCC CCL-10; *Mesocricetus auratus*) were maintained in MEM plus 10% FBS. Vero cells (*Cercopithecus aethiops*) were cultured in DMEM plus 5% FBS and *Aedes albopictus* C6/36 cells were grown in MEM plus 5% FBS (both cell lines were a gift of the Bowen laboratory at Colorado State University). All mammalian cells were split before cultures reached confluency by washing monolayers once with ice-cold phosphate buffered saline (PBS; Corning), incubating at 37°C with 0.25% trypsin solution (Fisher Scientific-Hyclone) until cells detached and ~1/10 of each culture re-seeded for passaging. Mosquito cells were passaged by scraping only. All cells were routinely screened for *Mycoplasma* contamination using the Universal *Mycoplasma* PCR-based detection kit (ATCC 30-1012K) and DAPI staining for extra-nuclear DNA detection by immunofluorescence microscopy to confirm PCR results. MDBK cells were screened frequently for non-cytopathic BVDV by RT-PCR (Ridpath et al. 1994) and by using

immunofluorescence microscopy with a monoclonal antibody that recognizes both cytopathic and non-cytopathic BVDV antigens (Veterinary Medical Research and Development, 3.12F1).

Virus production

Lentiviruses

Lentiviruses were generated with the pLKO.1 plasmid or one that produces an shRNA that targets XRN1 mRNA (Sigma Aldrich, TRCN0000049677) were generated as follows (described in Stewart et al. 2003). Equal amounts (10 μg) of each plasmid pCMVRΔ8.2, pVSV-G, and TRCN0000049677 (i.e. XRN1 shRNA containing pLK0.1) or pLK0.1 (vector only control) were added to 1 mL of calcium chloride solution (0.3 M) and mixed gently. One mL of 2x HBS buffer (10 mM D-glucose, 10 mM potassium chloride, 40 mM HEPES, 1.5 mM dibasic sodium phosphate, 270 mM sodium chloride, pH 7.1) was then added to the calcium chloride solution. This solution was then used to transfect a 50% confluent monolayer of 293T cells in a T-75 flask in 5 mL of maintenance medium (MEM with 10% FBS). Medium was replaced with fresh maintenance medium containing 60 μL of 5% butyric acid in PBS the following morning. Lentivirus was collected 48 hours later by centrifuging the medium to clarify at 1000xg for 10 minutes in a tabletop centrifuge at 4° C and immediately frozen in 1 mL aliquots at -80° C. Each aliquot was used once and discarded to avoid loss of lentivirus integrity due to repeated freeze-thaw cycles. Transductions of 293T cells were performed by rinsing a 75% confluent monolayer in a T-75 flask once with ice-cold PBS and adding 1 mL of lentivirus stock plus 3 mL fresh growth medium containing 5 μg/mL polybrene. The cells were incubated for 1-2 hours and rinsed once with PBS, then overlaid with fresh maintenance medium. The next day, the medium was replaced. On the third day post-transduction, the cells were fed with maintenance medium containing 5 μg/mL puromycin to select for cells expressing the puromycin resistance gene.

Puromycin-resistant cell pools were maintained in medium containing 1 μg/mL puromycin. XRN1 expression levels were determined by RT-qPCR using the primers reported in Table 3.

Flaviviruses

Dengue virus type 2 strain Jamaica 1409 (GenBank M20558.1; received from Dr. Irma Sanchez-Vargas at Colorado State University) was amplified by seeding T-25 flasks of C6/36 cells with a low multiplicity of infection (MOI) of a low passage virus stock (<4 passages) and incubated for 10 days in maintenance medium. Virus was harvested by scraping cells and clarified by centrifugation for 10 minutes at 1000xg at 4°C in a tabletop centrifuge. Viral stock-containing supernatants were adjusted to 20% FBS and 1 mL aliquots were immediately frozen at -80°C and were used once and discarded to avoid loss due to repeated freeze-thaw cycles. Viral stocks were titered by making ten-fold serial dilutions in cold DMEM with 10% FBS and plating 0.5 mL of each dilution per well of confluent monolayers of LLC-MK2 cells in 12 well plates. The virus was allowed to adsorb for 2 hours at 37°C in the incubator and then cultures were overlaid with a solution containing 2% methylcellulose in 0.5x MEM growth medium in PBS and allowed to incubate for 14 days at 37°C. Virus was inactivated by addition of 7% formaldehyde (v/v in PBS) and incubation at room temperature for 2 hours. The viscous overlay was removed by pipetting and monolayers were washed gently with cold water. Crystal violet stain (2% crystal violet in 80% methanol) was added to each monolayer for 10 minutes then rinsed multiple times with cold water to visualize plaques.

Kunjin virus (KUNV) strain FLSDX (GenBank AY274504.1; a gift from the Khromykh laboratory but initial stocks were grown by the Bowen laboratory) and the mutant KUNV IRAΔCS3 (described in Pijlman et al. 2008) were amplified on Vero or BHK-21 cells. At four days post infection (or when cytopathic effect was evident) virus was collected as described

above. The concentration of virus stocks was determined by plaque titrations on BHK-21 or Vero cells as described above, except that plates were incubated for 5 days.

For BVDV propagation, we first received an aliquot of cytopathic bovine viral diarrhea virus, Singer strain type 1a (GenBank DQ088995.2) from Dr. Hana van Campen (Colorado State University) and virus was amplified on MDBK cells. BVDV was collected at 3 days post infection, medium was clarified by centrifugation, and aliquots were frozen at -80°C. Virus was titered on MDBK cells for 8-10 days until plaques were visible as described above.

Viral infections

Possession of all viral stocks and basic uses thereof was approved by the CSU Biosafety Office. Viral infections were performed as follows. Sub-confluent 293T cells (flavivirus infections) or MDBK cells (BVDV infections) were infected at an MOI of 1 or higher as indicated for each experiment. Virus was adsorbed for 2 or more hours and washed twice with warm (37^{o}C) maintenance medium to remove residual viral particles. Cells were collected 24, 36, 48, or 96 hours later as indicated for analyses. Mock infected cells were also washed twice with warm maintenance medium. Hepatitis C virus infections (JFH-1 strain or using a replicon) were performed by Dr. Shelton Bradrick at Duke University and samples were collected for RNA isolation at 72 hours post infection.

Kunjin virus mutagenesis and analysis of small RNAs from the viral 3' UTR

Mutant Kunjin viruses predicted (by Chapman and Kieft, UC-Denver, personal communication and described in Chapman et al. 2014) to have defective sfRNA formation during infection were generated by overlap extension PCR. The FLSDXpro_HDVr Kunjin virus infectious clone (from the Khromykh laboratory; Liu et al. 2003) was used as a template for the construction of six individual mutant viruses. The high fidelity Phusion Hot Start II polymerase

(Thermo Scientific) was used for PCR using the mutagenic primers listed in Table 1 and assembled PCR products were inserted into the Age1 and Xho1 restriction sites. Plasmids were screened for the proper mutations by sequencing PCR amplicons or maxiprepped clones using the following primers: FLSDX Fw: 5'- ACTTTGTTAATTGTAAATAAATATTGTTAT; FLSDX Rv: 5'-GCGTGGGACGTTGATTCGCCTTTGT. Plasmids were linearized with Xho1 and *in vitro* transcriptions performed using the MEGAscript® SP6 transcription kit (Life Technologies) followed by Turbo DNase treatment to remove template. Viral RNAs were purified by phenol-chloroform-isoamyl alcohol (25:24:1) extraction and ethanol precipitation before RNA concentrations were determined. BHK-21 cells (one 90% confluent T-75 flask per virus) were electroporated with 5-10 µg of viral RNA, and virus was amplified by passaging once on BHK-21 cells to generate working stocks. Viral titers were assessed by plaque titrations, infections were performed in 293T cells (MOI of 10), and total cellular RNA was collected at 48 hpi using TRIzol™ (Invitrogen). Total RNA was treated with DNase I (Fermentas) to remove residual genomic DNA. Northern blotting was performed as described below using 2 µg of total RNA from each sample and sfRNAs detected by using a probe complementary to the entire KUNV 3' UTR.

Table 1. Mutagenic primers used for the construction of six KUNV mutants predicted to be defective in sfRNA formation.

Mutation/primer set	Forward	Reverse
Flanking primers	CATACCGGTCGGAAAAGTGATCGACCTTGG	CATCTCGAGCAATTGTTGTTGTTAACTTG
UCA10498	AGTGAGGATCACAGGCCGG	CCGGCCTGTGATCCTCACT
G10519	TTCCCGGCACCGGAAGTTGAG	CTCAACTTCCGGTGCCGGGAA
G10680	TGGCGTGGCACTCTGCGGAG	CTCCGCAGAGTGCCACGCCA
ACA10658	CAAGGCCCAAACACAGACCACG	CGTGGTCTGTGTTTGGGCCTTG

Plasmids

For mammalian transfections, the peGFP-N1 plasmid (Clontech; GenBank U55762.1) was used as a reporter plasmid. The DENV-2 3' UTR (Jamaica 1409, 10273-10723) was amplified by RT-PCR from infected cell RNA and cloned into the Not1 site of the 3' UTR of

eGFP. For *in vitro* transcription templates, viral sequences were inserted into the pGEM-4 (GenBank X65303.1) multiple cloning site to permit either SP6 or T7 transcription to generate reporter RNAs, competitor RNAs, or internally labeled riboprobes. The first stem-loop of the DENV-2 3' UTR was cloned into pGEM-4 in the XbaI and HindIII sites and was used as a reporter RNA for *in vitro* XRN1 decay assays (by John Anderson). For the DENV-2 competitor RNA, the 5' half of the viral 3' UTR was inserted into the XbaI and HindIII sites of pGEM-4 (by John Anderson). The HCV IRES element (nucleotides 1-389; Strain H77, GenBank AF009606.1) was cloned into pGEM-4 using the HCV16LUC plasmid (Bradrick et al. 2006) as a PCR template and inserted into the EcoRI and XbaI sites. The BVDV IRES element (nucleotides 1-440; GenBank DQ088995.2) was cloned into the EcoRI and HindIII sites of pGEM-4 using RNA from infected MDBK cells as RT-PCR template to amplify the BVDV insert. The first 200 nucleotides of the JEV 3' UTR (isolate TC2009-1 GenBank JF499790.1, nucleotides 10395-10965) was cloned by assembly PCR into pGEM-4 in the HindIII and EcoRI sites (by Benjamin Dodd). All sequences are reported in Table 2. The probe template for sfRNA-like decay intermediates from the peGFP-N1 plasmid containing the DENV-2 3' UTR was generated by cloning the 3' UTR of eGFP into the EcoRI and HindIII restriction sites of pGEM-4. All plasmids were verified by sequencing before use.

Table 2. Sequences inserted into the pGEM-4 or peGFP-N1 vectors for this study.

Insert	Sequence (5'-3')
DENV-2 SL-1	AAGAAGUCAGGCCAUCACAAAUGCCACAGCUUGAGUAAACUGUGCAGCCUGUAGCUCCACC
DENV-2 5' half of the 3' UTR	AAGGCAAAACUAACAUGAAACAAGGCUAAAAGUCAGGUCGGAUCAAGCCAUAGUACGGAAAAAA CUAUGCUACCUGUGAGCCCCGUCCAAGGACGUUAAAAGAAGUCAGGCCAUCACAAAUGC CACAGCUUGAGUAAACUGUGCAGCCUGUAGCUCCACCUGAGAAGGUGUAAAAAAUCUGGGA GGCCACAAACCAUGGAAGCUGUACGCAUGGCGUAG
DENV-2 3' UTR	AAGGCAAAACTAACATGAAACAAGGCTAAAAGTCAGGTCGGATCAAGCCATAGTACGGAAAAAA CTATGCTACCTGTGAGCCCCGTCCAAGGACGTTAAAAGAAGTCAGGCCATCACAAATGCCACAG CTTGAGTAAACTGTGCAGCCTGTAGCTCCACCTGAGAAGGTGTAAAAAATCTGGGAGGCCACAA ACCATGGAAGCTGTACGCATGGCGTAGTGGACTAGCGGTTAGAGGAGACCCCTCCCTTACAAAT CGCAGCAACAACGGGGGCCCAAGGTGAGATGAAGCTGTAGTCTCACTGGAAGGACTAGAGGTT AGAGGAGACCCCCCCAAAACAAAAAACAGCATATTGACGCTGGGAAAGACCAGAGATCCTGCTG TCTCCTCAGCATCATTCCAGGCACAGAACGCCAGAAAATGAATGGTGCTGTTGAATCAACAGGTTC T
JEV 5' end of 3' UTR	GACAGGATAAAGTCATGTGTGTAATGTGAGATAAGAAAATGTGCATGTGGAGTCAGGCCAGCAAC AGCTGCCACCGGATACTGAGTAGACGGTGCTGCCTGCGCCTCAGTCCCAGGAGGACTGGGTTAA CAAATCTGACAACGGAAGGTGGGAAAGCCCTCAGAACCGTCTCGGAAGCAGGTCCCTGCTCACC GGAAGTT
HCV IRES element	GCCAGCCCCCTGATGGGGGCGACACTCCACCATGAATCACTCCCCTGTGAGGAACTACTGTCTT CACGCAGAAAGCGTCTAGCCATGGCGTTAGTATGAGTGTCGTGCAGCCTCCAGGACCCCCCCTC CCGGGAGAGCCATAGTGGTCTGCGGAACCGGTGAGTACACCGGAATTGCCAGGACGACCGGGT CCTTTCTTGGATAAACCCGCTCAATGCCTGGAGATTTGGGCGTGCCCCCGCAAGACTGCTAGCC GAGTAGTGTTGGGTCGCGAAAGGCCTTGTGGTACTGCCTGATAGGGTGCTTGCGAGTGCCCCGG GAGGTCTCGTAGACCGTGCACCATGAGCACGAATCCTAAACCTCAAAGAAAAACCAAACGTAACA CCAAC
BVDV IRES element	ATTCGCCCTTCTCGTATACGTATTGGGGCAATTAAAATAATAATTAGGCCTAGGGAACAAAAGTCC CCCTCAGCGAAGGCCGAAAAGAGGCTAGCCATGCCCTTAGTAGGACTAGCATAAAGAGGGGGGT AGCAGCAGTGGTGAGTTCGTTGGATGGCTTAAGCCCTGAGTACAGGGTAGTCGTCAGTGGTTCG ACGCCTTGGAATAAAGGTCTCGAGATGCCACGTGGACGAGGGCATGCCCAAAGCACATCTTAAC CTGAGCGGGGGTCGCCCAGGTAAAAGCAGTTCTAACCGACTGTTACGGATACAGCCTGATAGGG TGCTGCAGAGGCCCACTGTTCTGCTACTAAAAATCTCTGCTGTACATGGCACATGGAGTTGATCA CAAATGAACTTTTATACAAAACTTACAAACAAAAACCCGTCAGGGTGGAAGAA

Templates for generation of radiolabeled RNA constructs

Templates for *in vitro* transcriptions to generate radiolabeled reporter or competitor RNAs were obtained by linearizing pGEM-4 plasmids containing segments of the DENV-2 or JEV 3' UTR or the HCV or BVDV IRES elements (as described above). To make the control reporter RNA or the DENV-2 sfRNA reporter, the pGEM-4 plasmid with or without the first stem-loop of the DENV-2 3' UTR (respectively) was linearized with Ear1 (Figure 6). In Figure 8, the 5' half of the DENV-2 and the 5' proximal 200 nt of the JEV reporter RNAs were generated by

linearizing the respective plasmids with HindIII. All DENV-2 competitor RNAs were generated by digesting the pGEM-4 plasmid containing the 5' half of the DENV-2 3' UTR with HindIII. For all competition assays, the control competitor template was made by digesting the empty pGEM-4 vector with Sml1, and the reporter RNA was generated by linearizing pGEM-4 with Ear1. The reporter and competitor RNAs containing the HCV or BVDV 5' UTRs were made by digesting the pGEM-4 plasmids containing the HCV or BVDV IRES elements with HindIII.

In vitro transcriptions and *in vitro* XRN1 decay assays

Radiolabeled, capped or monophosphorylated reporter or competitor RNAs were transcribed using SP6 polymerase with linearized pGEM-4 templates as previously described (Wilusz and Shenk 1988) and gel purified. Probes for northern blots were generated using T7 polymerase and EcoRI linearized pGEM-4 derivative templates (described above) and were also gel purified. Radiolabeled RNAs were generated using α ^{32}P-UTP with 10x molar excess 5' GMP or 7meGpppG cap analog to create 5' monophosphorylated (permissive) or 5' capped (non-permissive) substrates for XRN1. About 30 fmol of radioactive RNAs were incubated in mosquito C6/36 or human HeLa cell cytoplasmic extracts (S100, prepared as described in Sokoloski et al. 2008 and Ford et al. 1999, respectively) or with recombinant yeast XRN1 protein (New England Biolabs) and samples were collected at the indicated times by addition to 400 µL HSCB solution. For competition assays, a 30x molar excess of lightly radiolabeled DENV-2 or JEV 3' UTR or 66.7x molar excess of the BVDV or HCV 5' UTR constructs were incubated with ~30 fmol of the reporter RNA. RNAs were purified by phenol chloroform isoamyl alcohol (25:24:1) extraction and ethanol precipitation using tRNA or glycogen as carrier and resolved on 5% denaturing polyacrylamide gels containing 7M urea. Decay products were visualized by phosphorimaging.

Plasmid transfections

All plasmids were amplified in DH5α and purified using the Invitrogen PureLink HiPure plasmid maxiprep kit. Residual endotoxin was removed using the MiraClean endotoxin removal kit (Mirus). Human 293T cells were transfected using Lipofectamine 2000 (Life Technologies) with Opti-MEM1 Reduced Serum Medium according to the manufacturer's instructions. Total RNA from transfected cells was collected using TRIzol™ (Invitrogen).

Immunofluorescence assays

Cells were grown on coverslips or in 8-well chamber slides and at the indicated times post-infection were washed with cold PBS. Coverslips or chamber slides were then incubated with rocking at room temperature under 4% paraformaldehyde in PBS, then methanol, then 70% ethanol to fix and permeabilize cells. Cells were then blocked with 6% bovine serum albumin (Fraction V; Fisher) in PBS for 1 hour at room temperature or 4°C overnight and stained with primary antibody to BVDV (Veterinary Medical Research and Development; bovine viral diarrhea virus types 1 and 2 Mab 3.12F1; 1:100) in 0.6% bovine serum albumin in PBS overnight at 4°C with rocking. Coverslips were washed three times with PBS and incubated with secondary antibody (goat anti-mouse AlexaFluor 594; Life Technologies; 1:2,000) for 1 hour at room temperature, washed 5 times with PBS, and mounted using ProLong Gold with DAPI (Invitrogen). Cells were visualized using an Olympus IX71 inverted microscope and photographed using a digital camera (Q Imaging Retiga 2000R).

Western blots

Protein lysates from MDBK cells infected with BVDV for 24 hours or mock infected were generated by pelleting the cells, washing twice with cold PBS, and resuspending the pellets in RIPA buffer (50 mM Tris-Cl pH 7.5, 0.5% sodium deoxycholate [w/v], 1% NP-40 [v/v], 0.05%

sodium dodecyl sulfate (SDS) [w/v], 150 mM sodium chloride, 1 mM EDTA). Protein concentrations were determined by the Bradford assay (BioRad) and 20 μg (for anti-JUN blots) or 30 μg (for anti-FOS blots) total protein were separated by SDS-PAGE and transferred onto nitrocellulose membranes using a Trans-Blot Semi-dry Transfer cell (BioRad). Membranes were blocked with 5% milk in TBST (10 mM Tris -Cl pH 8, 150 mM sodium chloride, 1% Tween 20) overnight at 4°C or 1 hour at room temperature, and primary antibody (rabbit anti-c-JUN [H-79; Santa Cruz Biotechnology; 1:200]; rabbit anti-c-FOS [H-125; Santa Cruz Biotechnology; 1:1,000]; mouse anti-GAPDH [Millipore; 1:1,000]) was added to the blocking solution and rocked overnight at 4°C. Blots were washed three times with TBST and secondary antibody (goat anti-rabbit IgG HRP conjugate [BioRad; 1:20,000]; goat anti-mouse IgG HRP conjugate [Santa Cruz Biotechnology; 1:20,000]) in 5% milk (in TBST) was added and incubated for 1 hour at room temperature or overnight at 4°C. SuperSignal West Pico chemiluminescent substrate (Thermo Scientific) was used to visualize HRP conjugates using a VersaDoc Imager and ImageLab software (BioRad). Relative band quantification was done by volumetric analysis and c-JUN or c-FOS values were normalized to GAPDH.

Analysis of sfRNA-like decay intermediates by northern blotting

For analysis of intermediates generated from eGFP RNAs containing the DENV-2 3' UTR, 1 μg of total RNA from transfected cells at 48 hpt was analyzed by northern blotting (described below). To determine if treatment of cells transfected with peGFP-N1 +/- the DENV-2 3' UTR with an siRNA to eGFP enhanced the formation of the DENV-2 sfRNA-like decay intermediate, 1 μg of total RNA from cells collected at 24 hpt was analyzed. Decay intermediates generated from eGFP RNAs containing the BVDV or HCV IRES elements were detected at 48 hours post transfection in cells co-transfected with an anti-eGFP siRNA (described below) by northern blotting using 2 μg of total RNA from cells that had been exposed

to actinomycin D for 30 minutes. For flavivirus sfRNA detection, 1 μg of total RNA from cells infected with KUNV (0, 36, and 48 hpi) or DENV-2 (0, 3, and 4 dpi) was analyzed.

For the detection of sfRNA-like decay intermediates from eGFP reporters or sfRNAs from DENV-2 or KUNV infected cells, total cellular RNA (1 or 2 μg as indicated above) was separated on 5% denaturing polyacrylamide gels. To assess eGFP knockdown by northern blot, 5 μg of total RNA from transfected and infected (or mock-infected) cells was resolved on a denaturing agarose gel, and ethidium bromide-stained ribosomal RNA was visualized to ensure equal loading. RNA was then transferred onto a nylon membrane (Hybond-XL; GE Healthcare) by capillary action (agarose gels) or using a tank transfer unit (acrylamide gels). The blots were UV cross-linked before blocking for 30 minutes at 60°C in hybridization solution (50% formamide, 1 mg/mL bovine serum albumin, 750 mM sodium chloride, 75 mM sodium citrate, 0.1 mg/mL salmon sperm DNA, 1% SDS, 1 mg/mL polyvinylpyrrolidone, 1 mg/mL ficoll). *In vitro* transcribed, internally radiolabeled RNA probes (gel purified) complementary to the 3' UTR of either KUNV, DENV-2, or a probe complementary to a region surrounding the siRNA-cleavage site of the eGFP open reading frame were used to detect sfRNAs by probing in hybridization buffer overnight at 60°C. Blots were washed three times with wash solution (300 mM sodium chloride, 0.1% SDS, 30 mM sodium citrate) and three times with stringent wash solution (30 mM sodium chloride, 0.1% SDS, 3 mM sodium citrate) for twenty minutes each at 60°C. Hybridized RNAs were visualized by exposing the blot on storage phosphor screens and imaging on the Typhoon Trio Imager (GE Healthcare).

Analysis of mRNA stability and abundance

To generate mRNA decay curves, 293T cells were either mock infected or infected with DENV-2 (MOI of 1) or KUNV (MOI of 5), or MDBK cells were mock infected or infected with cytopathic BVDV (MOI of 10). At the indicated times post infection (3 or 4 dpi for DENV-2; 36 or

48 hpi for KUNV; 24 hpi for BVDV) the medium was replaced with fresh maintenance medium containing 5 μg/mL of actinomycin D (Sigma) and incubated for 30 minutes before collecting the initial time point by resuspending the cell monolayer in TRIzol™. The pLKO.1 and XRN1 shRNA expressing stable cell pools were analyzed after puromycin selection in the same manner. Analysis of mRNA stability in cells transiently transfected cells expressing the eGFP reporter with or without the DENV-2 3' UTR was done by transcriptional shutoffs at 48 hours post transfection. Following transcription shut-off, RNA was extracted following the manufacturer's protocol and treated with DNase I (Fermentas) to remove any residual genomic DNA. Total RNA from HCV (JFH-1 strain) infected Huh7.5 cells was obtained from Dr. Shelton Bradrick for half-life analysis. Reverse transcription using Improm-II reverse transcriptase (Promega) was performed by first annealing 0.5 or 1 μg of total RNA with random hexamer primers (0.5 μg per reaction in a total volume of 5 μL) at 70ºC for 5 minutes and reaction tubes were immediately placed on ice. Each reaction then received 4 μL reverse transcription buffer (5x), 5.6 μL water, 1 μL dNTPs (10 mM each), 2.4 μL magnesium chloride (25 mM), 1 μL RNase inhibitor, and 1 μL reverse transcriptase. The reactions were then incubated at 25ºC for 5 minutes, 42ºC for 1 hour, and 70ºC for 5 minutes in a thermocycler. The resulting cDNA was then diluted 1:1 with water to yield a total volume of 40 μL.

Quantitative PCR (qPCR) using the CFX96 real time PCR system (Bio-Rad) was then performed using SYBR green supermix. Each 10 μL qPCR reaction was generated by dividing a ~30 μL master mix containing 2.64 μL cDNA solution plus 15 μL SYBR green supermix, 10.2 μL water, and 1.2 μL each primer (at 2.5 μM) into 3 reactions. All qPCR reactions were done using a two-step amplification procedure with an annealing temperature of 60ºC using clear 96 well plates. The abundance of each transcript in each time point indicated was determined relative to *GAPDH* (human cells) or *ACTB* (bovine cells) using the ΔΔCt method and plotted to determine half-life using an exponential decay curve. Primers were designed using the NCBI Primer-

BLAST tool such that the annealing temperature was ~60ºC, the amplicon was ~100-200 nt in length, and all RNA isoforms in GenBank would be amplified (if applicable). Primers used for all qPCR experiments were standardized using ten-fold serial dilutions of plasmid or cDNA and only used if they had 89-110% efficiency (listed in Table 3). The average half-life plus or minus the standard deviation of two independent infections (for DENV-2 and KUNV infections) or three infections (BVDV and HCV) are reported, and Student's t-test was used to determine significance. Error bars indicate standard deviation of each qPCR measurement from a representative decay curve.

Table 3. Primers used for qPCR analyses.

Target	GenBank Accession Number	Organism/Virus	Forward	Reverse	Efficiency (%)
RN7SL1	*NR_002715.1*	*Homo sapiens*	GGAGTTCTGGGCTGTAGTGC	ATCAGCACGGGAGTTTTGAC	89
ACTB	AY141970.1	*Bos taurus*	CTGAGCGCAAGTACTCCGTG	CAGCTAACAGTCCGCCTAGA	92.5
AQP3	DQ083949.1	*Homo sapiens*	ACCAGCTTTTTGTTTCGGGC	GGCTGTGCCTATGAACTGGT	103.7
ARMCX4	NM_001256155.1	*Homo sapiens*	TGCAGTTGGCTGGACTAAGG	GTTTCTCCACTTCCCACCGT	94.2
BVDV	DQ088995.2	Bovine viral diarrhea virus (Singer)	ACCTGTGAGCGGGATCTACT	TCTTCAAAGAGCTCCAGCGG	92.7
CCL2	NM_002982.3	*Homo sapiens*	TGAAGCTCGCACTCTCGCCT	TGAGCGAGCCCTTGGGGAATGA	105.9
CLTC	NM_004859.3	*Homo sapiens*	CCTTGCAGGGTGCCAGATTA	ACCACACGATTTTGCTGTGC	100.1
CTNNB1	NM_001904.3	*Homo sapiens*	GCTGGGACCTTGCATAACCT	CCAAGCATTTTCACCAGGGC	101.6
CXCL11	NM_005409.4	*Homo sapiens*	CATGAGTGTGAAGGGCATGGCT	CCAGGGCCTATGCAAAGACAGCG	100.5
CXCL2	NM_002089.3	*Homo sapiens*	AGGGGTTCGCCGTTCTCGGA	ATGGGGCTCAGCAGGCGGTT	94
DENV 3' UTR	M20558.1	Dengue virus type 2 (Jamaica 1409)	AGGCCATCACAAATGCCACAGC	ACGCCATGCGTACAGCTTCCA	96.2
DENV ORF	M20558.1	Dengue virus type 2 (Jamaica 1409)	GTGCGTGTGCAAAGACCAACACC	AAGGCCATAGGTGCCGACTTGC	95.8
eGFP	U55762.1	N/A	GACGGCGACGTAAACGGCCA	CAGCTTGCCGGTGGTGCAGA	91.5
FOS	V01512.1	*Homo sapiens*	GTGGGAATGAAGTTGGCACT	CTACCACTCACCCGCAGACT	95.8
FOS	AY322482.1	*Bos taurus*	GCAAAACGCATGGAGTGTGT	AAAAGAGACGCAGACCCAGG	103.2
GAPDH	NM_002046.5	*Homo sapiens*	TCTTTTGCGTCGCCAGCCGA	ACCAGGCGCCCAATACGACC	94.9
HIF1A	NM_001530.3	*Homo sapiens*	GCGCGAACGACAAGAAA	GAAGTGGCAACTGATGAGCA	109.7
IL6	NM_000600.3	*Homo sapiens*	TCGAGCCCACCGGGAACGAA	GCAACTGGACCGAAGGCGCT	101
JUN	NM_001077827.1	*Bos taurus*	ACGACCTTCTACGACGATGC	GCCAGATTCAGGGTCATGCT	106.4
JUN	NM_002228.3	*Homo sapiens*	GCCAGGTCGGCAGTATA	TCTGGACACTCCCGAAAC	91.7

			GTC	AC	
KUNV 3' UTR	AY274504.1	Kunjin virus (FLSDX)	GGAGACCCCGTGCCGCAAAA	CACTGTGCCGTGTGGCTGGT	93.1
KUNV ORF	AY274504.1	Kunjin virus (FLSDX)	TGGACGGGGAATACCGACTTAGAGG	ACCCCAGCTGCTGCCACCTT	95
MOSPD2	NM_152581.3	*Homo sapiens*	CCACGGTTCCTTCGTCCATT	TGTATGTGTTCCCCTCCACG	103.3
MYC	NM_002467.4	*Homo sapiens*	TGTCAAGAGGCGAACACACA	ACCTTGGGGGCCTTTTCATT	90
OASL	NM_003733.3	*Homo sapiens*	TCCTTCAGCGAGCTGCAGAGAAAT	CCGGATCCAGGATGATGGGCCT	98.1
pGEM-4	X65303.1	N/A	GAATACACGGAATTCGAGCTCGGTA	TCATTAATGCAGCTGGCTTATCGAA	100.4
TUT1	NM_022830.2	*Homo sapiens*	AGGCAGCCCAAGAATGGTC	GCCACCACTCAGTCCTTTCA	98.6
VEGFA	NM_001171623.1	*Homo sapiens*	AGGAGGAGGGCAGAATCATCAC	ATGTCCACCAGGGTCTCGATTG	94
XRN1	NM_019001.4	*Homo sapiens*	GCGGCACCTGCCATCTTCTGA	GAACTGTCAGCTTGCTGTGCTCAA	106

For all mRNA abundance experiments, the average, plus or minus the standard deviation of three infections are reported. RNA from Kunjin virus infected 293T cells (MOI of 5) was analyzed at 48 hpi for *CXCL11*, *OASL*, *IL6*, and *CCL2* abundances. HCV (72 hpi) infected (or HCV replicon-expressing) purified cellular RNA was obtained from Dr. Shelton Bradrick. To determine the relative abundances of transcripts previously shown to be up-regulated upon AGO2 and/or DICER knockdown (Schmitter et al. 2006), human 293T cells were infected with KUNV (MOI of 10) or DENV-2 (MOI of 3) and RNA was collected at 60 hpi or 4 dpi (respectively). For transcript abundances in BVDV infections, MDBK cells were infected at a multiplicity of infection of 10 and RNA was collected at 24 hpi.

Global analysis of RNA stability by RNA-seq

To determine if XRN1 suppression by sfRNA was correlated with stabilization of host mRNAs in general, we performed global analyses of RNA stability using RNA-seq. Another positive-sense ssRNA arthropod-borne virus, SINV, was used as a control for these studies and was previously shown to alter cellular mRNA stability by sequestering the cellular HuR protein (Barnhart et al. 2013). Human 293T cells were mock infected or infected with SINV (strain MRE16; MOI of 10) or the Kunjin viruses (MOI of 5) in triplicate cultures. Cells were treated with

actinomycin D (5 μg/mL) for transcriptional shutoff at 24 hpi (Sindbis virus) or 48 hpi (KUNV or IRAΔCS3 KUNV). Four time points were collected: 0 (30 minutes post addition of actinomycin D), 0.5 hours, 1.5 hours, and 3 hours post shut-off. RNA was extracted from cell monolayers using TRIzol™ (Invitrogen) and 5 μg of total RNA were sent to Rutgers University- New Jersey Medical School for library preparation and bioinformatics analysis by Drs. Bin Tian, Mainul Hoque, and Liu Liang. The purity and quality of all RNA samples was verified using a Bioanalyzer (Agilent) before pooling each triplicate sample and processing. Relative RNA abundances were gleaned from the 0 time point. For mRNA abundance comparisons, only transcripts that were detected in both conditions (RPKM >0.01) were analyzed. Gene Ontology analyses were done using DAVID and functional annotation of transcripts was done using the GOTERM_BP_FAT tool (Huang et al. 2009(a), Huang et al. 2009(b)).

Global analysis of mRNA abundances by microarray

All microarray sample preparation and bioinformatic analyses were performed by Dr. Alexander Khromykh (University of Queensland, Brisbane, Australia), Dr. Yutaro Kumagai and Dr. Shizuo Akira (both at Osaka University, Suita, Osaka, Japan). Interferon-α receptor knock-out mouse embryonic fibroblasts (IFNAR-/- MEF) were infected with either the sfRNA-deficient mutant IRAΔCS3 KUNV or the wild-type KUNV (FLSDX) at an MOI of 1 (described in Pijlman et al. 2008). Total RNA was collected from the cell monolayers at 48 hpi using TRIzol™ (Invitrogen), purified using an RNeasy Mini kit (Qiagen) and cDNA libraries were generated with the WT-Ovation RNA Amplification System and Encore Biotin Module (Nugen). Mouse 430 2.0 Arrays (Affymetrix) were hybridized with the cDNA library and processed according to the manufacturer's recommendations. For analysis, robust multiarray analyses values were generated and genes with a 3-fold or higher difference after transforming to yield a mean value of 0 with standard deviation of 1 underwent hierarchical clustering according to Akaike's

information criteria to generate six clusters. The programs R and Bioconductor were used for all calculations.

Fractionation of capped and uncapped mRNAs

To determine the relative amount of uncapped transcripts in infected cells, RNA was extracted from cells at 4 dpi (DENV-2), 2 dpi (KUNV) or 3 dpi (HCV JFH-1 strain or from Huh7.5 cells expressing an HCV replicon from Dr. Shelton Bradrick) using TRIzol™ and 5 μg was fractionated by immunoprecipitation using an antibody to the m^3G and m^7G cap structure (Synaptic Systems) using the manufacturer's protocol with sepharose G beads. RNA was isolated from 10% of the input, the unbound supernatant fraction, and the immunoprecipitated fraction. RNA from all fractions was reverse transcribed for the analysis of mRNA stability as described above. qPCR was done to detect the relative abundance of two short-lived transcripts *FOS* and *TUT1*, using the uncapped *7SL* RNA as a reference gene to account for differences in fractionation efficiencies. For DENV-2 and KUNV infections, a representative graph depicting *FOS* and *TUT1* mRNA abundance in the supernatant fraction normalized to the 10% input is shown. For HCV infections and HCV replicon expressing cells, the average amount of *FOS* and *TUT1* relative to *7SL* in the supernatant fraction normalized to the 10% input is reported plus or minus standard deviation of values from three independent infections. The relative abundances of capped and polyadenylated mRNAs were determined by performing reverse transcriptions using equal volumes of immunoprecipitated (capped) RNA and oligo-d(T) primer. The ΔΔCt method was used to normalize each transcript to *GAPDH* using the primers reported in Table 3.

Co-immunoprecipitation of XRN1, AGO2, or DICER and viral RNAs

Human 293T cells were infected with KUNV (MOI of 5, 2 dpi) or DENV-2 (MOI of 1, 4 dpi), or MDBK cells were infected with BVDV (MOI of 10, 1 dpi). XRN1-RNA co-

immunoprecipitations from BVDV infected cells were performed as described in (Niranjanakumari et al. 2002) using the commercially available XRN1 C-1 antibody (Santa Cruz Biotechnology). For other immunoprecipitations, cells were washed three times with ice-cold PBS, overlaid with 1% formaldehyde (in PBS) to capture protein-RNA interactions, and rocked at room temperature for 15 minutes. To quench the reaction, glycine was added to a concentration of 0.25 M and cells were again rinsed with cold PBS three times. Cells were scraped into 500 μL of cold RIPA buffer plus 1 μL of RiboLock RNase Inhibitor (Fermentas) and frozen at -80°C. Samples were then thawed on ice, sonicated to lyse cells and were then centrifuged to clarify. To immunoprecipitate XRN1-RNA complexes, 10% of the input was saved at -80°C and lysate was incubated with either 2 μL of XRN1 antibody (a gift from Dr. Jens Lykke-Andersen, UCSD), 20μL of rabbit anti-DICER (Santa Cruz Biotechnology; clone H-212; sc-30226), 12 μL of rat anti-AGO2 (Millipore; clone 11A9; MABE253) or an equal amount of normal rabbit (Santa Cruz Biotechnology; sc-2027) or mouse (Santa Cruz Biotechnology; sc-2025) IgG plus 1 μL of RNase Inhibitor (Fermentas) for 1 hour, rotating at 4°C. Rehydrated Pansorbin Staph A-positive cells (Calbiochem) (or protein G sepharose 4 fast flow (GE Healthcare) for AGO2 immunoprecipitations) were then added to the lysates and rotated for 15 minutes at 4° C. Pansorbin cells were pelleted and resuspended in RIPA buffer containing 1 M urea and washed five times with vigorous intermittent vortexing. Pellets were resuspended finally in TEDS buffer (50 mM Tris-Cl pH 7.0, 5 mM EDTA, 1% SDS and 10 mM DTT). All samples (including the 10% input) were then incubated at 70° C with shaking for 45 minutes to reverse cross-links. Pansorbin was pelleted and RNA was isolated from supernatants using TRIzol™ and glycogen as a carrier. Any residual genomic DNA was removed by treating with DNase I (Fermentas), and an equal volume of RNA from each fraction was reverse transcribed with Improm-II reverse transcriptase as described above. Either semi-quantitative PCR using GoTaq Flexi polymerase (Promega) or quantitative real time PCR (SYBR green, as above) was

performed with primers to the DENV-2 3' UTR or open reading frame, the KUNV 3' UTR or open reading frame, or the BVDV 5' UTR (see Table 3 for sequence information). For qPCR quantification, the abundance of viral 3'UTR was compared to the abundance of viral open reading frame sequences and both were normalized to the 10% input fraction. For semi-quantitative PCR, products were resolved on a 2% agarose gel and stained with ethidium bromide.

eGFP knockdowns for RNA interference analysis

Human 293T cells were mock infected or infected with KUNV (MOI of 10) or DENV-2 (MOI of 3) and at 24 hpi (KUNV-2) or 3 dpi (DENV-2) cells were transfected with 1 μg of peGFP-N1 plasmid with an siRNA to eGFP (5'-GCAAGCUGACCCUGAAGUUCAU) or an equal volume of water. After 24 hours, cell monolayers were dissolved in TRIzol™ and RNA was extracted according to the manufacturer's protocol. Residual plasmid DNA was removed by digesting with *DpnI* and/or *EcoRI* (New England Biolabs) in the presence of RNase Inhibitor (Fermentas) followed by Turbo DNase treatment (Life Technologies) as done by Lee et al. (2012b). The abundance of eGFP mRNA in each sample was determined by northern blotting using 5 μg of total RNA and quantified using RT-qPCR as above using the primers to the eGFP open reading frame spanning the siRNA cleavage site, indicated in Table 3. To measure the relative amount of eGFP knockdown in each condition by RT-qPCR, eGFP abundance in the siRNA treated samples was determined relative to the eGFP plus water control, and *GAPDH* was used as a reference gene. A representative northern blot is shown from each infection and the average +/- the standard deviation of RT-qPCR measurements from two independent transfections per condition is reported.

Section I. Modulation of cellular mRNA stability by a non-coding flavivirus RNA

Dengue virus type 2 sfRNA is generated by XRN1-mediated decay

Previous studies implicated XRN1 in the formation of sfRNA by demonstrating that XRN1-depleted cells infected with KUNV or YFV generated less sfRNA than wild-type cells (Pijlman et al. 2008; Silva et al. 2010). Furthermore, incubation of RNAs containing the YFV 3' UTR with recombinant yeast XRN1 caused an sfRNA-like decay intermediate to form *in vitro* (Silva et al. 2010). We sought to expand these findings to determine if DENV-2 sfRNA formation by XRN1 was recapitulated in mammalian and mosquito systems. Because XRN1 specidically degrades monophosphorylated RNAs, we used 5' monophosphorylated radiolabeled reporter RNAs containing either a control sequence or the DENV-2 3' UTR to assess sfRNA formation in cytoplasmic extracts under conditions that favored 5'-3' decay by XRN1. Reactions using recombinant yeast XRN1 were also performed to generalize the findings reported in Silva et al. (2010) for YFV and determine if other cellular factors were required for sfRNA formation.

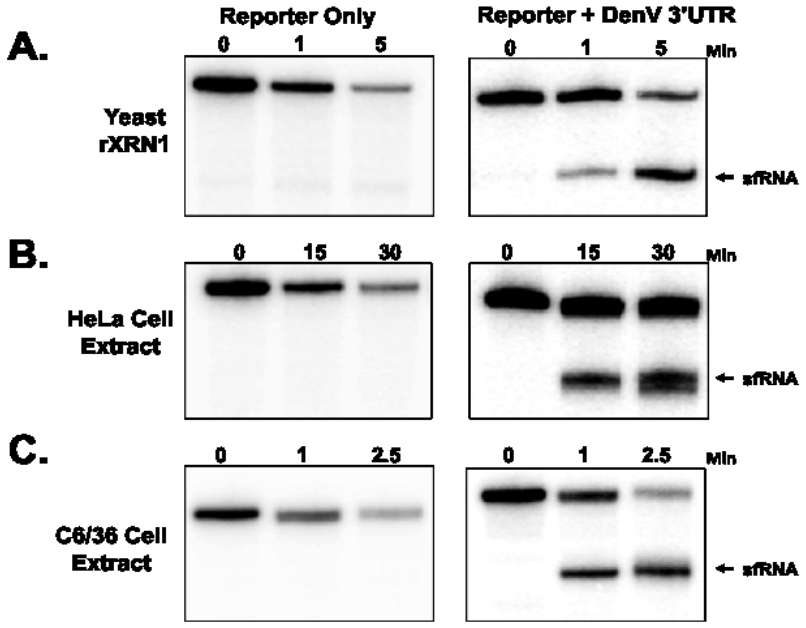

Figure 6. Dengue virus type 2 sfRNA is formed as XRN1 stalls on the viral 3' UTR. 5' monophosphorylated, radiolabeled reporter RNAs containing either the pGEM-4 plasmid control sequence (Reporter Only) or the dengue virus type 2 3' UTR (Reporter + DenV 3' UTR) were incubated with (A) recombinant yeast XRN1 enzyme, (B) HeLa cell cytoplasmic extract, or (C) C6/36 mosquito cell cytoplasmic extract for the indicated times under conditions that favored 5'-3' decay by XRN1. Decay products were separated on 5% polyacrylamide gels and visualized by phosphorimaging. sfRNA-like decay products are indicated at right. This experiment was performed in our laboratory by John R. Anderson.

When incubated with recombinant yeast XRN1, the control reporter RNA degraded rapidly and did not generate any decay intermediates. However, the addition of the DENV-2 3' UTR to the reporter RNA caused an sfRNA-like decay intermediate to accumulate as the full-length RNA was rapidly degraded (Figure 6A). Importantly, a robust sfRNA-like decay intermediate was also observed as the 3' UTR of DENV-2 was degraded in cytoplasmic extracts from HeLa cells (Figure 6B) or C6/36 mosquito cells (Figure 6C). These experiments strongly suggest that the structural elements in the DENV 3'UTR responsible for sfRNA formation can stall both mammalian and mosquito 5'-3' exoribonuclease (presumably XRN1) activity, and that cytoplasmic extracts lack other activities capable of efficiently degrading sfRNA.

sfRNA formation suppresses XRN1 activity

sfRNA accumulates to high levels during flavivirus infections (Pijlman et al. 2008) and therefore could potentially have a significant effect on cellular gene expression if it is able to sequester host factors.. Because XRN1 is highly processive and is able to degrade many endogenous highly structured RNAs (Jinek et al. 2011; Stevens 2001; Stevens 1978), and yeast XRN1 has been shown to stall on G-tracts or artificial C-G stem-loops (Decker and Parker 1993; Vreken and Raue 1992), we wondered if the stalling of XRN1 on flavivirus RNAs could also suppress XRN1 activity. If sfRNA remained associated with XRN1 for a time after stalling because the enzyme could not rapidly dissociate from the RNA substrate, then overall availability of XRN1 would be compromised by sfRNA formation and cellular substrates for

XRN1-mediated decay (i.e. decapped 5' monophosphorylated transcripts) would be stabilized, much as is seen when XRN1 is depleted in yeast (Blewett et al. 2011).

We used cytoplasmic extracts from HeLa and C6/36 cells as well as recombinant yeast XRN1 protein in competition assays to determine if the ability of XRN1 to degrade a monophosphorylated control RNA was impeded by sfRNA formation. Figure 7A shows the results of our competition assays in HeLa extract. On average, ~30% of a monophosphorylated reporter RNA remained after incubation in HeLa cytoplasmic extract for 30 minutes. Similar levels of the reporter RNA remained when a 30-fold molar excess of a lightly radiolabeled non-specific competitor transcript (generated from the linearized pGEM-4 vector) was added to the reaction. Interestingly, the addition of a 5' capped DENV-2 3' UTR competitor RNA that contains the necessary structures required for sfRNA formation but is not a substrate for XRN1 due to its blocked 5' end, had no effect on the decay of the reporter RNA as ~31% of the RNA remained after 30 minutes. However, when the DENV-2 3' UTR competitor RNA contains a 5' monophosphate and is therefore a substrate for XRN1, the reporter RNA was dramatically stabilized and ~70% of the RNA remained following the 30 minute incubation. Importantly, this effect was not only observed in human cell extracts, but also in C6/36 mosquito cell extracts (Figure 7B). Finally, the suppression of XRN1 activity observed in human and mosquito extracts did not require other cellular factors, as incubation of recombinant yeast XRN1 with the DENV-2 competitor RNA also caused the uncapped reporter RNA to become more stable (Figure 7C).

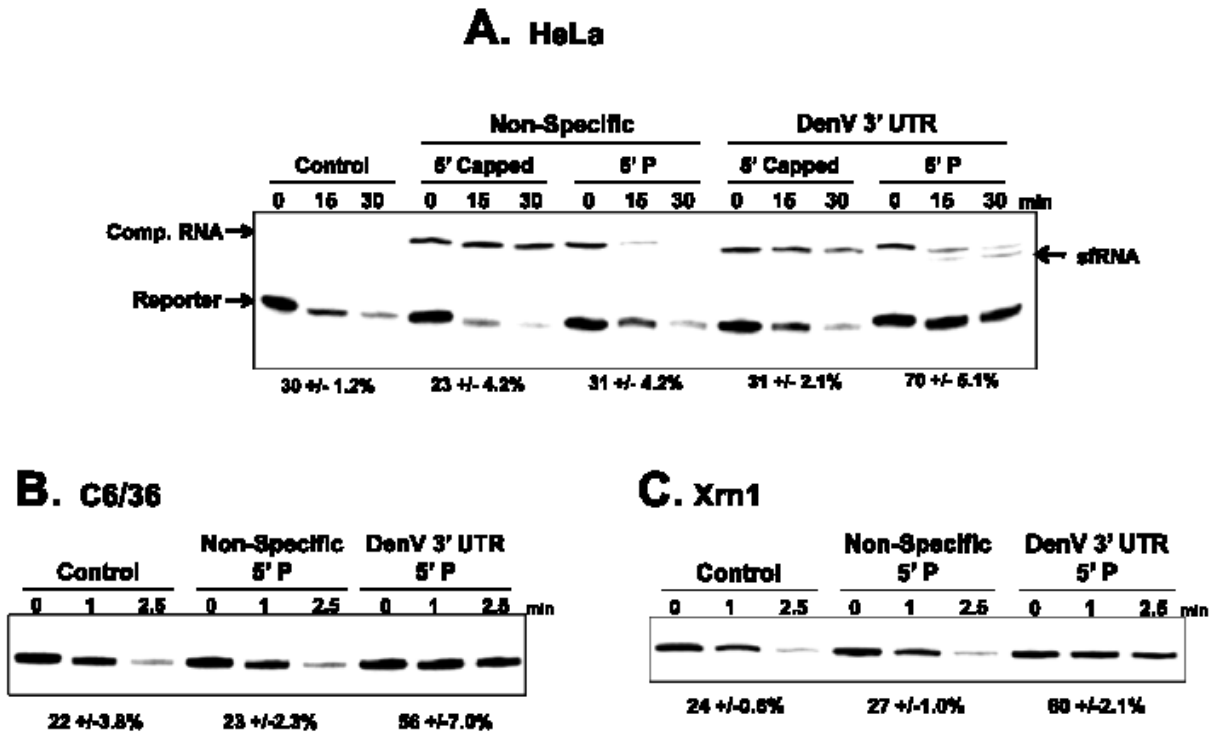

Figure 7. Subgenomic flavivirus RNA formation inhibits XRN1 activity. A 5' monophosphorylated RNA containing the DENV-2 3' UTR inhibits 5'-3' decay in (A) HeLa cell cytoplasmic extract, (B) C6/36 mosquito cell cytoplasmic extract and (C) with recombinant yeast XRN1 alone. The Control lanes do not contain competitor RNA. A lightly radiolabeled competitor RNA bearing either a 5' cap or monophosphate was used at 30X molar excess of the 5' monophosphorylated, radiolabeled reporter RNA for the indicated times. Non-specific competitor RNA was generated from a pGEM-4 template and compared to the DENV-2 3' UTR competitor containing the 5' half of the DENV-2 3' UTR. Products were resolved on 5% polyacrylamide gels and visualized by phophorimaging. Numbers below the gels are the average +/- standard deviation of the percent RNA remaining in the last time point from three independent experiments. This experiment was performed in our laboratory by John R. Anderson.

Suppression of XRN1 activity is likely a general property of sfRNAs

To determine if suppression of XRN1 activity is a general property of subgenomic flavivirus RNAs, we cloned the 5' proximal 200 nucleotides of the JEV 3' UTR which was predicted to harbor sfRNA-forming sequences/structures (Pijlman et al. 2008) and used our *in vitro* RNA decay assays to assess XRN1 activity. Figure 8A shows that a monophosphorylated reporter RNA containing the JEV 3' UTR formed an abundant sfRNA in HeLa cell extracts as well as when incubated with recombinant yeast XRN1 in the absence of any other factors. A

monophosphorylated RNA containing the 5' half of the DENV-2 3' UTR (a ~230 nt RNA) was used as a positive control in these experiments. Furthermore, the presence of the JEV 3' UTR radiolabeled competitor RNA provided at 30-fold molar excess was strongly associated with the stabilization of the monophosphorylated control RNA (Figure 8B), albeit not as potently as the DENV 3' UTR. The JEV 3' UTR RNA may have less apparent ability to suppress XRN1 activity compared to the DENV 3' UTR RNA in this experiment for two reasons. First, the DENV 3' UTR RNA harbors two XRN1-resistant structures capable of forming two sfRNAs (data not shown) and the JEV 3' UTR RNA has only one XRN1-resistant structure. The DENV 3' UTR RNA may therefore be more resistant to XRN1 than the JEV 3' UTR RNA because of additional secondary or tertiary RNA structural elements that stabilize the sfRNA. Second, the DENV 3' UTR RNA may be less susceptible to 3'-5' decay in HeLa cytoplasmic extract than the JEV 3' UTR RNA, as in Figure 8A we observe the depletion of the JEV sfRNA-like decay intermediate more rapidly than the DENV sfRNA-like decay intermediate, possibly through 3'-5' decay. Therefore, the suppression of 5'-3' exonucleolytic decay in HeLa cytoplasmic extract by the JEV 3' UTR (Figure 8B) could be less potent than that of the DENV 3' UTR because the JEV sfRNA-like decay intermediate is less stable (and therefore accumulates to lower levels) than the DENV sfRNA. These data indicate that sfRNA formation in and of itself is capable of repressing XRN1 activity, and this may be a conserved function of all flavivirus sfRNAs.

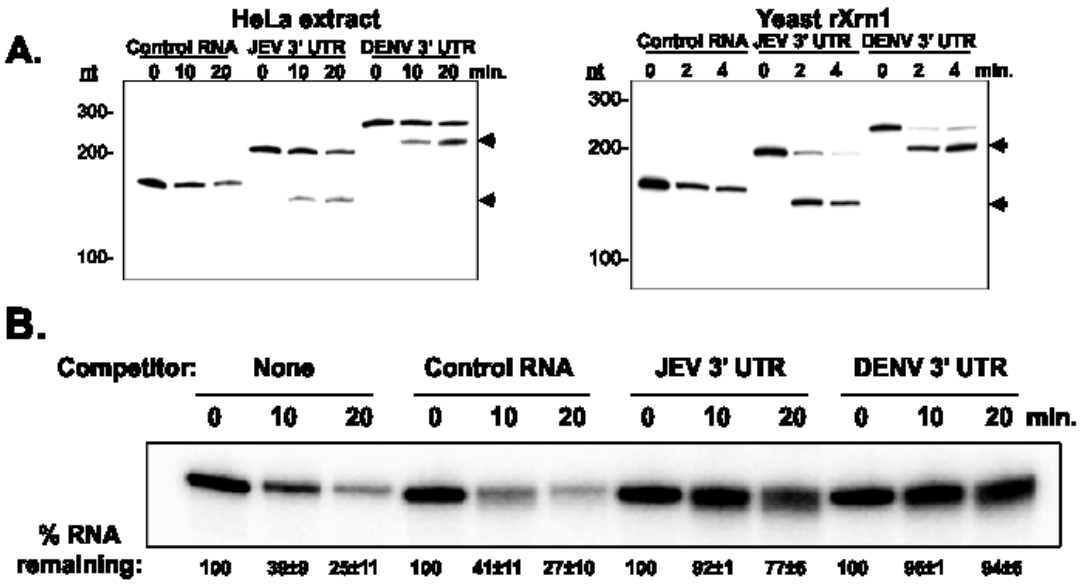

Figure 8. Suppression of XRN1 activity is likely a conserved function of flavivirus sfRNAs. (A) JEV sfRNA is formed as XRN1 stalls on the viral 3' UTR. Radiolabeled, 5' monophosphorylated reporter RNAs were incubated in HeLa cytoplasmic extract under conditions that favor 5'-3' decay (left panel) or with recombinant yeast XRN1 (right panel) containing either pGEM-4 reporter sequence (Control RNA), the 5' (proximal) 200 nt of the JEV 3' UTR, or the 5' half of the DENV-2 3' UTR (used as a positive control). (B) 5'-3' decay of a reporter RNA is inhibited in HeLa cytoplasmic extract in the presence of a competitor RNA containing the first 200 nt of the JEV 3' UTR. A 5' monophosphorylated radiolabeled reporter RNA containing the pGEM-4 sequence was incubated with a 30x molar excess of competitor RNA bearing a 5' monophosphate containing either pGEM-4 sequence (Control RNA), the first 200 nt of the JEV 3' UTR (JEV 3' UTR) or the 5' half of the DENV-2 3' UTR (DENV 3' UTR) in HeLa cytoplasmic extract. RNAs were isolated from the reaction at the indicated times, resolved on 5% denaturing polyacrylamide gels, and exposed to a phosphorimager screen to visualize. The numbers below the gel in (B) are the average percent RNA remaining in each time point +/- the standard deviation. The experiment shown in (B) was performed by John R. Anderson and the first 200 nucleotides of the JEV 3' UTR was assembled by PCR and cloned into pGEM-4 by Benjamin J. Dodd.

Finally, to determine if XRN1 activity is suppressed during infection of human cells with flaviviruses, we measured the relative abundance of uncapped cellular transcripts that would likely normally be substrates for XRN1. We used an antibody that recognizes 5' methylated RNA cap structure to fractionate total RNA purified from human 293T cells infected with DENV-2 when sfRNA had accumulated to high levels (4 days post infection; dpi) or from mock infected cells. Antibody was used in excess so that all capped RNAs would be immunoprecipitated away from the uncapped RNAs. We used the uncapped *7SL* RNA as a reference gene for RT-qPCR measurements and confirmed that its abundance was unchanged during viral infection. The

amount of uncapped transcripts in mock or DENV-2 infected cells relative to 10% of the RNA input was then determined. Figure 9 (top panels) shows that there was an increase in the relative abundance of two short-lived mRNAs, *FOS* and *TUT1*, in the uncapped fraction of RNA purified from DENV-2 infected cells relative to mock infected cells. Furthermore, this effect was not specific to DENV-2 infections, as uncapped mRNAs accumulated in KUNV infected cells (2 dpi; bottom panels of Figure 9). Importantly, this increase in uncapped mRNAs was strongly associated with sfRNA formation. Cells infected with a mutant KUNV that cannot generate sfRNA (the CS3ΔIRA mutant described in Pijlman et al. 2008) did not cause an increase in the relative abundance of uncapped cellular transcripts (Figure 9, bottom panels). Therefore, we have observed defects in XRN1 activity due to sfRNA accumulation using both cell extract-based experiments and cell culture models of infection.

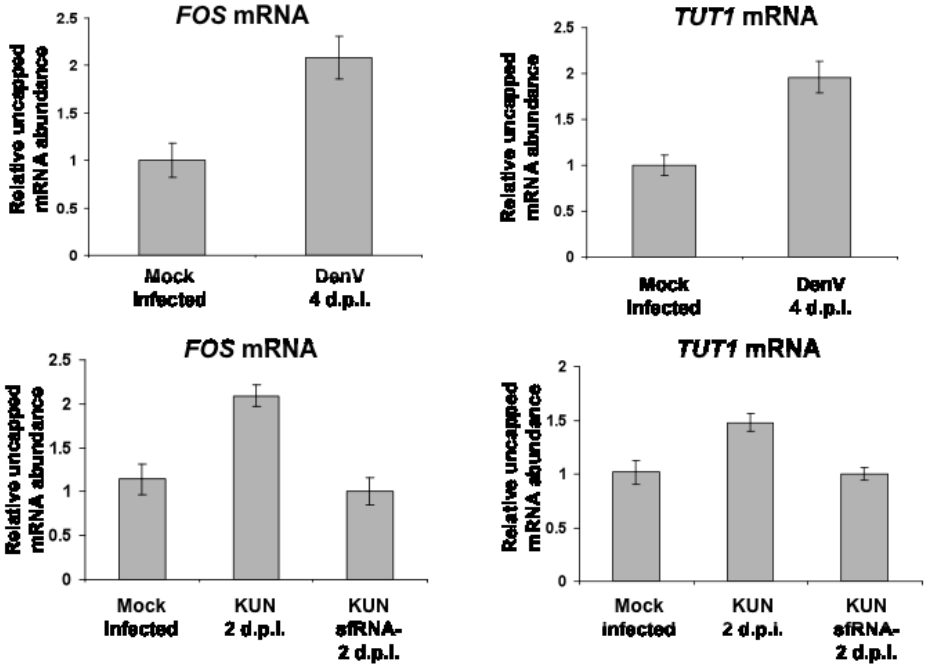

Figure 9. sfRNA accumulation during two flavivirus infections is correlated with an increase in the abundance of uncapped mRNAs. Human 293T cells were infected with dengue virus type 2 (DenV; top panels), Kunjin virus (KUN) or a Kunjin virus mutant that does not make sfRNA1 or sfRNA2 (KUN sfRNA-) at an MOI of 1, and total RNA collected 2 dpi or 4 dpi (respectively). Following fractionation of total RNA with an antibody to the 5' methylguanosine cap structure, RT-qPCR was performed to measure the relative abundance of two endogenous transcripts *FOS* and *TUT1*. Values shown above are from one representative experiment with standard error of the mean from three technical replicates.

XRN1 may be sequestered by sfRNA

If sfRNA formation inhibited XRN1 activity, we hypothesized that the most likely scenario by which this could occur would be if the sfRNA acted as a reversible inhibitor of the enzyme. Therefore, the RNA should be physically associated with XRN1 for a time, potentially due to a slow rate of dissociation as XRN1 frees itself from the stable RNA decay product. To look for an association between sfRNA and XRN1, cells were infected with DENV-2 or KUNV, and at 4 dpi or 2 dpi (respectively) we assessed the interaction between XRN1 and sfRNA by RNA co-immunoprecipitations using an antibody against XRN1. Protein-RNA interactions were stabilized in infected cells by formaldehyde cross-linking prior to cell lysis. As depicted in Figure 10A, we can observe the specific physical interaction between RNAs containing the DENV-2 or KUNV 3' UTRs and XRN1 by semi-quantitative RT-PCR. Furthermore, RNAs containing the viral 3' UTRs were enriched in the XRN1-co-immunoprecipitated fraction by ~4x or ~2x (respectively) compared to RNAs that contained the viral open reading frames as determined by qRT-PCR (Figure 10B). We normalized the abundances of the RNAs containing the viral 3' UTR or open reading frame (ORF) in the XRN1 immunoprecipitation fraction to the 10% input fraction to account for the minimal increase in the overall amount of viral 3' UTR-containing RNAs observed in infected cells due to sfRNA accumulation. Additionally, the efficiencies of the primers used to amplify the viral 3' UTR or ORF were within 2% of each other, and therefore differences in primer efficiency did not account for these observations. Overall, these data indicate that 3' UTR-containing RNAs (e.g. sfRNAs) were physically associated with XRN1 during infection.

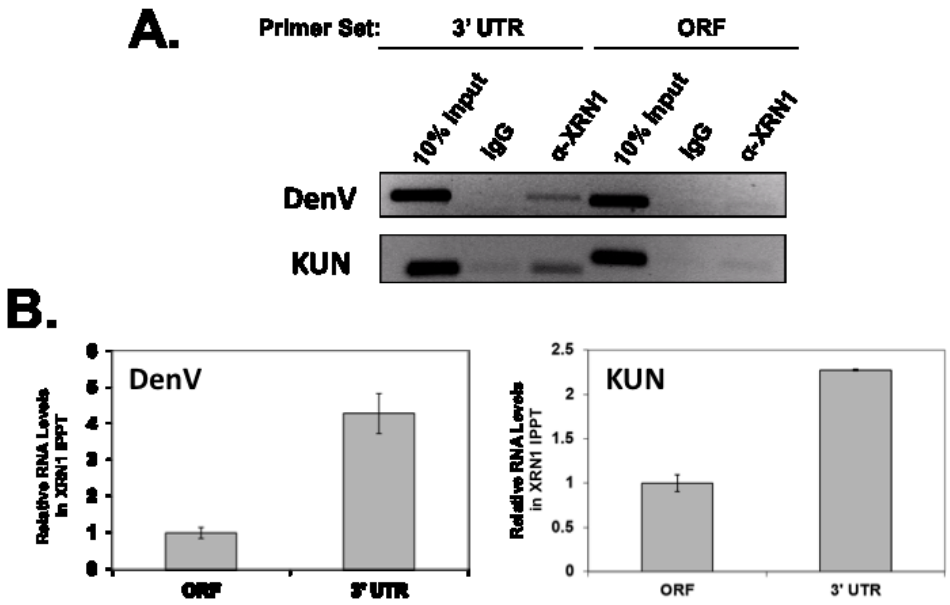

Figure 10. Subgenomic flavivirus RNA is physically associated with XRN1 during infection. Lysates generated from formaldehyde cross-linked 293T cells infected with dengue virus type 2 (DenV; MOI of 1) or Kunjin virus (KUN; MOI of 1) for 4 days or 2 days (respectively) were immunoprecipitated with XRN1 antibody (α-XRN1 lanes) or matched quantities of normal rabbit IgG (IgG lanes) and co-precipitating RNAs were detected by RT-PCR (A) or RT-qPCR (B) using primers to the viral open reading frame (ORF) or the 3' untranslated region (3' UTR). In (B), the relative RNA levels in the XRN1 immunoprecipitation (IPPT) fraction were determined by normalizing to the 10% input fractions.

Cellular mRNA stabilization is strongly associated with sfRNA accumulation

Because XRN1 is the major 5'-3' exoribonuclease in the cytoplasm of yeast and mammalian cells (Nagarajan et al. 2013; Bashkirov et al. 1997; Stevens 1978), and deletion or siRNA-mediated depletion of XRN1 results in increased mRNA stability in yeast (Blewett et al. 2011; Haimovich et al. 2013; Sun et al. 2013) and an ARE-containing reporter RNA in mammalian cells (Stoecklin et al. 2006), we wondered if defects in XRN1 activity due to sfRNA formation might influence the rate at which cellular mRNAs were degraded. Therefore, we first created a pool of human 293T cells stably expressing a short hairpin RNA (shRNA) to XRN1 to deplete the exonuclease. Figure 11A shows that the abundance of XRN1 mRNA in this cell pool was reduced to ~30% compared to cells stably expressing the pLKO.1 empty vector. To determine if XRN1 depletion alters the stability of endogenous cellular mRNAs, we performed

transcriptional shut-offs using actinomycin D and followed the degradation of two short-lived transcripts (*FOS* and *TUT1*) by RT-qPCR over a time course. Figure 11B shows that *TUT1* and *FOS* mRNAs are significantly stabilized in the cells deficient in XRN1 compared to the control cells harboring pLKO.1. The *TUT1* mRNA was 1.6-fold more stable and *FOS* was 1.8-fold more stable on average in cells depleted of XRN1 (average half-lives are reported in the graph insets in Figure 11). These transcripts, therefore, are very likely to be degraded by XRN1 in human 293T cells.

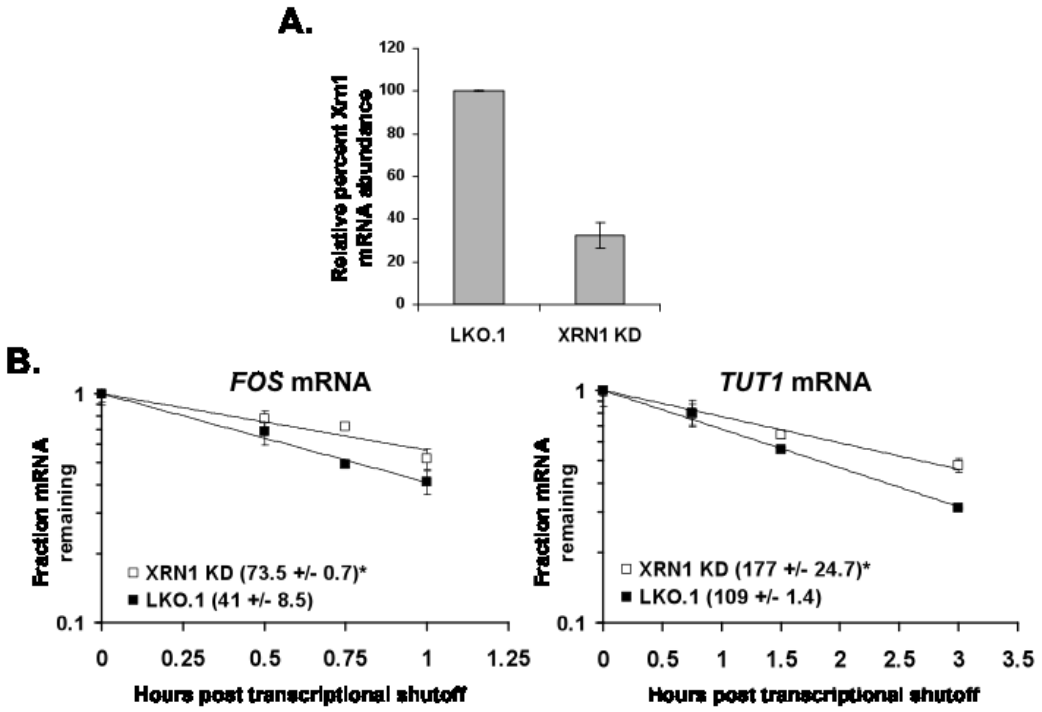

Figure 11. XRN1 depletion leads to increased stability of two short-lived transcripts in human 293T cells. (A) The abundance of XRN1 mRNA was assessed using RT-qPCR to show XRN1 knockdown efficiency in human 293T cells stably expressing an shRNA to XRN1(XRN1 KD) compared to cells expressing the empty vector pLKO.1 (LKO.1). (B) The stability of *FOS* and *TUT1* mRNAs was determined after transcriptional shutoff by actinomycin D treatment by RT-qPCR using *GAPDH* as a reference gene. Average half-lives (minutes) +/- the standard deviation are reported from two independent experiments. * indicates $p<0.05$ by Student's t-test.

As reduction of XRN1 activity leads to stabilization of cellular mRNAs (Figure 11) and sfRNA inhibits XRN1 in vitro (Figure 8) we predicted that cellular mRNAs were likely to be stabilized during flavivirus infections. To test this, we performed transcriptional shut-off

experiments by applying actinomycin D to mock infected or DENV-2 infected cells at 4 days post infection and collecting total RNA samples over a 3 hour time course at 3 or 4 days post infection. As DENV-2 sfRNA accumulated (Figure 12A), both *TUT1* and *FOS* mRNAs became more stable over the course of the DENV-2 infection (Figure 12B). By 4 dpi, when sfRNA was most abundant, *FOS* was 2.7-fold and *TUT1* was 2.1-fold more stable in DENV-2 infections than in mock infected cells. Therefore, the accumulation of sfRNA in a DENV-2 infection was associated with stabilization of two endogenous cellular transcripts that are likely substrates of XRN1. This indicates that XRN1 activity is repressed during DENV-2 infection.

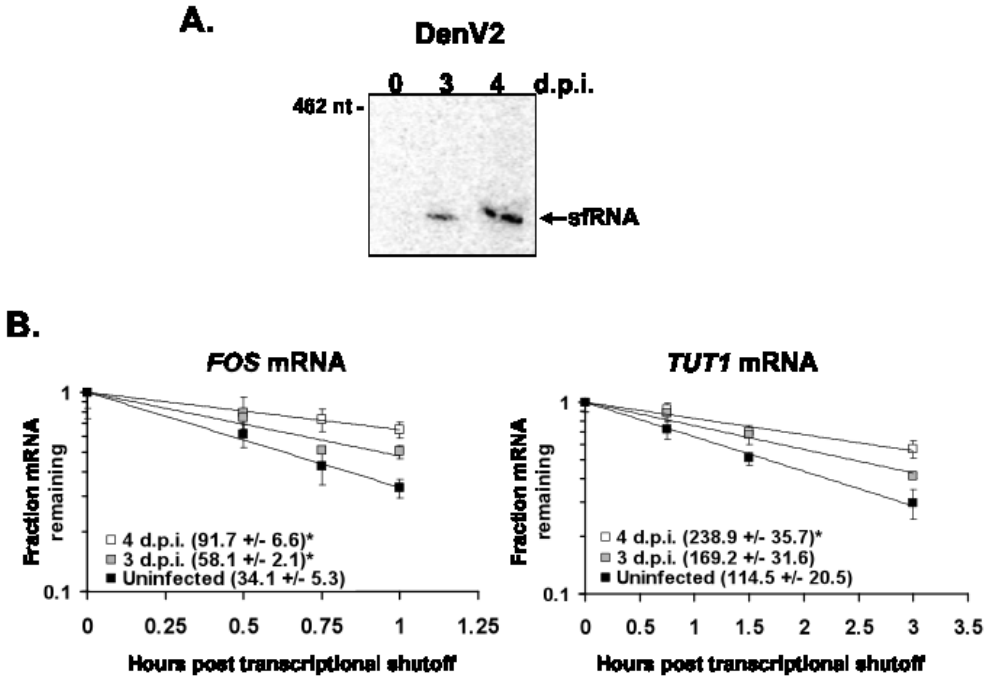

Figure 12. DENV-2 sfRNA accumulation is associated with stabilization of two short-lived cellular mRNAs. (A) Northern blotting was performed to visualize dengue virus type 2 (DenV2) sfRNA accumulation over the course of an infection (0, 3, and 4 days post infection). (B) The stability of *TUT1* and *FOS* mRNAs was assessed by actinomycin D transcriptional shutoff of cells infected with DENV-2 at 0, 3 and 4 days post infection by RT-qPCR using *GAPDH* as a reference gene. Average transcript half-life (minutes) plus or minus the standard deviation of two independent infections are shown. * indicates $p<0.05$ by Student's t-test.

To determine if mRNA stability was also altered in another flavivirus infection, we examined *TUT1* and *FOS* mRNA stability at 36 and 48 hpi with KUNV when sfRNA accumulated to high levels as assessed by northern blot (Figure 13A, left panel). Intriguingly,

both cellular transcripts were significantly stabilized in conjunction with sfRNA accumulation (Figure 13A, right panels). Furthermore, the stabilization of *FOS* and *TUT1* mRNAs only occurred during KUNV infection when sfRNA was present, as an sfRNA-deficient Kunjin virus (that replicated to the same level as wild-type KUNV, Figure 15C) did not alter cellular mRNA stability during infection (Figure 13B). Additionally, we later determined that *TUT1* mRNA is destabilized during Sindbis virus infection (Barnhart et al. 2013; Appendix 6). These results provide more substantial evidence that stabilization of cellular mRNAs is dependent on sfRNA production (and therefore XRN1 inhibition) rather than just a general cellular response to infection.

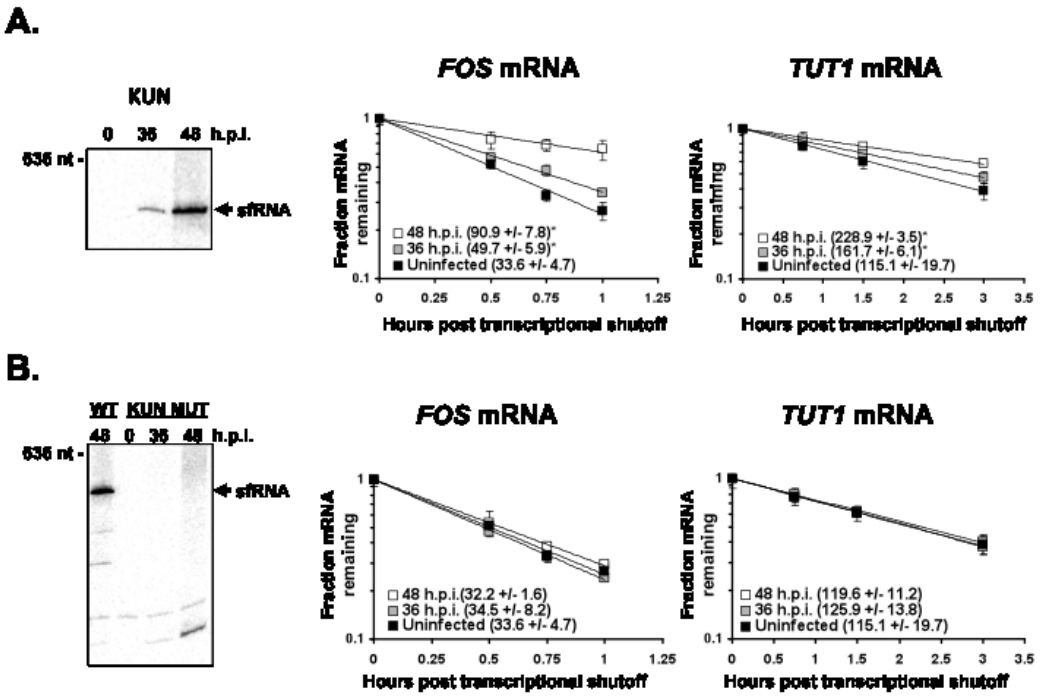

Figure 13. The stabilization of short-lived cellular mRNAs during Kunjin virus infection depends on sfRNA accumulation. Human 293T cells were infected with wild-type Kunjin virus (KUN) (A) or an sfRNA-deficient mutant Kunjin virus (KUN MUT) at an MOI of 1 (B) and transcription was inhibited by actinomycin-D treatment at 0, 36, and 48 hours post infection. Northern blotting was performed to assess sfRNA accumulation over the course of an infection (left panels) and mRNA stability of *TUT1* and *FOS* was determined by RT-qPCR using *GAPDH* as a reference gene (right panels). The average half-lives (minutes) from two independent infections +/- standard deviation are shown. * indicates $p<0.05$ using Student's t-test.

Although the results above demonstrated that sfRNA formation was necessary for the stabilization of cellular mRNAs (Figure 13), we also wished to determine whether sfRNA production is sufficient on its own to facilitate changes in mRNA stability in the complete absence of other aspects of a viral infection. We therefore cloned the DENV-2 3' UTR into the peGFP-N1 reporter plasmid to express GFP containing the 3' UTR of DENV-2 downstream of the GFP open reading frame. We transfected equal amounts of each peGFP plasmid into 293T cells and 48 hours post transfection performed transcriptional shut-offs with actinomycin D to assess changes in mRNA stability. As depicted in Figure 14A, the presence of the DENV-2 3' UTR facilitated the formation of an sfRNA-like RNA decay product that accumulated in transfected cells. Cells transfected with the sfRNA-producing DENV 3' UTR construct displayed a 2.1-fold increase in the half-lives of both *FOS* and *TUT1*. Of note, the stability of both *FOS* and *TUT1* mRNAs was not enhanced by the peGFP-N1 empty vector alone (Figure 14B).These results support that sfRNA formation in the absence of viral infection is capable of suppressing Xrn1 activity in human cells.

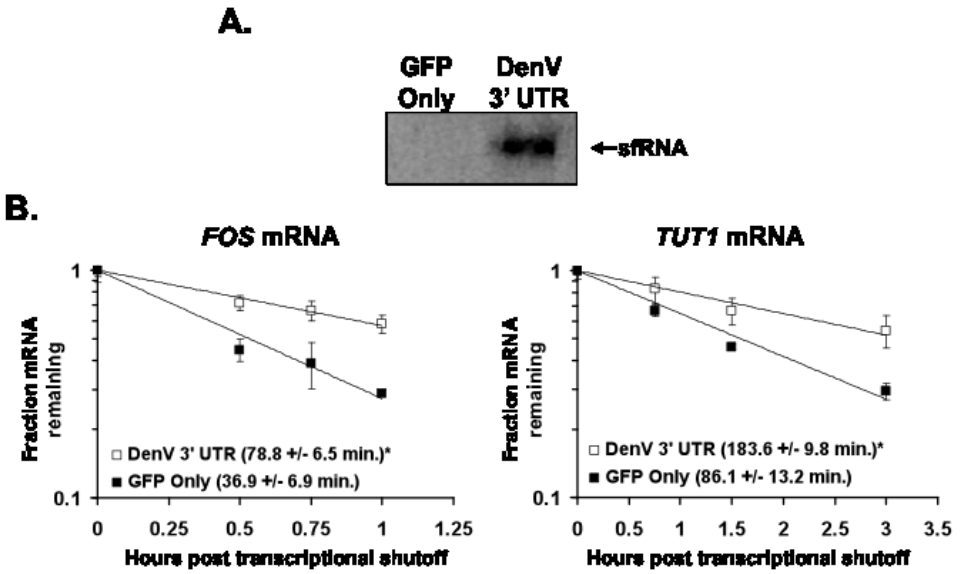

Figure 14. The accumulation of sfRNA in the absence of viral infection is associated with the stabilization of cellular transcripts. Plasmids expressing GFP alone ("GFP Only") or a GFP mRNA containing the dengue virus type 2 3' UTR in the GFP 3' UTR("DenV 3' UTR") were transfected into 293T cells and samples were taken 48 hours post transfection. (A) Northern blotting for the DENV2 3' UTR shows an sfRNA-like decay intermediate forms in transfected cells. (B) Transfected cells were treated with

actinomycin D to shut off transcription and *FOS* and *TUT1* mRNA stability was assessed by RT-qPCR using GAPDH as a reference gene. The mean of two independent experiments plus or minus the standard deviation are reported and * indicates $p<0.05$ by Student's t-test.

sfRNA accumulation is correlated with dramatic changes in cellular gene expression

Considering that sfRNA formation significantly stabilizes cellular transcripts during infections with two different flaviviruses and that changes in mRNA stability are often tightly coordinated with mRNA abundance, we sought to determine if sfRNA accumulation influences cellular gene expression during an infection. Our collaborators Dr. Khromykh (University of Queensland) and Drs. Kumagai and Akira (Osaka University) assessed changes in host gene expression at 48 hpi by microarray using mouse embryonic fibroblasts deficient in the interferon α/β receptor (IFNAR-/-). This cell line is highly permissive for KUNV replication and there was no difference in the intracellular level of wild-type and mutant KUNV RNA at 48 hpi when total RNA samples were collected (Figure 15C). For analysis, these cells were either mock infected, infected with the wild-type KUNV, or the sfRNA-deficient KUNV. Figure 15A depicts a heat map representing 416 mRNAs that were 3-fold or more over-expressed in the wild-type KUNV infected cells compared to mock infected cells. Importantly, 378 of these transcripts were not over-expressed upon infection with the sfRNA-deficient KUNV. Gene Ontology analysis of this set of transcripts revealed that factors involved in cell adhesion, innate immune response, inflammation, stress responses and cell proliferation were significantly over-represented ($p\leq0.01$). Furthermore, human 293T cells showed similar up-regulation of four of these immune factors as determined by RT-qPCR in the wild-type KUNV infected cells compared to the sfRNA-deficient KUNV infections (Figure 15B). In 293T cells the abundances of *OASL* and *CXCL11* were dramatically increased (by ~575- and ~472-fold, respectively) during wild-type KUNV infections versus mock infected cells. In contrast, the murine *Oasl1*, *Oasl2* and *Cxcl11* transcripts were elevated to a lesser extent as determined by microarray (by 20-, 12.97-, and

15.9-fold, respectively). These differences are likely due to the absence of type I interferon signaling in the IFNAR-/- MEFs compared to the interferon-competent human 293T cells. In contrast, the transcripts encoding interleukin-6 (*IL6*) and the chemokine *CCL2* were elevated by 4.5- and 3.5-fold (respectively) in human 293T cells, and by 15.2- and 4.71-fold (respectively) in the IFNAR-/- MEFs. These results both generalize our findings to other cell types (and species) and confirm the results derived from microarray analysis.

Interestingly, previous studies reported that transcripts encoding the four immune factors *IL6*, *OASL*, *CCL2*, and *CXCL11* were elevated in other flavivirus infections. The interferon-induced transcript *OASL* was shown to be elevated in DENV, HCV, and WNV infections and plays an important role in the host antiviral response (Fink et al. 2007; Schoggins et al. 2011; Yakub et al. 2005; Perelygin et al. 2002). The chemokine *CXCL11* is induced by type I interferon, NFκB, and/or pro-inflammatory cytokines and is a T cell chemoattractant that has been suggested to be involved in neuroinflammatory disorders (Cole et al. 1998). Furthermore, *CXCL11* was elevated in cell culture models of DENV infection and in human patients (Fink et al. 2007). Finally, *IL6* and *CCL2* have previously been shown to be elevated in WNV, DENV, JEV, and other flavivirus infections (Cheeran et al. 2005; Munoz-Erazo et al. 2012; Tolfvenstam et al. 2011; Nazmi et al. 2011; Palus et al. 2013). Therefore, sfRNA accumulation is likely contributing to dramatic changes in cellular gene expression in a cell-type independent manner that could substantially alter the host response to infection and potentially enhance immunopathogenesis.

Short-lived cellular transcripts may be elevated in flavivirus infections as a result of direct suppression of XRN1 activity leading to mRNA stabilization. However, transcripts might also be over-expressed as an indirect result of XRN1 suppression. We observed that the transcription factor *FOS* and the uridyl transferase *TUT1* were significantly stabilized at the mRNA level during WNV and DENV-2 infections. As discussed above, FOS over-expression could potentially contribute to increased transcription as part of the AP-1 transcription factor complex.

Furthermore, TUT1 modifies miRNAs by adding uridines to their 3' ends, causing a reduction in miRNA abundance likely by targeting the miRNAs for decay (Wyman et al. 2011; Knouf et al. 2013). Therefore, because *TUT1* was stabilized in several flavivirus infections in an sfRNA-dependent manner, this protein is likely upregulated during infection. Consequently, the observed over-expression of transcripts in wild-type KUNV infections could also result from elevated levels of transcription factors and repressors of miRNA-mediated decay like FOS and TUT1.

Interestingly, a subset of mRNAs was less abundant in the wild-type KUNV infected cells compared to mock infected cells and cells infected with the sfRNA-deficient KUNV (bottom portion of the heat map shown in Figure 15A). Gene Ontology analysis of the down-regulated transcripts showed that stress responses, cellular response to viral infection, and negative regulators of apoptosis were over-represented ($p \leq 0.01$). These changes in gene expression could be either direct or indirect effects of sfRNA accumulation. Because XRN1 has been previously demonstrated in yeast systems to directly affect transcription, transcripts that are reduced in abundance during sfRNA-producing viral infections could be down-regulated as a direct result of XRN1-suppression (Sun et al. 2013; Haimovich et al. 2013). Otherwise, suppression of XRN1 by sfRNA could indirectly reduce the abundance of many mRNAs by causing the stabilization (and up-regulation) of other RNA-decay factors.

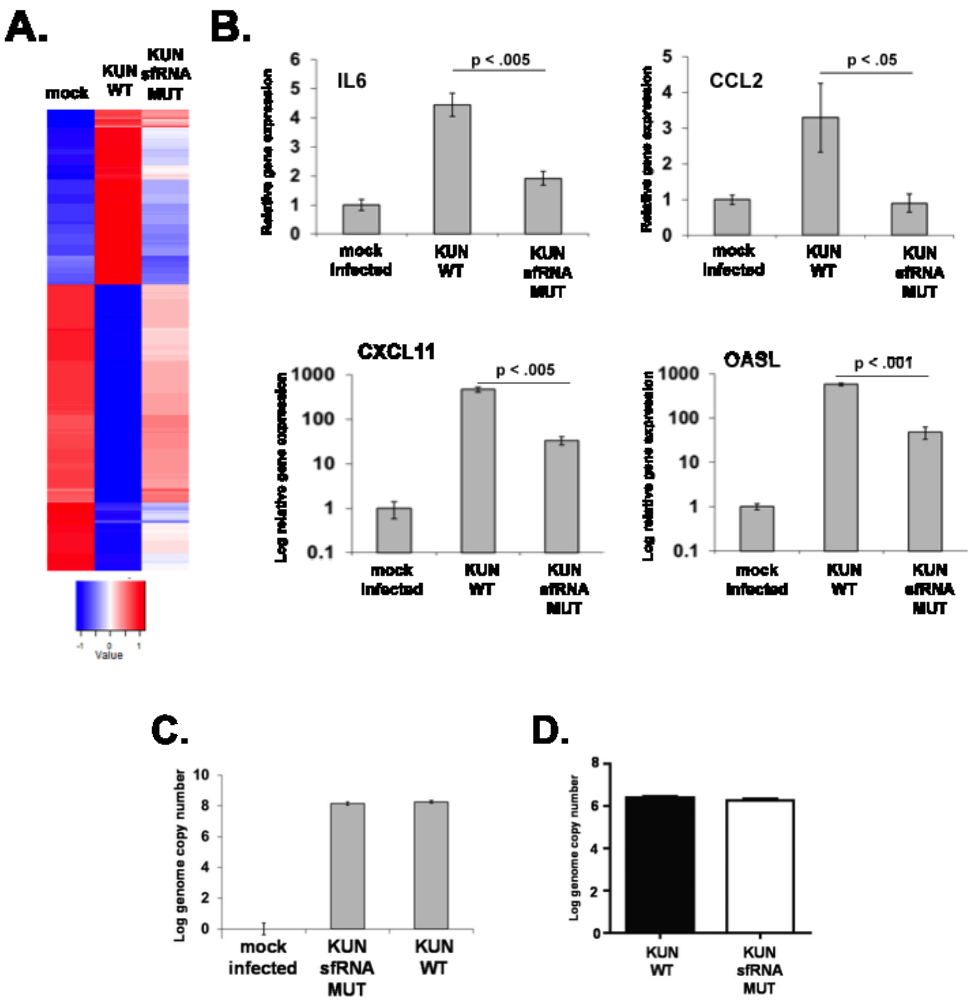

Figure 15. sfRNA accumulation leads to dramatic changes in cellular gene expression. (A) Mouse embryonic fibroblasts lacking the interferon α/β receptor (MEF IFNAR-/-) were mock treated or infected with Kunjin virus (KUN WT) or an sfRNA deficient mutant Kunjin virus (KUN sfRNA MUT) and total RNA was isolated from each sample at 48 hours post infection. The relative abundance of cellular transcripts was determined by microarray analysis and following robust multiarray analysis (RMA), hierarchical clustering was done for genes with threefold or more difference in RMA values after transformation to give a mean of 0 and a standard deviation of 1. The red-blue color key below the heat map depicts the transformed values. (B) The relative abundances of four transcripts shown to be up-regulated in wild-type KUNV infected MEF IFNAR-/- cells in (A), *IL6*, *CCL2*, *CXCL11*, and *OASL* were assessed in infected 293T cells (48 hours post infection) using RT-qPCR with *GAPDH* set as a reference gene. The average +/- standard deviations of three independent infections are shown and significance determined by Student's t-test. The sfRNA-deficient mutant KUNV replicate to similar levels in (C) 293T cells and in (D) MEF IFNAR-/- as determined by RT-qPCR for the Kunjin virus open reading frame from total RNA isolated at 48 hours post infection. Average genome copy number +/- standard deviation from three independent infections is shown. Experiments and results shown in (A) and (D) were performed by the Akira laboratory at Osaka University.

Global changes in cellular mRNA stability in arthropod-borne virus infections

Because sfRNA accumulation appears to correlate with (1) stabilization of two short-lived transcripts and (2) dysregulation of cellular mRNA abundances, we next sought to determine the global impact of sfRNA accumulation on cellular RNA stability during infection. Therefore, we compared cellular RNA stability in mock-infected cells or cells infected with either wild-type KUNV or two viruses that do not generate sfRNA (Sindbis virus and the sfRNA-deficient CS3ΔIRA Kunjin virus). Human 293T cells were mock infected or infected with Sindbis virus (MOI of 5), wild-type or the CS3ΔIRA Kunjin virus (MOI of 5) and transcription was halted using actinomycin D at 24 hpi (mock or SINV) or 48 hpi (the Kunjin viruses). Samples were collected in triplicate at 0 (30 minutes post-actinomycin D addition), 0.75, 1.5, and 3 hours post transcriptional shut-off. Mike Barnhart performed transcriptional shutoffs and RNA isolations from the SINV and mock infected cells. Total RNA was isolated from triplicate infections and Drs. Bin Tian, Mainul Hoque and Liu Liang performed library preparation and RNA-seq analysis at Rutgers New Jersey Medical School. For sequencing analyses, the triplicate samples collected for each time point in each infection were pooled.

Changes in mRNA abundance and stability in KUNV and SINV infections

We determined that ~3000 cellular RNAs had acceptable half-lives (i.e. they had $\geq$10 mapped reads in the '0' time point, a half-life > 0 and $p<0.05$ as determined by Dr. Liu Liang), and were present in both mock infected cells and cells infected with SINV, KUNV, or the sfRNA-deficient KUNV to enable direct comparisons of RNA stability (Figure 16A). Of note, the level of depth that these samples were sequenced at likely excluded an interesting set of transcripts that are of low abundance (<10 reads/sample) in mock infected cells. Therefore, short-lived transcripts may be under-represented in these datasets. Accordingly, neither *TUT1* nor *FOS* (that we analyzed previously (e.g. Figures 11-13) were present in these RNA-seq data sets.

However, we were able to observe some interesting trends in the analyses of the more abundant transcripts present in each condition.

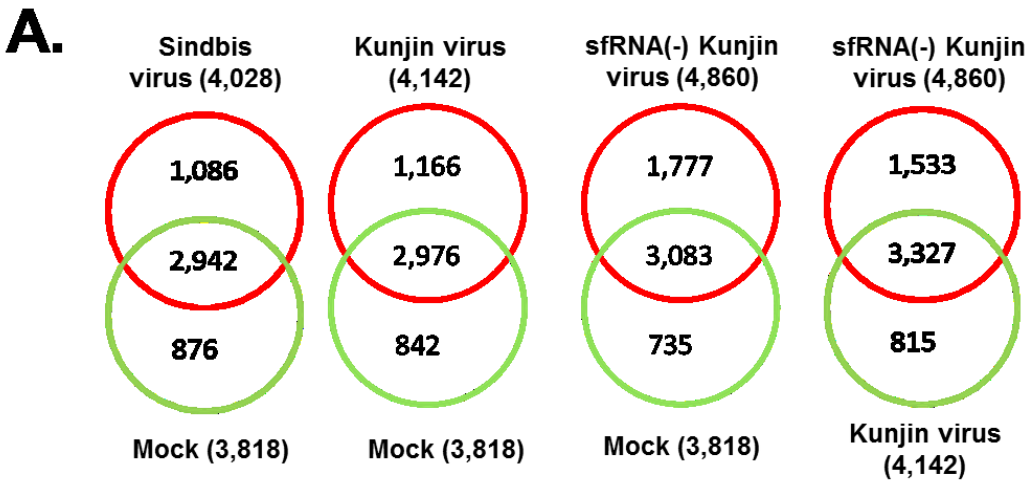

B.

Condition	Median half life (minutes)
Kunjin virus	243
Mock	214.2
Sindbis virus	211.2
sfRNA(-) Kunjin virus	171

Figure 16. Global analysis of mRNA stability in sfRNA-forming and sfRNA-deficient arthropod-borne virus infected cells. (A) Venn diagrams indicate the number of comparable half-lives generated in mock and Sindbis, Kunjin, or sfRNA(-) Kunjin virus infected cells that can be compared directly for analysis. (B) A list of the median RNA half-life (minutes) in each sample.

The median RNA half-life for each condition was compared to determine if sfRNA accumulation corresponded with overall stabilization of cellular RNA. Some interesting trends emerged from this comparison. As depicted above in Figure 16B, cellular RNA from KUNV infected cells had the longest median half-life at 243 minutes, and RNA from the sfRNA-deficient KUNV infected cells had the shortest median half-life of 171 minutes. The shorter median RNA half-life observed in cells infected with the sfRNA-deficient KUNV could be due to the induction of antiviral nucleases that target cellular mRNAs. Considering that KUNV infected cells have the most stable median RNA half-life and the sfRNA-deficient KUNV has the least

stable median RNA half-life, these results could potentially indicate that sfRNA formation leads to an overall stabilization of RNAs. This is consistent with the cellular RNA stabilization by sfRNA that we noted above (in Figures 11-13).

Intriguingly, some striking patterns emerge when we compare the distribution of RNAs that were determined to be ≥2x differentially stabilized during each infection compared to mock infected cells. Cells infected with KUNV have only 75 destabilized RNAs compared to mock infected cells, but the sfRNA-deficient KUNV infected cells had 478 destabilized RNAs (Figure 17A, left). Therefore, in the absence of sfRNA accumulation, Kunjin virus-infected cells have more destabilized RNAs than stabilized RNAs. If the normal cellular response to infection is to destabilize a substantial portion of transcripts, then suppression of XRN1 activity by sfRNA formation could impede the normal cellular response.

Correspondingly, cells infected with wild-type KUNV have many more stabilized RNAs (259) than those infected with the sfRNA-deficient KUNV (76; Figure 17A). Furthermore, when we directly compare the RNAs that were 2-fold or more stabilized or destabilized in KUNV infections with the sfRNA(-) KUNV infections, we can see very strong association between sfRNA accumulation and RNA stabilization (Figure 17A). Wild-type KUNV infected cells have 740 stabilized transcripts and only 58 destabilized transcripts when directly compared to the sfRNA-deficient KUNV infections (Figure 17B). It is important to note that with the size of these datasets (~3,000 RNAs/set), changes in stability or abundance that alter <150 RNAs could potentially be due to random chance (as 5% of a sample size of ~3,000 is ~150). Accordingly, analysis of RNAs from cells infected with SINV did not reveal dramatic differences in host mRNA stability. Figure 17C shows the distribution of ≥2x destabilized or stabilized RNAs in SINV infected cells and reveals a very slight over-representation of destabilized transcripts overall (which may not be significant). Thus, only infection with the sfRNA-forming KUNV shifts the distribution of differentially stabilized transcripts to yield more stabilized transcripts in general.

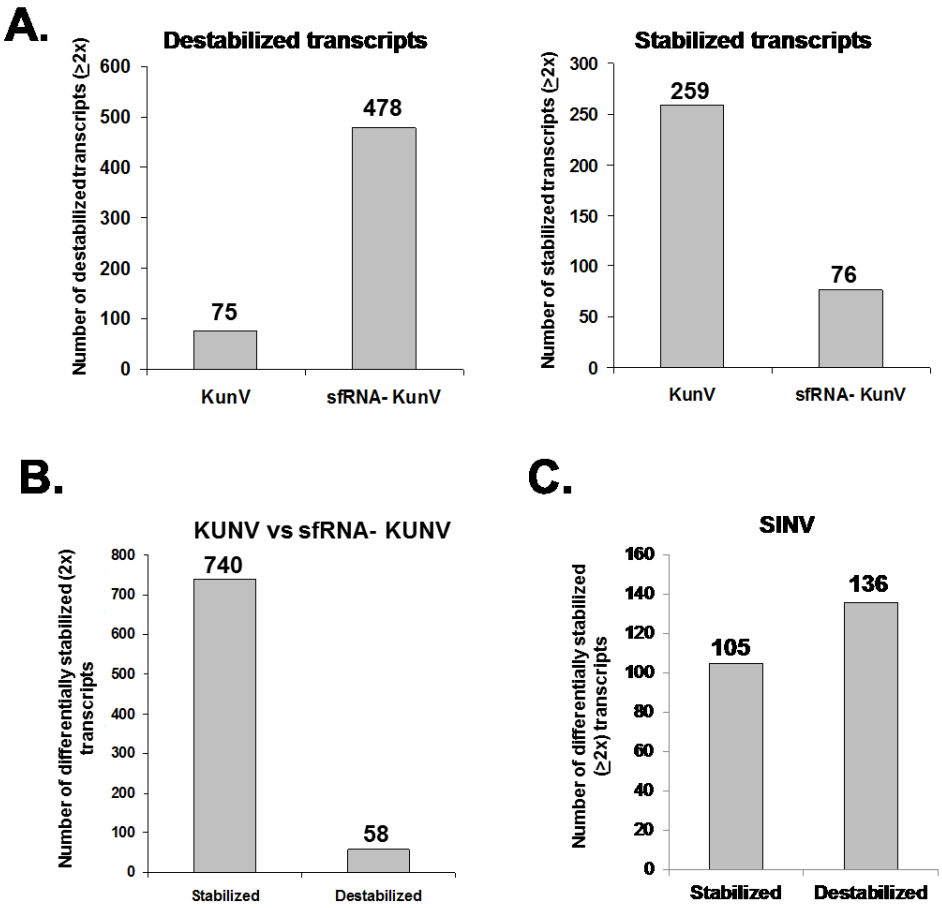

Figure 17. sfRNA accumulation is correlated with the stabilization of the majority of differentially stabilized transcripts in Kunjin virus infections. (A) The number of transcripts that were ≥2x or more destabilized in cells infected with the wild-type KUNV or the sfRNA-deficient KUNV (left panel), and the number of transcripts that were ≥2x or more stabilized in wild-type KUNV or sfRNA-deficient KUNV infected cells at 48 hpi (MOI of 5) compared to mock infected cells (right panel). (B) The RNAs that are ≥2x or more stabilized or destabilized in the wild-type KUNV infected cells compared directly to the sfRNA-deficient Kunjin virus infected cells are shown. (C) Differentially stabilized (≥2x vs mock) RNAs in cells infected with SINV at 24 hpi at an MOI of 5 are also reported.

We were next interested in ascertaining the relative changes in cellular RNA abundances of our subset of ~3,000 transcripts (Figure 16A) during each viral infection. We hypothesized that sfRNA-forming flavivirus infections would have more up-regulated transcripts than sfRNA-deficient virus infections, as sfRNA accumulation was previously shown to be associated with the stabilization of mRNAs. As depicted in Figure 18A , cells infected with KUNV had more transcripts that were 2-fold or more increased in abundance (323 RNAs) than transcripts that were 2-fold or more reduced in abundance (171 RNAs) compared to mock

infected cells. This is precisely what one might expect since sfRNA accumulation is strongly associated with stabilization of cellular mRNAs. Interestingly, cells infected with the sfRNA-deficient KUNV also had only slightly more up-regulated RNAs (242 RNAs) than down-regulated RNAs (196 RNAs; Figure 18B). This is again consistent with the absence of significant cellular mRNA stabilization due to the lack of sfRNA production by these viruses.

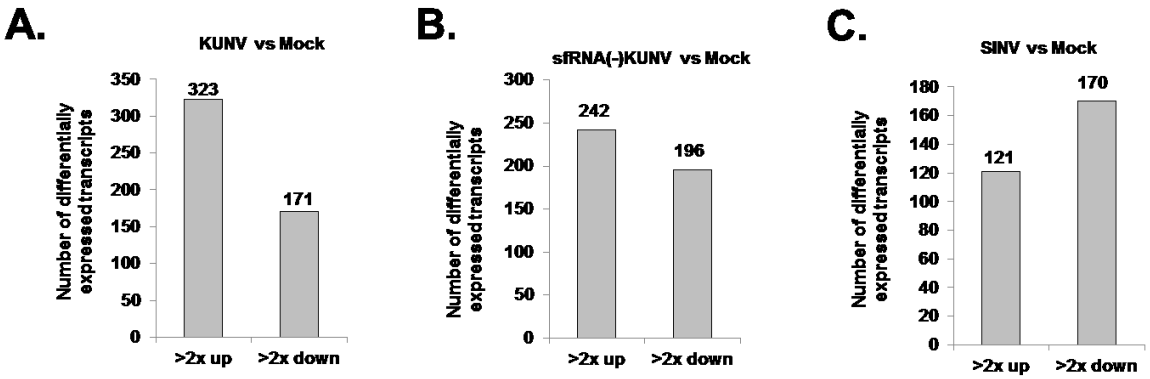

Figure 18. Transcripts that were ≥2x more or less abundant in virus infected cells compared to mock-infected cells by RNA-seq analysis. Values were derived from the '0' time point of actinomycin D shutoff samples. Only RNAs that were detectable (RPKM≥0.01) in both mock and infected cells were compared. Substantially up- or down-regulated RNAs in (A) Kunjin virus (KUNV) versus mock (B) sfRNA(-) Kunjin virus and (C) Sindbis virus (SINV) infected cells compared to mock infected cells are reported.

To reinforce this observation, we analyzed the dysregulation of cellular mRNA stability during SINV infections (which naturally do not make sfRNA). SINV-infected cells had slightly more RNAs that were reduced in abundance (170 RNAs) than were increased in abundance (121 RNAs) compared to mock infected cells (Figure 18C). The twenty transcripts that were most up- or down-regulated in each viral infection are reported in 3. Therefore, although limitations in the depth of sequencing performed may have excluded observations of the stability of many mRNAs in each infection, the available data do suggest that sfRNA formation is associated with increases in RNA abundances during infection.

Analysis of the relationship between transcript abundance and stability in arbovirus infected cells

During viral infection, one might expect that overall cellular gene expression would be significantly altered as the cell attempts to respond to the presence of foreign nucleic acids and proteins as well as the stresses of viral replication/remodeling of the cell. As described in the Introduction, recent studies suggest that transcription and mRNA decay are co-regulated in the cell by a crosstalk-type of mechanism that results in a significant buffering of mRNA abundances following disruption of decay or transcription (Sun et al. 2013; Haimovich et al. 2013). Studies in yeast suggest that XRN1 is involved in mediating this buffering mechanism (Sun et al. 2013). However, during the cellular response to infection, buffering is likely to be inactivated in order to allow mRNA decay and transcription to act together to achieve rapid changes in gene expression. Thus since we speculate that cells would likely substantially alter the level of many mRNAs upon infection, one might expect to see a positive correlation between mRNA half-lives and overall transcript abundance, as the buffering between transcription and mRNA stability is relaxed in infected cells to promote a more rapid response. As seen in Figure 19A, this is precisely what we observed in SINV infected cells. Buffering of gene expression appears to be relaxed as destabilized mRNAs are generally reduced in abundance and stabilized mRNAs are generally increased in abundance.

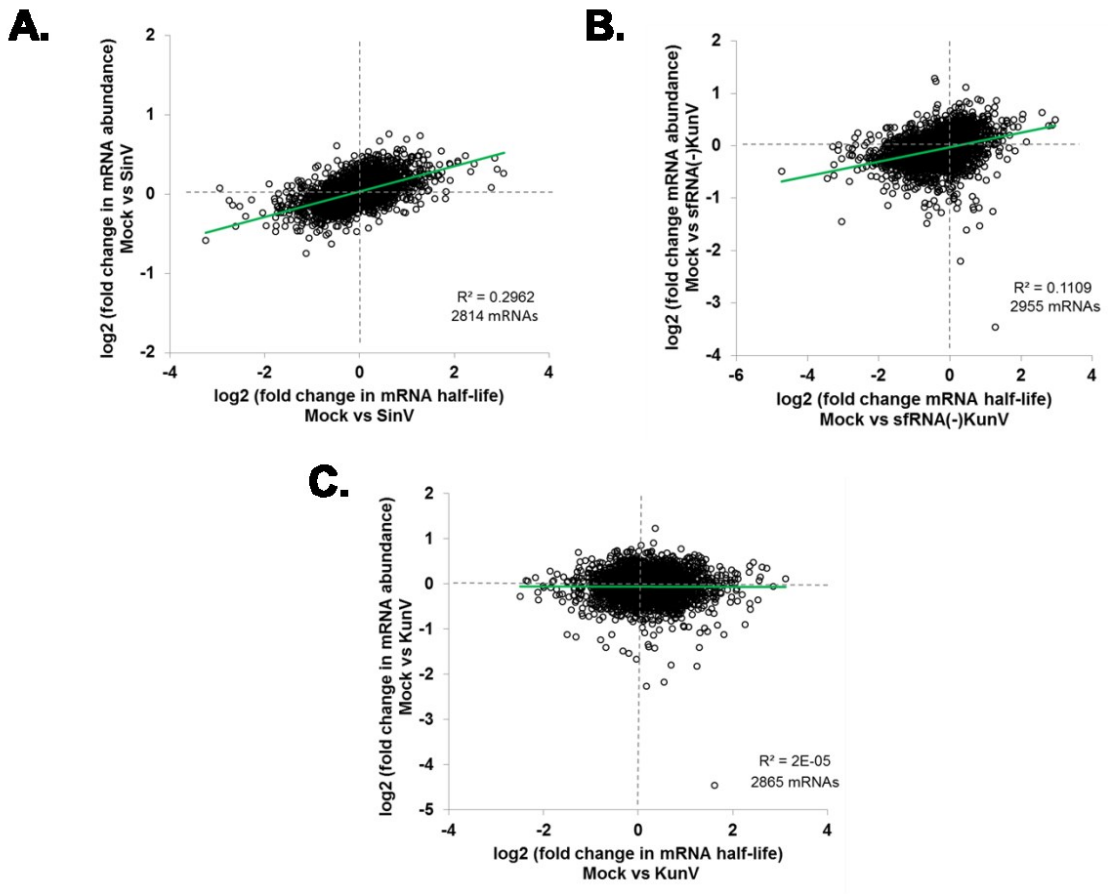

Figure 19. Relationships between mRNA abundance and stability in arthropod-borne virus infected cells. Log transformed fold-change values for transcripts that had acceptable abundances and stability in mock infected cells compared to (A) Sindbis virus infected cells (SinV), (B) sfRNA-deficient KUNV infected cells (sfRNA(-) KunV) and (C) wild-type Kunjin virus infected cells (KunV) reveal the degree to which changes in mRNA abundance correlate with changes in mRNA stability in each infection. Scatterplots were fit with a linear regression line and the R^2 value and number of transcripts per chart indicated in the inset panels. Abundance values were obtained from the '0' time point of actinomycin D shutoffs (30 minutes post drug application). Pearson coefficients were used to calculate statistical significance: Mock vs KunV p = 0.811; Mock vs sfRNA(-) KunV p<0.0001; Mock vs SinV p<0.0001.

As seen in Figure 19B, the exact same trend of relaxed buffering of cellular gene expression is observed in cells infected with the KUNV mutant that fails to express sfRNA. Interestingly, cells infected with wild-type KUNV that generates high levels of sfRNA during infection fail to show a positive correlation between cellular mRNA abundance and mRNA stability (Figure 19C). Given the recent suggestion that XRN1 may play a major role in regulating the buffering of gene expression in yeast (Sun et al. 2013; Haimovich et al. 2013), our observation that cells infected

with sfRNA-producing KUNV fail to be able to regulate buffering lends support to the idea that XRN1 also regulates this process in mammalian cells. These data also suggest that sfRNA-producing viruses are targeting not only mRNA decay/stability by repressing XRN1, but also are targeting transcriptional regulaton through interfering with the buffering process. Thus additional studies with KUNV and other sfRNA-producing viruses may allow insight into mechanistic aspects of the crosstalk between mRNA stability and transcription in mammalian cells.

Section II. Investigation of hepacivirus and pestivirus suppression of XRN1 activity

XRN1 stalls on RNA structures in the 5' UTR of hepaciviruses and pestiviruses

Our prior results showed that sfRNA formation was a highly conserved mechanism by which all arthropod-borne flaviviruses tested to date suppress XRN1 activity and dramatically alter cellular mRNA stability during infection. Although viruses in the *Flaviviridae* family in the *Hepacivirus* and *Pestivirus* genera do not form sfRNAs from their 3' UTRs (Pijlman et al. 2008), we wondered if they could use an analogous mechanism for suppressing XRN1 activity. Figure 20 shows representative predicted secondary structures of the 3' UTR of flaviviral RNAs and the 5' UTRs of hepacivirus and pestivirus RNAs (adapted from Liu et al. (2009a)). Interestingly, there are conserved secondary and higher-order structures predicted to occur within the 5' UTRs of HCV and BVDV RNAs that could potentially stall the XRN1 exoribonuclease.

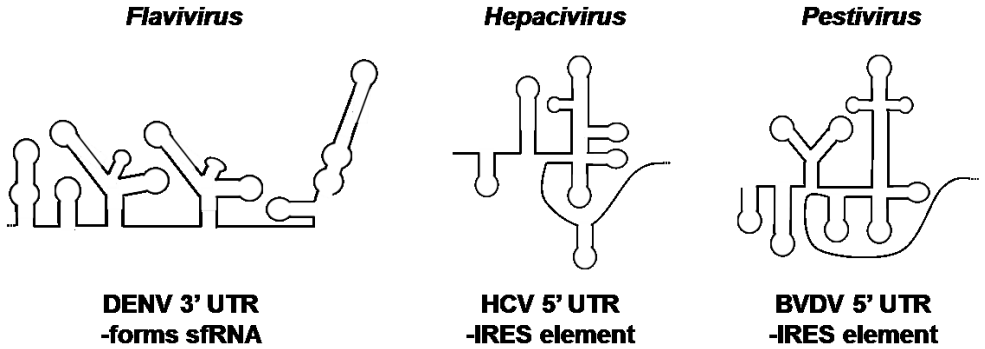

Figure 20. Diagrams of the predicted conserved secondary structures of representative flavivirus UTRs. The flavivirus 3' UTR is known to harbor pseudoknot

structures and additional structural elements implicated in sfRNA formation. Both hepacivirus and pestivirus 5' UTRs also have higher order structures that are implicated in cap-independent translation via internal ribosome entry site (IRES) elements (modified from Liu et al. 2009(a)). UTR = untranslated region; sfRNA = subgenomic flavivirus RNA.

To test the hypothesis that XRN1 stalls on the 5' UTRs of hepacivirus and pestivirus RNAs, we use our *in vitro* assay to compare the 5'-3' decay of reporter RNAs containing a control sequence or the HCV or BVDV 5' UTRs. As depicted in Figure 21A, the BVDV 5' UTR generated at least one distinct RNA decay intermediate when incubated with recombinant XRN1. Furthermore, the HCV 5' UTR also generated a decay intermediate in HeLa cell extract under conditions that favor 5'-3' decay (Figure 21B, left panel) and when the RNA is incubated with recombinant yeast XRN1 (Figure 21B, right panel). Therefore the ability of XRN1 to degrade these RNAs may be hampered by RNA structure in an analogous fashion to that used by the flaviviruses. An unconventional interaction between the liver-specific microRNA miR-122 (Lagos-Quintana et al. 2002) and the HCV 5' UTR was previously shown to facilitate viral replication (Jopling et al. 2005). Importantly, our results indicate that formation of the HCV RNA decay intermediate does not per se rely on the presence of miR-122, as this liver-specific microRNA is not expressed in HeLa cells nor is it present in the recombinant XRN1 assay.

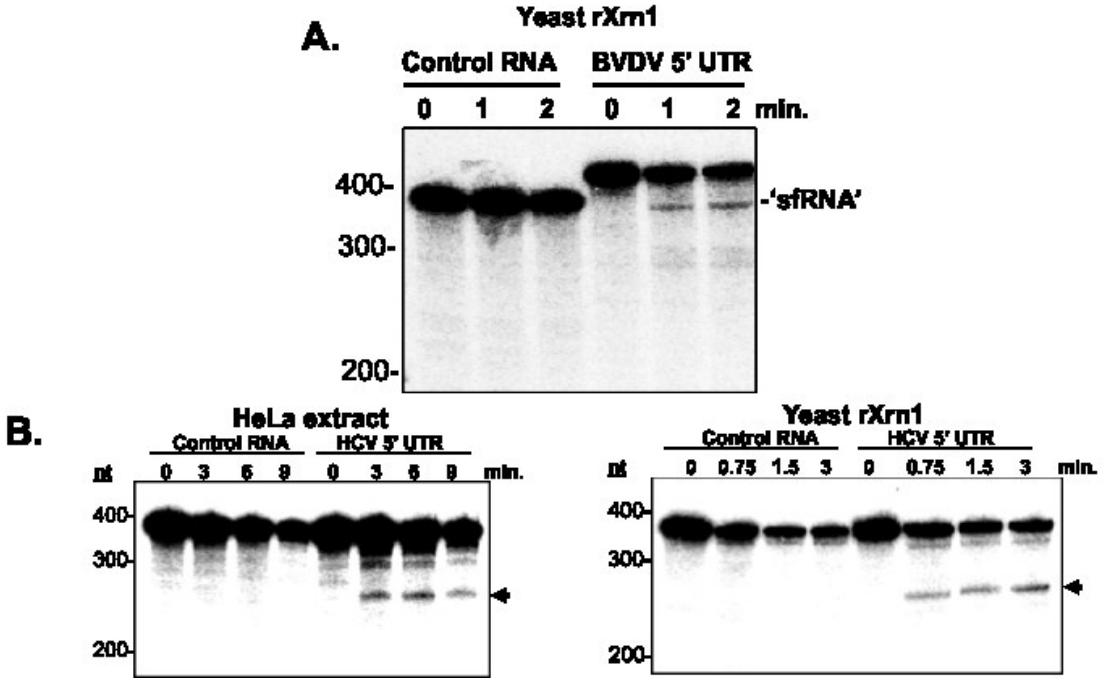

Figure 21. XRN1 stalls on the BVDV and HCV 5' untranslated regions. (A) A 5' monophosphorylated RNA containing the BVDV 5' UTR forms an sfRNA-like decay intermediate when degraded by recombinant yeast XRN1. This experiment was performed in our laboratory by John R. Anderson. (B) The hepatitis C virus 5' UTR also makes an sfRNA-like decay intermediate in HeLa cytoplasmic extract under conditions that highly favor 5'-3' decay (left panel) and when the RNA is incubated with recombinant yeast XRN1 (right panel). Arrows in (B) indicate the sfRNA-like decay intermediates formed as the HCV 5' UTR is degraded in the 5'-3' direction by XRN1.

We next wished to determine if HCV and BVDV 5' UTRs generated decay intermediates in human cells in culture using GFP reporter constructs, as we previously demonstrated that insertion of the DENV-2 3' UTR into the 3' UTR of GFP caused the formation of a distinct 5'-3' decay intermediate (Figure 14A). Human 293T cells were therefore transfected with the empty reporter plasmid peGFP-N1, or peGFP-N1 with the DENV-2 3' UTR, the HCV 5' UTR, or the BVDV 5' UTR inserted into the Not-1 site of the peGFP-N1 plasmid (shown in Figure 22A). As expected, we were able to detect a distinct 5'-3' decay intermediate in cells transfected with the DENV-2 3' UTR-containing GFP construct at 24 hours post transfection in 293T cells (Figure 22B, center lane). However, we were unable to detect distinct decay intermediates in cells transfected with the HCV or BVDV 5' UTR-containing reporter constructs alone (data not shown). Because the GFP reporter transcript is likely quite stable, we hypothesized that the addition of an siRNA that targets a region in the open reading frame of GFP (upstream of the 3' UTR) would stimulate 5'-3' decay of the reporter transcript following endonucleolytic cleavage by the loaded AGO2-containing RISC.

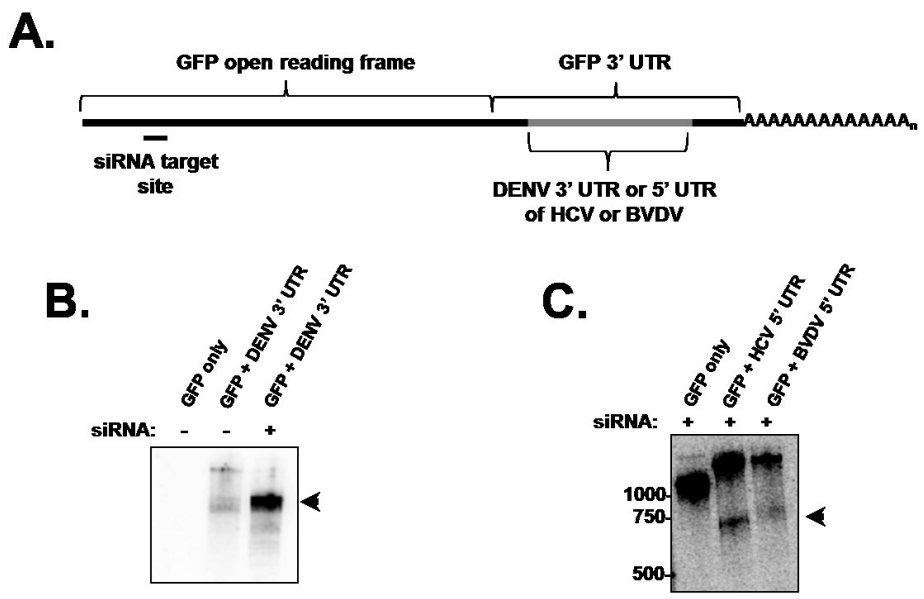

Figure 22. Distinct decay intermediates are generated from GFP reporter constructs containing the HCV and BVDV 5' UTRs. (A) Schematic of the transcript produced by the reporter constructs used for this experiment. The 3' UTR of DENV or the 5' UTR of either HCV or BVDV were inserted into the GFP 3' UTR of the peGFP-N1 reporter plasmid. (B) One µg of total RNA from 293T cells transfected with the empty GFP vector (GFP only) or GFP containing the DENV-2 3' UTR with or without treatment with anti-GFP siRNA (24 hours post transfection) was separated on a 5% denaturing PAGE gel and northern blots were done using a probe to the DENV-2 3' UTR. The sfRNA-like decay intermediates are indicated by the arrow. (C) The empty GFP vector (GFP only) or GFP with the HCV or BVDV 5' UTR inserted as indicated in (A) were transfected into 293T cells, all with siRNA against GFP added. Total RNA was collected 48 hours post transfection and 2 µgs of RNA were resolved on a 5% denaturing PAGE gel. Northern blots were done using a probe to the GFP 3' UTR (3' to the BVDV or HCV 5' UTR insertion) to detect 5'-3' decay intermediates. The sfRNA-like decay intermediates are indicated by the arrow at right. Both (B) and (C) show representative northern blots.

Figure 22B shows that when the anti-GFP siRNA is transfected into cells expressing the GFP + DENV-2 3' UTR reporter construct, the sfRNA-like decay intermediate accumulates to much higher levels. Furthermore, co-transfection of 293T cells with the anti-GFP siRNA and peGFP-N1 with the HCV 5' UTR or the BVDV 5' UTR revealed distinct sfRNA-like decay intermediates (Figure 22C). Therefore, the BVDV and HCV 5' UTRs can generate distinct 5'-3' decay intermediates in human cells, albeit to a lesser extent than those formed by as the DENV-2 3' UTR degrades. These results are consistent with our *in vitro* cell extract based experiments

that support the hypothesis that other host and viral factors are not required for the stalling of XRN1 on the HCV and BVCV 5' UTRs (Figure 21).

XRN1 enzymatic activity is repressed by the HCV and BVDV 5' UTRs

Because sfRNA was previously shown to stall and suppress XRN1 activity, we next wished to assess the ability of HCV and BVDV 5' UTRs to inhibit XRN1 activity. Using competition assays in HeLa cell extracts, we determined that the accumulation of decay intermediates from both the HCV and BVDV 5' UTRs was associated with suppression of XRN1-mediated decay of a reporter RNA (Figure 23). Interestingly, the RNA decay intermediates formed by HCV and BVDV are not as robust as those formed by DENV-2 and JEV in the same assay. However, we observed a significant increase in reporter RNA stability when the HCV and BVDV competitor RNAs were supplied at 66.7-fold the molar amount of the reporter RNA (versus 30-fold the molar amount of DENV-2 and JEV 3' UTRs used for the competition assays reported above in Figures 5 and 6). This may indicate that the HCV and BVDV 5' UTRs are not as strongly inhibitory as the DENV-2 and JEV 3' UTRs in our HeLa cell extract system.

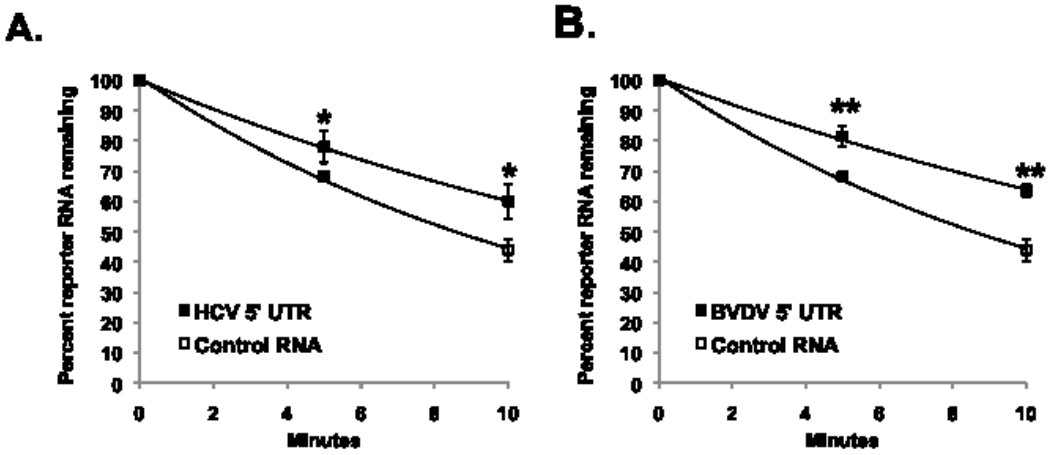

Figure 23. Subgenomic RNAs generated from hepacivirus and pestivirus 5' UTRs suppress XRN1 activity in HeLa cytoplasmic extracts. (A) A 5' monophosphorylated reporter RNA susceptible to XRN1-mediated decay was incubated with ~66.7x molar excess of 5' monophosphorylated competitor RNAs in HeLa cell extract and RNA was

isolated at 0, 5, and 10 minutes to resolve on a 5% denaturing polyacrylamide gel. The percent reporter RNA remaining was determined by quantification following phosphorimaging. (A) Shows the average +/- standard deviation of the percent reporter RNA remaining in each time point from three independent experiments with an HCV 5' UTR competitor RNA or a control competitor RNA. (B) Shows the average +/- standard deviation of the percent reporter RNA remaining at each time point in the presence of BVDV 5' UTR competitor or a control RNA competitor from two independent experiments. Student's t-test was used to assess significance, with * indicating $p \leq 0.05$ and ** $p \leq 0.01$. The above experiments were performed by John R. Anderson in our laboratory.

To determine if XRN1 activity was suppressed in human Huh7.5 cells infected with HCV, we analyzed the relative abundance of uncapped cellular transcripts. We hypothesized that if XRN1 activity was compromised by the formation of HCV subgenomic RNA, we would observe a significant increase in uncapped cellular RNAs compared to mock-infected cells. HCV infections were performed in collaboration with Dr. Shelton Bradrick (Duke University). As depicted in Figure 24A, human Huh7.5 liver cells infected with HCV (JFH-1 strain) showed a small but significant increase in the relative abundance of uncapped cellular mRNAs compared to mock infected cells. Interestingly, this effect was not dependent on the presence of HCV structural proteins, as Huh7.5 cells harboring a replicon HCV RNA also had an increase in the abundance of uncapped short-lived cellular transcripts (Figure 24B; the I_{389}/NS3-3′ replicon is described in Lohmann et al. 1999). Thus we conclude that XRN1 activity is likely suppressed in HCV infections, as uncapped mRNAs accumulate to a similar degree as observed in DENV-2 and KUNV infected cells (Figure 8) and the 5'-3' decay of a reporter transcript in HeLa cell extract is significantly reduced in the presence of HCV or BVDV 5' UTR competitor RNAs (Figure 23).

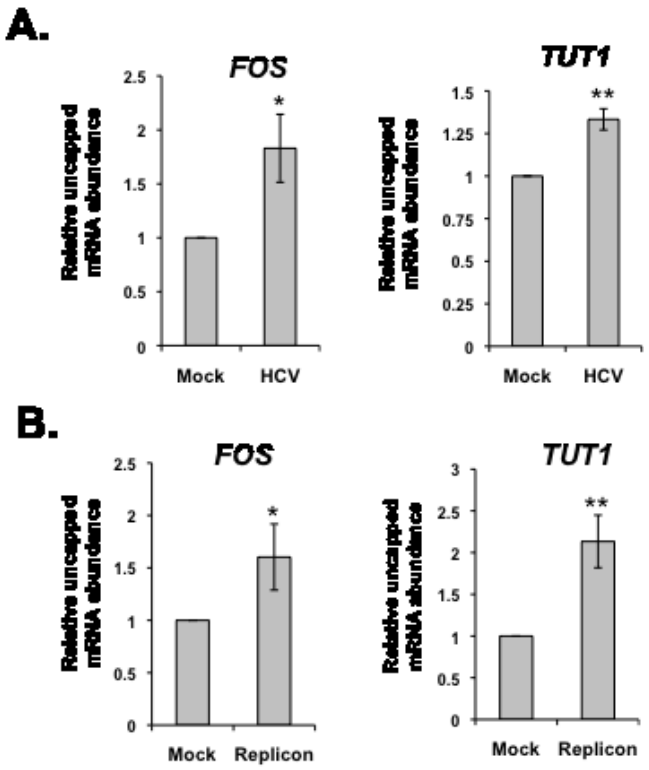

Figure 24. Uncapped mRNAs accumulate in HCV infected cells. (A) Total RNA from Huh7.5 cells either mock infected or infected with the JFH-1 strain of HCV (72 hpi) was fractionated into capped and uncapped portions, and the relative abundance of *FOS* and *TUT1* mRNAs in the uncapped fraction (normalized to the 10% input fraction) was determined by RT-qPCR using the uncapped *7SL* RNA as a reference gene. (B) RNA from Huh7.5 cells harboring an HCV replicon (I389/NS3-3'UTR) was fractionated and analyzed as in (A). Shown above are the averages +/- standard deviations of the relative abundances of each transcript from three independent infections. Infections and RNA extractions were performed by Dr. Shelton Bradrick at Duke University. Student's t-test was performed to assess significance, with * indicating $p \leq 0.05$ and ** $p \leq 0.001$.

Previously published data show that the HCV 5' UTR is degraded in the 5'-3' direction, presumably by XRN1 (Li et al. 2013(b)). Although it was not interpreted as stalling of the XRN1 exonuclease, the accumulation of what appears to be distinct 5'-3' decay intermediates of the 5' end of the HCV genome were observed (Li et al. 2013(b)). The authors of this study used an RNA ligation procedure to capture monophosphorylated HCV RNAs from infected cells in culture for cloning and sequence analysis of the HCV 5' UTR (Li et al. 2013(b)). Interestingly, the 5' end of the majority of these reported sequences was ~55 nt or ~80 nt from the end of the full-length 5' UTR of the HCV genomic RNA (Li et al. 2013(b)). Furthermore, it was recently demonstrated that an *in vitro* transcribed RNA containing the HCV 5' UTR physically associates

with XRN1 in 293T cells (Bradrick et al. 2013). These data indicate that the stalling of XRN1 on the HCV/BVDV 5' UTR may similarly cause a delay in the dissociation of the enzyme from the RNA substrate, leading to XRN1 suppression. Consistent with this, we have preliminary evidence indicating that BVDV RNA is associated with XRN1 during infections of bovine MDBK cells (Figure 25). Co-immunoprecipitation of XRN1 and associated RNAs from infected cells revealed a specific interaction between the BVDV genomic RNA and XRN1.

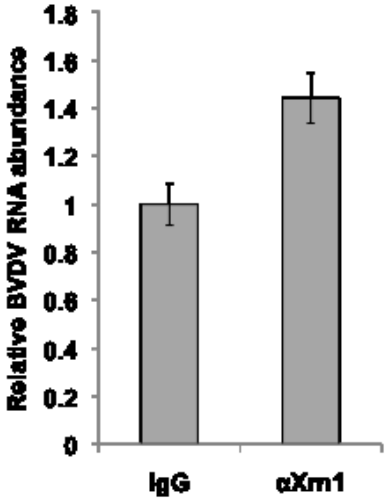

Figure 25. The BVDV genomic RNA is physically associated with XRN1 during infection. Bovine MDBK cells infected with cytopathic BVDV were formaldehyde cross-linked and lysed for co-immunoprecipitation with antibody to XRN1 (αXRN1) or a non-specific control antibody (IgG). Total RNA from the 10% input fraction and the immunoprecipitated fraction was reverse transcribed and the relative abundance of BVDV RNA was assessed in each fraction using primers to the BVDV 5' UTR. Shown above is an intriguing preliminary result from one experiment showing the relative amount of BVDV RNA +/- the error of measurement in the immunoprecipitation fraction relative to the 10% input fraction from one experiment.

The stability of mRNAs encoding oncogenes and angiogenic factors is dysregulated in hepacivirus and pestivirus infected cells

Previous studies have demonstrated that several oncogenes and angiogenic factors are up-regulated in various models of HCV infection and/or in patient tissues. The oncogene c-FOS has been shown to positively regulate HCV replication in cell culture (Kang et al. 2011(a)) and c-JUN over-expression can contribute to HCV-induced hepatocellular carcinoma (HCC) (Machida

et al. 2010). The oncogene c-myc is increased in the livers of HCV patients and in a transgenic mouse model of HCV infection (Higgs et al. 2013). Vascular endothelial growth factor A (VEGFA) is angiogenic and is known to be over-expressed in non-tumor regions of livers from patients with HCV-associated HCC (Chiang et al. 2008). Interestingly, VEGFA treatment was shown to increase liver mass by inducing liver sinusoidal endothelial cells to produce hepatocyte growth factor, ultimately leading to liver cell proliferation (LeCouter et al. 2003). Hypoxia inducible growth factor 1α (HIF1A) is another angiogenic factor that enhances HCV propagation and also stimulates the migration and altered cell polarity of hepatocytes in a cell culture model of metastasis (Wilson et al. 2012; Mee et al. 2010). Finally, chemokine (C-X-C motif) ligand 2 (CXCL2) is induced by the pro-inflammatory transcription factor NFκB, and is up-regulated in a tree-shrew (*Tupaia spp.)* hepatocyte model of HCV infection (Guitart et al. 2005). It follows then that hepatocellular carcinoma may be a result of the over-expression of potent oncogenic and angiogenic factors in HCV infected liver cells.

We previously demonstrated that sfRNA formation/XRN1 repression by arthropod-borne flaviviruses is correlated with increased expression of several pro-inflammatory factors and XRN1 suppression, and that HCV RNAs can inhibit XRN1 activity (Figures 14 and 22). We therefore sought to determine if changes in mRNA stability might account for the increased expression of several factors implicated in the development of hepatocellular carcinoma due to HCV. As seen in Figure 26A, the transcripts of three oncogenic factors, c-FOS (*FOS*), c-JUN (*JUN*), and c-myc (*MYC*), are significantly increased in abundance in HCV infected cells compared to mock infected cells. The three angiogenic factors vascular endothelial growth factor A (VEGFA), hypoxia induced factor 1α (*HIF1A*), and the chemokine *CXCL2* are also significantly increased compared to control cells. We next evaluated mRNA stability in cells infected with HCV (JFH-1 strain) or mock infected by actinomycin D transcriptional shut-offs at 72 hpi. Figure 26B shows representative mRNA decay curves of all six transcripts of oncogenes or angiogenic factors in mock and HCV infections and the average half-life from three

independent infections is also reported (graph insets). Strikingly, all six transcripts were significantly more stable in HCV infected cells when compared to mock infected cells. Therefore, changes in mRNA stability during HCV infection could account for the increased expression of several oncogenes and angiogenic factors implicated in HCV-induced hepatocellular carcinoma. One potential mechanism by which this could occur is by suppression of XRN1 by HCV RNAs, as we demonstrated occurs in flavivirus infections.

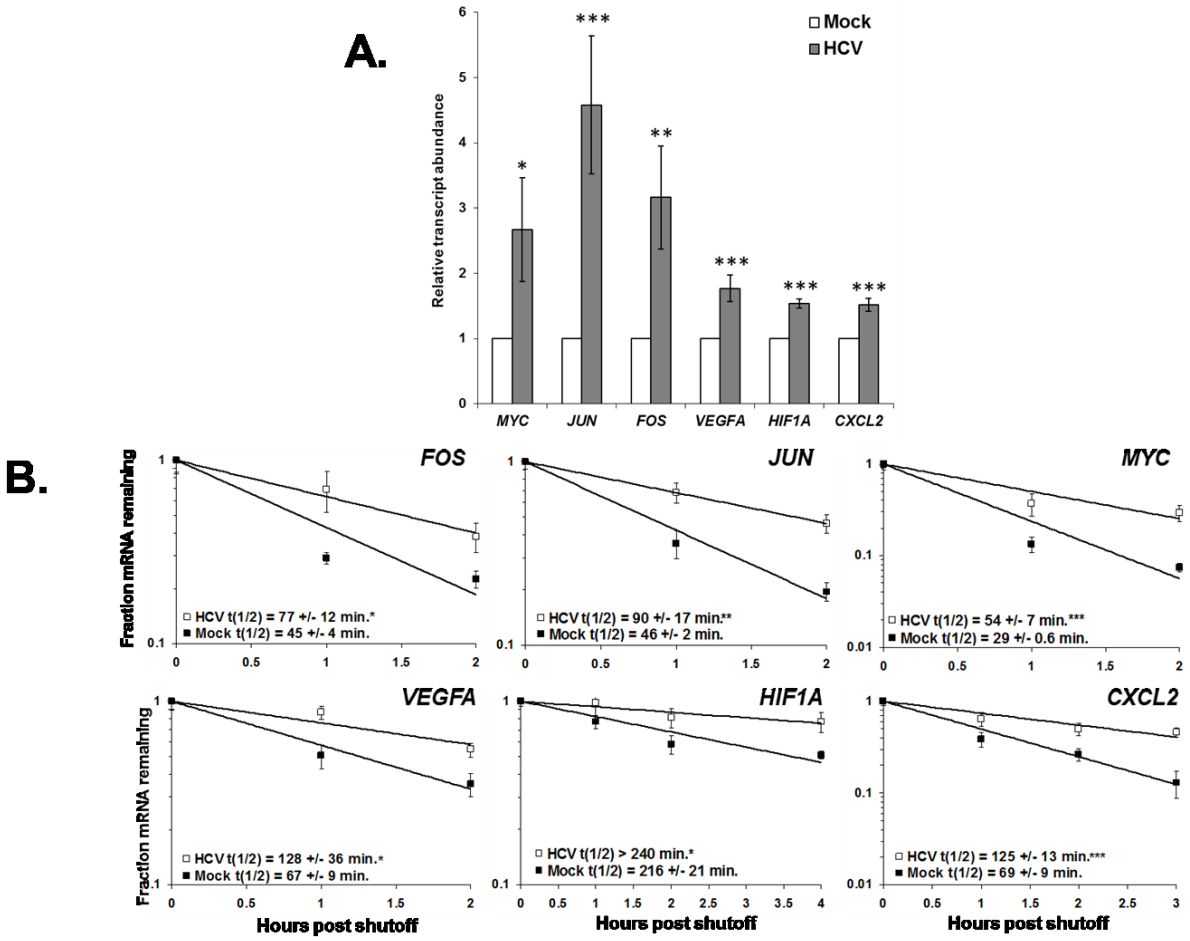

Figure 26. Six oncogenic or angiogenic factors implicated in HCV-induced hepatocellular carcinoma are up-regulated and stabilized at the mRNA level in HCV infected human cells. (A) Human Huh7.5 cells were infected with the JFH-1 strain of HCV and at 72 hpi RT-qPCR analysis was performed to assess the relative abundance of *FOS*, *JUN*, *MYC*, *VEGFA*, *HIF1A*, and *CXCL2* using *GAPDH* as a reference gene. Shown are the averages +/- standard deviations of the relative mRNA abundances from three independent infections. (B) The stability of each transcript was assessed by actinomycin D shut-off and RT-qPCR analysis of mock infected or HCV-infected cells (72 hpi). A representative decay curve for each transcript is shown with the average +/- standard deviation of the half-life (minutes) calculated from three independent infections in the inset panels. Hepatitis C virus infections and RNA isolations were done by Dr.

Shelton Bradrick at Duke University. Student's t-test was used to assess significance with * indicating $p \leq 0.05$, **$p \leq 0.01$, and ***$p \leq 0.005$.

If changes in mRNA stability during HCV infection were due to the stalling of XRN1 on highly structured viral RNAs, then we hypothesized that the related pestiviruses would also cause stabilization of short-lived cellular RNAs. To address this, we infected bovine MDBK cells with cytopathic BVDV and assessed the abundance and stability of two short-lived mRNAs, *JUN* and *FOS*, which were shown to be up-regulated and stabilized in human liver cells infected with HCV. Importantly, c-JUN and c-FOS are oncogenes, but are also known to play important roles in organism development and growth- and thus could have a major impact on the pathogenesis of BVDV infections. A large-scale bioinformatics and literature mining approach to identify novel transcription factors important for bovine embryo development identified c-FOS as one such factor (Turenne et al. 2012). Furthermore, studies using a murine cell culture model of mammalian development revealed that c-FOS and c-JUN expression can be induced only in differentiated cells, and c-JUN expression increases over the course of chemical-induced differentiation of mouse embryonal carcinoma cells (de Groot et al. 1990). In mammalian cells, c-FOS and c-JUN proteins can together form a heterodimer called the AP-1 transcription factor complex, which is specifically known to be important for proper bone development and growth (Wang et al. 1992) in addition to promoting carcinogenesis in certain systems (as discussed above). The c-FOS protein regulates mammalian bone development, growth, and hematopoiesis (Ruther et al. 1987; Wang et al. 1992). Intriguingly, c-FOS and c-JUN were shown to be up-regulated at the mRNA level in bovine B cell lymphosarcoma BL3 cells infected with cytopathic BVDV through an unknown mechanism (Neill and Ridpath 2008). Infection of pregnant heifers with BVDV can lead to abortions (Brownlie et al. 1989), defects in fetal growth (Grooms et al. 2004; Done et al. 1980), and fetal bone malformations (Webb et al. 2012; Webb et al. 2013). These developmental abnormalities could be contributed to by dysregulated host

gene expression resulting from BVDV infection, potentially by aberrant expression of short-lived growth factors including c-FOS or c-JUN in the developing embryo.

At 24 hpi, when all cells are infected with BVDV (as determined by immunofluorescence assays (Figure 27A), both *JUN* and *FOS* are significantly up-regulated at the mRNA level (Figure 27B). Furthermore, as observed in HCV infected cells, the stability of *JUN* and *FOS* mRNAs is significantly increased in cells infected with BVDV compared to mock infected cells (Figure 27C). These results indicate that significant changes in mRNA stability are observed in HCV and BVDV infections, possibly due to the suppression of XRN1 by highly structured viral RNAs. Because we have demonstrated that distinct decay intermediates are detected in cells transfected with reporter constructs bearing the 5' UTRs of BVDV and HCV (Figure 22), we are currently working to determine if changes in mRNA stability consistent with suppression of XRN1 activity occur in the absence of viral infection.

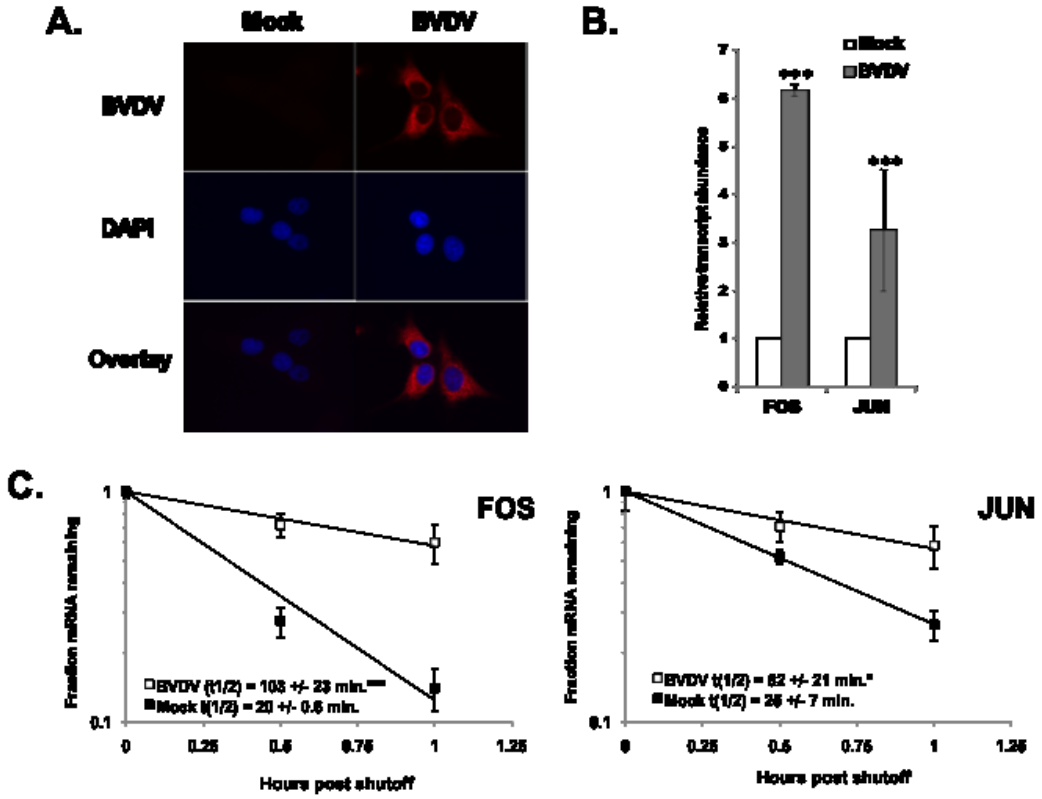

Figure 27. The abundance and stability of *FOS* and *JUN* mRNAs are significantly increased in BVDV infected cells. (A) Indirect immunofluorescence analysis of MDBK

cells mock infected or infected with BVDV (24 hpi, MOI of 10) using a primary antibody that recognizes all strains of cytopathic and non-cytopathic BVDV and a secondary antibody tagged with Alexafluor 594 (red). Nuclei are stained by DAPI and are shown in blue. Photographs are representative of three independent infections. (B) The two short-lived mRNAs *FOS* and *JUN* are more abundant in BVDV infected cells as determined by RT-qPCR analysis with beta actin (*ACTB*) set as the reference gene. The average +/- standard deviation of each transcript abundance from three independent infections are shown. (C) Both *FOS* and *JUN* are significantly stabilized during BVDV infection compared to mock-infected cells as determined by actinomycin D transcriptional shut-offs and RT-qPCR using *ACTB* as a reference gene. Representative decay curves are shown with the average +/- standard deviation of each half-life (minutes) from three independent replicates reported in the inset panels. Statistics reported in (B) and (C) are p-values from Student's t-test with * indicating $p \leq 0.05$, ** $p \leq 0.01$, *** $p \leq 0.005$.

Cellular mRNAs that are stabilized and increased in abundance in HCV and BVDV infections are intact and translatable

If the changes in post-transcriptional regulation of gene expression that were reported above in HCV and BVDV infected cells are contributing to changes in cell or organism biology as a result of infection (e.g. hepatocellular carcinoma due to HCV infection), then the proteins encoded in those transcripts must be expressed differentially. We therefore assessed the relative abundance of the translatable form (i.e. capped and polyadenylated) of the six transcripts we determined to be up-regulated and stabilized at the mRNA level in HCV infections (Figure 26). We fractionated total RNA from Huh7.5 cells mock infected or infected with HCV using an antibody that recognizes the 7-methylguanosine cap structure to generate a pool of RNA that contained capped RNAs only. We then reverse transcribed the capped RNA using an oligod(T) primer to capture polyadenylated RNAs. Using qPCR to quantify the relative abundance of each transcript in mock and HCV infected cells, we found a significant increase in the amount of capped and polyadenylated mRNAs encoding oncogenes or angiogenic factors in HCV infected cells (Figure 28A). Furthermore, bovine MDBK cells infected with BVDV showed a significant increase in the abundance of both FOS and JUN proteins as assessed by western blotting (Figure 28B). These results contrast with previous findings that FOS and JUN proteins are down-regulated in BL3 cells infected with BVDV, although the abundance of ACTIN was

also surprisingly severely reduced in BVDV infected samples in that study (Neill and Ridpath 2008). These data imply that there could be cell-type specific defects in general protein synthesis during BVDV infections. However, in MDBK cells, we did not observe a comparable decrease in the house-keeping protein GAPDH, and western blots were performed using equal quantities of total protein from mock and BVDV infected cells (Figure 28B). Furthermore, monocytes infected with cytopathic BVDV were shown to have no change in the abundance of actin protein by western blot in another study (Lee et al. 2008). Our results indicate that the abundance of polyadenylated and capped mRNAs or protein is positively correlated with the stability of several important cellular transcripts encoding oncogenic or growth factors in BVDV and HCV infected cells.

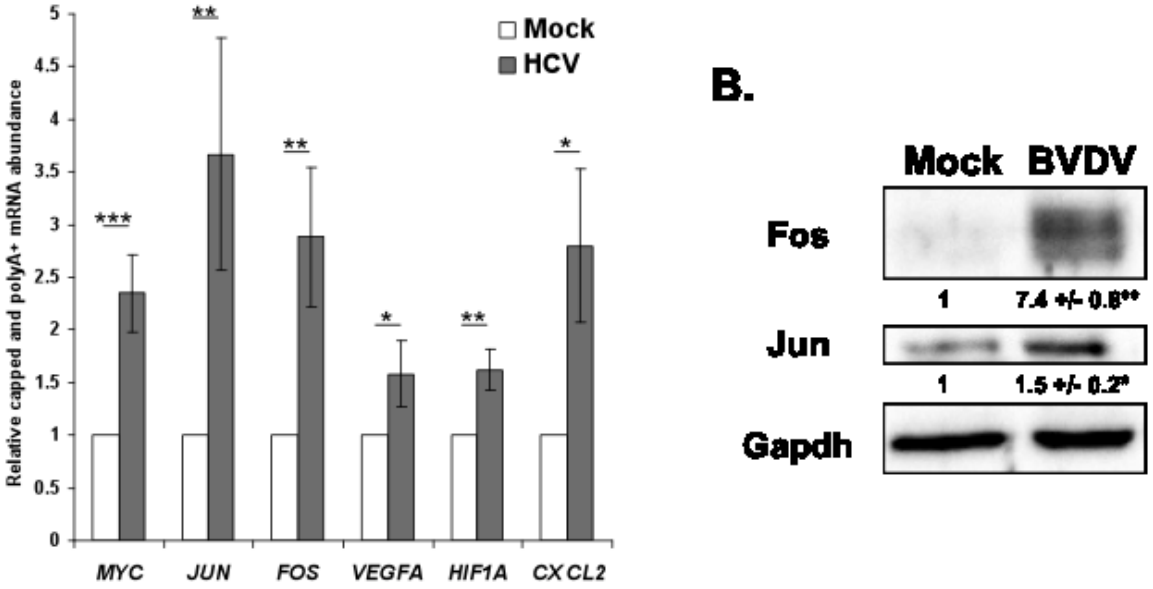

Figure 28. Inhibition of XRN1 may feedback and inhibit the entire 5'-3' decay pathway during HCV infection. (A) Stabilized, up-regulated transcripts encoding oncogenes and angiogenic factors are capped and polyadenylated. Total RNA from Huh7.5 cells mock infected or infected with HCV was fractionated to remove uncapped RNAs, and oligo d(T) was used to selectively reverse transcribe polyadenylated RNAs. The relative abundance of each mRNA was then assessed by qPCR using *GAPDH* as a reference gene. The average +/- standard deviation of three independent infections is shown above with significance assessed by Student's t-test (* indicates $p \leq 0.05$, ** $p \leq 0.01$, *** $p \leq 0.005$). Hepatitis C virus infections and isolation of total RNA were performed by Dr. Shelton Bradrick at Duke University. (B) Bovine MDBK cells infected with BVDV have increased levels of JUN and FOS proteins compared to mock infected

cells. Representative western blots are shown above with the average +/- standard deviation of the chemiluminescent signal from three independent infections is shown relative to GAPDH. Student's t-test was done to determine significance and * indicates $p<0.01$, ** indicates $p<0.001$.

Section III. Towards the elucidation of the structure of the XRN1-resistant sfRNA

Kunjin virus sfRNA formation requires a three-helix junction *in vivo*

Previous work identified several conserved pseudoknot-like structural motifs in the 3' UTRs of flaviviruses that were associated with sfRNA formation (Pijlman et al. 2008; Funk et al. 2010; Silva et al. 2010), but the exact structure required to stall XRN1 remained unknown. Recent work in the Kieft laboratory (University of Colorado, Denver, Anschutz School of Medicine) demonstrated that formation of sfRNA likely depends on a more complex structure that involves the interactions of several pseudoknots together to stabilize the RNA and prevent XRN1-mediated decay (Chapman et al. 2014; Chapman et al. *in press*). Using phylogenetic and biochemical approaches, each XRN1-resistant (sfRNA-forming) viral 3' UTR motif was shown to contain a conserved three-helix junction upstream from a pseudoknot and a hairpin. Importantly, the ~19 nucleotides required for these structures to form were conserved among all sfRNA-forming flaviviruses tested using *in silico* analyses (Chapman et al. 2014). Furthermore, the crystal structure of the XRN1-resisant sfRNA formed by the Murray Valley encephalitis virus (MVEV) 3' UTR determined by the Kieft laboratory (Chapman et al. *in press*) indicated that the resistance of these sfRNAs to XRN1 was likely conferred by a set of interwoven pseudoknots that stabilizes the 5' end of the viral RNA, keeping the 5' end from entering the active site of XRN1 (Chapman et al. *in press*). This complex three-dimensional structure was predicted to be stabilized by a short, highly conserved sequence element found in all sfRNA-forming flavivirus 3' UTRs.

We therefore generated six mutant Kunjin viruses using the FLSDX(pro)_HDV infectious clone (Liu et al. 2003) to determine the impact on XRN1 stalling in living cells of mutating conserved sequences in the 3' UTR predicted to be essential for sfRNA formation. Three sfRNAs are usually formed from the KUNV 3' UTR during infection. The largest one, sfRNA1, is the most abundant sfRNA in wild-type KUNV infections and sfRNAs 1 and 2 are likely the most biologically relevant. In support of this, the low cytopathogenic sfRNA-deficient KUNV (CS3ΔIRA) used in the studies depicted in section I of this results section fails to generate both sfRNA1 and sfRNA2, but sfRNA3 accumulates to low levels as shown in Figure12B. The CS3ΔIRA KUNV has a 3 nt substitution in stem-loop II of the KUNV 3' UTR that abrogates sfRNA1 formation, and a 10 nt deletion near stem-loop IV that abolishes sfRNA2 formation (Pijlman et al. 2008). In collaboration with the Kieft laboratory, we made targeted mutations in the KUNV 3' UTR that were predicted to abrogate the formation of sfRNA1 and/or sfRNA 2 (the sequences of each mutant virus 3' UTR are reported in Appendix 5). Based on biochemical, phylogenetics, and structural studies, the Kieft laboratory determined that C10519 and C10680 were required for stabilization of the interwoven pseudoknot structures that allowed the formation of sfRNA1 and sfRNA2 (respectively) in the KUNV 3' UTR.They also determined that nucleotides AGU10498-10500 and UGU10658-10660 were likely essential for KUNV sfRNA1 and sfRNA2 formation (respectively) based on the crystal structure of MVEV sfRNA (Chapman et al. *in press*). Therefore, three viruses with a G substituted for C10519 and/or C10680 were generated, and three viruses with AGU→UCA10498-10500 and/or UGU→ACA10658-10660 mutations were made to determine if these nucleotides were required for sfRNA formation in viral infections in cell culture.

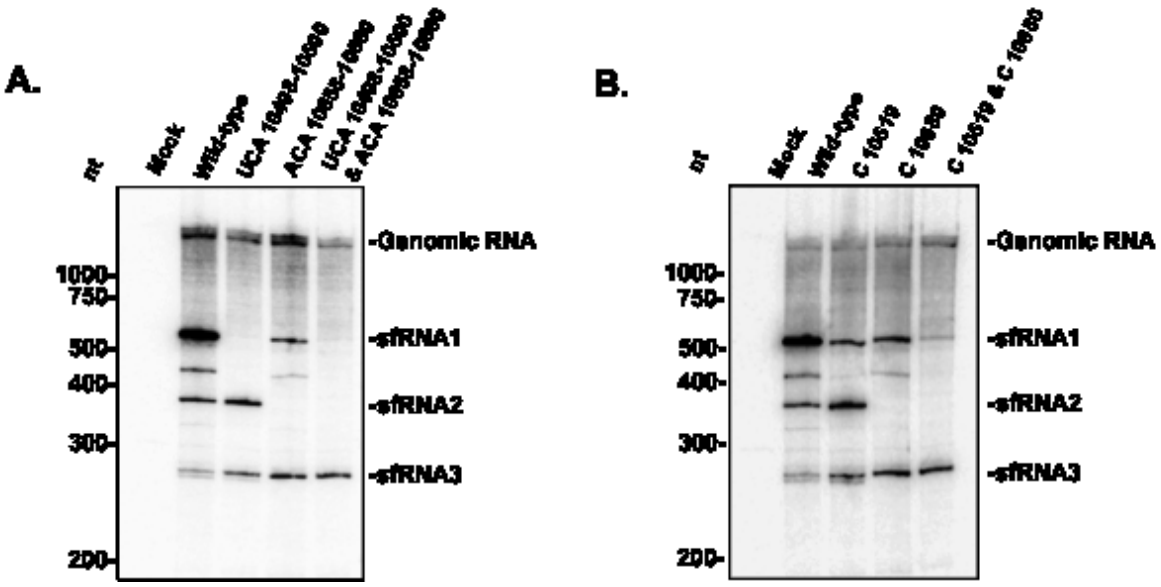

Figure 29. Kunjin virus sfRNA formation depends on the formation of a three-helix junction involving interwoven pseudoknots. Mutation of nucleotides in the 3' UTR of Kunjin virus predicted to disrupt (A) the closing of a ring structure to protect the viral RNA from XRN1-mediated decay or (B) the stabilization of a three-helix junction abrogate or severely limit sfRNA1 or sfRNA2 formation.

Human 293T cells were infected (MOI of 10) with each virus and total RNA collected at 48 hpi was separated on a 5% polyacrylamide gel for northern blotting to assess sfRNA formation. The northern blot shown in Figure 29A show that AGU10498-10500 and UGU10658-10660 are required for the formation of sfRNA1 and sfRNA2 (respectively). Similarly, the northern blot shown in Figure 29B shows that the C→G10519 and C→G10680 mutations also abrogated sfRNA1 and sfRNA2 formation as predicted. These data demonstrate that in the context of a KUNV infection of human cells, sfRNA formation relies on the formation of a complex three-dimensional structure that will be reported in detail in Chapman et al. (*in press* (b)).

Section IV. Additional functions of sfRNA: suppression of RNA interference

sfRNA-mediated inhibition of Argonaute-2 may inhibit RNAi

Our data indicate that one important role of sfRNA during viral infection is to suppress the host exoribonuclease XRN1. However, sfRNA from DENV-2 and WNV has also been shown to suppress RNA interference (RNAi) in non-human primate and mosquito cells, although the mechanism by which this occurs has not been fully characterized (Schnettler et al. 2012). Furthermore, the single previous study on sfRNA and RNAi that was published while our studies were ongoing used replicon constructs or RNA transfections in lieu of viral infections (Schnettler et al. 2012). Thus conclusions that can be drawn may be limited by this experimental design. One possible mechanism by which sfRNA suppresses RNAi is by acting as a competitive inhibitor or sink for DICER and/or AGO2 (the cytoplasmic effector proteins required for this process) due to its highly-structured nature (Rauscher et al. 1997).

Intriguingly, AGO2 can bind long hairpin-containing miRNA precursors (Cifuentes et al. 2010; Yang et al. 2010; Cheloufi et al. 2010) and shRNAs (Yang et al. 2012; Liu et al. 2013(b)) in vertebrate cells. These results indicate that AGO2 can bind and process RNAs that are larger than typical siRNAs or miRNAs. Therefore, we hypothesized that the mechanism by which sfRNA suppresses RNAi is through the binding and sequestration of Argonaute-2 (AGO2) and DICER. To test the hypothesis that AGO2 may be inhibited by sfRNA, we first assessed AGO2 activity in human cells during DENV-2 infection. Human 293T cells were infected with DENV-2 (MOI of 3) or mock infected, and 3 days later were transfected with a reporter plasmid encoding eGFP and an siRNA to eGFP or water as a negative control. After 24 hours, total RNA was collected from the cells and the abundance of eGFP mRNA was assessed by northern blotting (Figure 30A) or RT-qPCR (Figure 30B) to determine if there were any defects in eGFP knockdown by the siRNA during viral infection.

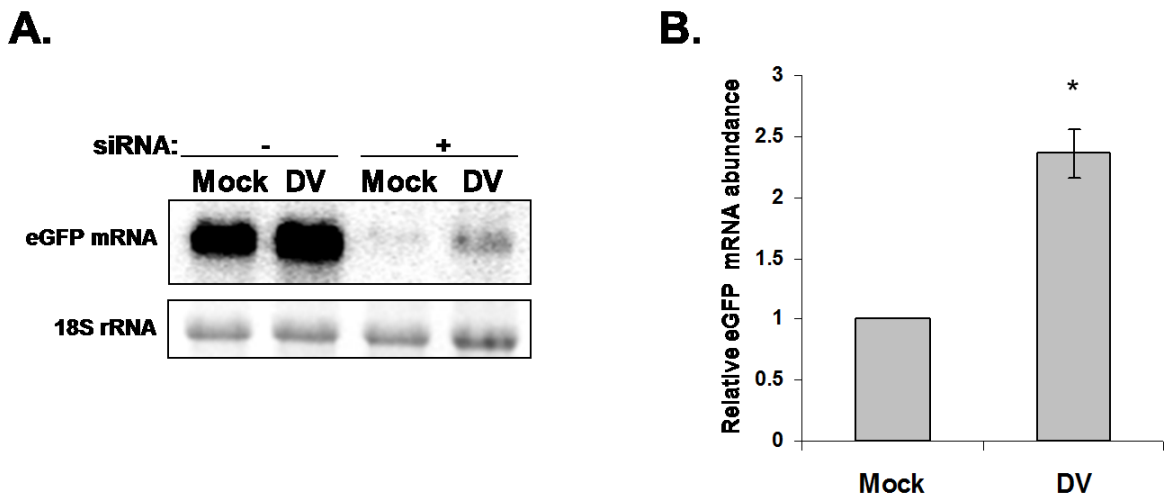

Figure 30. siRNA-mediated knockdown of the reporter eGFP is suppressed in DENV-2 infected cells when sfRNA is abundant. (A) A representative northern blot to detect eGFP mRNA using a probe that spans the siRNA-target site, with ethidium bromide-stained 18S rRNA as a loading control depicted at the bottom of the panel. Mock and DENV-2 infected cells (MOI of 3) were transfected with peGFP-N1 plasmid +/- an siRNA to eGFP (or water as the negative control) at 3 days post infection. Twenty-four hours later, total RNA was collected and 5 micrograms from each sample was resolved on a denaturing agarose gel and probed for eGFP. (B) To quantify the relative repression of eGFP knockdown in DENV-2 infected cells relative to mock infected cells, RT-qPCR was done using primers that span the siRNA-target site to detect the relative abundance of intact eGFP mRNA using *GAPDH* as a reference gene. The siRNA-containing samples were normalized to the samples that were not transfected with siRNA (water only). Shown above is the average +/- standard deviation of two independent infections. * indicates $p < 0.05$ by Student's t-test. Abbreviations: DV= dengue virus type 2.

As depicted in Figure 30A, eGFP mRNA was dramatically reduced in abundance by 24 hours post-transfection with an siRNA targeted to the eGFP open reading frame. Interestingly, human 293T cells infected with DENV-2 showed a repression of eGFP knockdown by siRNA as measured by northern blot (Figure 30A). For a more quantitative assessment of the relative suppression of siRNA-mediated eGFP knockdown, the relative abundance of intact eGFP mRNA was assessed using primers that span the siRNA-mediated AGO2 cleavage site (Figure 30B). This method was used to ensure that qRT-PCR measurements were actually measuring intact eGFP mRNA that was not cleaved endonucleolytically by the siRNA-AGO2 complex. We determined that cells infected with DENV-2 slightly (~2-fold) de-repress eGFP expression in the presence of anti-eGFP siRNA. This is in agreement with previous findings that Vero cells harboring a WNV or dengue virus type 1 replicon have a ~2-fold increase in luciferase activity in

the presence of anti-luciferase shRNA compared to untransfected Vero cells (Schnettler et al. 2012).

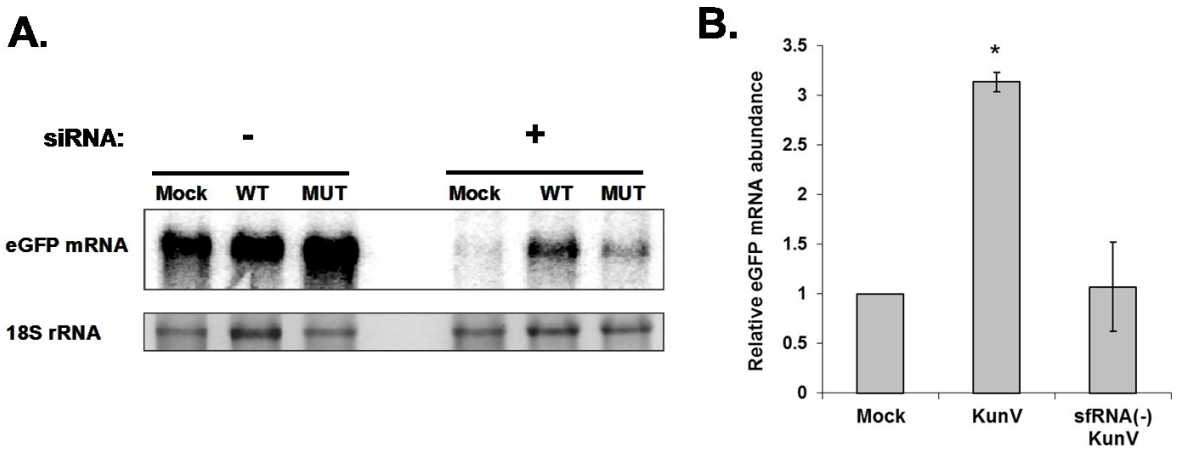

Figure 31. siRNA-mediated knockdown of the reporter eGFP is suppressed in an sfRNA-dependent manner in Kunjin virus infected 293T cells. (A) A representative northern blot showing eGFP mRNA abundance with 18S rRNA stained with ethidium bromide as a loading control. Human 293T cells were mock infected or infected with wild-type Kunjin virus (WT) or an sfRNA-deficient Kunjin virus (MUT) lacking sfRNA1 and sfRNA2 (MOI of 10). After 24 hours, the cells were transfected with peGFP-N1 and either water (- siRNA) or an siRNA to eGFP (+ siRNA). Total RNA from each sample was collected 48 hpi and 5 micrograms of each was resolved on a formaldehyde agarose gel and blotted using an RNA probe to the eGFP open reading frame. (B) RT-qPCR was done to quantify the relative knockdown of eGFP by siRNA using *GAPDH* as a reference gene. Results are the average +/- standard deviation of two independent infections. The * indicates $p<0.05$ using Student's t-test.

To determine if sfRNA formation is required for the de-repression of eGFP gene expression during other flavivirus infections, we infected human 293T cells with a wild-type Kunjin virus or an sfRNA-deficient Kunjin virus. As shown in Figure 31, KUNV infection also partially rescues eGFP mRNA expression in the presence of anti-eGFP siRNA. As determined by RT-qPCR of RNAs from mock infected and infected cells, the relative knockdown of eGFP is significantly decreased in wild-type but not sfRNA-deficient Kunjin virus infected cells. Similar to the DENV-2 infections, the reduction in eGFP knockdown was calculated to be ~3-fold. Of note, the sfRNA-deficient Kunjin virus used in this study is capable of generating at least one small sfRNA (sfRNA3, visible in the left panel of Figure 13B) that could be responsible for these small increases in gene expression. This may be particularly relevant in this experiment, as cells were infected at a high multiplicity of infection (10) and collected 60 hpi, when the smaller sfRNA3

had likely accumulated to a potentially significant level. Our results indicate that one major mechanism by which RNAi is suppressed by sfRNA in human cells is through the inhibition of AGO2 activity.

Schmitter et al. (2006) showed that when AGO2 and/or DICER are knocked down in 293T cells, subtle but significant changes in the abundance of many mRNAs results. Accordingly, as an alternative method of measuring AGO2 and/or DICER activity in cells infected with DENV-2 or KUNV, we looked for changes in the abundance of a set of transcripts that was shown to be increased (less than 2-fold) when AGO2 and/or DICER were depleted by shRNA-mediated knock-downs (Schmitter et al. 2006). This set of transcripts included aquaporin 3 (*AQP3*), armadillo repeat containing, X-linked 4 (*ARMCX4*), clathrin, heavy chain (*CLTC*), catenin (cadherin-associated protein) β 1 (*CTNNB1*), and motile sperm domain containing 2 (*MOSPD2*). Intriguingly, a small but significant increase in the expression of five transcripts shown to be elevated upon depletion of AGO2 and/or DICER was observed in cells infected with DENV-2 (Figure 32A). To assess the impact of sfRNA formation on these changes in mRNA abundances during infection and to determine if this was a DENV-2 specific effect, we next assessed the abundance of these transcripts in KUNV infected cells. Cells infected with wild-type KUNV had a significant increase in four out of five transcripts evaluated (Figure 32B, dark grey bars). Interestingly, although cells infected with the sfRNA-deficient KUNV also showed a slight increase in the abundance of two of these transcripts, overall the increased abundance of four of the transcripts correlated with sfRNA accumulation. However, as discussed above, the sfRNA-deficient KUNV generates a small sfRNA (sfRNA3), albeit to lower levels than sfRNA1 and sfRNA2 in wild-type virus infections. Therefore, the enhanced abundance of two of the four transcripts in the sfRNA-deficient KUNV infected cells could be due to the low amount of sfRNA3 that accumulates by 60 hpi.

As an aside, *AQP3*, *ARMCX4*, and *MOSPD2* were not represented in the RNA-seq datasets from KUNV or sfRNA-deficient KUNV infections (Figure 17). Furthermore, the

abundance of *CLTC* and *CTNNB1* were not substantially altered in KUNV or sfRNA-deficient KUNV infected cells (Figure 18). This is likely due to the lower multiplicity of infection and/or earlier time post infection that the RNA samples for sequencing analysis were collected at. However, our qRT-PCR results indicate that changes in gene expression consistent with AGO2 and/or DICER depletion are altered in flavivirus infected cells, potentially as a result of the direct inhibition of AGO2 or DICER activity by sfRNA.

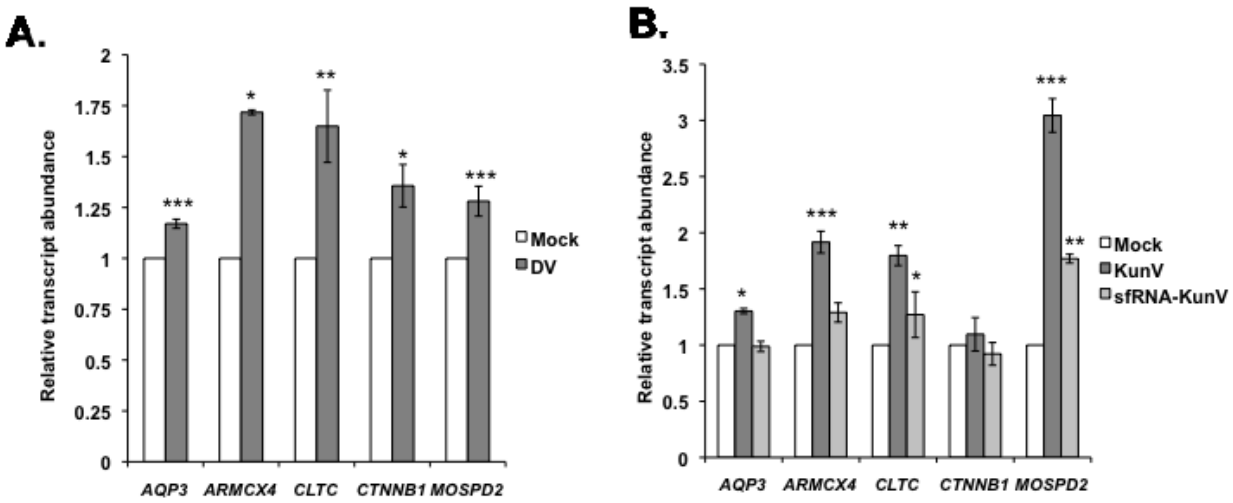

Figure 32. Changes in mRNA abundances in sfRNA-forming viral infections recapitulate those observed upon AGO2 and/or DICER knockdown. (A) Human 293T cells were infected with dengue virus type 2 (MOI of 3) or mock infected, and total RNA was collected 4 dpi. The relative abundance of five mRNAs, aquaporin 3 (*AQP3*), armadillo repeat containing, X-linked 4 (*ARMCX4*), clathrin, heavy chain (*CLTC*), catenin (cadherin-associated protein) β 1 (*CTNNB1*) and motile sperm domain containing 2 (*MOSPD2*) was assessed by RT-qPCR using *GAPDH* as a reference gene. (B) Total RNA from human 293T cells were mock infected or infected with Kunjin virus (KunV) or an sfRNA-deficient Kunjin virus (sfRNA-KunV) (MOI of 10) were collected 60 hpi and differences in mRNA abundances were assessed as in (A). The significance of the observed differences transcript abundance in infected cells compared to mock infected cells was evaluated using Student's t-test with * indicating $p<0.05$, **$p<0.01$, *** $p<0.005$.

sfRNA may bind and sequester AGO2 and DICER to alter RNA interference

One previous study indicated that DICER activity was specifically suppressed by sfRNA in WNV and DENV-2 replicon systems (Schnettler et al. 2006). However, our data suggest that AGO2 may also be suppressed by sfRNA. To test the hypothesis that sfRNA sequesters either

of these nucleases, we performed RNA-protein co-immunoprecipitation assays to determine if sfRNA was physically bound to either nuclease during infection.

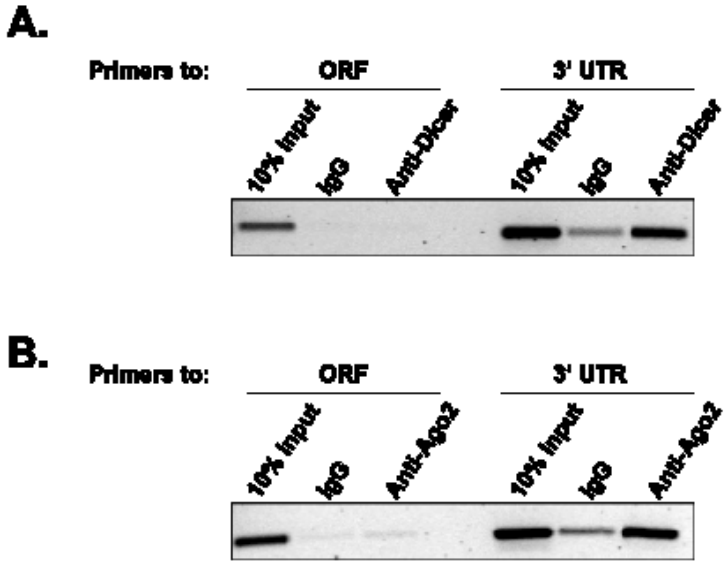

Figure 33. Kunjin virus sfRNA is physically associated with DICER and AGO2 during infection in human cells. Human 293T cells were infected with Kunjin virus (MOI of 10) and formaldehyde cross-linked to preserve RNA-protein interactions before immunoprecipitation with (A) anti-DICER antibody or (B) anti-AGO2 antibody. A normal IgG control antibody was used to account for non-specific interactions. Genomic RNAs were distinguished from sfRNAs by RT-PCR analysis using primers to the open reading frame (ORF) or the 3' untranslated region (3' UTR) as indicated above the panels. One co-immunoprecipitation experiment is shown.

Importantly, both DICER and AGO2 were shown to be physically associated with Kunjin virus RNAs containing the 3' UTR but not the viral open reading frame (Figure 33). These results will be validated by assessing DENV-2 sfRNA association with DICER and AGO2 and quantified by RT-qPCR. Future experiments will investigate the ability of DICER and AGO2 to bind to the highly structured sfRNAs using electrophoretic mobility shift assays. Finally, sfRNA may serve as an inhibitor of AGO2, DICER, and XRN1, leading to dysregulated gene expression during flavivirus infections in human cells.

DISCUSSION

The above studies sought to test the hypothesis that the formation of sfRNA during flavivirus infection suppresses the activity of the 5'-3' exoribonuclease XRN1. We demonstrated that sfRNA is formed by XRN1-mediated decay in mammalian, mosquito, and yeast systems as a result of highly structured conserved elements in the flaviviral 3' UTRs. The formation of sfRNA was then found to be strongly associated with defects in XRN1 activity as measured in cell-free extract systems and in infected cells in culture. Furthermore, global analysis of mRNA decay in cells infected with Kunjin virus or two sfRNA-deficient viruses revealed sfRNA-dependent changes in the relationship between stability and abundance of cellular RNAs consistent with XRN1 depletion observed in previous studies in yeast. Interestingly, these results may indicate that the cellular response to infection is compromised in sfRNA-producing viral infections. Finally, we demonstrated that suppression of XRN1 via highly structured viral RNAs may be conserved among all members of the *Flaviviridae*, as the 5' UTRs of HCV and BVDV form distinct decay intermediates upon 5'-3' decay by XRN1 and suppress XRN1 activity *in vitro*. These studies have therefore identified a novel mechanism by which all members of the *Flaviviridae* suppress a major aspect of the cellular RNA decay machinery, and this potentially contributes to virus-induced pathology.

Conserved structural elements in flaviviral untranslated regions suppress XRN1 activity

The results presented herein and findings from other laboratories demonstrate that the XRN1 exoribonuclease in yeast, mammal, and mosquito systems stalls on highly structured conserved viral RNA elements in the 3' UTRs of flavivirus RNAs. How do these RNAs disrupt XRN1-mediated decay of the viral genomic and/or messenger RNAs? Interestingly, although previous studies demonstrated that pseudoknot-like structures present in flavivirus 3' UTRs are

major contributors to the stalling of XRN1 (Pijlman et al. 2008; Silva et al. 2010; Funk et al. 2010), in collaboration with the Kieft laboratory (University of Colorado-Denver), we have demonstrated that sfRNA formation in cells relies on the interaction between multiple pseudoknots mediated by a conserved cytosine upstream of the stem-loops previously implicated in sfRNA formation (Chapman et al. 2014; Chapman et al. *in press*). Mutagenesis of the KUNV 3' UTR in which this essential cytosine was converted to a guanine completely abrogated sfRNA formation in infected 293T cells (Figure 29). Furthermore, structural analyses of the XRN1-resistant RNA structure in the MVEV sfRNA revealed that a three-helix junction centered on the conserved cytosine nucleotide was responsible for the stalling of XRN1 (Chapman et al. *in press*). Mutation of three nucleotides at the base of either of two stem-loops implicated in KUNV sfRNA formation predicted to disrupt this three-helix junction abrogated sfRNA formation in infected cells in culture (Figure 29). Importantly, these studies will likely enhance our ability to design effective drugs to target the sfRNA structure present in all flavivirus infections. Chemicals that disrupt the secondary structure of flavivirus RNAs could be used to potentially destabilize the structure and facilitate effective 5'-3' decay by XRN1. We are currently assessing the ability of small molecules used to disrupt stable stem-loop structures formed by CUG repeat elements in toxic RNAs observed in myotonic dystrophy (Lee et al. 2009; Coonrod et al. 2013) to abrogate sfRNA formation *in vitro* as a proof of concept. Furthermore, oligonucleotides with perfect complementarity to the regions in the flavivirus 3' UTR that span the base of each stem-loop could be applied to again facilitate XRN1-mediated decay by opening up the stable triple-helix structure. Finally, as has been suggested in other works (Pijlman et al. 2008; Liu et al. 2014), sfRNA-deficient flaviviruses should be tried as potential vaccine candidates as they are less pathogenic than wild-type viruses.

Intriguingly, we have observed that the HCV and BVDV 5' UTRs also stall XRN1, leading to the formation of distinct XRN1-mediated decay intermediates. We are currently cloning out the 5' ends of monophosphorylated BVDV and HCV RNAs that had been incubated with XRN1

to determine the exact RNA sequence/structures that stall XRN1. However, based on the sizes of the HCV and BVDV 5' UTR decay intermediates we observe in our cell extract and recombinant yeast XRN1 decay assays, we notice that the 5' ends of these decay intermediates roughly correspond with the bases of several predicted stem-loop structures conserved throughout the genera (Isken et al. 2007). We are currently generating deletion mutant constructs of the HCV 5' UTR to determine which region is required for the stalling of XRN1. Furthermore, because the stalling of XRN1 appears to be a common function of the IRES elements of both BVDV and HCV, we are currently working to determine if other viral IRES elements (e.g. Poliovirus) can stall XRN1. It will be interesting to determine if the stalling of XRN1 on distinct viral RNA structures is a function conserved among flaviviruses or potentially shared among viral RNAs that lack 5' methylated cap structures.

Intriguingly, other viral RNAs may also be resistant to XRN1-mediated decay. The RNAs generated by the yeast Narnavirus contain a long stem-loop at their 5' ends that was shown to block XRN1 (Esteban et al. 2008). However, this mechanism is likely distinct from what is observed in the decay of flavivirus RNAs. Rather than allow XRN1 to initiate degradation of these RNAs, this structure likely 'hides' the 5' end of the RNA. A recent study of the structure of *Drosophila* XRN1 revealed that the processive exonucleolytic activity of the enzyme works in concert with an unwinding activity to effectively process RNA duplexes only when a 5' overhang on the RNA is $\geq$8 in length (Jinek et al. 2011). Therefore, these RNAs likely do not act as competitive inhibitors of XRN1 to reduce XRN1 activity like sfRNAs. However, some plant viruses (e.g. Soybean dwarf virus and Red clover necrotic mosaic virus) are known to generate small subgenomic non-coding RNAs (<500 nt) that could potentially be a result of incomplete 5'-3' decay of the viral genome by XRN1 (Yamagishi et al. 2003; Iwakawa et al. 2008). Indeed, one study demonstrated that Red clover necrotic mosaic virus and other members of the *Dianthovirus* genus (positive-sense single-stranded RNA viruses of plants) generate these subgenomic RNAs as a result of incomplete 5'-3' decay in tobacco protoplast extracts (Iwakawa

et al. 2008). Furthermore, these RNAs appear have some ability to suppress viral translation (similar to what was observed in a study of the JEV sfRNA; Fan et al. 2011). However, unlike KUNV sfRNAs, the Red Clover Necrotic Mosaic virus subgenomic RNA appears to be packaged into nascent virions (Pijlman et al. 2008; Iwakawa et al. 2008). The role of these sgRNAs in viral pathogenesis remains uncharacterized.

Could endogenous cellular transcripts stall and suppress XRN1 activity?

One important finding from these studies is the observation that multiple viral RNAs are capable of stalling and suppressing XRN1 activity. Although we have discussed this capability in the context of viral infection and pathogenesis, it is possible that cellular transcripts also may encode XRN1-resistant structural elements. For example, some cellular transcripts are thought to be translated via IRES-mediated mechanisms, potentially to allow gene expression under conditions that suppress cap-mediated translation mechanisms (e.g. during mitosis or hypoxia) and/or to facilitate ribosome scanning through highly structured RNA elements (reviewed in Komar and Hatzoglou 2011; Le Quesne et al. 2001). If conserved structural elements in internal ribosome entry sites that are essential for translation initiation also happen to be resistant to XRN1-mediated decay, then cellular mRNAs that have been demonstrated to undergo IRES-mediated translation may stall and suppress XRN1 activity.

At least three other sets of transcripts with unique properties could be capable of stalling XRN1. First, a recent study demonstrated that the 3' UTRs of many transcripts in human and mouse cells are expressed at different levels than the associated open reading frames (Mercer et al. 2011). In other words, it appears that different regions of an mRNA show different abundances – which is strongly suggestive of differential decay of portions of the transcript. This study also demonstrated using *in situ* hybridization that the subcellular and/or tissue-specific localization of the 3' UTRs of three transcripts (*Col1a1*, *Nfia*, and *Myadm)* were different from

the corresponding open reading frames in mice during development (Mercer et al. 2011). Thus these cellular mRNAs could potentially be generating sfRNA-like decay intermediates from structured elements in their 3' UTRs. Second, transcripts that have been characterized as having unconventional transcription start sites or splice sites may potentially be generated as a result of incomplete degradation of the parent transcript by XRN1. Therefore, re-analyzing 5'-RACE data may reveal some interesting stall sites for RNA decay factors in cellular mRNAs. Finally, changes in the structure of mRNAs due to mutations or altered temperature could potentially facilitate the stalling of XRN1 on cellular mRNAs. For example, temperature-induced changes in RNA secondary structure have been described in Influenza A virus (Chursov et al. 2012) and tick-borne encephalitis virus (Elvang et al. 2011). A recent study demonstrated that up to 15% of transcribed single nucleotide variants cause local changes in mRNA structure in humans (Wan et al. 2014), indicating that small changes in the sequence of a transcript can impact RNA structure. Furthermore, recent studies demonstrated that single nucleotide variations in the 5' UTR of thrombin-activatable fibrinolysis inhibitor can significantly alter the structure and stability of the transcript (Boffa et al. 2008; Halvorsen et al. 2010). Therefore, because XRN1 is capable of stalling on structured viral RNAs, unique mRNA structures resulting from mutations or enhanced structural stability due to decreased temperature could potentially stall XRN1 in human cells. The identification of potential XRN1-resistant cellular transcripts will be important, because suppression of XRN1 could lead to defects in post-transcriptional regulatory mechanisms that may cause disease. Interestingly, transcripts that change conformation and adopt more stable higher-order structures at low temperatures and/or potentially during stress responses due to alterations in salt availability or concentration in the cytoplasm) and suppress XRN1 activity could dramatically alter the host response, potentially leading to disease.

Changes in gene expression during sfRNA-forming viral infections are consistent with studies of XRN1-deficient organisms

We hypothesized that sfRNA-forming viral infections would cause a global increase in the stability of cellular transcripts, and that this would also correspond with an overall increase in the steady-state abundance of cellular transcripts. In support of this hypothesis, we found that in conjunction with sfRNA-mediated suppression of the major exonuclease XRN1, there are substantial changes in the steady-state abundance of certain cellular RNAs including pro-inflammatory innate immune factors and the stability of short-lived transcripts was significantly increased (Figures 14, 16, 17). However, although we expected a substantial increase in the overall abundance of mRNAs as a result of XRN1 suppression in flavivirus infected cells, out of the ~3000 transcripts assessed in KUNV infections, the vast majority of transcripts were not substantially altered in abundance (e.g. most were less than 2-fold reduced or increased in abundance relative to mock infected cells). Fruit flies engineered to have reduced expression of the XRN1 homolog pacman also show few changes in the overall abundance of transcripts, although they also display dramatic phenotypic changes including developmental defects (Grima et al. 2008; Jones et al. 2013). Therefore, XRN1 depletion and/or enzymatic suppression can contribute to phenotypic changes without altering the steady-state abundance of the majority of mRNAs in a given system.

We also determined that sfRNA formation in Kunjin virus infections was strongly associated with the stabilization of cellular transcripts (Figure 17). In agreement with these findings, previous studies using XRN1-deficient yeast demonstrated that a majority of transcripts are generally more stable in these systems compared to wild-type yeast (He et al. 2003; Haimovich et al. 2013; Sun et al. 2013; Medina et al. 2014). The analysis of global changes in mRNA stability in KUNV and the sfRNA-deficient KUNV and SINV infections therefore provided another piece of evidence that XRN1 activity is suppressed as sfRNA accumulates. Although dramatic changes in overall mRNA abundance were not observed in *Drosophila* lacking XRN1,

it was also demonstrated that several mRNAs, including the mRNA of heat shock protein Hsp67Bc were increased in abundance in the XRN1-deficient Drosophila wing imaginal discs (Jones et al. 2013). Importantly, these changes in mRNA abundance were likely due to mRNA stabilization, as the abundance of the intron-containing pre-mRNAs were not substantially altered in the mutant flies compared to controls (Jones et al. 2013). These results indicate that changes in the post-transcriptional regulation of certain mRNAs could impact organism phenotype in the absence of global changes in mRNA abundance. Indeed, the *Arabidopsis* homolog of XRN1, XRN4, may have some sequence specificity (Rymarquis et al. 2011). However, this is potentially an indirect result, as certain transcripts undergoing 5'-3' turnover more rapidly than others and/or targeted for 5'-3' decay by RNA binding proteins (or miRNAs) that have sequence and/or RNA structure specificity might be over-represented in an XRN-deficient organism (Jones et al. 2012). Furthermore, the decapping complex can be specifically recruited to mRNAs that undergo miRNA-mediated decay, ARE-mediated decay, or to transcripts that contain other unique structural or sequence elements (reviewed in Ling et al. 2011). In this fashion, the suppression of XRN1 could lead to the stabilization and/or over-expression of a specific subset of transcripts, although the mammalian XRN1 exonuclease itself does not appear to exhibit sequence specificity.

Our global analyses RNA stability in arbovirus infected cells supports the idea that XRN1 suppression does not lead to the up-regulation of mRNAs on a global scale. Furthermore, these results may indicate that altered abundance and/or stability of a select subset of transcripts occurs upon XRN1 suppression, as appears to be the case in *Drosophila* wing morphogenesis (Jones et al. 2013). Although our RNA-seq approach to determine global changes in mRNA stability and abundance during arthropod-borne virus infections yielded important insights into the relationships between rates of mRNA decay and steady-state mRNA abundances, potentially very interesting groups of transcripts that are likely expressed at levels below the depth of sequencing were unfortunately not included in our datasets. These include *FOS*, *TUT1*

and the pro-inflammatory cytokines detected by qRT-PCR and microarray reported in Figure 15. Therefore, our global analyses of mRNA stability and abundance were not adequate for directly answering the question of whether or not short-lived transcripts induced by viral infections were stabilized by sfRNA. Importantly, we were able to directly assess the stability and steady-state abundance of a set of short-lived transcripts in HCV and BVDV infected cells known to be involved in pathologies associated with these viral infections. We determined that stabilization of these transcripts may be an important mechanism by which they are elevated in abundance overall. Therefore, XRN1 suppression by viral RNAs could contribute to pathology by altering the abundance and stability of a select group of normally short-lived transcripts.

Dysregulation of mRNA stability and abundance in arbovirus infections points to defects in homeostatic mechanisms that likely coordinate mRNA synthesis and decay

The relationship between mRNA stability and mRNA abundance in the constitutively expressed transcripts that likely serve a more general house-keeping function was analyzed using the datasets generated using RNA-seq for viral infections (Figures 16, 17 and 18). We demonstrated that sfRNA-deficient KUNV or SINV infected cells display a positive correlation between mRNA stability and abundance (Figure 19A and B). This might be expected if the cell undergoes a highly coordinated anti-viral response that requires concerted changes in mRNA abundance and stability. In contrast, cells infected with the sfRNA-forming KUNV displayed no correlation between changes in mRNA stability and abundance (Figures 18C and 19D). We hypothesize that this lack of coordination between mRNA stability and abundance in cells infected with sfRNA-forming flaviviruses indicates a defect in the host response to infection that may be involved in the sfRNA-dependent pathologies observed in other studies (Pijlman et al. 2008; Liu et al. 2014). How could this apparent defect in coordinated changes in cellular gene expression regulatory mechanisms contribute to pathology? If the cell is unable to rapidly react to the presence of viral pathogen associated molecular patterns (as discussed in the

Introduction), then the virus could gain a foothold in the cell for the establishment of replication complexes and host cell re-modeling earlier in the infection. Furthermore, post-transcriptional regulatory mechanisms are essential for controlling the expression of pro-inflammatory factors like TNF-α (also discussed in the Introduction). Defects in the coordinated regulation of transcription and mRNA decay could therefore promote excessive inflammation in infected cells that could perhaps not rapidly reduce the expression of pro-inflammatory factors. Exactly how mRNA decay processes influence mRNA synthesis in mammalian cells remains to be explored.

Coordination between XRN1 and early steps in the deadenylation-dependent RNA decay pathway

We demonstrated that short-lived oncogenes and angiogenic factors are more abundant and stable at the mRNA level in HCV and BVDV infected cells. Importantly, these mRNAs are not uncapped decay intermediates (although we determined that a small amount (~<10%) of cellular transcripts lacking 5' caps do accumulate in HCV, DENV-2, and KUNV infections) and the majority of these transcripts are polyadenylated, capped, and therefore theoretically translatable (Figure 28). In BVDV infected cells, c-FOS and c-JUN were more abundant at the RNA and protein levels, demonstrating that stabilization of these mRNAs could contribute to elevated gene expression. How could changes in XRN1 activity influence the abundance of capped and polyadenylated mRNAs and/or protein? Aside from mechanisms that mediate coordination of mRNA decay and synthesis as discussed above, it is also likely that the distinct enzymatic processes in the 5'-3' deadenylation-dependent decay pathway are also coordinated. There are three pieces of evidence that would support this idea. First, mRNA decay factors including CCR4-NOT family members, XRN1, DCP1a, DCP2, and AGO2 are often co-localized in discrete cytoplasmic foci (P-bodies) in human cells (Cougot et al. 2004; Liu et al. 2005; Sen and Blau et al. 2005), and XRN1 is known to directly interact with EDC4 in the decapping complex in human cells (Braun et al. 2012). Therefore these factors exist in close physical

proximity to one another and could directly or indirectly interact. Second, the decapping factor DCS1 has been shown to regulate XRN1 activity, potentially by causing a change in the XRN1 protein conformation and/or stabilizing the protein to increase the affinity of XRN1 for its RNA substrate (Sinturel et al. 2012). Therefore, there is precedence for the ability of a protein factor involved in a distinct mRNA decay process to regulate XRN1. Finally, as discussed in the Introduction, the proteins involved in deadenylation, decapping, and 5'-3' decay directly or indirectly interact through protein scaffolds, and the presence of disordered regions in many of these proteins may facilitate ribonucleoprotein aggregation (Decker et al. 2007; Reijns et al. 2008; Ozgur et al. 2010; Braun et al. 2012; Chang et al. 2014; Jonas and Izaurralde 2013). We have demonstrated that sfRNA formation directly inhibits XRN1 activity and that changes in mRNA stability consistent with XRN1-deficiency are observed in flavivirus infections. In addition to these findings, P-bodies are dispersed in DENV, WNV and HCV infected cells, indicating that the interactions between these various mRNA decay factors are potentially disturbed upon infection (Emara and Brinton 2007; Pager et al. 2013). Furthermore, as discussed in the Introduction, HeLa cells infected with WNV recruit XRN1, LSm1, TNRC6A, and the RNA helicases DDX3, and DDX6 to viral replication complexes (Chahar et al. 2013). The 3' UTR or sfRNA of DENV-2 was shown to interact with the P-body components DDX6 (Ward et al. 2011) and XRN1 (Figure 10). Furthermore, the HCV 5' UTR interacts with AGO2 (Conrad et al. 2013; Bradrick et al. 2013), LSm1-7 (Scheller et al. 2009) and XRN1 (Bradrick et al. 2013). It is therefore possible that viral RNAs (either full-length or sfRNAs/sfRNA-like HCV RNA decay intermediates) bind and sequester several RNA binding proteins normally present in ribonucleoprotein complexes that may coordinate disparate steps in the mRNA decay process. Therefore, the formation and accumulation of sfRNA/sfRNA-like decay intermediates could directly and indirectly perturb P-body formation by sequestering RNA binding proteins and nucleases like XRN1 and AGO2. Furthermore, recent studies have demonstrated that XRN1 may have the ability to act as a transcription factor in yeast (Sun et al. 2013; Haimovich et al.

2013; Medina et al. 2014), although XRN1 in mammalian and yeast cells is predominantly localized in the cytoplasm and therefore may not directly regulate transcription (Heyer et al. 1995; Ingelfinger et al. 2002). The potential sequestration of XRN1 on sfRNAs in flavivirus infected cells could also potentially disrupt feedback mechanisms that normally exist in the cell to coordinate mRNA synthesis in decay. Consequently, defects in coordination between early steps in the deadenylation-dependent mRNA decay pathway and coordination between mRNA synthesis and decay could be caused by XRN1-mediated formation of sfRNA as illustrated in Figure 34.

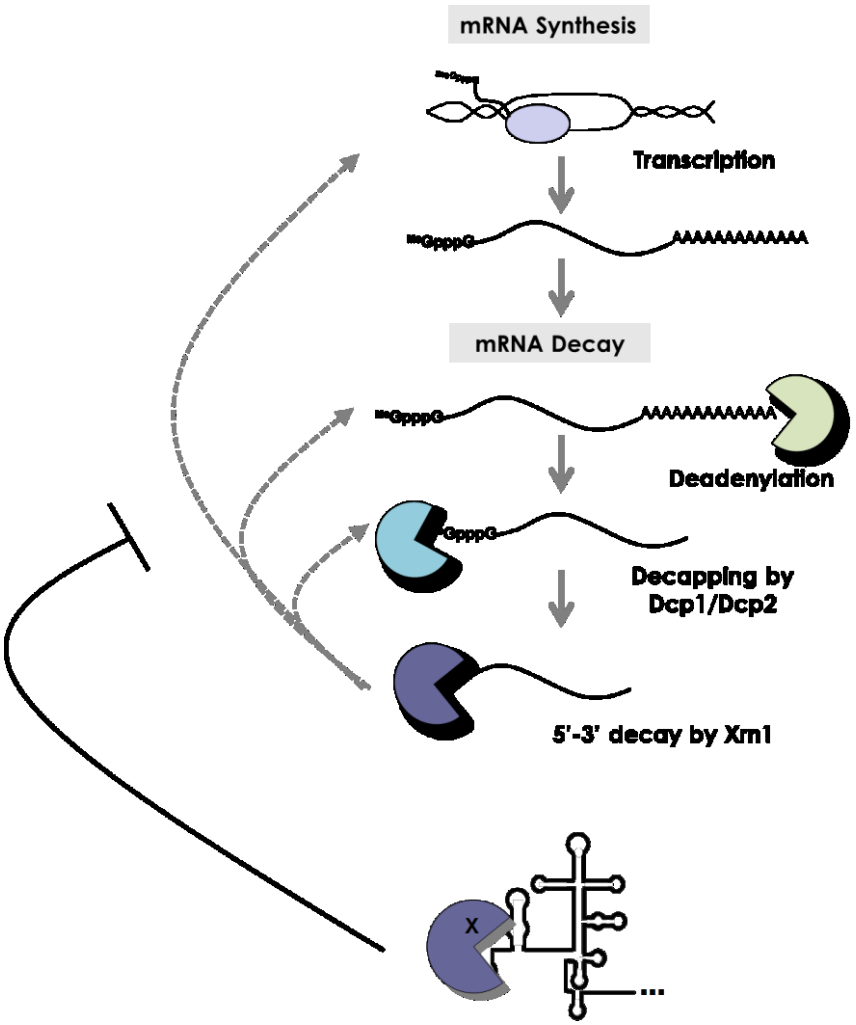

Figure 34. The suppression of XRN1 activity by highly structured flaviviral RNAs could disrupt normal feed-back mechanisms that regulate mRNA synthesis and decay. The coordination between XRN1 and other RNA decay factors (e.g. deadenylases and decapping factors) and/or transcription factors is represented by the gray dotted lines, and this coordination is likely dysregulated in flavivirus infections.

A role for XRN1 suppression in flavivirus-mediated pathology

Suppression of XRN1 activity by flaviviruses could lead to pathology by enhancing viral replication (either by stabilization of viral RNAs or other impacts on viral replication) or by dysregulating the host response to infection. We did not measure the rate of viral RNA decay during infection, although our data support the hypothesis that sfRNA accumulation would lead to increased viral RNA stability. This is highly likely, as a recent manuscript demonstrated that XRN1 is the primary exonuclease involved in degrading HCV RNAs (Li et al. 2013(b)) and the formation of sfRNAs in flavivirus infections relies on XRN1-mediated decay of the parent transcript. Furthermore, there are some clues in the literature that innate immune mechanisms are dysregulated during flavivirus infections of mammalian cells as a result of sfRNA accumulation (Schuessler et al. 2012, Chang et al. 2013). There are several potential mechanisms discussed below by which XRN1 suppression could contribute to flavivirus-, hepacivirus-, and pestivirus-induced pathology.

XRN1 is important for proper cell growth/proliferation and development

The suppression of XRN1 by highly structured flavivirus RNAs could contribute to changes in cell biology that may enhance or promote virus-induced pathology in the host. As discussed above, XRN1 depletion in yeast causes changes in mRNA stability- but how does XRN1 deficiency affect the biology of the cell? Several studies have demonstrated that XRN1 is likely important for regulating basic processes in cell growth, proliferation, and development. In the yeast *Schizosaccharomyces pombe*, XRN1 deficiency was shown to increase cell size, cause a loss of cell viability in the stationary phase, and also made these organisms hypersensitive to anti-mitotic drugs (Szankasi et al. 1996). Furthermore, *Saccharomyces cerevisiae* lacking XRN1 also have increased cell size and increased doubling time in conjunction with stabilization of cellular mRNAs (Larimer and Stevens 1990; Larimer et al.

1992). These studies demonstrate that XRN1 activity is strongly associated with defects in essential cell behaviors including cell growth and proliferation.

In more complex organisms, XRN1 has been implicated in the processes of development, response to stress/stimuli, and has even been suggested as a tumor suppressor protein. Studies in *Drosophila* demonstrate that XRN1 is differentially expressed during organism development, indicating that it may play an important regulatory role in mediating this complex process (Till et al. 1998). As discussed above, further studies in *Drosophila* showed that XRN1 is essential for normal wing development (Jones et al. 2013), epithelial sheet sealing (Grima et al. 2008) and spermatogenesis (Zabolotskaya et al. 2008). In mammals, less is known about the role of XRN1 in development and cell growth; however, a role for XRN1 in neuronal cell differentiation was proposed in one study. XRN1 expression can be induced by glial-cell derived neurotropic factor (GDNF) in human neuroblastoma cells (Shimoyama et al. 2003). Because GDNF induces differentiation of these neuronal cells, XRN1 could play a role in mediating this process (Shimoyama et al. 2003). Finally, XRN1 may potentially be important for the regulation of cell growth and proliferation, as it may be involved in the onset and/or progression of osteogenic sarcoma (Kruzelock et al. 1997; Zhang et al. 2002). Osteogenic sarcoma-derived cell lines and patient-derived osteogenic sarcoma biopsy specimens were shown to have reduced XRN1 expression when compared to a control human fetal osteoblast cell line (Zhang et al. 2002).

XRN1 activity in yeast is suppressed in the presence of lithium (Dichtl et al. 1997). Interestingly, lithium toxicity in yeast was abrogated by the overexpression of HAL2 protein, an enzyme known to break down adenosine 3', 5' bisphosphate (pAp) into 5' adenosine monophosphate and inorganic phosphate (Dichtl et al. 1997). The authors of this study demonstrated that XRN1 may be regulated in this context by the build-up of pAp as a result of lithium-mediated suppression of HAL2 activity as XRN1 activity was abrogated in vitro in the presence of pAp (Dichtl et al. 1997). A later study demonstrated that HAL2 expression is likely

regulated by BDF1, a member of the Fsh/Brd bromodomain-containing protein family, and that in the absence of BDF1 yeast cells were particularly sensitive to salt stress (Liu et al. 2009(b); Chen et al. 2013(b)). Over-expression of HAL2 rescued resistance to salt stress in a Bdf1 deletion strain (Chen et al. 2013(b)). These studies are potentially interesting in the context of mammalian development, because BRD4, another Fsh/Brd bromodomain-containing protein, was shown to be essential for normal development in mice (Houzelstein et al. 2002). Mice with reduced BRD4 expression have pre- and post-natal defects including malformation of the head, liver defects (including reduced liver cell proliferation), lack subcutaneous fat, and cataracts (Houzelstein et al. 2002). Mice lacking BRD4 completely are embryonic lethal (Houzelstein et al. 2002). If BRD4 similarly regulates HAL2 expression in mammalian cells as occurs in yeast, when BRD4 is under-expressed, we might expect to see a reduction in Hal2 expression. Reduced HAL2 expression could cause an accumulation of pAp, potentially leading to XRN1 suppression. Although these data are indirectly implicating XRN1 in the cellular response to lithium and salt stress, there are other pieces of evidence that implicate that XRN1 activity is important for organism response to stress. Intriguingly, the plant homolog of XRN1, XRN4, is known to be important for mediating the organism response to a variety of stresses, including heat and ethylene toxicity (Potuschak et al. 2006; Olmedo et al. 2006; Merret et al. 2013). Therefore, XRN1 might be important for mediating the cellular anti-flaviviral response.

Inhibition of RNA interference by sfRNA

RNA interference is arguably the most important innate immune response that arthropods use to protect themselves from flavivirus induced pathology (Blair 2011; Sanchez-Vargas et al. 2009). Therefore, the ability of flaviviruses to suppress the RNAi pathway to some degree is likely very important for these viruses to exist in the arthropod vector long enough to be transmitted to the next host. Our studies have demonstrated that siRNA-mediated silencing

of gene expression in mammalian cells is limited during DENV-2 and KUNV infections in an sfRNA-dependent fashion (Figures 29 and 30). Because RNAi is likely most important in the context of the viral infection of the arthropod vector, we are currently assessing the degree to which RNAi is suppressed *in vivo* in the mosquito vector. Although sfRNA formation in the mosquito vector has not been demonstrated in the literature, preliminary evidence suggests that sfRNA accumulates to high levels in DENV-2 infected *Aedes aegypti* mosquitoes (data not shown). Furthermore have demonstrated using cytoplasmic extracts from *Aedes albopictus* C6/36 cells that sfRNA also inhibits XRN1 activity in this system (Figure 7C). As discussed in the Introduction, there is some evidence that sfRNA reduces DICER activity in non-human mammalian cells (Schnettler et al. 2012) and a recent manuscript demonstrated that microRNAs are significantly reduced in abundance DENV-2 infected cells (Kakumani et al. 2013), possibly indicating that DICER and/or AGO2 activity is suppressed during flavivirus infections. Disruption of both AGO2 and DICER by sfRNA would be possible considering the importance of RNAi to the arthropod anti-viral response. However, another possibility that we are currently assessing is the potential for feedback mechanisms to exist between components of the RNAi pathway. If AGO2 suppression feeds back and reduces DICER activity, or if XRN1 (known to degrade AGO2-mediated endonucleolytic decay products; Orban and Izaurralde 2005) suppression feeds back and suppresses AGO2 activity, then sfRNA could be indirectly suppressing RNAi during infection. We are pursuing this by assessing the knockdown efficiency of a reporter RNA in cells deficient in XRN1, AGO2, or DICER. However, the intriguing preliminary finding that the 3' UTR of KUNV is directly associated with AGO2 and DICER in infected cells implies that sfRNA is likely a direct inhibitor of all three nucleases.

Future directions

Determine the impact of sfRNA formation on viral RNA stability

Co-opting cellular RNA stability factors can stabilize viral RNAs (Sokoloski et al. 2010), and the sponging of the host HuR protein by Sindbis virus RNAs can dramatically alter cellular mRNA stability and processing (Barnhart et al. 2013). Therefore, the suppression of the major cytoplasmic 5'-3' exoribonuclease XRN1 by sfRNA likely stabilizes both viral and cellular RNAs. We demonstrated that sfRNA formation requires XRN1 to actively degrade viral RNAs and that RNAi-mediated decay of a reporter transcript containing the DENV-2 3' UTR or the 5' UTR of HCV or BVDV enhances the formation of sfRNA. Therefore, some flaviviral genomes may act as bait for the RNA decay machinery to ultimately cause the stabilization of viral RNAs later in the infection. Answering this question of flaviviral RNA stability will require overcoming a technical limitation in the system. Although there is not currently a commercially available inhibitor of flavivirus transcription (homologous to actinomycin D in mammalian cells) to directly address this hypothesis, several other experimental approaches could be undertaken. A broad-spectrum antiviral drug, HPA-23 ($(NH_4)_{18}(NaW_{21}Sb_9O_{86})_{17}$), was demonstrated to inhibit transcription of a diverse array of viruses (Werner et al. 1976; Tsiang et al. 1978), including DENV-2 (Bartholomeusz et al. 1994). Initial experiments using HPA-23 were not successful in shutting off flaviral transcription in our laboratory, perhaps due to the low solubility and perhaps stability of this compound in aqueous solutions. Alternatively, a metabolic labeling approach in which labeled ribonucleosides are applied to infected cells in culture and integrated into nascent viral genomes may also be attempted (assuming viral RNA dependent RNA polymerases can efficiently incorporate these modified ribonucleotides) as reported in Azarkh et al. (2011). Finally, as was done in Sokoloski et al. (2010), the use of a temperature-sensitive flaviviruses engineered to lose RdRp activity upon transfer to a higher temperature could yield viral RNA stability data. However, no temperature sensitive mutants with defects in the flaviviral

polymerase have been described in the literature to our knowledge, although targeted mutations predicted to abrogate polymerase activity at higher temperatures by disrupting the tertiary structure of the enzyme could be employed to potentially generate such mutants. Therefore, future studies should seek to address the role of XRN1 suppression in the stabilization of flavivirus RNAs.

Examine the mechanisms by which flavivirus RNAs are degraded in the cell

Although XRN1 is likely a key player in mediating the degradation of flavivirus RNAs, as demonstrated by sfRNA accumulation, the initial steps in the decay of flavivirus RNAs are unknown. It would be interesting to determine if induced nucleases (e.g. RNase L) contribute to endonucleolytic cleavage of viral RNAs to facilitate XRN1-mediated decay of 5' phosphorylated RNAs. Furthermore, although RNAi is likely not a major mechanism by which viral RNAs are targeted for decay in mammalian somatic cells, AGO2-mediated decay of viral transcripts in mammalian cells has been recently documented (Li et al. 2013(c); Maillard et al. 2013). Indeed, we demonstrated that targeting a reporter RNA containing the 3' UTR of DENV-2 or the HCV or BVDV 5' UTR with an upstream siRNA lead to increased accumulation of sfRNA-like decay intermediates in human 293T cells. Because flavivirus RNAs are not polyadenylated but contain 5' methylguanosine caps, it would be interesting to determine if they are shunted directly into the decapping and 5'-3' decay pathway. Interestingly, there is some evidence that the YFV genome undergoes 3'-5' decay, as a 3' truncated sfRNA was detected in infected mammalian cells (Silva et al. 2010). The hepacivirus and pestivirus RNAs lack methylated 5' caps, and because XRN1 is unable to effectively degrade 5' triphosphorylated RNAs (Jinek et al. 2011) it would be interesting to determine how these RNAs are dephosphorylated to allow XRN1-mediated decay. It is also likely that viral RNAs can be targeted by quality control pathways in the cell, considering that they (1) do not have a nuclear experience and thus are not present in

proper ribonucleoprotein complexes (Wilusz and Wilusz 2010) and (2) viral RNA-dependent RNA polymerases are error-prone and likely integrate premature termination codons, fail to add a termination codon, or highly structured viral RNAs could stall on the ribosome during translation. Using a combination of RNAi-mediated gene silencing of key endo- and exonucleases and assessment of viral RNA stability using one of the methods described above should enable the elucidation of how flavivirus RNAs are degraded in the cell.

Directly assess the role of XRN1 suppression in pathology

Although we have demonstrated that the major 5'-3' exoribonuclease XRN1 is suppressed by sfRNAs and that significant changes gene expression occur in association with sfRNA accumulation, future studies should directly address the hypothesis that XRN1 inhibition during viral infection leads to pathology. Two studies have demonstrated that sfRNA is important for KUNV and DENV-2 mediated cytotoxicity/pathogenicity in either a mouse model of infection or in cell culture (Pijlman et al. 2008; Liu et al. 2014). How exactly do sfRNAs from diverse flaviviruses mediate pathology, and could the sfRNA-like decay intermediates observed in BVDV and HCV infections also contribute to pathology?

Because XRN1 has been implicated as a tumor suppressor protein (Zhang et al. 2002), it is possible that the suppression of XRN1 by sfRNA-like decay intermediates observed in HCV infections could contribute to the onset of HCV-induced HCC. We are currently assessing the relationship between carcinogenesis and XRN1 suppression using focus formation assays in Huh7 and NIH3T3 cell culture models. Hepatitis C virus infections can also cause fibrosis (Razavi et al. 2013), and XRN1 has been demonstrated to be important for epithelial sheet sealing in Drosophila, a model for wound healing. To determine if XRN1 suppression by viral RNAs could contribute to defects in wound healing/fibrosis during infection, we are also performing in vitro wound healing/cell migration assays (as done in Lee et al. 2012(b)).

As discussed above, XRN1 is important for proper organismic development, cell growth/proliferation, and respond to various stimuli. It has therefore been postulated that XRN1 coordinates a proper cellular response to various cues that permit a dramatic change in global gene expression (Jones et al. 2012). Because we observed dramatic changes in cellular gene expression in flavivirus infections that occurred in an sfRNA-dependent fashion, it is possible that XRN1 is also important for mediating the proper cellular response to viral infection. The observation that transcript abundances were generally not correlated with transcript stability in wild-type KUNV infected cells, but that there is a positive correlation between these values in two sfRNA-deficient RNA virus infections supports the hypothesis that sfRNA disrupts the normal cellular response to infection.

Gene ontology analysis of the transcripts that were $\geq$2-fold more stable in KUNV infected cells relative to the sfRNA-deficient KUNV infected cells revealed that several biological processes may be altered as a result of sfRNA formation. There was a significant enrichment ($p \leq 0.001$) in transcripts encoding factors involved in the cell cycle process, microtubule cytoskeleton organization, nuclear division, ribosome biogenesis, and the cellular response to stress. As discussed in the Introduction, organisms that have defects in XRN1 expression also display abnormalities in many of these processes, including cell proliferation (Jones et al. 2012; Nagarajan et al. 2013). These results lend further support to the idea that sfRNA suppresses XRN1 activity during infection. Furthermore, the transcripts that were selectively stabilized in association with sfRNA formation may encode factors that are particularly important for the cellular response to viral infection. Gene ontology analysis revealed a significant enrichment ($p \leq 0.001$) in transcripts of proteins involved in RNA processing, RNA splicing, protein catabolism, macromolecular complex subunit organization, regulation of protein ubiquitination, and other processes that are likely important for remodeling the cell by altering cellular gene expression. The full list of GO terms that are significantly enriched ($p \leq 0.001$) is reported in Appendix 4.

Flavivirus infected cells undergo ER stress, as demonstrated by several studies (e.g. Yu et al. 2013; Ambrose and Mackenzie 2011). This is further supported by our RNA-seq data as GO analysis of the transcripts $\geq$2x increased in abundance in KUNV or sfRNA(-) KUNV infections showed a significant ($p<0.01$) enrichment in transcripts encoding factors involved in the response to ER stress, ER overload response, and the unfolded protein response. Therefore, one possible experiment to demonstrate the importance of XRN1 in mediating cell responses to stress would be to deplete human cells of XRN1 (by shRNA-mediated gene silencing) or treat cells with sfRNA-forming constructs, and challenge cells with chemical inducers of ER stress (e.g. brefeldin A; Klausner et al. 1992) to determine if post-transcriptional changes in gene expression and/or cytotoxicity are observed in association with XRN1 suppression. These studies will provide insight into the direct mechanisms by which XRN1 suppression could lead to pathology during a viral infection.

Determine if XRN1 suppression enhances viral RNA recombination

As described above in the Introduction, the gene expression strategy of flaviviruses relies on the translation and proteolytic processing of a polyprotein encoded in a single viral RNA. However, the organization of the viral genome and the generation of distinct viral proteins can be greatly influenced by changes in the viral RNA sequence caused by mutation or recombination events. Furthermore, sfRNAs have been shown to be essential for Kunjin virus pathogenesis (Pijlman et al. 2008). Theoretically, changes in the organization /sequence of the viral RNA due to recombination events or mutations could alter the RNA structures such that sfRNA formation is enhanced or suppressed. Therefore, changes in the flaviviral RNA sequence due to recombination or mutation could ultimately contribute to viral pathogenesis.

It is likely that mutation of nascent viral genomes due to error-prone flavivirus RdRp activity is the primary mechanism by which genetic diversity is expanded in these viruses. For

example, the error rate of DENV RdRp is known to be fairly high and is in the same range as other single stranded RNA viruses at 10^{-3}-10^{-5} mutations per nucleotide (Jin et al. 2011; Drake 1993; Holmes and Burch 2000). Similarly, HCV mutation rates were estimated to be ~3×10^{-5} mutations per nucleotide in human patients (Ribeiro et al. 2012). However, recombination of viral RNA genomes can occur as viral RdRps dissociate from one template and re-initiate transcription on another template to generate a novel RNA sequence (i.e. template switching; Simon-Loriere and Holmes 2011). Recombination can therefore change the genome structure and substantially alter the protein products generated by a virus. Interestingly, viral genomes of members of all three genera in the *Flaviviridae* family have been reported to undergo RNA recombination events, the outcome of which leads to either deletion of internal segments or results in the insertion of host or viral RNA sequences into the viral genome (Tautz et al. 1994; Tautz et al. 1996; Meyers et al. 1989; Meyers et al. 1998; Simon-Loriere and Holmes 2011 Pesko et al. 2012). Although some phylogenetic studies have pin-pointed specific instances in which certain flaviviruses including DENV have likely undergone recombination events, experimental evidence indicates that flavivirus recombination is probably a rare event (Holmes et al. 1999; Tolou et al. 2001; Uzcatequi et al. 2001; Taucher et al. 2010; Faye et al. 2014). However, the pestiviruses and hepaciviruses are known to undergo recombination events quite frequently (Gallei et al. 2005; Cristina and Colina 2006; Moreno et al. 2006; Reiter et al. 2011; Simon-Loriere and Holmes 2011; Scheel et al. 2013). Importantly, recombination is a significant mechanism by which changes in cytopathogenicity of BVDV infections can occur (Meyers et al. 1991; Gallei et al. 2005). In some cases, viral or host protease recognition sites are inserted into the BVDV genome between NS2 and NS3 (likely through recombination events) leading to proteolysis; however, some insertions do not have an obvious proteolysis target site and cause cleavage of NS2 and NS3 through unknown mechanisms (Tautz et al. 1996, Meyers et al. 1989; Meyers et al. 1991, Mendez et al. 1998; Becher et al. 2002).

Intriguingly, studies in plants have demonstrated that XRN1 is likely involved in suppressing viral RNA recombination events (Serviene et al. 2005; Cheng et al. 2006; Jaag and Nagy 2009). This may be because XRN1 is involved in degrading viral and cellular transcripts, effectively removing decapped (and therefore potential substrates for RNA-RNA recombination) RNAs from the cytoplasm that could be incorporated into nascent viral genomic RNAs during RdRp template switching. Importantly, as discussed above, non-cytopathic BVDV can transform into cytopathic BVDV and therefore cause severe mucosal disease in infected animals (Tautz et al. 1998). Therefore, if XRN1 suppression enhances viral recombination events in mammalian systems as well as plant systems, then this could be an important mechanism by which flaviviruses evolve to become more pathogenic.

It would be particularly interesting to determine if the suppression of XRN1 by viral RNAs could increase the recombination frequency in flavivirus infections. There are three experiments that could be done to test this hypothesis. First, SINV is known to undergo RNA-RNA recombination (Weiss and Schlesinger 1991; Raju et al. 1995) in tissue culture models of infection. The 3' UTR of DENV-2 or the 5' UTRs of HCV or BVDV could be provided in *trans* to determine if (1) there are more viral recombinants (by sequence) or (2) there is an increase in defective interfering particles (non-infectious virions that likely increase in abundance in association with increased RNA-RNA recombination events). Finally, we are currently working to determing the exact sequences/structures necessary in the BVDV and 5' UTRs by deletion mutagenesis that facilitates XRN1 suppression. This should facilitate the construction of replicon constructs and/or infectious clones that lack the XRN1 resistance element that can be used to screen for viral RNA recombinants.

Development of a novel screening assay for anti-flavivirals

Although there are accepted vaccines in use for several flaviviruses including YFV and JEV, there are no targeted, highly effective treatments for any pathogens in the *Flavivirus* genus. There is a profound need for novel, targeted anti-flaviviral therapies. Because all of these viruses have similar replication cycles, they likely use similar aspects of the cellular gene expression machinery to promote viral proliferation that could be targeted for new anti-viral therapeutics. The research presented herein describes a unique mechanism that all members of the *Flaviviridae* may use to successfully interact with the host RNA decay machinery.

The formation of sfRNA during flavivirus infection has been shown to be important for viral replication in certain cell lines (Pijlman et al. 2008; Silva et al. 2010). Furthermore, we have demonstrated that the up-regulation of cytokines, chemokines, and other pro-inflammatory factors is dramatically enhanced by sfRNA formation in Kunjin virus infections. Cells infected with HCV and BVDV have significant defects in mRNA stability consistent with XRN1 suppression that likely contribute to the over-expression of cellular transcripts implicated in viral pathogenesis including hepatocellular carcinoma due to HCV infection. Because these viruses also appear to suppress XRN1 activity through unique structures in their 5' UTRs, anti-viral compounds that destabilize the RNA structures required for XRN1 suppression will likely have two important functions: suppression of both viral replication and pathogenesis. A high throughput cell-free drug screening assay in which sfRNA formation is monitored could therefore provide a starting point for the generation of novel anti-viral compounds that could potentially mitigate disease caused by any virus in the *Flaviviridae* family. Importantly, carcinogenesis due to HCV could potentially be inhibited through treatment with one such compound.

Conclusions

Through the experiments presented herein, we have demonstrated several important findings. First, the stalling of XRN1 on complex, conserved structural elements in flavivirus 3' UTRs also suppress XRN1 activity. Secondly, other members of the *Flaviviridae* family, namely hepatitis C virus and bovine viral diarrhea virus, generate XRN1-mediated decay intermediates from their highly structured 5' UTRs. Furthermore, the stalling of XRN1 on these RNA structures also suppresses XRN1 activity, indicating that inhibition of the major 5'-3' exonuclease XRN1 is likely conserved among all members of the *Flaviviridae*. Third, XRN1 suppression by viral RNAs contributes to dramatic changes in cellular mRNA stability and likely dampens the host response to infection. This could contribute to the enhancement of virus-induced pathology that is observed in wild-type sfRNA forming KUNV and DENV-2 infections but not during infections with mutant viruses deficient in sfRNA formation (Pijlman et al. 2008; Liu et al. 2014). The studies presented herein will therefore contribute to our understanding of how post-transcriptional mechanisms regulate cellular gene expression in the context of viral infection. Additionally, our studies suggest that one mechanism by which sfRNA suppresses RNA interference is by binding to AGO2 and DICER to suppress their activities during infection. This is potentially important for persistent infections of the arthropod vectors of many of the flaviviruses, as RNAi is an essential antiviral immune mechanism in these organisms (Blair 2011). Finally, we provide a foundation for the further study of how viruses evade and suppress the host cellular RNA decay machinery to promote a productive infection.

CITATIONS

Acosta EG, Castilla V, Damonte EB. Functional entry of dengue virus into Aedes albopictus mosquito cells is dependent on clathrin-mediated endocytosis. J Gen Virol. 2008 Feb;89(Pt 2):474-84

Adler B, Adler H, Pfister H, Jungi TW, Peterhans E. Macrophages infected with cytopathic bovine viral diarrhea virus release a factor(s) capable of priming uninfected macrophages for activation-induced apoptosis. J Virol. 1997 Apr;71(4):3255-8.

Akira S, Uematsu S, Takeuchi O. Pathogen recognition and innate immunity. Cell. 2006 Feb 24;124(4):783-801.

Al-Haj L, Blackshear PJ, Khabar KS. Regulation of p21/CIP1/WAF-1 mediated cell-cycle arrest by RNase L and tristetraprolin, and involvement of AU-rich elements. Nucleic Acids Res. 2012 Sep;40(16):7739-52.

Alvarez DE, Lodeiro MF, Ludueña SJ, Pietrasanta LI, Gamarnik AV. Long-range RNA-RNA interactions circularize the dengue virus genome. J Virol. 2005 Jun;79(11):6631-43.

Amberg DC, Goldstein AL, Cole CN. Isolation and characterization of RAT1: an essential gene of Saccharomyces cerevisiae required for the efficient nucleocytoplasmic trafficking of mRNA. Genes Dev. 1992 Jul;6(7):1173-89.

Ambrose RL, Mackenzie JM. West Nile virus differentially modulates the unfolded protein response to facilitate replication and immune evasion. J Virol. 2011 Mar;85(6):2723-32.

Anderson JS, Parker RP. The 3' to 5' degradation of yeast mRNAs is a general mechanism for mRNA turnover that requires the SKI2 DEVH box protein and 3' to 5' exonucleases of the exosome complex. EMBO J. 1998 Mar 2;17(5):1497-506.

Anderson P. Intrinsic mRNA stability helps compose the inflammatory symphony. Nat Immunol. 2009 Mar;10(3):233-4.

Angusti A, Manfredini S, Durini E, Ciliberti N, Vertuani S, Solaroli N, Pricl S, Ferrone M, Fermeglia M, Loddo R, Secci B, Visioli A, Sanna T, Collu G, Pezzullo M, La Colla P. Design, synthesis and anti flaviviridae activity of N(6)-, 5',3'-O- and 5',2'-O-substituted adenine nucleoside analogs. Chem Pharm Bull (Tokyo). 2008 Apr;56(4):423-32.

Ariumi Y, Kuroki M, Kushima Y, Osugi K, Hijikata M, Maki M, Ikeda M, Kato N. Hepatitis C virus hijacks P-body and stress granule components around lipid droplets. J Virol. 2011 Jul;85(14):6882-92.

Armstrong GL, Wasley A, Simard EP, McQuillan GM, Kuhnert WL, Alter MJ. The prevalence of hepatitis C virus infection in the United States, 1999 through 2002. Ann Intern Med. 2006 May 16;144(10):705-14.

Ashour J, Laurent-Rolle M, Shi PY, García-Sastre A. NS5 of dengue virus mediates STAT2 binding and degradation. J Virol. 2009 Jun;83(11):5408-18.

Azarkh Y, Dölken L, Nagel M, Gilden D, Cohrs RJ. Synthesis and decay of varicella zoster virus transcripts. J Neurovirol. 2011 Jun;17(3):281-7.

Backes S, Shapiro JS, Sabin LR, Pham AM, Reyes I, Moss B, Cherry S, tenOever BR. Degradation of host microRNAs by poxvirus poly(A) polymerase reveals terminal RNA methylation as a protective antiviral mechanism. Cell Host Microbe. 2012 Aug 16;12(2):200-10.

Baillat D, Shiekhattar R. Functional dissection of the human TNRC6 (TNRC6A-related) family of proteins. Mol Cell Biol. 2009 Aug;29(15):4144-55.

Banerjee A, Ray RB, Ray R. Oncogenic potential of hepatitis C virus proteins. Viruses. 2010 Sep;2(9):2108-33.

Barnhart MD, Moon SL, Emch AW, Wilusz CJ, Wilusz J. Changes in cellular mRNA stability, splicing, and polyadenylation through HuR protein sequestration by a cytoplasmic RNA virus. Cell Rep. 2013 Nov 27;5(4):909-17.

Bartel DP. MicroRNAs: genomics, biogenesis, mechanism, and function. Cell. 2004 Jan 23;116(2):281-97

Bartel DP. MicroRNAs: target recognition and regulatory functions. Cell. 2009 Jan 23;136(2):215-33.

Bartenschlager R, Ahlborn-Laake L, Mous J, Jacobsen H. Kinetic and structural analyses of hepatitis C virus polyprotein processing. J Virol. 1994 Aug;68(8):5045-55.

Bartholomeusz A, Tomlinson E, Wright PJ, Birch C, Locarnini S, Weigold H, Marcuccio S, Holan G. Use of a flavivirus RNA-dependent RNA polymerase assay to investigate the antiviral activity of selected compounds. Antiviral Res. 1994 Aug;24(4):341-50.

Bashkirov VI, Scherthan H, Solinger JA, Buerstedde JM, Heyer WD. A mouse cytoplasmic exoribonuclease (mXRN1p) with preference for G4 tetraplex substrates. J Cell Biol. 1997 Feb 24;136(4):761-73.

Basu A, Chaturvedi UC. Vascular endothelium: the battlefield of dengue viruses. FEMS Immunol Med Microbiol. 2008 Aug;53(3):287-99.

Bauhofer O, Summerfield A, Sakoda Y, Tratschin JD, Hofmann MA, Ruggli N. Classical swine fever virus Npro interacts with interferon regulatory factor 3 and induces its proteasomal degradation. J Virol. 2007 Apr;81(7):3087-96.

Becher P, Avalos Ramirez R, Orlich M, Cedillo Rosales S, König M, Schweizer M, Stalder H, Schirrmeier H, Thiel HJ.Genetic and antigenic characterization of novel pestivirus genotypes: implications for classification. Virology. 2003 Jun 20;311(1):96-104.

Becher P, Orlich M, Thiel HJ. Complete genomic sequence of border disease virus, a pestivirus from sheep. J Virol. 1998 Jun;72(6):5165-73.

Becher P, Thiel HJ, Collins M, Brownlie J, Orlich M. Cellular sequences in pestivirus genomes encoding gamma-aminobutyric acid (A) receptor-associated protein and Golgi-associated ATPase enhancer of 16 kilodaltons. J Virol. 2002 Dec;76(24):13069-76.

Beckham CJ, Parker R. P bodies, stress granules, and viral life cycles. Cell Host Microbe. 2008 Apr 17;3(4):206-12.

Beelman CA, Stevens A, Caponigro G, LaGrandeur TE, Hatfield L, Fortner DM, Parker R. An essential component of the decapping enzyme required for normal rates of mRNA turnover. Nature. 1996 Aug 15;382(6592):642-6.

Ben-Ami O, Pencovich N, Lotem J, Levanon D, Groner Y. A regulatory interplay between miR-27a and Runx1 during megakaryopoiesis. Proc Natl Acad Sci U S A. 2009 Jan 6;106(1):238-43.

Benelli R, Lorusso G, Albini A, Noonan DM. Cytokines and chemokines as regulators of angiogenesis in health and disease. Curr Pharm Des. 2006;12(24):3101-15.

Berezhna SY, Supekova L, Sever MJ, Schultz PG, Deniz AA. Dual regulation of hepatitis C viral RNA by cellular RNAi requires partitioning of AGO2 to lipid droplets and P-bodies. RNA. 2011 Oct;17(10):1831-45.

Bergqvist A, Rice CM. Transcriptional activation of the interleukin-2 promoter by hepatitis C virus core protein. J Virol. 2001 Jan;75(2):772-81.

Berry KE, Waghray S, Doudna JA. The HCV IRES pseudoknot positions the initiation codon on the 40S ribosomal subunit. RNA. 2010 Aug;16(8):1559-69.

Bhattacharyya S, Sen U, Vrati S. Regulated IRE1-dependent decay pathway is activated during Japanese encephalitis virus-induced unfolded protein response and benefits viral replication. J Gen Virol. 2014 Jan;95(Pt 1):71-9.

Bhattacharyya SN, Habermacher R, Martine U, Closs EI, Filipowicz W. Stress-induced reversal of microRNA repression and mRNA P-body localization in human cells. Cold Spring Harb Symp Quant Biol. 2006;71:513-21.

Bielefeldt-Ohmann H, Smirnova NP, Tolnay AE, Webb BT, Antoniazzi AQ, van Campen H, Hansen TR. Neuro-invasion by a 'Trojan Horse' strategy and vasculopathy during intrauterine flavivirus infection. Int J Exp Pathol. 2012 Feb;93(1):24-33.

Bisbal C, Silverman RH. Diverse functions of RNase L and implications in pathology. Biochimie. 2007 Jun-Jul;89(6-7):789-98.

Blair CD. Mosquito RNAi is the major innate immune pathway controlling arbovirus infection and transmission. Future Microbiol. 2011 Mar;6(3):265-77.

Blanchard E, Belouzard S, Goueslain L, Wakita T, Dubuisson J, Wychowski C, Rouillé Y. Hepatitis C virus entry depends on clathrin-mediated endocytosis. J Virol. 2006 Jul;80(14):6964-72.

Blewett N, Coller J, Goldstrohm A. A quantitative assay for measuring mRNA decapping by splinted ligation reverse transcription polymerase chain reaction: qSL-RT-PCR. RNA. 2011 Mar;17(3):535-43.

Boege U, Heinz FX, Wengler G, Kunz C. Amino acid compositions and amino-terminal sequences of the structural proteins of a flavivirus, European Tick-Borne Encephalitis virus. Virology. 1983 Apr 30;126(2):651-7.

Boffa MB, Maret D, Hamill JD, Bastajian N, Crainich P, Jenny NS, Tang Z, Macy EM, Tracy RP, Franco RF, Nesheim ME, Koschinsky ML. Effect of single nucleotide polymorphisms on expression of the gene encoding thrombin-activatable fibrinolysis inhibitor: a functional analysis. Blood. 2008 Jan 1;111(1):183-9.

Bouveret E, Rigaut G, Shevchenko A, Wilm M, Séraphin B. A Sm-like protein complex that participates in mRNA degradation. EMBO J. 2000 Apr 3;19(7):1661-71.

Brackenbury LS, Carr BV, Charleston B. Aspects of the innate and adaptive immune responses to acute infections with BVDV. Vet Microbiol. 2003 Nov 7;96(4):337-44.

Bradrick SS, Nagyal S, Novatt H. A miRNA-responsive cell-free translation system facilitates isolation of hepatitis C virus miRNP complexes. RNA. 2013 Aug;19(8):1159-69.

Bradrick SS, Walters RW, Gromeier M. The hepatitis C virus 3'-untranslated region or a poly(A) tract promote efficient translation subsequent to the initiation phase. Nucleic Acids Res. 2006 Mar 1;34(4):1293-303.

Braun JE, Truffault V, Boland A, Huntzinger E, Chang CT, Haas G, Weichenrieder O, Coles M, Izaurralde E. A direct interaction between DCP1 and XRN1 couples mRNA decapping to 5' exonucleolytic degradation. Nat Struct Mol Biol. 2012 Dec; 19(12):1324-31.

Brawerman G, Mendecki J, Lee SY. A procedure for the isolation of mammalian messenger ribonucleic acid. Biochemistry. 1972 Feb 15;11(4):637-41.

Brawerman G. Eukaryotic messenger RNA. Annu Rev Biochem. 1974;43(0):621-42.

Brengues M, Teixeira D, Parker R. Movement of eukaryotic mRNAs between polysomes and cytoplasmic processing bodies. Science. 2005 Oct 21;310(5747):486-9.

Brinton MA, Dispoto JH. Sequence and secondary structure analysis of the 5'-terminal region of flavivirus genome RNA. Virology. 1988 Feb;162(2):290-9.

Brinton MA, Fernandez AV, Dispoto JH. The 3'-nucleotides of flavivirus genomic RNA form a conserved secondary structure. Virology. 1986 Aug;153(1):113-21.

Brinton MA, Perelygin AA. Genetic resistance to flaviviruses. Adv Virus Res. 2003;60:43-85.

Brinton MA. Replication cycle and molecular biology of the West Nile virus. Viruses. 2013 Dec 27;6(1):13-53.

Brown CE, Tarun SZ Jr, Boeck R, Sachs AB. PAN3 encodes a subunit of the Pab1p-dependent poly(A) nuclease in Saccharomyces cerevisiae. Mol Cell Biol. 1996 Oct;16(10):5744-53.

Brown EA, Zhang H, Ping LH, Lemon SM. Secondary structure of the 5' nontranslated regions of hepatitis C virus and pestivirus genomic RNAs. Nucleic Acids Res. 1992 Oct 11;20(19):5041-5.

Brown JA, Valenstein ML, Yario TA, Tycowski KT, Steitz JA. Formation of triple-helical structures by the 3'-end sequences of MALAT1 and MENβ noncoding RNAs. Proc Natl Acad Sci U S A. 2012 Nov 20;109(47):19202-7.

Brownell J, Polyak SJ. Molecular pathways: hepatitis C virus, CXCL10, and the inflammatory road to liver cancer. Clin Cancer Res. 2013 Mar 15;19(6):1347-52.

Brownlie J, Clarke MC, Howard CJ. Experimental infection of cattle in early pregnancy with a cytopathic strain of bovine virus diarrhoea virus. Res Vet Sci. 1989 May;46(3):307-11.

Brownlie J, Clarke MC, Howard CJ. Experimental production of fatal mucosal disease in cattle. Vet Rec. 1984 Jun 2;114(22):535-6.

Buchan JR, Muhlrad D, Parker R. P bodies promote stress granule assembly in Saccharomyces cerevisiae. J Cell Biol. 2008 Nov 3;183(3):441-55.

Buchan JR, Parker R. Eukaryotic stress granules: the ins and outs of translation. Mol Cell. 2009 Dec 25;36(6):932-41.

Buck AH, Perot J, Chisholm MA, Kumar DS, Tuddenham L, Cognat V, Marcinowski L, Dölken L, Pfeffer S. Post-transcriptional regulation of miR-27 in murine cytomegalovirus infection. RNA. 2010 Feb;16(2):307-15.

Bukh J, Purcell RH, Miller RH. Sequence analysis of the 5' noncoding region of hepatitis C virus. Proc Natl Acad Sci U S A. 1992 Jun 1;89(11):4942-6.

Burbelo PD, Dubovi EJ, Simmonds P, Medina JL, Henriquez JA, Mishra N, Wagner J, Tokarz R, Cullen JM, Iadarola MJ, Rice CM, Lipkin WI, Kapoor A. Serology-enabled discovery of genetically diverse hepaciviruses in a new host. J Virol. 2012 Jun;86(11):6171-8.

Burke DS and Monath TP. 2001. Flaviviruses. In Knipe DM and Howley PM (eds), Fields Virology. Lippincott-Williams & Wilkins, Philadelphia, PA, pp. 1043–1125.

Caillet-Saguy C, Lim SP, Shi PY, Lescar J, Bressanelli S. Polymerases of hepatitis C viruses and flaviviruses: Structural and mechanistic insights and drug development. Antiviral Res. 2014 Feb 19. pii: S0166-3542(14)00049-7.

Campbell CL, Black WC 4th, Hess AM, Foy BD. Comparative genomics of small RNA regulatory pathway components in vector mosquitoes. BMC Genomics. 2008 Sep 18;9:425.

Caplen NJ, Parrish S, Imani F, Fire A, Morgan RA. Specific inhibition of gene expression by small double-stranded RNAs in invertebrate and vertebrate systems. Proc Natl Acad Sci U S A. 2001 Aug 14;98(17):9742-7.

Caput D, Beutler B, Hartog K, Thayer R, Brown-Shimer S, Cerami A. Identification of a common nucleotide sequence in the 3'-untranslated region of mRNA molecules specifying inflammatory mediators. Proc Natl Acad Sci U S A. 1986 Mar;83(6):1670-4.

Carballo E, Lai WS, Blackshear PJ. Evidence that tristetraprolin is a physiological regulator of granulocyte-macrophage colony-stimulating factor messenger RNA deadenylation and stability. Blood. 2000 Mar 15;95(6):1891-9.

Carballo E, Lai WS, Blackshear PJ. Feedback inhibition of macrophage tumor necrosis factor-alpha production by tristetraprolin. Science. 1998 Aug 14;281(5379):1001-5.

Carod-Artal FJ, Wichmann O, Farrar J, Gascón J. Neurological complications of dengue virus infection. Lancet Neurol. 2013 Sep;12(9):906-19.

Castelli JC, Hassel BA, Wood KA, Li XL, Amemiya K, Dalakas MC, Torrence PF, Youle RJ. A study of the interferon antiviral mechanism: apoptosis activation by the 2-5A system. J Exp Med. 1997 Sep 15; 186(6):967-72.

Cathcart AL, Rozovics JM, Semler BL. Cellular mRNA decay protein AUF1 negatively regulates enterovirus and human rhinovirus infections. J Virol. 2013 Oct;87(19):10423-34.

Cazalla D, Yario T, Steitz JA. Down-regulation of a host microRNA by a Herpesvirus saimiri noncoding RNA. Science. 2010 Jun 18;328(5985):1563-6.

Centers for Disease Control and Prevention (2012). Dengue. Retrieved from http://www.cdc.gov/dengue/

Centers for Disease Control and Prevention. Locally acquired Dengue--Key West, Florida, 2009-2010. MMWR Morb Mortal Wkly Rep. 2010 May 21;59(19):577-81.

Chahar HS, Chen S, Manjunath N. P-body components LSM1, TNRC6A, DDX3, DDX6 and XRN1 are recruited to WNV replication sites and positively regulate viral replication. Virology. 2013 Feb 5;436(1):1-7.

Chambers TJ, Hahn CS, Galler R, Rice CM. Flavivirus genome organization, expression, and replication. Annu Rev Microbiol. 1990;44:649-88.

Chandriani S, Skewes-Cox P, Zhong W, Ganem DE, Divers TJ, Van Blaricum AJ, Tennant BC, Kistler AL. Identification of a previously undescribed divergent virus from the Flaviviridae family in an outbreak of equine serum hepatitis. Proc Natl Acad Sci U S A. 2013 Apr 9;110(15):E1407-15.

Chang CT, Bercovich N, Loh B, Jonas S, Izaurralde E. The activation of the decapping enzyme DCP2 by DCP1 occurs on the EDC4 scaffold and involves a conserved loop in DCP1. Nucleic Acids Res. 2014 Feb 8

Chang KS, Luo G. The polypyrimidine tract-binding protein (PTB) is required for efficient replication of hepatitis C virus (HCV) RNA. Virus Res. 2006 Jan;115(1):1-8.

Chang RY, Hsu TW, Chen YL, Liu SF, Tsai YJ, Lin YT, Chen YS, Fan YH. Japanese encephalitis virus non-coding RNA inhibits activation of interferon by blocking nuclear translocation of interferon regulatory factor 3. Vet Microbiol. 2013 Sep 27;166(1-2):11-21.

Chapman EG, Moon SL, Wilusz J, Kieft JS. RNA Structures that Resist Degradation by XRN1 Produce a Pathogenic Dengue Virus RNA. eLife 2014;3:e01892.

Chapman EG, Costantino DA, Rabe JL, Moon SL, Wilusz J, Nix JC, Kieft JS. The structural basis of pathogenic flavivirus subgenomic RNA (sfRNA) production. Science. *in press*.

Charleston B, Fray MD, Baigent S, Carr BV, Morrison WI.Establishment of persistent infection with non-cytopathic bovine viral diarrhoea virus in cattle is associated with a failure to induce type I interferon. J Gen Virol. 2001 Aug;82(Pt 8):1893-7.

(a) Cheadle C, Fan J, Cho-Chung YS, Werner T, Ray J, Do L, Gorospe M, Becker KG. Control of gene expression during T cell activation: alternate regulation of mRNA transcription and mRNA stability. BMC Genomics. 2005 May 20;6:75.

(b) Cheadle C, Fan J, Cho-Chung YS, Werner T, Ray J, Do L, Gorospe M, Becker KG. Stability regulation of mRNA and the control of gene expression. Ann N Y Acad Sci. 2005 Nov;1058:196-204.

Cheeran MC, Hu S, Sheng WS, Rashid A, Peterson PK, Lokensgard JR. Differential responses of human brain cells to West Nile virus infection. J Neurovirol. 2005 Dec;11(6):512-24.

Chekulaeva M, Mathys H, Zipprich JT, Attig J, Colic M, Parker R, Filipowicz W.miRNA repression involves TNRC6A-mediated recruitment of CCR4-NOT through conserved W-containing motifs. Nat Struct Mol Biol. 2011 Oct 7;18(11):1218-26.

Cheloufi S, Dos Santos CO, Chong MM, Hannon GJ. A DICER-independent miRNA biogenesis pathway that requires Ago catalysis. Nature. 2010 Jun 3;465(7298):584-9.

Chen CY, Zheng D, Xia Z, Shyu AB. Ago-TNRC6 triggers microRNA-mediated decay by promoting two deadenylation steps. Nat Struct Mol Biol. 2009 Nov;16(11):1160-6.

(a) Chen Y, Chen J, Wang H, Shi J, Wu K, Liu S, Liu Y, Wu J. HCV-induced miR-21 contributes to evasion of host immune system by targeting MyD88 and IRAK1. PLoS Pathog. 2013;9(4):e1003248.

(b) Chen L, Liu L, Wang M, Fu J, Zhang Z, Hou J, Bao X. Hal2p functions in Bdf1p-involved salt stress response in Saccharomyces cerevisiae. PLoS One. 2013 Apr 17;8(4):e62110.

Chen Y, Maguire T, Hileman RE, Fromm JR, Esko JD, Linhardt RJ, Marks RM. Dengue virus infectivity depends on envelope protein binding to target cell heparan sulfate. Nat Med. 1997 Aug;3(8):866-71.

Chen Z, Rijnbrand R, Jangra RK, Devaraj SG, Qu L, Ma Y, Lemon SM, Li K. Ubiquitination and proteasomal degradation of interferon regulatory factor-3 induced by Npro from a cytopathic bovine viral diarrhea virus. Virology. 2007 Sep 30;366(2):277-92.

Cheng CP, Serviene E, Nagy PD. Suppression of viral RNA recombination by a host exoribonuclease. J Virol. 2006 Mar;80(6):2631-40

Chiang DY, Villanueva A, Hoshida Y, Peix J, Newell P, Minguez B, LeBlanc AC, Donovan DJ, Thung SN, Solé M, Tovar V, Alsinet C, Ramos AH, Barretina J, Roayaie S, Schwartz M, Waxman S, Bruix J, Mazzaferro V, Ligon AH, Najfeld V, Friedman SL, Sellers WR, Meyerson M, Llovet JM. Focal gains of VEGFA and molecular classification of hepatocellular carcinoma. Cancer Res. 2008 Aug 15;68(16):6779-88.

Chowdhury A, Mukhopadhyay J, Tharun S. The decapping activator Lsm1p-7p-Pat1p complex has the intrinsic ability to distinguish between oligoadenylated and polyadenylated RNAs. RNA. 2007 Jul;13(7):998-1016.

Christie M, Boland A, Huntzinger E, Weichenrieder O, Izaurralde E. Structure of the PAN3 pseudokinase reveals the basis for interactions with the PAN2 deadenylase and the TNRC6A proteins. Mol Cell. 2013 Aug 8;51(3):360-73.

Chu JJ, Ng ML. Infectious entry of West Nile virus occurs through a clathrin-mediated endocytic pathway. J Virol. 2004 Oct;78(19):10543-55.

Chursov A, Kopetzky SJ, Leshchiner I, Kondofersky I, Theis FJ, Frishman D, Shneider A. Specific temperature-induced perturbations of secondary mRNA structures are associated with the cold-adapted temperature-sensitive phenotype of influenza A virus. RNA Biol. 2012 Oct;9(10):1266-74.

Cifuentes D, Xue H, Taylor DW, Patnode H, Mishima Y, Cheloufi S, Ma E, Mane S, Hannon GJ, Lawson ND, Wolfe SA, Giraldez AJ. A novel miRNA processing pathway independent of DICER requires Argonaute2 catalytic activity. Science. 2010 Jun 25;328(5986):1694-8.

Clyde K, Harris E.RNA secondary structure in the coding region of dengue virus type 2 directs translation start codon selection and is required for viral replication. J Virol. 2006 Mar;80(5):2170-82.

Clyde K, Barrera J, Harris E. The capsid-coding region hairpin element (cHP) is a critical determinant of dengue virus and West Nile virus RNA synthesis. Virology. 2008 Sep 30;379(2):314-23.

Cole KE, Strick CA, Paradis TJ, Ogborne KT, Loetscher M, Gladue RP, Lin W, Boyd JG, Moser B, Wood DE, Sahagan BG, Neote K. Interferon-inducible T cell alpha chemoattractant (I-TAC): a novel non-ELR CXC chemokine with potent activity on activated T cells through selective high affinity binding to CXCR3. J Exp Med. 1998 Jun 15;187(12):2009-21.

Collart MA, Panasenko OO, Nikolaev SI. The Not3/5 subunit of the Ccr4-Not complex: a central regulator of gene expression that integrates signals between the cytoplasm and the nucleus in eukaryotic cells. Cell Signal. 2013 Apr;25(4):743-51.

Collart MA. Global control of gene expression in yeast by the Ccr4-Not complex. Gene. 2003 Aug 14;313:1-16.

Collins ME, Heaney J, Thomas CJ, Brownlie J. Infectivity of pestivirus following persistence of acute infection. Vet Microbiol. 2009 Sep 18;138(3-4):289-96.

Conrad KD, Giering F, Erfurth C, Neumann A, Fehr C, Meister G, Niepmann M. MicroRNA-122 dependent binding of AGO2 protein to hepatitis C virus RNA is associated with enhanced RNA stability and translation stimulation. PLoS One. 2013;8(2):e56272.

Coonrod LA, Nakamori M, Wang W, Carrell S, Hilton CL, Bodner MJ, Siboni RB, Docter AG, Haley MM, Thornton CA, Berglund JA. Reducing levels of toxic RNA with small molecules. ACS Chem Biol. 2013 Nov 15;8(11):2528-37.

Cooper DA, Jha BK, Silverman RH, Hesselberth JR, Barton DJ. Ribonuclease L and metal-ion-independent endoribonuclease cleavage sites in host and viral RNAs. Nucleic Acids Res. 2014 Feb 5.

Costa VV, Fagundes CT, Souza DG, Teixeira MM. Inflammatory and innate immune responses in dengue infection: protection versus disease induction. Am J Pathol. 2013 Jun;182(6):1950-61.

Cougot N, Babajko S, Séraphin B. Cytoplasmic foci are sites of mRNA decay in human cells. J Cell Biol. 2004 Apr;165(1):31-40.

Coulon C, Georgiadou M, Roncal C, De Bock K, Langenberg T, Carmeliet P. From vessel sprouting to normalization: role of the prolyl hydroxylase domain protein/hypoxia-inducible factor oxygen-sensing machinery. Arterioscler Thromb Vasc Biol. 2010 Dec;30(12):2331-6.

Courtney SC, Di H, Stockman BM, Liu H, Scherbik SV, Brinton MA. Identification of novel host cell binding partners of Oas1b, the protein conferring resistance to flavivirus-induced disease in mice. J Virol. 2012 Aug;86(15):7953-63.

Coussens LM, Werb Z. Inflammation and cancer. Nature. 2002 Dec 19-26;420(6917):860-7.

Crist CG, Montarras D, Pallafacchina G, Rocancourt D, Cumano A, Conway SJ, Buckingham M. Muscle stem cell behavior is modified by microRNA-27 regulation of Pax3 expression. Proc Natl Acad Sci U S A. 2009 Aug 11;106(32):13383-7.

Cristina J, Colina R. Evidence of structural genomic region recombination in Hepatitis C virus. Virol J. 2006 Jun 30;3:53.

Cullen BR, Cherry S, tenOever BR. Is RNA interference a physiologically relevant innate antiviral immune response in mammals? Cell Host Microbe. 2013 Oct 16;14(4):374-8.

Daffis S, Szretter KJ, Schriewer J, Li J, Youn S, Errett J, Lin TY, Schneller S, Zust R, Dong H, Thiel V, Sen GC, Fensterl V, Klimstra WB, Pierson TC, Buller RM, Gale M Jr, Shi PY, Diamond MS. 2'-O methylation of the viral mRNA cap evades host restriction by IFIT family members. Nature. 2010 Nov 18;468(7322):452-6.

de Groot RP, Schoorlemmer J, van Genesen ST, Kruijer W. Differential expression of jun and fos genes during differentiation of mouse P19 embryonal carcinoma cells. Nucleic Acids Res. 1990 Jun 11;18(11):3195-202.

Decker CJ, Parker R. A turnover pathway for both stable and unstable mRNAs in yeast: evidence for a requirement for deadenylation. Genes Dev. 1993 Aug;7(8):1632-43.

Decker CJ, Teixeira D, Parker R. EDC3p and a glutamine/asparagine-rich domain of Lsm4p function in processing body assembly in Saccharomyces cerevisiae. J Cell Biol. 2007 Nov 5; 179(3):437-49.

Deng R, Brock KV. 5' and 3' untranslated regions of pestivirus genome: primary and secondary structure analyses. Nucleic Acids Res. 1993 Apr 25;21(8):1949-57.

Depner K, Bauer T, Liess B. Thermal and pH stability of pestiviruses. Rev Sci Tech. 1992 Sep;11(3):885-93.

Dichtl B, Stevens A, Tollervey D. Lithium toxicity in yeast is due to the inhibition of RNA processing enzymes. EMBO J. 1997 Dec 1;16(23):7184-95.

Dickson AM, Anderson JR, Barnhart MD, Sokoloski KJ, Oko L, Opyrchal M, Galanis E, Wilusz CJ, Morrison TE, Wilusz J. Dephosphorylation of HuR protein during alphavirus infection is associated with HuR relocalization to the cytoplasm. J Biol Chem. 2012 Oct 19;287(43):36229-38.

Doll D, Keller L, Maak M, Boulesteix AL, Siewert JR, Holzmann B, Janssen KP. Differential expression of the chemokines GRO-2, GRO-3, and interleukin-8 in colon cancer and their impact on metastatic disease and survival. Int J Colorectal Dis. 2010 May;25(5):573-81.

Doma MK, Parker R. Endonucleolytic cleavage of eukaryotic mRNAs with stalls in translation elongation. Nature. 2006 Mar 23;440(7083):561-4.

Domingues RB, Kuster GW, Onuki-Castro FL, Souza VA, Levi JE, Pannuti CS. Involvement of the central nervous system in patients with dengue virus infection. J Neurol Sci. 2008 Apr 15;267(1-2):36-40.

Done JT, Terlecki S, Richardson C, Harkness JW, Sands JJ, Patterson DS, Sweasey D, Shaw IG, Winkler CE, Duffell SJ. Bovine virus diarrhoea-mucosal disease virus: pathogenicity for the fetal calf following maternal infection. Vet Rec. 1980 Jun 7;106(23):473-9.

Dong QM, Zhang JQ, Li Q, Bracher JC, Hendricks DT, Zhao XH. Clinical significance of serum expression of GROβ in esophageal squamous cell carcinoma. World J Gastroenterol. 2011 Jun 7;17(21):2658-62.

Dong XY, Liu WJ, Zhao MQ, Wang JY, Pei JJ, Luo YW, Ju CM, Chen JD. Classical swine fever virus triggers RIG-I and MDA5-dependent signaling pathway to IRF-3 and NF-κB activation to promote secretion of interferon and inflammatory cytokines in porcine alveolar macrophages. Virol J. 2013 Sep 13;10:286.

Donis RO, Dubovi EJ. Differences in virus-induced polypeptides in cells infected by cytopathic and noncytopathic biotypes of bovine virus diarrhea-mucosal disease virus. Virology. 1987 May;158(1):168-73.

Dorner M, Horwitz JA, Robbins JB, Barry WT, Feng Q, Mu K, Jones CT, Schoggins JW, Catanese MT, Burton DR, Law M, Rice CM, Ploss A. A genetically humanized mouse model for hepatitis C virus infection. Nature. 2011 Jun 8;474(7350):208-11.

Dougherty JD, White JP, Lloyd RE. Poliovirus-mediated disruption of cytoplasmic processing bodies. J Virol. 2011 Jan;85(1):64-75.

Drake JW. Rates of spontaneous mutation among RNA viruses. Proc Natl Acad Sci U S A. 1993 May 1;90(9):4171-5.

Drexler JF, Corman VM, Müller MA, Lukashev AN, Gmyl A, Coutard B, Adam A, Ritz D, Leijten LM, van Riel D, Kallies R, Klose SM, Gloza-Rausch F, Binger T, Annan A, Adu-Sarkodie Y,

Oppong S, Bourgarel M, Rupp D, Hoffmann B, Schlegel M, Kümmerer BM, Krüger DH, Schmidt-Chanasit J, Setién AA, Cottontail VM, Hemachudha T, Wacharapluesadee S, Osterrieder K, Bartenschlager R, Matthee S, Beer M, Kuiken T, Reusken C, Leroy EM, Ulrich RG, Drosten C. Evidence for novel hepaciviruses in rodents. PLoS Pathog. 2013;9(6):e1003438.

Duan R, Rhie BH, Ryu HY, Ahn SH. The RNA polymerase II Rpb4/7 subcomplex regulates cellular lifespan through an mRNA decay process. Biochem Biophys Res Commun. 2013 Nov 8;441(1):266-70.

Dukhan D, Leroy F, Peyronnet J, Bosc E, Chaves D, Durka M, Storer R, La Colla P, Seela F, Gosselin G. Synthesis of 5-aza-7-deazaguanine nucleoside derivatives as potential anti-flavivirus agents. Nucleosides Nucleotides Nucleic Acids. 2005;24(5-7):671-4.

Dunckley T, Parker R. The DCP2 protein is required for mRNA decapping in Saccharomyces cerevisiae and contains a functional MutT motif. EMBO J. 1999 Oct 1;18(19):5411-22.

Dunckley T, Tucker M, Parker R. Two related proteins, EDC1p and EDC2p, stimulate mRNA decapping in Saccharomyces cerevisiae. Genetics. 2001 Jan;157(1):27-37.

Eberle AB, Lykke-Andersen S, Mühlemann O, Jensen TH. SMG6 promotes endonucleolytic cleavage of nonsense mRNA in human cells. Nat Struct Mol Biol. 2009 Jan;16(1):49-55.

Ebos JM, Lee CR, Cruz-Munoz W, Bjarnason GA, Christensen JG, Kerbel RS. Accelerated metastasis after short-term treatment with a potent inhibitor of tumor angiogenesis. Cancer Cell. 2009 Mar 3;15(3):232-9.

Egger D, Wölk B, Gosert R, Bianchi L, Blum HE, Moradpour D, Bienz K. Expression of hepatitis C virus proteins induces distinct membrane alterations including a candidate viral replication complex. J Virol. 2002 Jun;76(12):5974-84.

Eksioglu EA, Zhu H, Bayouth L, Bess J, Liu HY, Nelson DR, Liu C. Characterization of HCV interactions with Toll-like receptors and RIG-I in liver cells. PLoS One. 2011;6(6):e21186.

Elshuber S, Allison SL, Heinz FX, Mandl CW. Cleavage of protein prM is necessary for infection of BHK-21 cells by tick-borne encephalitis virus. J Gen Virol. 2003 Jan;84(Pt 1):183-91.

Elvang A, Melik W, Bertrand Y, Lönn M, Johansson M. Sequencing of a tick-borne encephalitis virus from Ixodes ricinus reveals a thermosensitive RNA switch significant for virus propagation in ectothermic arthropods. Vector Borne Zoonotic Dis. 2011 Jun;11(6):649-58.

Emara MM, Brinton MA. Interaction of TIA-1/TIAR with West Nile and dengue virus products in infected cells interferes with stress granule formation and processing body assembly. Proc Natl Acad Sci U S A. 2007 May 22;104(21):9041-6.

Epstein JH, Quan PL, Briese T, Street C, Jabado O, Conlan S, Ali Khan S, Verdugo D, Hossain MJ, Hutchison SK, Egholm M, Luby SP, Daszak P, Lipkin WI. Identification of GBV-D, a novel GB-like flavivirus from old world frugivorous bats (Pteropus giganteus) in Bangladesh. PLoS Pathog. 2010 Jul 1;6:e1000972.

Errett JS, Suthar MS, McMillan A, Diamond MS, Gale M Jr. The essential, nonredundant roles of RIG-I and MDA5 in detecting and controlling West Nile virus infection. J Virol. 2013 Nov;87(21):11416-25

Esteban R, Vega L, Fujimura T. 20S RNA narnavirus defies the antiviral activity of SKI1/XRN1 in Saccharomyces cerevisiae. J Biol Chem. 2008 Sep 19;283(38):25812-20.

Evans MJ, von Hahn T, Tscherne DM, Syder AJ, Panis M, Wölk B, Hatziioannou T, McKeating JA, Bieniasz PD, Rice CM. Claudin-1 is a hepatitis C virus co-receptor required for a late step in entry. Nature. 2007 Apr 12;446(7137):801-5.

Eystathioy T, Jakymiw A, Chan EK, Séraphin B, Cougot N, Fritzler MJ. The TNRC6A protein colocalizes with mRNA degradation associated proteins hDCP1 and hLSm4 in cytoplasmic GW bodies. RNA. 2003 Oct;9(10):1171-3.

Fabian MR, Cieplak MK, Frank F, Morita M, Green J, Srikumar T, Nagar B, Yamamoto T, Raught B, Duchaine TF, Sonenberg N. miRNA-mediated deadenylation is orchestrated by TNRC6A through two conserved motifs that interact with CCR4-NOT. Nat Struct Mol Biol. 2011 Oct 7;18(11):1211-7.

Failla C, Tomei L, De Francesco R. Both NS3 and NS4A are required for proteolytic processing of hepatitis C virus nonstructural proteins. J Virol. 1994 Jun;68(6):3753-60.

Fan XC, Steitz JA. Overexpression of HuR, a nuclear-cytoplasmic shuttling protein, increases the in vivo stability of ARE-containing mRNAs. EMBO J. 1998 Jun 15;17(12):3448-60.

Faye O, Freire CC, Iamarino A, Faye O, de Oliveira JV, Diallo M, Zanotto PM, Sall AA. Molecular evolution of Zika virus during its emergence in the 20(th) century. PLoS Negl Trop Dis. 2014 Jan 9;8(1):e2636.

Feng Q, Hato SV, Langereis MA, Zoll J, Virgen-Slane R, Peisley A, Hur S, Semler BL, van Rij RP, van Kuppeveld FJ. MDA5 detects the double-stranded RNA replicative form in picornavirus-infected cells. Cell Rep. 2012 Nov 29;2(5):1187-96.

Fenger-Gron M, Fillman C, Norrild B, Lykke-Andersen J. Multiple processing body factors and the ARE binding protein TTP activate mRNA decapping. Mol Cell. 2005 Dec 22;20(6):905-15.

Filomatori CV, Iglesias NG, Villordo SM, Alvarez DE, Gamarnik AV. RNA sequences and structures required for the recruitment and activity of the dengue virus polymerase. J Biol Chem. 2011 Mar 4;286(9):6929-39.

Filomatori CV, Lodeiro MF, Alvarez DE, Samsa MM, Pietrasanta L, Gamarnik AV. A 5' RNA element promotes dengue virus RNA synthesis on a circular genome. Genes Dev. 2006 Aug 15;20(16):2238-49.

Fink J, Gu F, Ling L, Tolfvenstam T, Olfat F, Chin KC, Aw P, George J, Kuznetsov VA, Schreiber M, Vasudevan SG, Hibberd ML. Host gene expression profiling of dengue virus infection in cell lines and patients. PLoS Negl Trop Dis. 2007 Nov 21;1(2):e86.

Flecken T, Spangenberg HC, Thimme R. Immunobiology of hepatocellular carcinoma. Langenbecks Arch Surg. 2012 Jun;397(5):673-80.

Flemr M, Malik R, Franke V, Nejepinska J, Sedlacek R, Vlahovicek K, Svoboda P. A retrotransposon-driven DICER isoform directs endogenous small interfering RNA production in mouse oocytes. Cell. 2013 Nov 7;155(4):807-16.

Fletcher SP, Jackson RJ. Pestivirus internal ribosome entry site (IRES) structure and function: elements in the 5' untranslated region important for IRES function. J Virol. 2002 May;76(10):5024-33.

Flores EF, Kreutz LC, Donis RO. Swine and ruminant pestiviruses require the same cellular factor to enter bovine cells. J Gen Virol. 1996 Jun;77 (Pt 6):1295-303.

Floyd-Smith G, Slattery E, Lengyel P. Interferon action: RNA cleavage pattern of a (2'-5') oligoadenylate-dependent endonuclease. Science. 1981 May 29;212(4498):1030-2.

Franks TM, Singh G, Lykke-Andersen J. Upf1 ATPase-dependent mRNP disassembly is required for completion of nonsense- mediated mRNA decay. Cell. 2010 Dec 10;143(6):938-50.

Fredericksen BL, Keller BC, Fornek J, Katze MG, Gale M Jr. Establishment and maintenance of the innate antiviral response to West Nile Virus involves both RIG-I and MDA5 signaling through IPS-1. J Virol. 2008 Jan;82(2):609-16.

Friebe P, Bartenschlager R. Genetic analysis of sequences in the 3' nontranslated region of hepatitis C virus that are important for RNA replication. J Virol. 2002 Jun;76(11):5326-38.

Friebe P, Boudet J, Simorre JP, Bartenschlager R. Kissing-loop interaction in the 3' end of the hepatitis C virus genome essential for RNA replication.J Virol. 2005 Jan;79(1):380-92

Friebe P, Harris E. Interplay of RNA elements in the dengue virus 5' and 3' ends required for viral RNA replication. J Virol. 2010 Jun;84(12):6103-18.

Frischmeyer PA, van Hoof A, O'Donnell K, Guerrerio AL, Parker R, Dietz HC. An mRNA surveillance mechanism that eliminates transcripts lacking termination codons. Science. 2002 Mar 22;295(5563):2258-61.

Fulton RW, Briggs RE, Ridpath JF, Saliki JT, Confer AW, Payton ME, Duff GC, Step DL, Walker DA.Transmission of bovine viral diarrhea virus 1b to susceptible and vaccinated calves by exposure to persistently infected calves. Can J Vet Res. 2005 Jul;69(3):161-9.

Funk A, Truong K, Nagasaki T, Torres S, Floden N, Balmori Melian E, Edmonds J, Dong H, Shi PY, Khromykh AA. RNA structures required for production of subgenomic flavivirus RNA. J Virol. 2010 Nov;84(21):11407-17.

Furuichi Y, Morgan M, Shatkin AJ, Jelinek W, Salditt-Georgieff M, Darnell JE. Methylated, blocked 5 termini in HeLa cell mRNA. Proc Natl Acad Sci U S A. 1975 May;72(5):1904-8.

Gallei A, Orlich M, Thiel HJ, Becher P. Noncytopathogenic pestivirus strains generated by nonhomologous RNA recombination: alterations in the NS4A/NS4B coding region. J Virol. 2005 Nov;79(22):14261-70.

Garneau NL, Sokoloski KJ, Opyrchal M, Neff CP, Wilusz CJ, Wilusz J. The 3' untranslated region of sindbis virus represses deadenylation of viral transcripts in mosquito and Mammalian cells. J Virol. 2008 Jan;82(2):880-92.

Geerlings TH, Vos JC, Raue HA. The final step in the formation of 25S rRNA in Saccharomyces cerevisiae is performed by 5'-->3' exonucleases. RNA. 2000 Dec;6(12):1698-703.

Germi R, Crance JM, Garin D, Guimet J, Lortat-Jacob H, Ruigrok RW, Zarski JP, Drouet E. Cellular glycosaminoglycans and low density lipoprotein receptor are involved in hepatitis C virus adsorption. J Med Virol. 2002 Oct;68(2):206-15.

Ghoshal A, Das S, Ghosh S, Mishra MK, Sharma V, Koli P, Sen E, Basu A. Proinflammatory mediators released by activated microglia induces neuronal death in Japanese encephalitis. Glia. 2007 Apr 1;55(5):483-96.

Gil LH, van Olphen AL, Mittal SK, Donis RO. Modulation of PKR activity in cells infected by bovine viral diarrhea virus. Virus Res. 2006 Mar;116(1-2):69-77.

Gilfoy FD, Mason PW. West Nile virus-induced interferon production is mediated by the double-stranded RNA-dependent protein kinase PKR. J Virol. 2007 Oct;81(20):11148-58.

Goel HL, Mercurio AM. VEGF targets the tumour cell. Nat Rev Cancer. 2013 Dec;13(12):871-82.

Goler-Baron V, Selitrennik M, Barkai O, Haimovich G, Lotan R, Choder M. Transcription in the nucleus and mRNA decay in the cytoplasm are coupled processes. Genes Dev. 2008 Aug 1;22(15):2022-7.

Gollins SW, Porterfield JS. Flavivirus infection enhancement in macrophages: an electron microscopic study of viral cellular entry. J Gen Virol. 1985 Sep;66 (Pt 9):1969-82.

Gottipati K, Ruggli N, Gerber M, Tratschin JD, Benning M, Bellamy H, Choi KH. The structure of classical swine fever virus N(pro): a novel cysteine Autoprotease and zinc-binding protein involved in subversion of type I interferon induction. PLoS Pathog. 2013;9(10):e1003704.

Gouttenoire J, Roingeard P, Penin F, Moradpour D. Amphipathic alpha-helix AH2 is a major determinant for the oligomerization of hepatitis C virus nonstructural protein 4B. J Virol. 2010 Dec;84(24):12529-37.

Green AM, Beatty PR, Hadjilaou A, Harris E. Innate Immunity to Dengue Virus Infection and Subversion of Antiviral Responses. J Mol Biol. 2014 Mar 20;426(6):1148-1160.

Greiser-Wilke I, Dittmar KE, Liess B, Moennig V. Heterogeneous expression of the non-structural protein p80/p125 in cells infected with different pestiviruses. J Gen Virol. 1992 Jan;73 (Pt 1):47-52.

Griffin SD, Beales LP, Clarke DS, Worsfold O, Evans SD, Jaeger J, Harris MP, Rowlands DJ. The p7 protein of hepatitis C virus forms an ion channel that is blocked by the antiviral drug, Amantadine. FEBS Lett. 2003 Jan 30;535(1-3):34-8.

Grima DP, Sullivan M, Zabolotskaya MV, Browne C, Seago J, Wan KC, Okada Y, Newbury SF. The 5'-3' exoribonuclease pacman is required for epithelial sheet sealing in Drosophila and genetically interacts with the phosphatase puckered. Biol Cell. 2008 Dec;100(12):687-701.

Grooms DL. Reproductive consequences of infection with bovine viral diarrhea virus. Vet Clin North Am Food Anim Pract. 2004 Mar;20(1):5-19.

Grossmann V, Kern W, Harbich S, Alpermann T, Jeromin S, Schnittger S, Haferlach C, Haferlach T, Kohlmann A. Prognostic relevance of RUNX1 mutations in T-cell acute lymphoblastic leukemia. Haematologica. 2011 Dec;96(12):1874-7

Grummer B, Grotha S, Greiser-Wilke I. Bovine viral diarrhoea virus is internalized by clathrin-dependent receptor-mediated endocytosis. J Vet Med B Infect Dis Vet Public Health. 2004 Dec;51(10):427-32.

Gu M, Rice CM. Structures of hepatitis C virus nonstructural proteins required for replicase assembly and function. Curr Opin Virol. 2013 Apr;3(2):129-36.

Gubler DJ. Dengue, Urbanization and Globalization: The Unholy Trinity of the 21(st) Century. Trop Med Health. 2011 Dec;39(4 Suppl):3-11.

Guidotti LG, Chisari FV. Immunobiology and pathogenesis of viral hepatitis. Annu Rev Pathol. 2006;1:23-61.

Guirakhoo F, Bolin RA, Roehrig JT. The Murray Valley encephalitis virus prM protein confers acid resistance to virus particles and alters the expression of epitopes within the R2 domain of E glycoprotein. Virology. 1992 Dec;191(2):921-31.

Guitart A, Riezu-Boj JI, Elizalde E, Larrea E, Berasain C, Aldabe R, Civeira MP, Prieto J. Hepatitis C virus infection of primary tupaia hepatocytes leads to selection of quasispecies variants, induction of interferon-stimulated genes and NF-kappaB nuclear translocation. J Gen Virol. 2005 Nov;86(Pt 11):3065-74.

Guo J, Hui DJ, Merrick WC, Sen GC. A new pathway of translational regulation mediated by eukaryotic initiation factor 3. EMBO J. 2000 Dec 15;19(24):6891-9.

Guttilla IK, White BA. Coordinate regulation of FOXO1 by miR-27a, miR-96, and miR-182 in breast cancer cells. J Biol Chem. 2009 Aug 28;284(35):23204-16.

Gy I, Gasciolli V, Lauressergues D, Morel JB, Gombert J, Proux F, Proux C, Vaucheret H, Mallory AC. Arabidopsis FIERY1, XRN2, and XRN3 are endogenous RNA silencing suppressors. Plant Cell. 2007 Nov;19(11):3451-61.
Hahn CS, Hahn YS, Rice CM, Lee E, Dalgarno L, Strauss EG, Strauss JH. Conserved elements in the 3' untranslated region of flavivirus RNAs and potential cyclization sequences. J Mol Biol. 1987 Nov 5;198(1):33-41.

Haimovich G, Medina DA, Causse SZ, Garber M, Millán-Zambrano G, Barkai O, Chávez S, Pérez-Ortín JE, Darzacq X, Choder M. Gene expression is circular: factors for mRNA degradation also foster mRNA synthesis. Cell. 2013 May 23;153(5):1000-11.

Halvorsen M, Martin JS, Broadaway S, Laederach A. Disease-associated mutations that alter the RNA structural ensemble. PLoS Genet. 2010 Aug 19;6(8):e1001074.

Han JQ, Barton DJ. Activation and evasion of the antiviral 2'-5' oligoadenylate synthetase/ribonuclease L pathway by hepatitis C virus mRNA. RNA. 2002 Apr;8(4):512-25.

Han JQ, Townsend HL, Jha BK, Paranjape JM, Silverman RH, Barton DJ. A phylogenetically conserved RNA structure in the poliovirus open reading frame inhibits the antiviral endoribonuclease RNase L. J Virol. 2007 Jun;81(11):5561-72.

Hansen TR, Smirnova NP, Van Campen H, Shoemaker ML, Ptitsyn AA, Bielefeldt-Ohmann H. Maternal and fetal response to fetal persistent infection with bovine viral diarrhea virus. Am J Reprod Immunol. 2010 Oct;64(4):295-306.

Hao JH, Yu M, Li HK, Shi YR, Li Q, Hao XS. Inhibitory effect of antisense vascular endothelial growth factor RNA on the profile of hepatocellular carcinoma cell line in vitro and in vivo. World J Gastroenterol. 2006 Feb 21;12(7):1140-3.

Hao S, Baltimore D. The stability of mRNA influences the temporal order of the induction of genes encoding inflammatory molecules. Nat Immunol. 2009 Mar;10(3):281-8.

Harada T, Tautz N, Thiel HJ. E2-p7 region of the bovine viral diarrhea virus polyprotein: processing and functional studies. J Virol. 2000 Oct;74(20):9498-506.

Harel-Sharvit L, Eldad N, Haimovich G, Barkai O, Duek L, Choder M. RNA polymerase II subunits link transcription and mRNA decay to translation. Cell. 2010 Nov 12;143(4):552-63.

Harigaya Y, Parker R. No-go decay: a quality control mechanism for RNA in translation. Wiley Interdiscip Rev RNA. 2010 Jul-Aug;1(1):132-41.

He F, Li X, Spatrick P, Casillo R, Dong S, Jacobson A. Genome-wide analysis of mRNAs regulated by the nonsense-mediated and 5' to 3' mRNA decay pathways in yeast. Mol Cell. 2003 Dec;12(6):1439-52.

Heinz FX, Stiasny K. Flaviviruses and flavivirus vaccines. Vaccine. 2012 Jun 19;30(29):4301-6.

Henry Y, Wood H, Morrissey JP, Petfalski E, Kearsey S, Tollervey D. The 5' end of yeast 5.8S rRNA is generated by exonucleases from an upstream cleavage site. EMBO J. 1994 May 15;13(10):2452-63.

Heuer C, Healy A, Zerbini C. Economic effects of exposure to bovine viral diarrhea virus on dairy herds in New Zealand. J Dairy Sci. 2007 Dec;90(12):5428-38.

Heyer WD, Johnson AW, Reinhart U, Kolodner RD. Regulation and intracellular localization of Saccharomyces cerevisiae strand exchange protein 1 (Sep1/XRN1/Kem1), a multifunctional exonuclease. Mol Cell Biol. 1995 May;15(5):2728-36.

Higgs MR, Lerat H, Pawlotsky JM. Hepatitis C virus-induced activation of β-catenin promotes c-Myc expression and a cascade of pro-carcinogenetic events. Oncogene. 2013 Sep 26;32(39):4683-93.

Hilgard P, Stockert R. Heparan sulfate proteoglycans initiate dengue virus infection of hepatocytes. Hepatology. 2000 Nov;32(5):1069-77.

Hogg JR, Goff SP. Upf1 senses 3'UTR length to potentiate mRNA decay. Cell. 2010 Oct 29;143(3):379-89.

Holmes EC, Burch SS.The causes and consequences of genetic variation in dengue virus. Trends Microbiol. 2000 Feb;8(2):74-7.

Holmes EC, Worobey M, Rambaut A. Phylogenetic evidence for recombination in dengue virus. Mol Biol Evol. 1999 Mar;16(3):405-9.

Hovanessian AG, Wood J, Meurs E, Montagnier L. Increased nuclease activity in cells treated with pppA2'p5'A2'p5' A. Proc Natl Acad Sci U S A. 1979 Jul;76(7):3261-5.

Hoover S, Striker R. Thiopurines inhibit bovine viral diarrhea virus production in a thiopurine methyltransferase-dependent manner. J Gen Virol. 2008 Apr;89(Pt 4):1000-9.

Hopkins KC, McLane LM, Maqbool T, Panda D, Gordesky-Gold B, Cherry S. A genome-wide RNAi screen reveals that mRNA decapping restricts bunyaviral replication by limiting the pools of DCP2-accessible targets for cap-snatching. Genes Dev. 2013 Jul 1;27(13):1511-25.

Horner SM. Activation and Evasion of Antiviral Innate Immunity by Hepatitis C Virus. J Mol Biol. 2014 Mar 20;426(6):1198-1209.

Horvath CM. The Jak-STAT pathway stimulated by interferon alpha or interferon beta. Sci STKE. 2004 Nov 23;2004(260):tr10.

Houzelstein D, Bullock SL, Lynch DE, Grigorieva EF, Wilson VA, Beddington RS. Growth and early postimplantation defects in mice deficient for the bromodomain-containing protein Brd4. Mol Cell Biol. 2002 Jun;22(11):3794-802.

Hsu CL, Stevens A. Yeast cells lacking 5'-->3' exoribonuclease 1 contain mRNA species that are poly(A) deficient and partially lack the 5' cap structure. Mol Cell Biol. 1993 Aug;13(8):4826-35.

(a) Huang DW, Sherman BT, Lempicki RA. Bioinformatics enrichment tools: paths toward the comprehensive functional analysis of large gene lists. Nucleic Acids Res. 2009;37(1):1-13.

(b) Huang DW, Sherman BT, Lempicki RA. Systematic and integrative analysis of large gene lists using DAVID Bioinformatics Resources. Nature Protoc. 2009;4(1):44-57.

Huang H, Zeqiraj E, Dong B, Jha BK, Duffy NM, Orlicky S, Thevakumaran N, Talukdar M, Pillon MC, Ceccarelli DF, Wan LC, Juang YC, Mao DY, Gaughan C, Brinton MA, Perelygin AA, Kourinov I, Guarné A, Silverman RH, Sicheri F. Dimeric Structure of Pseudokinase RNase L Bound to 2-5A Reveals a Basis for Interferon-Induced Antiviral Activity. Mol Cell. 2014 Jan 23;53(2):221-34.

Hui DJ, Terenzi F, Merrick WC, Sen GC. Mouse p56 blocks a distinct function of eukaryotic initiation factor 3 in translation initiation. J Biol Chem. 2005 Feb 4;280(5):3433-40.

Hulst MM, Moormann RJ. Inhibition of pestivirus infection in cell culture by envelope proteins E(rns) and E2 of classical swine fever virus: E(rns) and E2 interact with different receptors. J Gen Virol. 1997 Nov;78 (Pt 11):2779-87.

Huntzinger E, Kuzuoglu-Öztürk D, Braun JE, Eulalio A, Wohlbold L, Izaurralde E. The interactions of TNRC6A proteins with PABP and deadenylases are required for both translational repression and degradation of miRNA targets. Nucleic Acids Res. 2013 Jan;41(2):978-94.

Hyde JL, Gardner CL, Kimura T, White JP, Liu G, Trobaugh DW, Huang C, Tonelli M, Paessler S, Takeda K, Klimstra WB, Amarasinghe GK, Diamond MS. A viral RNA structural element alters host recognition of nonself RNA. Science. 2014 Feb 14;343(6172):783-7.

Ichikawa M, Asai T, Chiba S, Kurokawa M, Ogawa S. Runx1/AML-1 ranks as a master regulator of adult hematopoiesis. Cell Cycle. 2004 Jun;3(6):722-4.

Iliopoulos D, Hirsch HA, Struhl K. An epigenetic switch involving NF-kappaB, Lin28, Let-7 MicroRNA, and IL6 links inflammation to cell transformation. Cell. 2009 Nov 13;139(4):693-706.

Ingelfinger D, Arndt-Jovin DJ, Lührmann R, Achsel T. The human LSm1-7 proteins colocalize with the mRNA-degrading enzymes DCP1/2 and Xrnl in distinct cytoplasmic foci. RNA. 2002 Dec;8(12):1489-501.

Iqbal M, Flick-Smith H, McCauley JW. Interactions of bovine viral diarrhoea virus glycoprotein E(rns) with cell surface glycosaminoglycans. J Gen Virol. 2000 Feb;81(Pt 2):451-9.

Isken O, Baroth M, Grassmann CW, Weinlich S, Ostareck DH, Ostareck-Lederer A, Behrens SE. Nuclear factors are involved in hepatitis C virus RNA replication. RNA. 2007 Oct;13(10):1675-92.

Isken O, Grassmann CW, Sarisky RT, Kann M, Zhang S, Grosse F, Kao PN, Behrens SE. Members of the NF90/NFAR protein group are involved in the life cycle of a positive-strand RNA virus. EMBO J. 2003 Nov 3;22(21):5655-65.

Isken O, Grassmann CW, Yu H, Behrens SE. Complex signals in the genomic 3' nontranslated region of bovine viral diarrhea virus coordinate translation and replication of the viral RNA. RNA. 2004 Oct;10(10):1637-52.

Issur M, Geiss BJ, Bougie I, Picard-Jean F, Despins S, Mayette J, Hobdey SE, Bisaillon M. The flavivirus NS5 protein is a true RNA guanylyltransferase that catalyzes a two-step reaction to form the RNA cap structure. RNA. 2009 Dec;15(12):2340-50.

Iwakawa HO, Mizumoto H, Nagano H, Imoto Y, Takigawa K, Sarawaneeyaruk S, Kaido M, Mise K, Okuno T. A viral noncoding RNA generated by cis-element-mediated protection against 5'->3' RNA decay represses both cap-independent and cap-dependent translation. J Virol. 2008 Oct;82(20):10162-74.

Jaag HM, Nagy PD. Silencing of Nicotiana benthamiana XRN4p exoribonuclease promotes tombusvirus RNA accumulation and recombination. Virology. 2009 Apr 10;386(2):344-52.

Jangra RK, Yi M, Lemon SM. Regulation of hepatitis C virus translation and infectious virus production by the microRNA miR-122. J Virol. 2010 Jul;84(13):6615-25.

Januszyk K, Lima CD. The eukaryotic RNA exosome. Curr Opin Struct Biol. 2014 Feb 10;24C:132-140.

Jensen S, Thomsen AR. Sensing of RNA viruses: a review of innate immune receptors involved in recognizing RNA virus invasion. J Virol. 2012 Mar;86(6):2900-10.

Jia XY, Briese T, Jordan I, Rambaut A, Chi HC, Mackenzie JS, Hall RA, Scherret J, Lipkin WI. Genetic analysis of West Nile New York 1999 encephalitis virus. Lancet. 1999 Dec 4;354(9194):1971-2.

Jimeno-Gonzalez S, Schmid M, Malagon F, Haaning LL, Jensen TH. Rat1p maintains RNA polymerase II CTD phosphorylation balance. RNA. 2014 Apr;20(4):551-8.

Jin Z, Deval J, Johnson KA, Swinney DC. Characterization of the elongation complex of dengue virus RNA polymerase: assembly, kinetics of nucleotide incorporation, and fidelity. J Biol Chem. 2011 Jan 21;286(3):2067-77.

Jinek M, Coyle SM, Doudna JA. Coupled 5' nucleotide recognition and processivity in XRN1-mediated mRNA decay. Mol Cell. 2011 Mar 4;41(5):600-8.

Jonas S, Izaurralde E. The role of disordered protein regions in the assembly of decapping complexes and RNP granules. Genes Dev. 2013 Dec 15;27(24):2628-41.

Jones CI, Grima DP, Waldron JA, Jones S, Parker HN, Newbury SF. The 5'-3' exoribonuclease Pacman (XRN1) regulates expression of the heat shock protein Hsp67Bc and the microRNA miR-277-3p in Drosophila wing imaginal discs. RNA Biol. 2013 Aug 1;10(8):1345-55.

Jones CI, Zabolotskaya MV, Newbury SF. The 5' → 3' exoribonuclease XRN1/Pacman and its functions in cellular processes and development. Wiley Interdiscip Rev RNA. 2012 Jul-Aug;3(4):455-68.

Jones CT, Murray CL, Eastman DK, Tassello J, Rice CM. Hepatitis C virus p7 and NS2 proteins are essential for production of infectious virus. J Virol. 2007 Aug;81(16):8374-83.

Jopling CL, Schütz S, Sarnow P. Position-dependent function for a tandem microRNA miR-122-binding site located in the hepatitis C virus RNA genome. Cell Host Microbe. 2008 Jul 17;4(1):77-85

Jopling CL, Yi M, Lancaster AM, Lemon SM, Sarnow P. Modulation of hepatitis C virus RNA abundance by a liver-specific MicroRNA. Science. 2005 Sep 2;309(5740):1577-81.

Junjhon J, Edwards TJ, Utaipat U, Bowman VD, Holdaway HA, Zhang W, Keelapang P, Puttikhunt C, Perera R, Chipman PR, Kasinrerk W, Malasit P, Kuhn RJ, Sittisombut N. Influence of pr-M cleavage on the heterogeneity of extracellular dengue virus particles. J Virol. 2010 Aug;84(16):8353-8.

Kakumani PK, Ponia SS, S RK, Sood V, Chinnappan M, Banerjea AC, Medigeshi GR, Malhotra P, Mukherjee SK, Bhatnagar RK. Role of RNA interference (RNAi) in dengue virus replication and identification of NS4B as an RNAi suppressor. J Virol. 2013 Aug;87(16):8870-83.

(a) Kang SM, Lim S, Won SJ, Shin YJ, Lim YS, Ahn BY, Hwang SB. c-FOS regulates hepatitis C virus propagation. FEBS Lett. 2011 Oct 20;585(20):3236-44.

(b) Kang JG, Amar MJ, Remaley AT, Kwon J, Blackshear PJ, Wang PY, Hwang PM. Zinc finger protein tristetraprolin interacts with CCL3 mRNA and regulates tissue inflammation. J Immunol. 2011 Sep 1;187(5):2696-701.

Kapoor A, Simmonds P, Gerold G, Qaisar N, Jain K, Henriquez JA, Firth C, Hirschberg DL, Rice CM, Shields S, Lipkin WI. Characterization of a canine homolog of hepatitis C virus. Proc Natl Acad Sci U S A. 2011 Jul 12;108(28):11608-13.

Kapoor A, Simmonds P, Scheel TK, Hjelle B, Cullen JM, Burbelo PD, Chauhan LV, Duraisamy R, Sanchez Leon M, Jain K, Vandegrift KJ, Calisher CH, Rice CM, Lipkin WI. Identification of rodent homologs of hepatitis C virus and pegiviruses. MBio. 2013 Apr 9;4(2):e00216-13.

Kato H, Sato S, Yoneyama M, Yamamoto M, Uematsu S, Matsui K, Tsujimura T, Takeda K, Fujita T, Takeuchi O, Akira S. Cell type-specific involvement of RIG-I in antiviral response. Immunity. 2005 Jul;23(1):19-28.

Kato H, Takeuchi O, Mikamo-Satoh E, Hirai R, Kawai T, Matsushita K, Hiiragi A, Dermody TS, Fujita T, Akira S. Length-dependent recognition of double-stranded ribonucleic acids by retinoic acid-inducible gene-I and melanoma differentiation-associated gene 5. J Exp Med. 2008 Jul 7;205(7):1601-10.

Kato H, Takeuchi O, Sato S, Yoneyama M, Yamamoto M, Matsui K, Uematsu S, Jung A, Kawai T, Ishii KJ, Yamaguchi O, Otsu K, Tsujimura T, Koh CS, Reis e Sousa C, Matsuura Y, Fujita T, Akira S. Differential roles of MDA5 and RIG-I helicases in the recognition of RNA viruses. Nature. 2006 May 4;441(7089):101-5.

Katoh H, Okamoto T, Fukuhara T, Kambara H, Morita E, Mori Y, Kamitani W, Matsuura Y. Japanese encephalitis virus core protein inhibits stress granule formation through an interaction with Caprin-1 and facilitates viral propagation. J Virol. 2013 Jan;87(1):489-502.

Kaufusi PH, Kelley JF, Yanagihara R, Nerurkar VR. Induction of endoplasmic reticulum-derived replication-competent membrane structures by West Nile virus non-structural protein 4B. PLoS One. 2014 Jan 20;9(1):e84040.

Kaushik DK, Gupta M, Kumawat KL, Basu A. NLRP3 inflammasome: key mediator of neuroinflammation in murine Japanese encephalitis. PLoS One. 2012;7(2):e32270.

Kavandi L, Collier MA, Nguyen H, Syed V. Progesterone and calcitriol attenuate inflammatory cytokines CXCL1 and CXCL2 in ovarian and endometrial cancer cells. J Cell Biochem. 2012 Oct;113(10):3143-52.

Kawai T, Akira S. Toll-like receptor and RIG-I-like receptor signaling. Ann N Y Acad Sci. 2008 Nov;1143:1-20.

Kedersha NL, Gupta M, Li W, Miller I, Anderson P. RNA-binding proteins TIA-1 and TIAR link the phosphorylation of eIF-2 alpha to the assembly of mammalian stress granules. J Cell Biol. 1999 Dec 27;147(7):1431-42.

Kenna M, Stevens A, McCammon M, Douglas MG. An essential yeast gene with homology to the exonuclease-encoding XRN1/KEM1 gene also encodes a protein with exoribonuclease activity. Mol Cell Biol. 1993 Jan;13(1):341-50.

Kerr SC, Azzouz N, Fuchs SM, Collart MA, Strahl BD, Corbett AH, Laribee RN. The Ccr4-Not complex interacts with the mRNA export machinery. PLoS One. 2011 Mar 28;6(3):e18302.

Khabar KS, Siddiqui YM, al-Zoghaibi F, al-Haj L, Dhalla M, Zhou A, Dong B, Whitmore M, Paranjape J, Al-Ahdal MN, Al-Mohanna F, Williams BR, Silverman RH. RNase L mediates transient control of the interferon response through modulation of the double-stranded RNA-dependent protein kinase PKR.J Biol Chem. 2003 May 30; 278(22):20124-32.

Khromykh AA, Meka H, Guyatt KJ, Westaway EG. Essential role of cyclization sequences in flavivirus RNA replication. J Virol. 2001 Jul;75(14):6719-28.

Kieft JS, Zhou K, Jubin R, Doudna JA. Mechanism of ribosome recruitment by hepatitis C IRES RNA. RNA. 2001 Feb;7(2):194-206.

Kim CW, Chang KM. Hepatitis C virus: virology and life cycle. Clin Mol Hepatol. 2013 Mar;19(1):17-25.

Kim J, Kim J. KEM1 is involved in filamentous growth of Saccharomyces cerevisiae. FEMS Microbiol Lett. 2002 Oct 29;216(1):33-8.

Kim M, Krogan NJ, Vasiljeva L, Rando OJ, Nedea E, Greenblatt JF, Buratowski S. The yeast Rat1 exonuclease promotes transcription termination by RNA polymerase II. Nature. 2004 Nov 25; 432(7016):517-22.

Kim YK, Kim CS, Lee SH, Jang SK. Domains I and II in the 5' nontranslated region of the HCV genome are required for RNA replication. Biochem Biophys Res Commun. 2002 Jan 11;290(1):105-12.

King E, Trabue C, Yin D, Yao ZQ, Moorman JP. Hepatitis C: the complications of immune dysfunction. Expert Rev Clin Immunol. 2007 Mar;3(2):145-57.

Kishore S, Jaskiewicz L, Burger L, Hausser J, Khorshid M, Zavolan M. A quantitative analysis of CLIP methods for identifying binding sites of RNA-binding proteins. Nat Methods. 2011 May 15;8(7):559-64.

Kiyosawa K, Tanaka E, Sodeyama T. Hepatitis C virus and hepatocellular carcinoma. Curr Stud Hematol Blood Transfus. 1998;(62):161-80

Klauer AA, van Hoof A. Degradation of mRNAs that lack a stop codon: a decade of nonstop progress. Wiley Interdiscip Rev RNA. 2012 Sep-Oct;3(5):649-60.

Klausner RD, Donaldson JG, Lippincott-Schwartz J. Brefeldin A: insights into the control of membrane traffic and organelle structure. J Cell Biol. 1992 Mar;116(5):1071-80.

Knouf EC, Wyman SK, Tewari M. The human TUT1 nucleotidyl transferase as a global regulator of microRNA abundance. PLoS One. 2013 Jul 18;8(7):e69630.

Kollmar O, Junker B, Rupertus K, Scheuer C, Menger MD, Schilling MK. Liver resection-associated macrophage inflammatory protein-2 stimulates engraftment but not growth of colorectal metastasis at extrahepatic sites. J Surg Res. 2008 Apr;145(2):295-302.

Kollmar O, Scheuer C, Menger MD, Schilling MK. Macrophage inflammatory protein-2 promotes angiogenesis, cell migration, and tumor growth in hepatic metastasis. Ann Surg Oncol. 2006 Feb;13(2):263-75.

Kolykhalov AA, Feinstone SM, Rice CM. Identification of a highly conserved sequence element at the 3' terminus of hepatitis C virus genome RNA. J Virol. 1996 Jun;70(6):3363-71.

Komar AA, Hatzoglou M. Cellular IRES-mediated translation: the war of ITAFs in pathophysiological states. Cell Cycle. 2011 Jan 15;10(2):229-40.

Krey T, Thiel HJ, Rümenapf T. Acid-resistant bovine pestivirus requires activation for pH-triggered fusion during entry. J Virol. 2005 Apr;79(7):4191-200.

Krohn N, Kapoor S, Enami Y, Follenzi A, Bandi S, Joseph B, Gupta S. Hepatocyte transplantation-induced liver inflammation is driven by cytokines-chemokines associated with neutrophils and Kupffer cells. Gastroenterology. 2009 May;136(5):1806-17.

Kruzelock RP, Murphy EC, Strong LC, Naylor SL, Hansen MF. Localization of a novel tumor suppressor locus on human chromosome 3q important in osteosarcoma tumorigenesis. Cancer Res. 1997 Jan 1;57(1):106-9.

Kumthip K, Chusri P, Jilg N, Zhao L, Fusco DN, Zhao H, Goto K, Cheng D, Schaefer EA, Zhang L, Pantip C, Thongsawat S, O'Brien A, Peng LF, Maneekarn N, Chung RT, Lin W. Hepatitis C virus NS5A disrupts STAT1 phosphorylation and suppresses type I interferon signaling. J Virol. 2012 Aug;86(16):8581-91.

Kundu P, Fabian MR, Sonenberg N, Bhattacharyya SN, Filipowicz W. HuR protein attenuates miRNA-mediated repression by promoting miRISC dissociation from the target RNA. Nucleic Acids Res. 2012 Jun;40(11):5088-100.

Kuo MC, Liang DC, Huang CF, Shih YS, Wu JH, Lin TL, Shih LY. RUNX1 mutations are frequent in chronic myelomonocytic leukemia and mutations at the C-terminal region might predict acute myeloid leukemia transformation. Leukemia. 2009 Aug;23(8):1426-31.

Lagos-Quintana M, Rauhut R, Yalcin A, Meyer J, Lendeckel W, Tuschl T. Identification of tissue-specific microRNAs from mouse. Curr Biol. 2002 Apr 30;12(9):735-9.

Lai WS, Carballo E, Strum JR, Kennington EA, Phillips RS, Blackshear PJ. Evidence that tristetraprolin binds to AU-rich elements and promotes the deadenylation and destabilization of tumor necrosis factor alpha mRNA. Mol Cell Biol. 1999 Jun;19(6):4311-23.

Lanford RE, Hildebrandt-Eriksen ES, Petri A, Persson R, Lindow M, Munk ME, Kauppinen S, Ørum H. Therapeutic silencing of microRNA-122 in primates with chronic hepatitis C virus infection. Science. 2010 Jan 8;327(5962):198-201.

Langlois RA, Albrecht RA, Kimble B, Sutton T, Shapiro JS, Finch C, Angel M, Chua MA, Gonzalez-Reiche AS, Xu K, Perez D, García-Sastre A, tenOever BR. MicroRNA-based strategy to mitigate the risk of gain-of-function influenza studies. Nat Biotechnol. 2013 Sep;31(9):844-7.

Lanyon SR, Hill FI, Reichel MP, Brownlie J. Bovine viral diarrhoea: Pathogenesis and diagnosis. Vet J. 2014 Feb;199(2):201-209.

Larimer FW, Hsu CL, Maupin MK, Stevens A. Characterization of the XRN1 gene encoding a 5'-->3' exoribonuclease: sequence data and analysis of disparate protein and mRNA levels of gene-disrupted yeast cells. Gene. 1992 Oct 12;120(1):51-7.

Larimer FW, Stevens A. Disruption of the gene XRN1, coding for a 5'→3' exoribonuclease, restricts yeast cell growth. Gene. 1990 Oct 30;95(1):85-90.

Laroia G, Cuesta R, Brewer G, Schneider RJ. Control of mRNA decay by heat shock-ubiquitin-proteasome pathway. Science. 1999 Apr 16;284(5413):499-502.

Le Quesne JP, Stoneley M, Fraser GA, Willis AE. Derivation of a structural model for the c-myc IRES. J Mol Biol. 2001 Jun 29;310(1):111-26.

Le SY, Siddiqui A, Maizel JV Jr. A common structural core in the internal ribosome entry sites of picornavirus, hepatitis C virus, and pestivirus. Virus Genes. 1996;12(2):135-47.

Lebedeva S, Jens M, Theil K, Schwanhäusser B, Selbach M, Landthaler M, Rajewsky N. Transcriptome-wide analysis of regulatory interactions of the RNA-binding protein HuR. Mol Cell. 2011 Aug 5;43(3):340-52.

LeCouter J, Moritz DR, Li B, Phillips GL, Liang XH, Gerber HP, Hillan KJ, Ferrara N. Angiogenesis-independent endothelial protection of liver: role of VEGFR-1. Science. 2003 Feb 7;299(5608):890-3.

Lee E, Stocks CE, Amberg SM, Rice CM, Lobigs M. Mutagenesis of the signal sequence of yellow fever virus prM protein: enhancement of signalase cleavage In vitro is lethal for virus production. J Virol. 2000 Jan;74(1):24-32.

(b) Lee JE, Lee JY, Trembly J, Wilusz J, Tian B, Wilusz CJ. The PARN deadenylase targets a discrete set of mRNAs for decay and regulates cell motility in mouse myoblasts. PLoS Genet. 2012;8(8):e1002901.

(a) Lee KG, Xu S, Kang ZH, Huo J, Huang M, Liu D, Takeuchi O, Akira S, Lam KP.Bruton's tyrosine kinase phosphorylates Toll-like receptor 3 to initiate antiviral response. Proc Natl Acad Sci U S A. 2012 Apr 10;109(15):5791-6. (a)

Lee MM, Pushechnikov A, Disney MD. Rational and modular design of potent ligands targeting the RNA that causes myotonic dystrophy 2. ACS Chem Biol. 2009 May 15;4(5):345-55.

Lee SI, Murthy SC, Trimble JJ, Desrosiers RC, Steitz JA. Four novel U RNAs are encoded by a herpesvirus. Cell. 1988 Aug 26;54(5):599-607.

Lee SR, Pharr GT, Boyd BL, Pinchuk LM. Bovine viral diarrhea viruses modulate toll-like receptors, cytokines and co-stimulatory molecules genes expression in bovine peripheral blood monocytes. Comp Immunol Microbiol Infect Dis. 2008 Sep;31(5):403-18.

Lejeune F, Li X, Maquat LE. Nonsense-mediated mRNA decay in mammalian cells involves decapping, deadenylating, and exonucleolytic activities. Mol Cell. 2003 Sep;12(3):675-87.

Lemon SM, McGivern DR. Is hepatitis C virus carcinogenic? Gastroenterology. 2012 May;142(6):1274-8.

Leopardi R, Vainionpää R, Hurme M, Siljander P, Salmi AA. Measles virus infection enhances IL-1 beta but reduces tumor necrosis factor-alpha expression in human monocytes. J Immunol. 1992 Oct 1;149(7):2397-401.

Li CH, Irmer H, Gudjonsdottir-Planck D, Freese S, Salm H, Haile S, Estévez AM, Clayton C. Roles of a Trypanosoma brucei 5'->3' exoribonuclease homolog in mRNA degradation. RNA. 2006 Dec;12(12):2171-86.

Li K, Lemon SM. Innate immune responses in hepatitis C virus infection. Semin Immunopathol. 2013 Jan;35(1):53-72.

Li K, Li NL, Wei D, Pfeffer SR, Fan M, Pfeffer LM. Activation of chemokine and inflammatory cytokine response in hepatitis C virus-infected hepatocytes depends on Toll-like receptor 3 sensing of hepatitis C virus double-stranded RNA intermediates. Hepatology. 2012 Mar;55(3):666-75.

Li L, Lok SM, Yu IM, Zhang Y, Kuhn RJ, Chen J, Rossmann MG. The flavivirus precursor membrane-envelope protein complex: structure and maturation.Science. 2008 Mar 28;319(5871):1830-4.

(a) Li SH, Dong H, Li XF, Xie X, Zhao H, Deng YQ, Wang XY, Ye Q, Zhu SY, Wang HJ, Zhang B, Leng QB, Zuest R, Qin ED, Qin CF, Shi PY. Rational design of a flavivirus vaccine by abolishing viral RNA 2'-O methylation. J Virol. 2013 May;87(10):5812-9.

Li W, Li Y, Kedersha N, Anderson P, Emara M, Swiderek KM, Moreno GT, Brinton MA. Cell proteins TIA-1 and TIAR interact with the 3' stem-loop of the West Nile virus complementary minus-strand RNA and facilitate virus replication. J Virol. 2002 Dec;76(23):11989-2000.

Li XL, Blackford JA, Judge CS, Liu M, Xiao W, Kalvakolanu DV, Hassel BA. RNase-L-dependent destabilization of interferon-induced mRNAs. A role for the 2-5A system in attenuation of the interferon response. J Biol Chem. 2000 Mar 24; 275(12):8880-8.

(c)Li Y, Lu J, Han Y, Fan X, Ding SW. RNA interference functions as an antiviral immunity mechanism in mammals.Science. 2013 Oct 11;342(6155):231-4.

(b) Li Y, Masaki T, Yamane D, McGivern DR, Lemon SM. Competing and noncompeting activities of miR-122 and the 5' exonuclease XRN1 in regulation of hepatitis C virus replication. Proc Natl Acad Sci U S A. 2013 Jan 29;110(5):1881-6.

(a) Li XL, Ezelle HJ, Hsi TY, Hassel BA. A central role for RNA in the induction and biological activities of type 1 interferons. Wiley Interdiscip Rev RNA. 2011 Jan-Feb;2(1):58-78.

(b) Li Y, Song M, Kiledjian M. Differential utilization of decapping enzymes in mammalian mRNA decay pathways. RNA. 2011 Mar;17(3):419-28.

Libri V, Helwak A, Miesen P, Santhakumar D, Borger JG, Kudla G, Grey F, Tollervey D, Buck AH. Murine cytomegalovirus encodes a miR-27 inhibitor disguised as a target. Proc Natl Acad Sci U S A. 2012 Jan 3;109(1):279-84.

Lin C, Lindenbach BD, Prágai BM, McCourt DW, Rice CM. Processing in the hepatitis C virus E2-NS2 region: identification of p7 and two distinct E2-specific products with different C termini. J Virol. 1994 Aug;68(8):5063-73.

Lin RJ, Chien HL, Lin SY, Chang BL, Yu HP, Tang WC, Lin YL. MCPIP1 ribonuclease exhibits broad-spectrum antiviral effects through viral RNA binding and degradation. Nucleic Acids Res. 2013 Mar 1;41(5):3314-26.

Lindenbach BD and Rice,CM. 2001.Flaviviridae: the viruses and their replication. In Knipe DM and Howley PM (eds), Fields Virology. Lippincott-Williams & Wilkins, Philadelphia, PA, pp. 991–1041.

Liu H, Rodgers ND, Jiao X, Kiledjian M. The scavenger mRNA decapping enzyme DCPS is a member of the HIT family of pyrophosphatases. EMBO J. 2002 Sep 2;21(17):4699-708.

Liu J, Valencia-Sanchez MA, Hannon GJ, Parker R. MicroRNA-dependent localization of targeted mRNAs to mammalian P-bodies. Nat Cell Biol. 2005;7:719–723.

(a) Liu S, Qiu C, Miao R, Zhou J, Lee A, Liu B, Lester SN, Fu W, Zhu L, Zhang L, Xu J, Fan D, Li K, Fu M, Wang T. MCPIP1 restricts HIV infection and is rapidly degraded in activated CD4+ T cells. Proc Natl Acad Sci U S A. 2013 Nov 19;110(47):19083-8.

Liu WJ, Chen HB, Khromykh AA. Molecular and functional analyses of Kunjin virus infectious cDNA clones demonstrate the essential roles for NS2A in virus assembly and for a nonconservative residue in NS3 in RNA replication. J Virol. 2003 Jul;77(14):7804-13.

(b) Liu X, Yang H, Zhang X, Liu L, Lei M, Zhang Z, Bao X. Bdf1p deletion affects mitochondrial function and causes apoptotic cell death under salt stress. FEMS Yeast Res. 2009 Mar;9(2):240-6.

Liu Y, Liu H, Zou J, Zhang B, Yuan Z. Dengue virus subgenomic RNA induces apoptosis through the Bcl-2-mediated PI3k/Akt signaling pathway. Virology. 2014 Jan 5;448:15-25.

(a) Liu Y, Wimmer E, Paul AV. Cis-acting RNA elements in human and animal plus-strand RNA viruses. Biochim Biophys Acta. 2009 Sep-Oct;1789(9-10):495-517.

(b) Liu YP, Schopman NC, Berkhout B. DICER-independent processing of short hairpin RNAs. Nucleic Acids Res. 2013 Apr 1;41(6):3723-33.

Lloyd RE. Regulation of stress granules and P-bodies during RNA virus infection. Wiley Interdiscip Rev RNA. 2013 May-Jun;4(3):317-31.

Lodeiro MF, Filomatori CV, Gamarnik AV. Structural and functional studies of the promoter element for dengue virus RNA replication. J Virol. 2009 Jan;83(2):993-1008.

Loh B, Jonas S, Izaurralde E. The SMG5-SMG7 heterodimer directly recruits the CCR4-NOT deadenylase complex to mRNAs containing nonsense codons via interaction with POP2. Genes Dev. 2013 Oct 1;27(19):2125-38.

Lohmann V, Körner F, Koch J, Herian U, Theilmann L, Bartenschlager R. Replication of subgenomic hepatitis C virus RNAs in a hepatoma cell line. Science. 1999 Jul 2;285(5424):110-3.

Loo YM, Fornek J, Crochet N, Bajwa G, Perwitasari O, Martinez-Sobrido L, Akira S, Gill MA, García-Sastre A, Katze MG, Gale M Jr. Distinct RIG-I and MDA5 signaling by RNA viruses in innate immunity. J Virol. 2008 Jan;82(1):335-45.

Loo YM, Gale M Jr. Immune signaling by RIG-I-like receptors. Immunity. 2011 May 27;34(5):680-92.

Lubas M, Damgaard CK, Tomecki R, Cysewski D, Jensen TH, Dziembowski A. Exonuclease hDIS3L2 specifies an exosome-independent 3'-5' degradation pathway of human cytoplasmic mRNA. EMBO J. 2013 Jul 3;32(13):1855-68.

Lukavsky PJ. Structure and function of HCV IRES domains. Virus Res. 2009 Feb;139(2):166-71.

Luo D, Xu T, Watson RP, Scherer-Becker D, Sampath A, Jahnke W, Yeong SS, Wang CH, Lim SP, Strongin A, Vasudevan SG, Lescar J. Insights into RNA unwinding and ATP hydrolysis by the flavivirus NS3 protein. EMBO J. 2008 Dec 3;27(23):3209-19.

Luo G. Cellular proteins bind to the poly(U) tract of the 3' untranslated region of hepatitis C virus RNA genome. Virology. 1999 Mar 30;256(1):105-18.

Ma E, MacRae IJ, Kirsch JF, Doudna JA. Autoinhibition of human DICER by its internal helicase domain. J Mol Biol. 2008 Jun 27;380(1):237-43.

Machida K, Tsukamoto H, Liu JC, Han YP, Govindarajan S, Lai MM, Akira S, Ou JH. c-JUN mediates hepatitis C virus hepatocarcinogenesis through signal transducer and activator of transcription 3 and nitric oxide-dependent impairment of oxidative DNA repair. Hepatology. 2010 Aug;52(2):480-92.

Machlin ES, Sarnow P, Sagan SM. Masking the 5' terminal nucleotides of the hepatitis C virus genome by an unconventional microRNA-target RNA complex. Proc Natl Acad Sci U S A. 2011 Feb 22;108(8):3193-8.

Mackenzie JM, Khromykh AA, Jones MK, Westaway EG. Subcellular localization and some biochemical properties of the flavivirus Kunjin nonstructural proteins NS2A and NS4A. Virology. 1998 Jun 5;245(2):203-15.

Magkouras I, Mätzener P, Rümenapf T, Peterhans E, Schweizer M. RNase-dependent inhibition of extracellular, but not intracellular, dsRNA-induced interferon synthesis by Erns of pestiviruses. J Gen Virol. 2008 Oct;89(Pt 10):2501-6.

Maillard PV, Ciaudo C, Marchais A, Li Y, Jay F, Ding SW, Voinnet O. Antiviral RNA interference in mammalian cells. Science. 2013 Oct 11;342(6155):235-8.

Malathi K, Dong B, Gale M Jr, Silverman RH. Small self-RNA generated by RNase L amplifies antiviral innate immunity. Nature. 2007 Aug 16;448(7155):816-9.

Malathi K, Saito T, Crochet N, Barton DJ, Gale M Jr, Silverman RH. RNase L releases a small RNA from HCV RNA that refolds into a potent PAMP. RNA. 2010 Nov;16(11):2108-19.

Malecki M, Viegas SC, Carneiro T, Golik P, Dressaire C, Ferreira MG, Arraiano CM. The exoribonuclease Dis3L2 defines a novel eukaryotic RNA degradation pathway. EMBO J. 2013 Jul 3;32(13):1842-54

Mandl CW, Kroschewski H, Allison SL, Kofler R, Holzmann H, Meixner T, Heinz FX. Adaptation of tick-borne encephalitis virus to BHK-21 cells results in the formation of multiple heparan sulfate binding sites in the envelope protein and attenuation in vivo. J Virol. 2001 Jun;75(12):5627-37.

Mangus DA, Evans MC, Agrin NS, Smith M, Gongidi P, Jacobson A. Positive and negative regulation of poly(A) nuclease. Mol Cell Biol. 2004 Jun;24(12):5521-33.

Maquat LE, Gong C. Gene expression networks: competing mRNA decay pathways in mammalian cells. Biochem Soc Trans. 2009 Dec;37(Pt 6):1287-92.

Marcinowski L, Tanguy M, Krmpotic A, Rädle B, Lisnić VJ, Tuddenham L, Chane-Woon-Ming B, Ruzsics Z, Erhard F, Benkartek C, Babic M, Zimmer R, Trgovcich J, Koszinowski UH, Jonjic S, Pfeffer S, Dölken L. Degradation of cellular mir-27 by a novel, highly abundant viral transcript is important for efficient virus replication in vivo. PLoS Pathog. 2012 Feb;8(2):e1002510.

Markoff L, Chang A, Falgout B. Processing of flavivirus structural glycoproteins: stable membrane insertion of premembrane requires the envelope signal peptide. Virology. 1994 Nov 1;204(2):526-40.

Martinez NJ, Gregory RI. Argonaute2 expression is post-transcriptionally coupled to microRNA abundance. RNA. 2013 May;19(5):605-12.

Marusawa H, Hijikata M, Chiba T, Shimotohno K. Hepatitis C virus core protein inhibits Fas- and tumor necrosis factor alpha-mediated apoptosis via NF-kappaB activation. J Virol. 1999 Jun;73(6):4713-20.

Mathapati BS, Mishra N, Rajukumar K, Nema RK, Behera SP, Dubey SC. Entry of bovine viral diarrhea virus into ovine cells occurs through clathrin-dependent endocytosis and low pH-dependent fusion. In Vitro Cell Dev Biol Anim. 2010 May;46(5):403-7.

Matsuki H, Takahashi M, Higuchi M, Makokha GN, Oie M, Fujii M. Both G3BP1 and G3BP2 contribute to stress granule formation. Genes Cells. 2013 Feb;18(2):135-46.

Matsushita K, Takeuchi O, Standley DM, Kumagai Y, Kawagoe T, Miyake T, Satoh T, Kato H, Tsujimura T, Nakamura H, Akira S. Zc3h12a is an RNase essential for controlling immune responses by regulating mRNA decay. Nature. 2009 Apr 30;458(7242):1185-90.

Matsuzaki K, Murata M, Yoshida K, Sekimoto G, Uemura Y, Sakaida N, Kaibori M, Kamiyama Y, Nishizawa M, Fujisawa J, Okazaki K, Seki T. Chronic inflammation associated with hepatitis C virus infection perturbs hepatic transforming growth factor beta signaling, promoting cirrhosis and hepatocellular carcinoma. Hepatology. 2007 Jul;46(1):48-57.

Matzener P, Magkouras I, Rümenapf T, Peterhans E, Schweizer M.The viral RNase E(rns) prevents IFN type-I triggering by pestiviral single- and double-stranded RNAs. Virus Res. 2009 Mar;140(1-2):15-23.

Maurer K, Krey T, Moennig V, Thiel HJ, Rümenapf T. CD46 is a cellular receptor for bovine viral diarrhea virus. J Virol. 2004 Feb;78(4):1792-9.

McMullan LK, Grakoui A, Evans MJ, Mihalik K, Puig M, Branch AD, Feinstone SM, Rice CM. Evidence for a functional RNA element in the hepatitis C virus core gene. Proc Natl Acad Sci U S A. 2007 Feb 20;104(8):2879-84.

Medina DA, Jordán-Pla A, Millán-Zambrano G, Chávez S, Choder M, Pérez-Ortín JE. Cytoplasmic 5'-3' exonuclease XRN1p is also a genome-wide transcription factor in yeast. Front Genet. 2014 Feb 6;5:1.

Mee CJ, Farquhar MJ, Harris HJ, Hu K, Ramma W, Ahmed A, Maurel P, Bicknell R, Balfe P, McKeating JA. Hepatitis C virus infection reduces hepatocellular polarity in a vascular endothelial growth factor-dependent manner. Gastroenterology. 2010 Mar;138(3):1134-42.

Mercer TR, Wilhelm D, Dinger ME, Soldà G, Korbie DJ, Glazov EA, Truong V, Schwenke M, Simons C, Matthaei KI, Saint R, Koopman P, Mattick JS. Expression of distinct RNAs from 3' untranslated regions. Nucleic Acids Res. 2011 Mar;39(6):2393-403.

Merret R, Descombin J, Juan YT, Favory JJ, Carpentier MC, Chaparro C, Charng YY, Deragon JM, Bousquet-Antonelli C. XRN4 and LARP1 are required for a heat-triggered mRNA decay pathway involved in plant acclimation and survival during thermal stress. Cell Rep. 2013 Dec 12;5(5):1279-93.

Meyers G, Ege A, Fetzer C, von Freyburg M, Elbers K, Carr V, Prentice H, Charleston B, Schürmann EM. Bovine viral diarrhea virus: prevention of persistent fetal infection by a combination of two mutations affecting Erns RNase and Npro protease. J Virol. 2007 Apr;81(7):3327-38.

Meyers G, Rümenapf T, Thiel HJ. Ubiquitin in a togavirus. Nature. 1989 Oct 12;341(6242):491.

Meyers G, Stoll D, Gunn M. Insertion of a sequence encoding light chain 3 of microtubule-associated proteins 1A and 1B in a pestivirus genome: connection with virus cytopathogenicity and induction of lethal disease in cattle. J Virol. 1998 May;72(5):4139-48.

Meyers G, Tautz N, Dubovi EJ, Thiel HJ. Viral cytopathogenicity correlated with integration of ubiquitin-coding sequences. Virology. 1991 Feb;180(2):602-16.

Meyers G, Thiel HJ. Molecular characterization of pestiviruses. Adv Virus Res. 1996;47:53-118.

Miki TS, Richter H, Rüegger S, Großhans H. PAXT-1 promotes XRN2 activity by stabilizing it through a conserved domain. Mol Cell. 2014 Jan 23;53(2):351-60.

Miller S, Kastner S, Krijnse-Locker J, Bühler S, Bartenschlager R. The non-structural protein 4A of dengue virus is an integral membrane protein inducing membrane alterations in a 2K-regulated manner.J Biol Chem. 2007 Mar 23;282(12):8873-82

Miller S, Sparacio S, Bartenschlager R. Subcellular localization and membrane topology of the Dengue virus type 2 Non-structural protein 4B. J Biol Chem. 2006 Mar 31;281(13):8854-63.

Miorin L, Romero-Brey I, Maiuri P, Hoppe S, Krijnse-Locker J, Bartenschlager R, Marcello A. Three-dimensional architecture of tick-borne encephalitis virus replication sites and trafficking of the replicated RNA. J Virol. 2013 Jun;87(11):6469-81.

Mir MA, Duran WA, Hjelle BL, Ye C, Panganiban AT. Storage of cellular 5' mRNA caps in P bodies for viral cap-snatching. Proc Natl Acad Sci U S A. 2008 Dec 9;105(49):19294-9.

Mittal S, Aslam A, Doidge R, Medica R, Winkler GS. The Ccr4a (CNOT6) and Ccr4b (CNOT6L) deadenylase subunits of the human Ccr4-Not complex contribute to the prevention of cell death and senescence. Mol Biol Cell. 2011 Mar 15;22(6):748-58.

Mitton-Fry RM, DeGregorio SJ, Wang J, Steitz TA, Steitz JA. Poly(A) tail recognition by a viral RNA element through assembly of a triple helix. Science. 2010 Nov 26;330(6008):1244-7.

Modis Y, Ogata S, Clements D, Harrison SC. A ligand-binding pocket in the dengue virus envelope glycoprotein. Proc Natl Acad Sci U S A. 2003 Jun 10;100(12):6986-91.

Moes L, Wirth M. The internal initiation of translation in bovine viral diarrhea virus RNA depends on the presence of an RNA pseudoknot upstream of the initiation codon. Virol J. 2007 Nov 22;4:124.

Molle C, Zhang T, Ysebrant de Lendonck L, Gueydan C, Andrianne M, Sherer F, Van Simaeys G, Blackshear PJ, Leo O, Goriely S. Tristetraprolin regulation of interleukin 23 mRNA stability prevents a spontaneous inflammatory disease. J Exp Med. 2013 Aug 26;210(9):1675-84.

Moon SL, Wilusz J. Cytoplasmic viruses: rage against the (cellular RNA decay) machine. PLoS Pathog. 2013 Dec;9(12):e1003762.

Moreno MP, Casane D, López L, Cristina J. Evidence of recombination in quasispecies populations of a Hepatitis C Virus patient undergoing anti-viral therapy. Virol J. 2006 Oct 24;3:87.

Moriya K, Fujie H, Shintani Y, Yotsuyanagi H, Tsutsumi T, Ishibashi K, Matsuura Y, Kimura S, Miyamura T, Koike K. The core protein of hepatitis C virus induces hepatocellular carcinoma in transgenic mice. Nat Med. 1998 Sep;4(9):1065-7

Morrison J, Laurent-Rolle M, Maestre AM, Rajsbaum R, Pisanelli G, Simon V, Mulder LC, Fernandez-Sesma A, García-Sastre A. Dengue virus co-opts UBR4 to degrade STAT2 and antagonize type I interferon signaling. PLoS Pathog. 2013 Mar;9(3):e1003265.

Mortimer SA, Doudna JA. Unconventional miR-122 binding stabilizes the HCV genome by forming a trimolecular RNA structure. Nucleic Acids Res. 2013 Apr;41(7):4230-40.

Muhlrad D, Decker CJ, Parker R. Deadenylation of the unstable mRNA encoded by the yeast MFA2 gene leads to decapping followed by 5'-->3' digestion of the transcript. Genes Dev. 1994 Apr 1;8(7):855-66.

Muhlrad D, Parker R. Mutations affecting stability and deadenylation of the yeast MFA2 transcript. Genes Dev. 1992 Nov;6(11):2100-11.

Muhlrad D, Parker R. The yeast EDC1 mRNA undergoes deadenylation-independent decapping stimulated by Not2p, Not4p, and Not5p. EMBO J. 2005 Mar 9;24(5):1033-45.

Mukherjee N, Corcoran DL, Nusbaum JD, Reid DW, Georgiev S, Hafner M, Ascano M Jr, Tuschl T, Ohler U, Keene JD. Integrative regulatory mapping indicates that the RNA-binding protein HuR couples pre-mRNA processing and mRNA stability. Mol Cell. 2011 Aug 5;43(3):327-39.

Munoz-Erazo L, Natoli R, Provis JM, Madigan MC, King NJ. Microarray analysis of gene expression in West Nile virus-infected human retinal pigment epithelium. Mol Vis. 2012;18:730-43.

Munoz-Jordán JL, Laurent-Rolle M, Ashour J, Martínez-Sobrido L, Ashok M, Lipkin WI, García-Sastre A. Inhibition of alpha/beta interferon signaling by the NS4B protein of flaviviruses. J Virol. 2005 Jul;79(13):8004-13.

Nagarajan VK, Jones CI, Newbury SF, Green PJ. XRN 5'→3' exoribonucleases: structure, mechanisms and functions. Biochim Biophys Acta. 2013 Jun-Jul;1829(6-7):590-603.

Nakazato H, Kopp DW, Edmonds M. Localization of the polyadenylate sequences in messenger ribonucleic acid and in the heterogeneous nuclear ribonucleic acid of HeLa cells. J Biol Chem. 1973 Feb 25;248(4):1472-6.

Nayak A, Berry B, Tassetto M, Kunitomi M, Acevedo A, Deng C, Krutchinsky A, Gross J, Antoniewski C, Andino R. Cricket paralysis virus antagonizes Argonaute 2 to modulate antiviral defense in Drosophila. Nat Struct Mol Biol. 2010 May;17(5):547-54.

Nazmi A, Dutta K, Basu A. RIG-I mediates innate immune response in mouse neurons following Japanese encephalitis virus infection. PLoS One. 2011;6(6):e21761.

Neill JD, Ridpath JF. Increase in proto-oncogene mRNA transcript levels in bovine lymphoid cells infected with a cytopathic type 2 bovine viral diarrhea virus. Virus Res. 2008 Aug;135(2):326-31.

Newbury S, Woollard A. The 5'-3' exoribonuclease xrn-1 is essential for ventral epithelial enclosure during C. elegans embryogenesis. RNA. 2004 Jan;10(1):59-65.

Newcomer BW, Givens MD. Approved and experimental countermeasures against pestiviral diseases: Bovine viral diarrhea, classical swine fever and border disease. Antiviral Res. 2013 Oct;100(1):133-50.

Ng ML. Ultrastructural studies of Kunjin virus-infected Aedes albopictus cells. J Gen Virol. 1987 Feb;68 (Pt 2):577-82.

Niranjanakumari S, Lasda E, Brazas R, Garcia-Blanco MA. Reversible cross-linking combined with immunoprecipitation to study RNA-protein interactions in vivo.Methods. 2002 Feb;26(2):182-90.

Nishitsuji H, Funami K, Shimizu Y, Ujino S, Sugiyama K, Seya T, Takaku H, Shimotohno K. Hepatitis C virus infection induces inflammatory cytokines and chemokines mediated by the cross talk between hepatocytes and stellate cells. J Virol. 2013 Jul;87(14):8169-78.

(a) Nomoto A, Detjen B, Pozzatti R, Wimmer E. The location of the polio genome protein in viral RNAs and its implication for RNA synthesis. Nature. 1977 Jul 21;268(5617):208-13.

(b) Nomoto A, Kitamura N, Golini F, Wimmer E. The 5'-terminal structures of poliovirion RNA and poliovirus mRNA differ only in the genome-linked protein VPg. Proc Natl Acad Sci U S A. 1977 Dec;74(12):5345-9.

Olmedo G, Guo H, Gregory BD, Nourizadeh SD, Aguilar-Henonin L, Li H, An F, Guzman P, Ecker JR. ETHYLENE-INSENSITIVE5 encodes a 5'-->3' exoribonuclease required for regulation of the EIN3-targeting F-box proteins EBF1/2. Proc Natl Acad Sci U S A. 2006 Sep 5;103(36):13286-93.

Orban TI, Izaurralde E. Decay of mRNAs targeted by RISC requires XRN1, the Ski complex, and the exosome. RNA. 2005 Apr;11(4):459-69.

Oue E, Lee JW, Sakamoto K, Iimura T, Aoki K, Kayamori K, Michi Y, Yamashiro M, Harada K, Amagasa T, Yamaguchi A. CXCL2 synthesized by oral squamous cell carcinoma is involved in cancer-associated bone destruction. Biochem Biophys Res Commun. 2012 Aug 3;424(3):456-61.

Ozgur S, Chekulaeva M, Stoecklin G. Human Pat1b connects deadenylation with mRNA decapping and controls the assembly of processing bodies. Mol Cell Biol. 2010 Sep;30(17):4308-23.

Pager CT, Schütz S, Abraham TM, Luo G, Sarnow P. Modulation of hepatitis C virus RNA abundance and virus release by dispersion of processing bodies and enrichment of stress granules. Virology. 2013 Jan 20;435(2):472-84.

Palomares RA, Walz HG, Brock KV. Expression of type I interferon-induced antiviral state and pro-apoptosis markers during experimental infection with low or high virulence bovine viral diarrhea virus in beef calves. Virus Res. 2013 May;173(2):260-9.

Palus M, Vojtiskova J, Salat J, Kopecky J, Grubhoffer L, Lipoldova M, Demant P, Ruzek D. Mice with different susceptibility to tick-borne encephalitis virus infection show selective neutralizing antibody response and inflammatory reaction in the central nervous system. J Neuroinflammation. 2013 Jun 27;10:77.

Palusa S, Ndaluka C, Bowen RA, Wilusz CJ, Wilusz J. The 3' untranslated region of the rabies virus glycoprotein mRNA specifically interacts with cellular PCBP2 protein and promotes transcript stability. PLoS One. 2012;7(3):e33561.

Paul D, Bartenschlager R. Architecture and biogenesis of plus-strand RNA virus replication factories. World J Virol. 2013 May 12;2(2):32-48.

Pavlovic D, Neville DC, Argaud O, Blumberg B, Dwek RA, Fischer WB, Zitzmann N. The hepatitis C virus p7 protein forms an ion channel that is inhibited by long-alkyl-chain iminosugar derivatives. Proc Natl Acad Sci U S A. 2003 May 13;100(10):6104-8.

Peng SS, Chen CY, Xu N, Shyu AB. RNA stabilization by the AU-rich element binding protein, HuR, an ELAV protein. EMBO J. 1998 Jun 15;17(12):3461-70.

Perelygin AA, Scherbik SV, Zhulin IB, Stockman BM, Li Y, Brinton MA. Positional cloning of the murine flavivirus resistance gene. Proc Natl Acad Sci U S A. 2002 Jul 9;99(14):9322-7.

Perez-Vilaro G, Scheller N, Saludes V, Díez J. Hepatitis C virus infection alters P-body composition but is independent of P-body granules. J Virol. 2012 Aug;86(16):8740-9.

Pesko KN, Fitzpatrick KA, Ryan EM, Shi PY, Zhang B, Lennon NJ, Newman RM, Henn MR, Ebel GD. Internally deleted WNV genomes isolated from exotic birds in New Mexico: function in cells, mosquitoes, and mice. Virology. 2012 May 25;427(1):10-7.

Pestova TV, Borukhov SI, Hellen CU. Eukaryotic ribosomes require initiation factors 1 and 1A to locate initiation codons. Nature.1998 Aug 27;394(6696):854-9.

Peterhans E, Bachofen C, Stalder H, Schweizer M. Cytopathic bovine viral diarrhea viruses (BVDV): emerging pestiviruses doomed to extinction. Vet Res. 2010 Nov-Dec;41(6):44.

Peterhans E, Schweizer M. Pestiviruses: how to outmaneuver your hosts. Vet Microbiol. 2010 Apr 21;142(1-2):18-25.

Pichlmair A, Schulz O, Tan CP, Rehwinkel J, Kato H, Takeuchi O, Akira S, Way M, Schiavo G, Reis e Sousa C. Activation of MDA5 requires higher-order RNA structures generated during virus infection. J Virol. 2009 Oct;83(20):10761-9.

Pichlmair A, Lassnig C, Eberle CA, Górna MW, Baumann CL, Burkard TR, Bürckstümmer T, Stefanovic A, Krieger S, Bennett KL, Rülicke T, Weber F, Colinge J, Müller M, Superti-Furga G. IFIT1 is an antiviral protein that recognizes 5'-triphosphate RNA. Nat Immunol. 2011 Jun 5;12(7):624-30.

Pierson TC, Kielian M. Flaviviruses: braking the entering. Curr Opin Virol. 2013 Feb;3(1):3-12.

Pijlman GP, Funk A, Kondratieva N, Leung J, Torres S, van der Aa L, Liu WJ, Palmenberg AC, Shi PY, Hall RA, Khromykh AA. A highly structured, nuclease-resistant, noncoding RNA produced by flaviviruses is required for pathogenicity. Cell Host Microbe. 2008 Dec 11;4(6):579-91.

Ploss A, Evans MJ, Gaysinskaya VA, Panis M, You H, de Jong YP, Rice CM. Human occludin is a hepatitis C virus entry factor required for infection of mouse cells. Nature. 2009 Feb 12;457(7231):882-6.

Polacek C, Foley JE, Harris E. Conformational changes in the solution structure of the dengue virus 5' end in the presence and absence of the 3' untranslated region. J Virol. 2009 Jan;83(2):1161-6.

Papadopoulos JS, Agarwala R. COBALT: constraint-based alignment tool for multiple protein sequences. Bioinformatics. 2007 May 1;23(9):1073-9.

Porta C, Larghi P, Rimoldi M, Totaro MG, Allavena P, Mantovani A, Sica A. Cellular and molecular pathways linking inflammation and cancer. Immunobiology. 2009;214(9-10):761-77.

Potuschak T, Vansiri A, Binder BM, Lechner E, Vierstra RD, Genschik P. The exoribonuclease XRN4 is a component of the ethylene response pathway in Arabidopsis. Plant Cell. 2006 Nov;18(11):3047-57.

Premkumar A, Wilson L, Ewart GD, Gage PW. Cation-selective ion channels formed by p7 of hepatitis C virus are blocked by hexamethylene amiloride. FEBS Lett. 2004 Jan 16;557(1-3):99-103.

Proutski V, Gould EA, Holmes EC. Secondary structure of the 3' untranslated region of flaviviruses: similarities and differences. Nucleic Acids Res. 1997 Mar 15;25(6):1194-202.

Quan PL, Firth C, Conte JM, Williams SH, Zambrana-Torrelio CM, Anthony SJ, Ellison JA, Gilbert AT, Kuzmin IV, Niezgoda M, Osinubi MO, Recuenco S, Markotter W, Breiman RF, Kalemba L, Malekani J, Lindblade KA, Rostal MK, Ojeda-Flores R, Suzan G, Davis LB, Blau DM, Ogunkoya AB, Alvarez Castillo DA, Moran D, Ngam S, Akaibe D, Agwanda B, Briese T, Epstein JH, Daszak P, Rupprecht CE, Holmes EC, Lipkin WI. Bats are a major natural reservoir for hepaciviruses and pegiviruses. Proc Natl Acad Sci U S A. 2013 May 14;110(20):8194-9.

Racaniello, VR. 2001. Picornaviridae: the viruses and their replication. In Knipe DM and Howley PM (eds), Fields Virology. Lippincott-Williams & Wilkins, Philadelphia, PA, pp. 685-722.

Raghavan A, Ogilvie RL, Reilly C, Abelson ML, Raghavan S, Vasdewani J, Krathwohl M, Bohjanen PR. Genome-wide analysis of mRNA decay in resting and activated primary human T lymphocytes. Nucleic Acids Res. 2002 Dec 15;30(24):5529-38.

Raju R, Raju L, Hacker D, Garcin D, Compans R, Kolakofsky D. Nontemplated bases at the 5' ends of Tacaribe virus mRNAs. Virology. 1990 Jan;174(1):53-9.

Raju R, Subramaniam SV, Hajjou M. Genesis of Sindbis virus by in vivo recombination of nonreplicative RNA precursors. J Virol. 1995 Dec;69(12):7391-401.

Rauscher S, Flamm C, Mandl CW, Heinz FX, Stadler PF. Secondary structure of the 3'-noncoding region of flavivirus genomes: comparative analysis of base pairing probabilities. RNA. 1997 Jul;3(7):779-91.

Ray RB, Meyer K, Steele R, Shrivastava A, Aggarwal BB, Ray R. Inhibition of tumor necrosis factor (TNF-alpha)-mediated apoptosis by hepatitis C virus core protein. J Biol Chem. 1998 Jan 23;273(4):2256-9.

Ray RB, Steele R, Meyer K, Ray R. Transcriptional repression of p53 promoter by hepatitis C virus core protein. J Biol Chem. 1997 Apr 25;272(17):10983-6.

Razavi H, Elkhoury AC, Elbasha E, Estes C, Pasini K, Poynard T, Kumar R. Chronic hepatitis C virus (HCV) disease burden and cost in the United States. Hepatology. 2013 Jun;57(6):2164-70.

Rehwinkel J, Behm-Ansmant I, Gatfield D, Izaurralde E. A crucial role for TNRC6A and the DCP1:DCP2 decapping complex in miRNA-mediated gene silencing. RNA. 2005 Nov;11(11):1640-7.

Reijns MA, Alexander RD, Spiller MP, Beggs JD. A role for Q/N-rich aggregation-prone regions in P-body localization.J Cell Sci. 2008 Aug 1;121(Pt 15):2463-72.

Reiter J, Pérez-Vilaró G, Scheller N, Mina LB, Díez J, Meyerhans A. Hepatitis C virus RNA recombination in cell culture. J Hepatol. 2011 Oct;55(4):777-83.

Rhee WJ, Ni CW, Zheng Z, Chang K, Jo H, Bao G. HuR regulates the expression of stress-sensitive genes and mediates inflammatory response in human umbilical vein endothelial cells. Proc Natl Acad Sci U S A. 2010 Apr 13;107(15):6858-63.

Ribeiro RM, Li H, Wang S, Stoddard MB, Learn GH, Korber BT, Bhattacharya T, Guedj J, Parrish EH, Hahn BH, Shaw GM, Perelson AS. Quantifying the diversification of hepatitis C virus (HCV) during primary infection: estimates of the in vivo mutation rate. PLoS Pathog. 2012;8(8):e1002881.

Ridpath JF, Bolin SR, Dubovi EJ. Segregation of bovine viral diarrhea virus into genotypes. Virology. 1994 Nov 15;205(1):66-74.

Ridpath JF. Immunology of BVDV vaccines. Biologicals. 2013 Jan;41(1):14-9.

Roby JA, Pijlman GP, Wilusz J, Khromykh AA. Noncoding Subgenomic Flavivirus RNA: Multiple Functions in West Nile Virus Pathogenesis and Modulation of Host Responses. Viruses. 2014 Jan 27;6(2):404-27.

Romagnani P, Lasagni L, Annunziato F, Serio M, Romagnani S. CXC chemokines: the regulatory link between inflammation and angiogenesis. Trends Immunol. 2004 Apr;25(4):201-9.

Romero TA, Tumban E, Jun J, Lott WB, Hanley KA. Secondary structure of dengue virus type 4 3' untranslated region: impact of deletion and substitution mutations. J Gen Virol. 2006 Nov;87(Pt 11):3291-6.

Romero-Brey I, Merz A, Chiramel A, Lee JY, Chlanda P, Haselman U, Santarella-Mellwig R, Habermann A, Hoppe S, Kallis S, Walther P, Antony C, Krijnse-Locker J, Bartenschlager R. Three-dimensional architecture and biogenesis of membrane structures associated with hepatitis C virus replication. PLoS Pathog. 2012;8(12):e1003056.

Romero-Lopez C, Berzal-Herranz A. A long-range RNA-RNA interaction between the 5' and 3' ends of the HCV genome. RNA. 2009 Sep;15(9):1740-52.

Rossi CR, Kiesel GK. Factors affecting the production of bovine type I interferon on bovine embryonic lung cells by polyriboinosinic-polyribocytidylic acid.Am J Vet Res. 1980 Apr;41(4):557-60.

Rossini G, Landini MP, Gelsomino F, Sambri V, Varani S. Innate host responses to West Nile virus: Implications for central nervous system immunopathology. World J Virol. 2013 May 12;2(2):49-56.

Rothman AL. Immunity to dengue virus: a tale of original antigenic sin and tropical cytokine storms. Nat Rev Immunol. 2011 Jul 15;11(8):532-43.

Rozovics JM, Chase AJ, Cathcart AL, Chou W, Gershon PD, Palusa S, Wilusz J, Semler BL. Picornavirus modification of a host mRNA decay protein. MBio. 2012 Nov 6;3(6):e00431-12.

Ruggli N, Tratschin JD, Schweizer M, McCullough KC, Hofmann MA, Summerfield A. Classical swine fever virus interferes with cellular antiviral defense: evidence for a novel function of N(pro). J Virol. 2003 Jul;77(13):7645-54.

Ruther U, Garber C, Komitowski D, Müller R, Wagner EF. Deregulated c-FOS expression interferes with normal bone development in transgenic mice. Nature. 1987 Jan 29-Feb 4;325(6103):412-6.

Rymarquis LA, Souret FF, Green PJ. Evidence that XRN4, an Arabidopsis homolog of exoribonuclease XRN1, preferentially impacts transcripts with certain sequences or in particular functional categories. RNA. 2011 Mar;17(3):501-11.

Saito T, Owen DM, Jiang F, Marcotrigiano J, Gale M Jr. Innate immunity induced by composition-dependent RIG-I recognition of hepatitis C virus RNA. Nature. 2008 Jul 24;454(7203):523-7.

Sakai A, Claire MS, Faulk K, Govindarajan S, Emerson SU, Purcell RH, Bukh J. The p7 polypeptide of hepatitis C virus is critical for infectivity and contains functionally important genotype-specific sequences. Proc Natl Acad Sci U S A. 2003 Sep 30;100(20):11646-51.

Sakamuro D, Furukawa T, Takegami T. Hepatitis C virus nonstructural protein NS3 transforms NIH 3T3 cells.J Virol. 1995 Jun;69(6):3893-6

Samuel MA, Whitby K, Keller BC, Marri A, Barchet W, Williams BR, Silverman RH, Gale M Jr, Diamond MS. PKR and RNase L contribute to protection against lethal West Nile Virus infection by controlling early viral spread in the periphery and replication in neurons. J Virol. 2006 Jul;80(14):7009-19.

Sanchez-Vargas I, Scott JC, Poole-Smith BK, Franz AW, Barbosa-Solomieu V, Wilusz J, Olson KE, Blair CD. Dengue virus type 2 infections of Aedes aegypti are modulated by the mosquito's RNA interference pathway. PLoS Pathog. 2009 Feb;5(2):e1000299.

Scarselli E, Ansuini H, Cerino R, Roccasecca RM, Acali S, Filocamo G, Traboni C, Nicosia A, Cortese R, Vitelli A.The human scavenger receptor class B type I is a novel candidate receptor for the hepatitis C virus. EMBO J. 2002 Oct 1;21(19):5017-25.

Scheel TK, Galli A, Li YP, Mikkelsen LS, Gottwein JM, Bukh J. Productive homologous and non-homologous recombination of hepatitis C virus in cell culture. PLoS Pathog. 2013 Mar;9(3):e1003228.

Scheel TK, Rice CM. Understanding the hepatitis C virus life cycle paves the way for highly effective therapies. Nat Med. 2013 Jul;19(7):837-49.

Scheller N, Mina LB, Galão RP, Chari A, Giménez-Barcons M, Noueiry A, Fischer U, Meyerhans A, Díez J. Translation and replication of hepatitis C virus genomic RNA depends on

ancient cellular proteins that control mRNA fates. Proc Natl Acad Sci U S A. 2009 Aug 11;106(32):13517-22.

Scherbik SV, Paranjape JM, Stockman BM, Silverman RH, Brinton MA. RNase L plays a role in the antiviral response to West Nile virus. J Virol. 2006 Mar;80(6):2987-99.

Schmitter D, Filkowski J, Sewer A, Pillai RS, Oakeley EJ, Zavolan M, Svoboda P, Filipowicz W. Effects of DICER and Argonaute down-regulation on mRNA levels in human HEK293 cells. Nucleic Acids Res. 2006;34(17):4801-15.

Schnell G, Loo YM, Marcotrigiano J, Gale M Jr. Uridine composition of the poly-U/UC tract of HCV RNA defines non-self recognition by RIG-I. PLoS Pathog. 2012;8(8):e1002839.

Schnell MJ, McGettigan JP, Wirblich C, Papaneri A. The cell biology of rabies virus: using stealth to reach the brain. Nat Rev Microbiol. 2010 Jan;8(1):51-61.

Schnettler E, Sterken MG, Leung JY, Metz SW, Geertsema C, Goldbach RW, Vlak JM, Kohl A, Khromykh AA, Pijlman GP. Noncoding flavivirus RNA displays RNA interference suppressor activity in insect and Mammalian cells. J Virol. 2012 Dec;86(24):13486-500.

Schnittger S, Dicker F, Kern W, Wendland N, Sundermann J, Alpermann T, Haferlach C, Haferlach T. RUNX1 mutations are frequent in de novo AML with noncomplex karyotype and confer an unfavorable prognosis. Blood. 2011 Feb 24;117(8):2348-57.

Schoggins JW, Wilson SJ, Panis M, Murphy MY, Jones CT, Bieniasz P, Rice CM. A diverse range of gene products are effectors of the type I interferon antiviral response. Nature. 2011 Apr 28;472(7344):481-5.

Schuessler A, Funk A, Lazear HM, Cooper DA, Torres S, Daffis S, Jha BK, Kumagai Y, Takeuchi O, Hertzog P, Silverman R, Akira S, Barton DJ, Diamond MS, Khromykh AA. West Nile virus noncoding subgenomic RNA contributes to viral evasion of the type I interferon-mediated antiviral response. J Virol. 2012 May;86(10):5708-18.

Schwartz D, Decker CJ, Parker R. The enhancer of decapping proteins, EDC1p and EDC2p, bind RNA and stimulate the activity of the decapping enzyme. RNA. 2003 Feb;9(2):239-51.

Schwede A, Ellis L, Luther J, Carrington M, Stoecklin G, Clayton C. A role for Caf1 in mRNA deadenylation and decay in trypanosomes and human cells. Nucleic Acids Res. 2008 Jun;36(10):3374-88.

Scortegagna M, Cataisson C, Martin RJ, Hicklin DJ, Schreiber RD, Yuspa SH, Arbeit JM. HIF-1alpha regulates epithelial inflammation by cell autonomous NFkappaB activation and paracrine stromal remodeling. Blood. 2008 Apr 1;111(7):3343-54.

Seago J, Hilton L, Reid E, Doceul V, Jeyatheesan J, Moganeradj K, McCauley J, Charleston B, Goodbourn S. The Npro product of classical swine fever virus and bovine viral diarrhea virus uses a conserved mechanism to target interferon regulatory factor-3. J Gen Virol. 2007 Nov;88(Pt 11):3002-6.

Sen GL, Blau HM. Argonaute 2/RISC resides in sites of mammalian mRNA decay known as cytoplasmic bodies. Nat Cell Biol. 2005;7:633–636.

Serviene E, Shapka N, Cheng CP, Panavas T, Phuangrat B, Baker J, Nagy PD. Genome-wide screen identifies host genes affecting viral RNA recombination. Proc Natl Acad Sci U S A. 2005 Jul 26;102(30):10545-50.

Shapiro JS, Langlois RA, Pham AM, Tenoever BR. Evidence for a cytoplasmic microprocessor of pri-miRNAs. RNA. 2012 Jul;18(7):1338-46.

Shaw G, Kamen R. A conserved AU sequence from the 3' untranslated region of GM-CSF mRNA mediates selective mRNA degradation. Cell. 1986 Aug 29;46(5):659-67.

She M, Decker CJ, Svergun DI, Round A, Chen N, Muhlrad D, Parker R, Song H. Structural basis of DCP2 recognition and activation by DCP1. Mol Cell. 2008 Feb 15;29(3):337-49.

Sheth U, Parker R. Decapping and decay of messenger RNA occur in cytoplasmic processing bodies. Science. 2003 May 2;300(5620):805-8.

Shimakami T, Yamane D, Jangra RK, Kempf BJ, Spaniel C, Barton DJ, Lemon SM. Stabilization of hepatitis C virus RNA by an AGO2-miR-122 complex. Proc Natl Acad Sci U S A. 2012 Jan 17;109(3):941-6.

Shimizu H, Miyazaki M, Wakabayashi Y, Mitsuhashi N, Kato A, Ito H, Nakagawa K, Yoshidome H, Kataoka M, Nakajima N. Vascular endothelial growth factor secreted by replicating hepatocytes induces sinusoidal endothelial cell proliferation during regeneration after partial hepatectomy in rats. J Hepatol. 2001 May;34(5):683-9.

Shimoyama Y, Morikawa Y, Ichihara M, Kodama Y, Fukuda N, Hayashi H, Morinaga T, Iwashita T, Murakumo Y, Takahashi M. Identification of human SEP1 as a glial cell line-derived neurotrophic factor-inducible protein and its expression in the nervous system. Neuroscience. 2003;121(4):899-906.

Shin D, Richards SL, Alto BW, Bettinardi DJ, Smartt CT. Genome sequence analysis of dengue virus 1 isolated in Key West, Florida. PLoS One. 2013 Sep 30;8(9):e74582.

Shyu AB, Belasco JG, Greenberg ME. Two distinct destabilizing elements in the c-FOS message trigger deadenylation as a first step in rapid mRNA decay. Genes Dev. 1991 Feb;5(2):221-31.

Siddiqui N, Mangus DA, Chang TC, Palermino JM, Shyu AB, Gehring K. Poly(A) nuclease interacts with the C-terminal domain of polyadenylate-binding protein domain from poly(A)-binding protein. J Biol Chem. 2007 Aug 24;282(34):25067-75.

Silva PA, Pereira CF, Dalebout TJ, Spaan WJ, Bredenbeek PJ. An RNA pseudoknot is required for production of yellow fever virus subgenomic RNA by the host nuclease XRN1. J Virol. 2010 Nov;84(21):11395-406.

Simon-Loriere E, Holmes EC. Why do RNA viruses recombine? Nat Rev Microbiol. 2011 Jul 4;9(8):617-26.

Sinturel F, Bréchemier-Baey D, Kiledjian M, Condon C, Bénard L. Activation of 5'-3' exoribonuclease XRN1 by cofactor DCS1 is essential for mitochondrial function in yeast. Proc Natl Acad Sci U S A. 2012 May 22;109(21):8264-9.

Sips GJ, Wilschut J, Smit JM. Neuroinvasive flavivirus infections. Rev Med Virol. 2012 Mar;22(2):69-87.

Sizova DV, Kolupaeva VG, Pestova TV, Shatsky IN, Hellen CU. Specific interaction of eukaryotic translation initiation factor 3 with the 5' nontranslated regions of hepatitis C virus and classical swine fever virus RNAs. J Virol. 1998 Jun;72(6):4775-82.

Smibert P, Yang JS, Azzam G, Liu JL, Lai EC. Homeostatic control of Argonaute stability by microRNA availability. Nat Struct Mol Biol. 2013 Jul;20(7):789-95.

Smietanski M, Werner M, Purta E, Kaminska KH, Stepinski J, Darzynkiewicz E, Nowotny M, Bujnicki JM. Structural analysis of human 2'-O-ribose methyltransferases involved in mRNA cap structure formation. Nat Commun. 2014;5:3004.

Smirnova NP, Bielefeldt-Ohmann H, Van Campen H, Austin KJ, Han H, Montgomery DL, Shoemaker ML, van Olphen AL, Hansen TR. Acute non-cytopathic bovine viral diarrhea virus infection induces pronounced type I interferon response in pregnant cows and fetuses. Virus Res. 2008 Mar;132(1-2):49-58.

Smirnova NP, Webb BT, Bielefeldt-Ohmann H, Van Campen H, Antoniazzi AQ, Morarie SE, Hansen TR. Development of fetal and placental innate immune responses during establishment of persistent infection with bovine viral diarrhea virus. Virus Res. 2012 Aug;167(2):329-36.

Smit JM, Moesker B, Rodenhuis-Zybert I, Wilschut J. Flavivirus cell entry and membrane fusion. Viruses. 2011 Feb;3(2):160-71.

Smith BD, Morgan RL, Beckett GA, Falck-Ytter Y, Holtzman D, Ward JW. Hepatitis C virus testing of persons born during 1945-1965: recommendations from the Centers for Disease Control and Prevention. Ann Intern Med. 2012 Dec 4;157(11):817-22.

Sokoloski KJ, Dickson AM, Chaskey EL, Garneau NL, Wilusz CJ, Wilusz J. Sindbis virus usurps the cellular HuR protein to stabilize its transcripts and promote productive infections in mammalian and mosquito cells. Cell Host Microbe. 2010 Aug 19;8(2):196-207.

Solomon S, Xu Y, Wang B, David MD, Schubert P, Kennedy D, Schrader JW. Distinct structural features of caprin-1 mediate its interaction with G3BP-1 and its induction of phosphorylation of eukaryotic translation initiation factor 2alpha, entry to cytoplasmic stress granules, and selective interaction with a subset of mRNAs. Mol Cell Biol. 2007 Mar;27(6):2324-42

Song MG, Bail S, Kiledjian M. Multiple Nudix family proteins possess mRNA decapping activity. RNA. 2013 Mar;19(3):390-9.

Song Y, Friebe P, Tzima E, Jünemann C, Bartenschlager R, Niepmann M. The hepatitis C virus RNA 3'-untranslated region strongly enhances translation directed by the internal ribosome entry site. J Virol. 2006 Dec;80(23):11579-88.

St Laurent G 3rd, Shtokalo D, Heydarian M, Palyanov A, Babiy D, Zhou J, Kumar A, Urcuqui-Inchima S Insights from the HuR-interacting transcriptome: ncRNAs, ubiquitin pathways, and patterns of secondary structure dependent RNA interactions. Mol Genet Genomics. 2012 Dec;287(11-12):867-79.

Stadler K, Allison SL, Schalich J, Heinz FX. Proteolytic activation of tick-borne encephalitis virus by furin. J Virol. 1997 Nov;71(11):8475-81.

Stapleton JT, Foung S, Muerhoff AS, Bukh J, Simmonds P. The GB viruses: a review and proposed classification of GBV-A, GBV-C (HGV), and GBV-D in genus Pegivirus within the family Flaviviridae. J Gen Virol. 2011 Feb;92(Pt 2):233-46.

Stark R, Meyers G, Rümenapf T, Thiel HJ. Processing of pestivirus polyprotein: cleavage site between autoprotease and nucleocapsid protein of classical swine fever virus. J Virol. 1993 Dec;67(12):7088-95.

Stauffer JK, Scarzello AJ, Jiang Q, Wiltrout RH. Chronic inflammation, immune escape, and oncogenesis in the liver: a unique neighborhood for novel intersections. Hepatology. 2012 Oct;56(4):1567-74.

Steiger M, Carr-Schmid A, Schwartz DC, Kiledjian M, Parker R. Analysis of recombinant yeast decapping enzyme. RNA. 2003 Feb;9(2):231-8.

Stewart SA, Dykxhoorn DM, Palliser D, Mizuno H, Yu EY, An DS, Sabatini DM, Chen IS, Hahn WC, Sharp PA, Weinberg RA, Novina CD. Lentivirus-delivered stable gene silencing by RNAi in primary cells. RNA. 2003 Apr;9(4):493-501.

Stevens A. 5'-exoribonuclease 1: XRN1. Methods Enzymol. 2001;342:251-9.

Stevens A. An exoribonuclease from Saccharomyces cerevisiae: effect of modifications of 5' end groups on the hydrolysis of substrates to 5' mononucleotides. Biochem Biophys Res Commun. 1978 Mar 30;81(2):656-61.

Stevens A. An mRNA decapping enzyme from ribosomes of Saccharomyces cerevisiae. Biochem Biophys Res Commun. 1980 Oct 16;96(3):1150-5.

Stevens A, Hsu CL, Isham KR, Larimer FW. Fragments of the internal transcribed spacer 1 of pre-rRNA accumulate in Saccharomyces cerevisiae lacking 5'----3' exoribonuclease 1. J Bacteriol. 1991 Nov;173(21):7024-8.

Stevens A, Poole TL. 5'-exonuclease-2 of Saccharomyces cerevisiae. Purification and features of ribonuclease activity with comparison to 5'-exonuclease-1. J Biol Chem. 1995 Jul 7;270(27):16063-9.

Stiasny K, Allison SL, Schalich J, Heinz FX. Membrane interactions of the tick-borne encephalitis virus fusion protein E at low pH. J Virol. 2002 Apr;76(8):3784-90.

Stoecklin G, Mayo T, Anderson P. ARE-mRNA degradation requires the 5'-3' decay pathway. EMBO Rep. 2006 Jan;7(1):72-7.

Suksanpaisan L, Susantad T, Smith DR. Characterization of dengue virus entry into HepG2 cells. J Biomed Sci. 2009 Feb 4;16:17.

Sumpter R Jr, Loo YM, Foy E, Li K, Yoneyama M, Fujita T, Lemon SM, Gale M Jr. Regulating intracellular antiviral defense and permissiveness to hepatitis C virus RNA replication through a cellular RNA helicase, RIG-I. J Virol. 2005 Mar;79(5):2689-99.

Sun M, Schwalb B, Pirkl N, Maier KC, Schenk A, Failmezger H, Tresch A, Cramer P. Global analysis of eukaryotic mRNA degradation reveals XRN1-dependent buffering of transcript levels. Mol Cell. 2013 Oct 10;52(1):52-62.

Suthar MS, Diamond MS, Gale M Jr. West Nile virus infection and immunity. Nat Rev Microbiol. 2013 Feb;11(2):115-28.

Suthar MS, Ma DY, Thomas S, Lund JM, Zhang N, Daffis S, Rudensky AY, Bevan MJ, Clark EA, Kaja MK, Diamond MS, Gale M Jr. IPS-1 is essential for the control of West Nile virus infection and immunity. PLoS Pathog. 2010 Feb 5;6(2):e1000757.

Suthar MS, Ramos HJ, Brassil MM, Netland J, Chappell CP, Blahnik G, McMillan A, Diamond MS, Clark EA, Bevan MJ, Gale M Jr. The RIG-I-like receptor LGP2 controls CD8(+) T cell survival and fitness. Immunity. 2012 Aug 24;37(2):235-48.

Swarup V, Das S, Ghosh S, Basu A. Tumor necrosis factor receptor-1-induced neuronal death by TRADD contributes to the pathogenesis of Japanese encephalitis. J Neurochem. 2007 Oct;103(2):771-83

Szankasi P, Smith GR. Requirement of S. pombe exonuclease II, a homologue of S. cerevisiae Sep1, for normal mitotic growth and viability. Curr Genet. 1996 Sep;30(4):284-93.

Szretter KJ, Daniels BP, Cho H, Gainey MD, Yokoyama WM, Gale M Jr, Virgin HW, Klein RS, Sen GC, Diamond MS. 2'-O methylation of the viral mRNA cap by West Nile virus evades ifit1-dependent and -independent mechanisms of host restriction in vivo. PLoS Pathog. 2012;8(5):e1002698.

Takimoto K, Wakiyama M, Yokoyama S. Mammalian TNRC6A contains multiple Argonaute-binding sites and functions in microRNA-mediated translational repression. RNA. 2009 Jun;15(6):1078-89.

Tanaka T, Kato N, Cho MJ, Sugiyama K, Shimotohno K. Structure of the 3' terminus of the hepatitis C virus genome. J Virol. 1996 May;70(5):3307-12.

Tanji Y, Hijikata M, Hirowatari Y, Shimotohno K. Hepatitis C virus polyprotein processing: kinetics and mutagenic analysis of serine proteinase-dependent cleavage. J Virol. 1994 Dec;68(12):8418-22.

Taucher C, Berger A, Mandl CW. A trans-complementing recombination trap demonstrates a low propensity of flaviviruses for intermolecular recombination. J Virol. 2010 Jan;84(1):599-611.

Tautz N, Meyers G, Stark R, Dubovi EJ, Thiel HJ. Cytopathogenicity of a pestivirus correlates with a 27-nucleotide insertion. J Virol. 1996 Nov;70(11):7851-8.

Tautz N, Meyers G, Thiel HJ. Pathogenesis of mucosal disease, a deadly disease of cattle caused by a pestivirus. Clin Diagn Virol. 1998 Jul 15;10(2-3):121-7.

Taylor GA, Carballo E, Lee DM, Lai WS, Thompson MJ, Patel DD, Schenkman DI, Gilkeson GS, Broxmeyer HE, Haynes BF, Blackshear PJ. A pathogenetic role for TNF alpha in the syndrome of cachexia, arthritis, and autoimmunity resulting from tristetraprolin (TTP) deficiency. Immunity. 1996 May;4(5):445-54.

Tenoever BR, Ng SL, Chua MA, McWhirter SM, García-Sastre A, Maniatis T. Multiple functions of the IKK-related kinase IKKepsilon in interferon-mediated antiviral immunity. Science. 2007 Mar 2;315(5816):1274-8.

Tharun S, He W, Mayes AE, Lennertz P, Beggs JD, Parker R. Yeast Sm-like proteins function in mRNA decapping and decay. Nature. 2000 Mar 30;404(6777):515-8.

Thoren F, Romero A, Lindh M, Dahlgren C, Hellstrand K. A hepatitis C virus-encoded, nonstructural protein (NS3) triggers dysfunction and apoptosis in lymphocytes: role of NADPH oxidase-derived oxygen radicals. J Leukoc Biol. 2004 Dec;76(6):1180-6.

Thurner C, Witwer C, Hofacker IL, Stadler PF. Conserved RNA secondary structures in Flaviviridae genomes. J Gen Virol. 2004 May;85(Pt 5):1113-24.

Till DD, Linz B, Seago JE, Elgar SJ, Marujo PE, Elias ML, Arraiano CM, McClellan JA, McCarthy JE, Newbury SF. Identification and developmental expression of a 5'-3' exoribonuclease from Drosophila melanogaster. Mech Dev. 1998 Dec;79(1-2):51-5.

Tishkoff DX, Johnson AW, Kolodner RD. Molecular and genetic analysis of the gene encoding the Saccharomyces cerevisiae strand exchange protein Sep1. Mol Cell Biol. 1991 May;11(5):2593-608.

Tolfvenstam T, Lindblom A, Schreiber MJ, Ling L, Chow A, Ooi EE, Hibberd ML. Characterization of early host responses in adults with dengue disease. BMC Infect Dis. 2011 Aug 2;11:209.

Tolou HJ, Couissinier-Paris P, Durand JP, Mercier V, de Pina JJ, de Micco P, Billoir F, Charrel RN, de Lamballerie X. Evidence for recombination in natural populations of dengue virus type 1 based on the analysis of complete genome sequences. J Gen Virol. 2001 Jun;82(Pt 6):1283-90.

Totaro A, Renzi F, La Fata G, Mattioli C, Raabe M, Urlaub H, Achsel T. The human Pat1b protein: a novel mRNA deadenylation factor identified by a new immunoprecipitation technique. Nucleic Acids Res. 2011 Jan;39(2):635-47.

Townsend HL, Jha BK, Han JQ, Maluf NK, Silverman RH, Barton DJ. A viral RNA competitively inhibits the antiviral endoribonuclease domain of RNase L. RNA. 2008 Jun;14(6):1026-36.

Trent DW. Antigenic characterization of flavivirus structural proteins separated by isoelectric focusing. J Virol. 1977 Jun;22(3):608-18.

Triantafilou K, Vakakis E, Kar S, Richer E, Evans GL, Triantafilou M. Visualisation of direct interaction of MDA5 and the dsRNA replicative intermediate form of positive strand RNA viruses. J Cell Sci. 2012 Oct 15;125(Pt 20):4761-9.

Tscherne DM, Jones CT, Evans MJ, Lindenbach BD, McKeating JA, Rice CM. Time- and temperature-dependent activation of hepatitis C virus for low-pH-triggered entry. J Virol. 2006 Feb;80(4):1734-41.

Tsiang H, Atanasiu P, Chermann JC, Jasmin C. Inhibition of rabies virus in vitro by the ammonium-5-tungsto-2-antimoniate. J Gen Virol. 1978 Sep;40(3):665-8.

Tsuchihara K, Tanaka T, Hijikata M, Kuge S, Toyoda H, Nomoto A, Yamamoto N, Shimotohno K. Specific interaction of polypyrimidine tract-binding protein with the extreme 3'-terminal structure of the hepatitis C virus genome, the 3'X. J Virol. 1997 Sep;71(9):6720-6.

Turenne N, Tiys E, Ivanisenko V, Yudin N, Ignatieva E, Valour D, Degrelle SA, Hue I. Finding biomarkers in non-model species: literature mining of transcription factors involved in bovine embryo development. BioData Min. 2012 Aug 29;5(1):12.

Tycowski KT, Shu MD, Borah S, Shi M, Steitz JA. Conservation of a triple-helix-forming RNA stability element in noncoding and genomic RNAs of diverse viruses. Cell Rep. 2012 Jul 26;2(1):26-32.

Uchida N, Hoshino S, Katada T. Identification of a human cytoplasmic poly(A) nuclease complex stimulated by poly(A)-binding protein. J Biol Chem. 2004 Jan 9;279(2):1383-91.

Uehata T, Akira S. mRNA degradation by the endoribonuclease Regnase-1/ZC3H12a/MCPIP-1. Biochim Biophys Acta. 2013 Jun-Jul;1829(6-7):708-13.

Uzcategui NY, Camacho D, Comach G, Cuello de Uzcategui R, Holmes EC, Gould EA. Molecular epidemiology of dengue type 2 virus in Venezuela: evidence for in situ virus evolution and recombination. J Gen Virol. 2001 Dec;82(Pt 12):2945-53.

van der Schaar HM, Rust MJ, Chen C, van der Ende-Metselaar H, Wilschut J, Zhuang X, Smit JM. Dissecting the cell entry pathway of dengue virus by single-particle tracking in living cells. PLoS Pathog. 2008 Dec;4(12):e1000244.

van Hoof A, Frischmeyer PA, Dietz HC, Parker R. Exosome-mediated recognition and degradation of mRNAs lacking a termination codon. Science. 2002 Mar 22;295(5563):2262-4.

van Mierlo JT, Bronkhorst AW, Overheul GJ, Sadanandan SA, Ekström JO, Heestermans M, Hultmark D, Antoniewski C, van Rij RP. Convergent evolution of argonaute-2 slicer antagonism in two distinct insect RNA viruses. PLoS Pathog. 2012;8(8):e1002872.

Van Tubergen E, Vander Broek R, Lee J, Wolf G, Carey T, Bradford C, Prince M, Kirkwood KL, D'Silva NJ. Tristetraprolin regulates interleukin-6, which is correlated with tumor progression in patients with head and neck squamous cell carcinoma. Cancer. 2011 Jun 15;117(12):2677-89.

Vassilaki N, Friebe P, Meuleman P, Kallis S, Kaul A, Paranhos-Baccalà G, Leroux-Roels G, Mavromara P, Bartenschlager R. Role of the hepatitis C virus core+1 open reading frame and core cis-acting RNA elements in viral RNA translation and replication. J Virol. 2008 Dec;82(23):11503-15.

Vasudevan S, Peltz SW, Wilusz CJ. Non-stop decay--a new mRNA surveillance pathway. Bioessays. 2002 Sep;24(9):785-8.

Vilcek S, Paton D, Lowings P, Björklund H, Nettleton P, Belák S. Genetic analysis of pestiviruses at the 3' end of the genome. Virus Genes. 1999;18(2):107-14.

Vreken P, Raue HA. The rate-limiting step in yeast PGK1 mRNA degradation is an endonucleolytic cleavage in the 3'-terminal part of the coding region. Mol Cell Biol. 1992 Jul;12(7):2986-96.

Wan Y, Qu K, Zhang QC, Flynn RA, Manor O, Ouyang Z, Zhang J, Spitale RC, Snyder MP, Segal E, Chang HY. Landscape and variation of RNA secondary structure across the human transcriptome. Nature. 2014 Jan 30;505(7485):706-9.

Wang C, Pflugheber J, Sumpter R Jr, Sodora DL, Hui D, Sen GC, Gale M Jr. Alpha interferon induces distinct translational control programs to suppress hepatitis C virus RNA replication. J Virol. 2003 Apr;77(7):3898-912.

Wang C, Sarnow P, Siddiqui A. Translation of human hepatitis C virus RNA in cultured cells is mediated by an internal ribosome-binding mechanism. J Virol. 1993 Jun;67(6):3338-44.

Wang CC, Huang ZS, Chiang PL, Chen CT, Wu HN. Analysis of the nucleoside triphosphatase, RNA triphosphatase, and unwinding activities of the helicase domain of dengue virus NS3 protein. FEBS Lett. 2009 Feb 18;583(4):691-6.

Wang JG, Collinge M, Ramgolam V, Ayalon O, Fan XC, Pardi R, Bender JR. LFA-1-dependent HuR nuclear export and cytokine mRNA stabilization in T cell activation. J Immunol. 2006 Feb 15;176(4):2105-13.

Wang L, Jeng KS, Lai MM. Poly(C)-binding protein 2 interacts with sequences required for viral replication in the hepatitis C virus (HCV) 5' untranslated region and directs HCV RNA replication through circularizing the viral genome. J Virol. 2011 Aug;85(16):7954-64.

Wang T, Town T, Alexopoulou L, Anderson JF, Fikrig E, Flavell RA. Toll-like receptor 3 mediates West Nile virus entry into the brain causing lethal encephalitis. Nat Med. 2004 Dec;10(12):1366-73.

Wang Z, Jiao X, Carr-Schmid A, Kiledjian M. The hDCP2 protein is a mammalian mRNA decapping enzyme. Proc Natl Acad Sci U S A. 2002 Oct 1;99(20):12663-8.

Wang Z, Kiledjian M. Functional link between the mammalian exosome and mRNA decapping. Cell. 2001 Dec 14;107(6):751-62.

Wang ZQ, Ovitt C, Grigoriadis AE, Möhle-Steinlein U, Rüther U, Wagner EF. Bone and haematopoietic defects in mice lacking c-FOS. Nature. 1992 Dec 24-31;360(6406):741-5.

Ward AM, Bidet K, Yinglin A, Ler SG, Hogue K, Blackstock W, Gunaratne J, Garcia-Blanco MA. Quantitative mass spectrometry of DENV-2 RNA-interacting proteins reveals that the DEAD-box RNA helicase DDX6 binds the DB1 and DB2 3' UTR structures. RNA Biol. 2011 Nov-Dec;8(6):1173-86.

Washenberger CL, Han JQ, Kechris KJ, Jha BK, Silverman RH, Barton DJ. Hepatitis C virus RNA: dinucleotide frequencies and cleavage by RNase L. Virus Res. 2007 Dec;130(1-2):85-95.

Webb BT, McGilvray KC, Smirnova NP, Hansen TR, Norrdin RW. Effects of in utero pestivirus infection on bovine fetal bone geometry, biomechanical properties and composition. Vet J. 2013 Nov;198(2):376-81.

Webb BT, Norrdin RW, Smirnova NP, Van Campen H, Weiner CM, Antoniazzi AQ, Bielefeldt-Ohmann H, Hansen TR. Bovine viral diarrhea virus cyclically impairs long bone trabecular modeling in experimental persistently infected fetuses. Vet Pathol. 2012 Nov;49(6):930-40.

Weber M, Gawanbacht A, Habjan M, Rang A, Borner C, Schmidt AM, Veitinger S, Jacob R, Devignot S, Kochs G, García-Sastre A, Weber F. Incoming RNA virus nucleocapsids containing a 5'-triphosphorylated genome activate RIG-I and antiviral signaling. Cell Host Microbe. 2013 Mar 13;13(3):336-46.

Weiner CM, Smirnova NP, Webb BT, Van Campen H, Hansen TR. Interferon stimulated genes, CXCR4 and immune cell responses in peripheral blood mononuclear cells infected with bovine viral diarrhea virus. Res Vet Sci. 2012 Oct;93(2):1081-8.

Weiskircher E, Aligo J, Ning G, Konan KV. Bovine viral diarrhea virus NS4B protein is an integral membrane protein associated with Golgi markers and rearranged host membranes. Virol J. 2009 Nov 3;6:185.

Weiss BG, Schlesinger S. Recombination between Sindbis virus RNAs. J Virol. 1991 Aug;65(8):4017-25.

Werner GH, Jasmin C, Chermann JC. Effect of ammonium 5-tungsto-2-antimoniate on encephalomyocarditis and vesicular stomatitis virus infections in mice. J Gen Virol. 1976 Apr;31(1):59-64.

Werner M, Purta E, Kaminska KH, Cymerman IA, Campbell DA, Mittra B, Zamudio JR, Sturm NR, Jaworski J, Bujnicki JM. 2'-O-ribose methylation of cap2 in human: function and evolution in a horizontally mobile family. Nucleic Acids Res. 2011 Jun;39(11):4756-68.

Westaway EG, Mackenzie JM, Khromykh AA. Replication and gene function in Kunjin virus. Curr Top Microbiol Immunol. 2002;267:323-51.

Wilson GK, Brimacombe CL, Rowe IA, Reynolds GM, Fletcher NF, Stamataki Z, Bhogal RH, Simões ML, Ashcroft M, Afford SC, Mitry RR, Dhawan A, Mee CJ, Hübscher SG, Balfe P, McKeating JA. A dual role for hypoxia inducible factor-1α in the hepatitis C virus lifecycle and hepatoma migration. J Hepatol. 2012 Apr;56(4):803-9.

Wilson T, Treisman R. Removal of poly(A) and consequent degradation of c-FOS mRNA facilitated by 3' AU-rich sequences. Nature. 1988 Nov 24;336(6197):396-9.

Wilusz CJ, Wilusz J. Consequences of mRNA wardrobe malfunctions. Cell. 2010 Dec 10;143(6):863-5.

Wilusz J, Shenk T. A 64 kd nuclear protein binds to RNA segments that include the AAUAAA polyadenylation motif. Cell. 1988 Jan 29;52(2):221-8.

Wise M, Finelli L, Sorvillo F. Prognostic factors associated with hepatitis C disease: a case-control study utilizing U.S. multiple-cause-of-death data. Public Health Rep. 2010 May-Jun;125(3):414-22.

Wiskerchen M, Belzer SK, Collett MS. Pestivirus gene expression: the first protein product of the bovine viral diarrhea virus large open reading frame, p20, possesses proteolytic activity. J Virol. 1991 Aug;65(8):4508-14.

Withers JB, Beemon KL. Structural features in the Rous sarcoma virus RNA stability element are necessary for sensing the correct termination codon. Retrovirology. 2010 Aug 5;7:65.

Wong J, Si X, Angeles A, Zhang J, Shi J, Fung G, Jagdeo J, Wang T, Zhong Z, Jan E, Luo H. Cytoplasmic redistribution and cleavage of AUF1 during coxsackievirus infection enhance the stability of its viral genome. FASEB J. 2013 Jul;27(7):2777-87.

Wozniak AL, Griffin S, Rowlands D, Harris M, Yi M, Lemon SM, Weinman SA. Intracellular proton conductance of the hepatitis C virus p7 protein and its contribution to infectious virus production. PLoS Pathog. 2010 Sep 2;6(9):e1001087.

Wu D, Muhlrad D, Bowler MW, Jiang S, Liu Z, Parker R, Song H. Lsm2 and Lsm3 bridge the interaction of the Lsm1-7 complex with Pat1 for decapping activation. Cell Res. 2014 Feb;24(2):233-46.

Wu M, Reuter M, Lilie H, Liu Y, Wahle E, Song H. Structural insight into poly(A) binding and catalytic mechanism of human PARN. EMBO J. 2005 Dec 7;24(23):4082-93.

Wyman SK, Knouf EC, Parkin RK, Fritz BR, Lin DW, Dennis LM, Krouse MA, Webster PJ, Tewari M. Post-transcriptional generation of miRNA variants by multiple nucleotidyl transferases contributes to miRNA transcriptome complexity. Genome Res. 2011 Sep;21(9):1450-61

Xia H, Vijayaraghavan B, Belák S, Liu L. Detection and identification of the atypical bovine pestiviruses in commercial foetal bovine serum batches. PLoS One. 2011;6(12):e28553.

Xiang S, Cooper-Morgan A, Jiao X, Kiledjian M, Manley JL, Tong L. Structure and function of the 5'→3' exoribonuclease Rat1 and its activating partner Rai1. Nature. 2009 Apr 9; 458(7239):784-8.

Xue Y, Bai X, Lee I, Kallstrom G, Ho J, Brown J, Stevens A, Johnson AW. Saccharomyces cerevisiae RAI1 (YGL246c) is homologous to human DOM3Z and encodes a protein that binds the nuclear exoribonuclease Rat1p. Mol Cell Biol. 2000 Jun;20(11):4006-15.

Yacoub S, Mongkolsapaya J, Screaton G. The pathogenesis of dengue. Curr Opin Infect Dis. 2013 Jun;26(3):284-9.

Yakub I, Lillibridge KM, Moran A, Gonzalez OY, Belmont J, Gibbs RA, Tweardy DJ. Single nucleotide polymorphisms in genes for 2'-5'-oligoadenylate synthetase and RNase L inpatients hospitalized with West Nile virus infection. J Infect Dis. 2005 Nov 15;192(10):1741-8.

Yamada N, Tanihara K, Takada A, Yorihuzi T, Tsutsumi M, Shimomura H, Tsuji T, Date T. Genetic organization and diversity of the 3' noncoding region of the hepatitis C virus genome. Virology. 1996 Sep 1;223(1):255-61.

Yamagishi N, Terauchi H, Kanematsu S, Hidaka S. Characterization of the small subgenomic RNA of Soybean dwarf virus. Arch Virol. 2003 Sep;148(9):1827-34.

Yamashita A, Chang TC, Yamashita Y, Zhu W, Zhong Z, Chen CY, Shyu AB. Concerted action of poly(A) nucleases and decapping enzyme in mammalian mRNA turnover. Nat Struct Mol Biol. 2005 Dec;12(12):1054-63.

Yamshchikov VF, Compans RW. Processing of the intracellular form of the west Nile virus capsid protein by the viral NS2B-NS3 protease: an in vitro study. J Virol. 1994 Sep;68(9):5765-71.

Yamshchikov VF, Trent DW, Compans RW. Upregulation of signalase processing and induction of prM-E secretion by the flavivirus NS2B-NS3 protease: roles of protease components. J Virol. 1997 Jun;71(6):4364-71.

Yan YB. Deadenylation: enzymes, regulation, and functional implications. Wiley Interdiscip Rev RNA. 2014 Feb 12.

Yang JS, Maurin T, Lai EC. Functional parameters of DICER-independent microRNA biogenesis. RNA. 2012 May;18(5):945-57.

Yang JS, Maurin T, Robine N, Rasmussen KD, Jeffrey KL, Chandwani R, Papapetrou EP, Sadelain M, O'Carroll D, Lai EC. Conserved vertebrate mir-451 provides a platform for DICER-independent, AGO2-mediated microRNA biogenesis. Proc. Natl Acad. Sci. USA. 2010;107:15163–15168.

Yang S, He M, Liu X, Li X, Fan B, Zhao S. Japanese encephalitis virus infects porcine kidney epithelial PK15 cells via clathrin- and cholesterol-dependent endocytosis. Virol J. 2013 Aug 12;10:258.

Yap LJ, Luo D, Chung KY, Lim SP, Bodenreider C, Noble C, Shi PY, Lescar J. Crystal structure of the dengue virus methyltransferase bound to a 5'-capped octameric RNA. PLoS One. 2010 Sep 17;5(9).

Yi M, Lemon SM. Structure-function analysis of the 3' stem-loop of hepatitis C virus genomic RNA and its role in viral RNA replication. RNA. 2003 Mar;9(3):331-45.

Yoneyama M, Kikuchi M, Natsukawa T, Shinobu N, Imaizumi T, Miyagishi M, Taira K, Akira S, Fujita T. The RNA helicase RIG-I has an essential function in double-stranded RNA-induced innate antiviral responses. Nat Immunol. 2004 Jul;5(7):730-7.

You S, Rice CM. 3' RNA elements in hepatitis C virus replication: kissing partners and long poly(U). J Virol. 2008 Jan;82(1):184-95.

You S, Stump DD, Branch AD, Rice CM. A cis-acting replication element in the sequence encoding the NS5B RNA-dependent RNA polymerase is required for hepatitis C virus RNA replication. J Virol. 2004 Feb;78(3):1352-66.

Yu C, Achazi K, Niedrig M. Tick-borne encephalitis virus triggers inositol-requiring enzyme 1 (IRE1) and transcription factor 6 (ATF6) pathways of unfolded protein response. Virus Res. 2013 Dec 26;178(2):471-7.

Yu H, Grassmann CW, Behrens SE. Sequence and structural elements at the 3' terminus of bovine viral diarrhea virus genomic RNA: functional role during RNA replication. J Virol. 1999 May;73(5):3638-48.

Yu H, Isken O, Grassmann CW, Behrens SE. A stem-loop motif formed by the immediate 5' terminus of the bovine viral diarrhea virus genome modulates translation as well as replication of the viral RNA. J Virol. 2000 Jul;74(13):5825-35.

Yu IM, Zhang W, Holdaway HA, Li L, Kostyuchenko VA, Chipman PR, Kuhn RJ, Rossmann MG, Chen J. Structure of the immature dengue virus at low pH primes proteolytic maturation. Science. 2008 Mar 28;319(5871):1834-7.

Zabolotskaya MV, Grima DP, Lin MD, Chou TB, Newbury SF. The 5'-3' exoribonuclease Pacman is required for normal male fertility and is dynamically localized in cytoplasmic particles in Drosophila testis cells. Biochem J. 2008 Dec 15;416(3):327-35.

Zenz R, Eferl R, Scheinecker C, Redlich K, Smolen J, Schonthaler HB, Kenner L, Tschachler E, Wagner EF. Activator protein 1 (Fos/Jun) functions in inflammatory bone and skin disease. Arthritis Res Ther. 2008;10(1):201.

Zhang K, Dion N, Fuchs B, Damron T, Gitelis S, Irwin R, O'Connor M, Schwartz H, Scully SP, Rock MG, Bolander ME, Sarkar G. The human homolog of yeast SEP1 is a novel candidate tumor suppressor gene in osteogenic sarcoma. Gene. 2002 Oct 2;298(2):121-7.

Zhang R, Jha BK, Ogden KM, Dong B, Zhao L, Elliott R, Patton JT, Silverman RH, Weiss SR. Homologous 2',5'-phosphodiesterases from disparate RNA viruses antagonize antiviral innate immunity. Proc Natl Acad Sci U S A. 2013 Aug 6;110(32):13114-9.

Zhang W, Chipman PR, Corver J, Johnson PR, Zhang Y, Mukhopadhyay S, Baker TS, Strauss JH, Rossmann MG, Kuhn RJ. Visualization of membrane protein domains by cryo-electron microscopy of dengue virus. Nat Struct Biol. 2003 Nov;10(11):907-12.

Zhou A, Paranjape JM, Hassel BA, Nie H, Shah S, Galinski B, Silverman RH. Impact of RNase L overexpression on viral and cellular growth and death. J Interferon Cytokine Res. 1998 Nov; 18(11):953-61.

Zhu H, Zhou HL, Hasman RA, Lou H. Hu proteins regulate polyadenylation by blocking sites containing U-rich sequences. J Biol Chem. 2007 Jan 26;282(4):2203-10.

Zust R, Cervantes-Barragan L, Habjan M, Maier R, Neuman BW, Ziebuhr J, Szretter KJ, Baker SC, Barchet W, Diamond MS, Siddell SG, Ludewig B, Thiel V. Ribose 2'-O-methylation provides a molecular signature for the distinction of self and non-self mRNA dependent on the RNA sensor Mda5. Nat Immunol. 2011 Feb;12(2):137-43.

APPENDICES

Appendix 1. List of abbreviations used.

AGO2	argonaute 2
ARE	AU-rich element
BDV	border disease virus
BVDV	bovine viral diarrhea virus
C	core or capsid protein
CDC	Centers for Disease Control
cHP	capsid hairpin
CNS	central nervous system
CSFV	classic swine fever virus
DENV	dengue virus
DENV-2	dengue virus type 2
DMEM	Dulbecco's modified Eagle's medium
dsRNA	double stranded RNA
E	envelope protein
eiF3	eukaryotic translation initiation factor 3
ER	endoplasmic reticulum
G	glycoprotein
GBV	G.B. viruses
GFP	green fluorescent protein
GO	gene ontology
HCC	hepatocellular carcinoma
HCV	hepatitis C virus
HIF1A	hypoxia inducible factor 1A
HIV-1	human immunodeficiency virus type 1
HVS	herpesvirus saimiri
IFIT	interferon induced proteins with tetratricopeptide repeats
IFN	interferon
IFNAR1	IFNα and IFNβ receptor complex 1
IL	interleukin
IRES	internal ribosome entry site
IRF	interferon response factor
ISG	interferon stimulated gene
JEV	japanese encephalitis virus
KUNV	Kunjin virus
MAVS	mitochondrial antiviral signaling
mCMV	murine cytomegalovirus
MDA5	melanoma differentiation antigen 5
MDBK	Madin-Darby bovine kidney
MEF	mouse embryonic fibroblasts
MEM	modified Eagle's medium
miR/miRNA	microRNA

mRNA	messenger RNA
MYD88	myeloid differentiation 88
NFκB	nuclear factor κ B
NLRP3	NOD, LRR and pyrin domain containing 3
NMD	nonsense-mediated decay
NS	nonstructural protein
OAS	oligoadenylate synthetase
ORF	open reading frame
PABP	poly(A) binding protein
PAGE	polyacrylamide gel electrophoresis
PAMP	pathogen associated molecular pattern
PAN	polyadenylated nuclear
PARN	poly(A) specific ribonuclease
P-body	processing body
PBS	phosphate buffered saline
PCBP2	poly(C) binding protein 2
PCR	polymerase chain reaction
PRR	pathogen recognition receptor
qPCR	quantitative polymerase chain reaction
RdRp	RNA-dependent RNA polymerase
RIG-I	official symbol: DDX58; retinoic acid-inducible gene 1
RISC	RNA induced silencing complex
RNAi	RNA interference
RNase L	ribonuclease L
RNP	ribonucleoprotein
RT	reverse transcription
SD	standard deviation
SEM	standard error of the mean
sfRNA	subgenomic flavivirus RNA
SG	stress granule
SINV	sindbis virus
siRNA	small-inderfering RNAs
SL	stem-loop
STAT	signal transducer and activator of transcription
TLR	Toll-like receptors
TNF	tumor necrosis factor
TRIF	TIR domain-containing adaptor inducing IFNβ
UTR	untranslated region
VEGF	vascular endothelial growth factor
VpG	viral protein, genome-linked
WNV	West Nile virus
XRN1	exoribonuclease 1
XRN2	exoribonuclease 2

YFV	yellow fever virus

Appendix 2. Conservation of the amino acid sequences of XRN1.

Amino acid sequences of XRN1 homologs in human, fruit fly, house mouse, mosquito, and two species of yeast were aligned using COBALT (Papadopoulos and Agarwala 2007). The full protein name, species, and NCBI or GenBank reference sequence are indicated below.

Name	Species	ID
5'-3' exoribonuclease 1 isoform a	*Homo sapiens*	NP_061874.3
pacman, isoform a	*Drosophila melanogaster*	AAF48958.1
5'-3' exoribonuclease 1	*Mus musculus*	NP_036046.2
5'-3' exoribonuclease 1	*Culex quinquefasciatus*	EDS29953.1
KLLA0F22385p	*Kluyveromyces lactis*	CAG98788.1
5'-3' exoribonuclease	*Saccharomyces cerevisiae*	AAA35219.1

COBALT alignment of XRN1 homolog amino acid sequences.

```
H. sap.  1     MGVPKFYRWISERYPCLSEVVKEHQIPEFDNLYLDMNGIIHQCSHPNDDDVHFRISDDKIFTDIFHYLEVLFRIIKPRKV  80
D. mel.  1     MGVPKFFRYISERYPCLSELAREHCIPEFDNLYLDMNGIVHNCSHPDDNNIHFHLEEEQIFQEIFNYVDKLFYLIKPQRL  80
M. mus.  1     MGVPKFYRWISERYPCLSEVVKEHQIPEFDNLYLDMNGIIHQCSHPNDDDVHFRISDDKIFTDIFHYLEVLFRIIKPRKV  80
C. qui.  1     MGVPKFFRYMSERYPCLGELVRENQVPDFDNLYLDMNGIIHNCSHPNDSDVFFRITEEQIFSDIFHYLEFLFRMIRPQKL  80
K. lac.  1     MGIPKFFHFISERWPQISQLIDGSQIPEFDNLYLDMNSILHNCTHGDGSEVNSRLSEEEVYSKIFSYIDHLFHTIKPKQT  80
S. cer.  1     MGIPKFFRYISERWPMILQLIEGTQIPEFDNLYLDMNSILHNCTHGNDDDVTKRLTEEEVFAKICTYIDHLFQTIKPKKI  80

H. sap.  81    FFMAVDGVAPRAKMNQQRGRRFRSAKEAEDKIKKAIEKGETLPTEARFDSNCITPGTEFMARLHEHLKYFVNMKISTDKS  160
D. mel.  81    FFLSVDGVAPRAKMNQQRSRRFRTAREAEQQEAKAAQRGELRE-HERFDSNCITPGTEFMVRLQEGLRAFLKTKISTDPL  159
M. mus.  81    FFMAVDGVAPRAKMNQQRGRRFRSAKEAEDKIKKAIEKGETLPTEARFDSNCITPGTEFMARLHEHLKYFVNMKISTDKS  160
C. qui.  81    FFIAVDGVAPRAKMNQQRGRRFRSAREAQEQVEQAEKKGDVLPLEARFDSNCITPGTSFMVRLQRALEHFIKVKVSTNPL  160
K. lac.  81    FYMAIDGVAPRAKMNQQRARRFRTAMDAEKALQKAIENGDELPKGEPFDSNAITPGTEFMAKLTENLKYFIHDKITNDTR  160
S. cer.  81    FYMAIDGVAPRAKMNQQRARRFRTAMDAEKALKKAIENGDEIPKGEPFDSNSITPGTEFMAKLTKNLQYFIHDKISNDSK  160

H. sap.  161   WQGVTIYFSGHETPGEGEHKIMEFIRSEKAKPDHDPNTRHCLYGLDADLIMLGLTSHEAHFSLLREEVRFgGKKTQRVCA  240
D. mel.  160   WQRCTVILSGQEAPGEGEHKIMDYIRYMKTQPDYDPNTRHCLYGLDADLIILGLCTHELHFVVLREEVKF-GRNVKRTS-  237
M. mus.  161   WQGVTIYFSGHETPGEGEHKIMEFIRSEKAKPDHDPNTRHCLYGLDADLIMLGLTSHEAHFSLLREEVRFgGKKTQRVCA  240
C. qui.  161   WKHCKVVLSGHETPGEGEHKIMEYIRHAKASPGFDSNTRHCLYGLDADLIMLGLCTHERHFSLLREEVKF-GKNDKKSSI  239
K. lac.  161   WQNVKVIFSGHEVPGEGEHKIMDYIRAIRAQEDYNPNTRHCIYGLDADLIILGLSTHDHHFCLLREEVTF-GKRSSSVKT  239
S. cer.  161   WREVQIIFSGHEVPGEGEHKIMNFIRHLKSQKDFNQNTRHCIYGLDADLIMLGLSTHGPHFALLREEVTF-GRRNSEKKS  239

H. sap.  241   PEETTFHLLHLSLMREYIDYEFSVLK-EKITFKYDIERIIDDWILMGFLVGNDFIPHLPHLHINHDALPLLYGTYVTILP  319
D. mel.  238   VEETRFFLLHLGLLREYLELEFDALRtDEHKLDIA--QLIDDWVLMGFLVGNDFIPHLPCLHISSNALPLLYRTYIGIYP  315
M. mus.  241   PEETTFHLLHLSLMREYIDYEFSALK-EKITFKYDIEKIIDDWILMGFLVGNDFIPHLPHLHINHDALPLLYGTYIAILP  319
C. qui.  240   VEETRFYLLHLTLLREYLELEFAPVR-DKLKFEFNPYKLIDDWVLMGYMVGNDFIPHLPNLHINENALPTLFQAYMDVLP  318
K. lac.  240   LETQNFFLLHLSILREYLALEFEEIT-DSVQFEYDFERVLDDFIFVLFTIGNDFLPNLPDLHLKKGAFPVLLQTFKEALQ  318
S. cer.  240   LEHQNFYLLHLSLLREYMELEFKEIA-DEMQFEYNFERILDDFILVMFVIGNDFLPNLPDLHLNKGAFPVLLQTFKEALL  318

H. sap.  320   ELGGYINESGHLNLPRFEKYLVKLSDFDREHFSEVFVDLKWFESKVG-NKYLNEAAGVAAEEARNYKEKKKLKGQE      394
D. mel.  316   TLGGNINENGKLNLRRLQIFISALTEVELDHFKEHADDLKYMN-----NK--SEAFDMDVGEITESQNLDSDLGAL      384
M. mus.  320   ELGGYINESGHLNLPRFERYLVKLSDFDREHFSEVFVDLKWFESKVG-NKYLNEAAGAAAEEAKNCKEKRKPKGQE      394
C. qui.  319   GLDGYINEGGILNLERLEVLMERLARFDRDIFLENYTDLQYFKAKRG--ANDTEAFDVTLEEIK--ADMDMDLSAL      390
K. lac.  319   HMDGYINEQGKINLARFSIWLKYLSDFEYLNFEKKDIDVEWFNQQLEnISLEGERKRTRMGKKLLMKQQKKLIGAV[51]  445
S. cer.  319   HTDGYINEHGKINLKRLGVWLNYLSQFELLNFEKDDIDVEWFNKQLEnISLEGERKRQRVGKKLLVKQQKKLIGSI[51]  445
```

Appendix 2. Continued.

```
H. sap.  395   NSLCWTAL    DKNEGEMITSKDNL    EDETEDDDLFETEFRQYKRTYYMTKMGVDVVSDDFLADQAACYVQAIQWI  466
D. mel.  385   INKSMLLY    DDDSE---------    EDCSDENAVLLKEFQNYKRNFYRNKFKR-DPNDELIEELCHHYVNALQWV  446
M. mus.  395   NSLSWAAL    DKSEGEGVASRDNF    EDETEDDDLFETEFRQYKRTYYMTKMGVDVVSDEFLANQAACYVQAIQWI  466
C. qui.  391   IKASEDMF    LDDDEDGGGERYST    EDIENDPELFEKEFAAYKRNYYMTKMGYGDFNEETRAEQAECYIRALQWT  462
K. lac.  446   HSKSKDLY[11]QETDEEHEARIHET[16]EELEEEREIYSERFVEWKDQYYKDKLDFSINDTDSLKEMTENYVGGLQWV  544
S. cer.  446   HSKSKGSY[11]DETEEEFQNRVNSI[16]EELETEKTIYNERFERWKHEYYHDKLKFTTDSEEKVRDLAKDYVEGLQWV  544

H. sap.  467   LHYYYHGVQSWSWYYPYHYAPFLSDIHNISTLKIHFELGKPFKPFEQLLAVLPAASKNLLPACYQHLMTNEDSPIIEYYP  546
D. mel.  447   LDYYYRGVQSWDWYYPFHYTPFISDLKNIEQVEIAFHMGTPFLPFQQLLAVLPAASAKLLPVAYHDLMLLPTSPLAEFYP  526
M. mus.  467   LHYYYHGVQSWSWYYPYHYAPFLSDIRSISTLKIHFELGKPFKPFEQLLAVLPSASKNLLPTCYQHLMTSEDSPIIEYYP  546
C. qui.  463   LLYYYRGVSSWAWYYPHHYAPFISDVQNFKNIKLNFEMGKPFLPFQQLLSVLPAASKDHLPTAYHKLMTDPDSSVIDYYP  542
K. lac.  545   LYYYYRGCPSWSWYYRYHYAPRISDVIKGIDQNIEFHKGQPFKPFQQLMAVLPERSKNLIPVVYRPLMYDEHSPILDFYP  624
S. cer.  545   LYYYYRGCPSWSWYYPHHYAPRISDLAKGLDQDIEFDLSKPFTPFQQLMAVLPERSKNLIPPAFRPLMYDEQSPIHDFYP  624

H. sap.  547   PDFKTDLNGKQQEWEAVVLIPFIDEKRLLEAMETCNHSLKKEERKRNQHSECLMCWYDRDTEFIYPSPWPEKFPAIER--  624
D. mel.  527   LEFESDLNGKKHDWEAVVLIPFIDEGRLLAAMLPCEAQLSLEERERNRHGPMYVYKYSTVAQGPMPAYPPLRALPVLY--  604
M. mus.  547   PDFKTDLNGKQQEWEAVVLIPFIDETRLLEAMETCNHSLKKEERKRNQHSECLMCWYDRDTEFTYSSPWPEKFPAIER--  624
C. qui.  543   ENFGTDLNGKQQAWEAVVLIPFIDEKRLLKAMEPCDAFLTDEEKQRNVHGPMMLFQYDEQGSAFLGANYGLDDVAELK--  620
K. lac.  625   NEVELDLNGKTADWEAVVKISFVDQKRLVEAMAPYDAKLSPDEKKRNSFGTDLIFIFNPQVDTVYKTPLAGLFNDIEHnh  704
S. cer.  625   AEVQLDKNGKTADWEAVVLISFVDEKRLIEAMQPYLRKLSPEEKTRNQFGKDLIYSFNPQVDNLYKSPLGGIFSDIEHnh  704

H. sap.  625   -CCTRYKIISLDAWRVDINKNKITRIDQKAL----YFCGFPTLKHIRHKFFLKKSGVQVFQQSSRGENMMLEILVDAESD  699
D. mel.  605   -C----TEVAKWSHEIAVNLPYSVCIELPNAArtvFFPGFPTMQHLPFDFELRNDRVKVFEQVSRNQNIVLKP--RKRQL  677
M. mus.  625   -CCTRYKMISLDAWRVDINKNKITRVDQKAL----YFCGFPTLKHIKHKFFLKKSGVQVFQQSSRGENLMLEISVNAEPD  699
C. qui.  621   -----VKEIPIYRDDLYVPENKLVLGPSKGAIldgYIKGFPTMKHLKYHGILKEIRVKVFNFPSRNASMVVAI--DKEGD  693
K. lac.  705   cIEREFIPESMENVKFLFGLPKGAKLGASSLA------GFPSLKTLPLTAELAYNSSVVFNFPSKQQSMVLHIQDLYKEN  778
S. cer.  705   cVEKEYITIPLDSSEIRYGLLPNAKLGAEMLA------GFPTLLSLPFTSSLEYNETMVFQQPSKQQSMVLQITDIYKTN  778

H. sap.  700   ELTVENVASSVLGKSVFVNWPHLEEARVVAVSDGETKFYLEEPpGTQKLYSGRTAPPSKVVHLGDKEQSNWAKeVQGISE  779
D. mel.  678   EDTLTAVASQYLGKVIHVGWPHLVKAIVVRVATRDQRV------------------DSEGITLNDSRRFDSEC--KALQE  737
M. mus.  700   ELRIENIASAVLGKAVFVNWPHLEEARVVAVSDGETKFYIEEPpGTQKVYLGKTAPPSKVIQLTDKEQSNWTKeIQGISE  779
C. qui.  694   DKSTAQLAQELLGSIVYVSWPHLTEAKVVKVADAKTVYEKDRE------------------ERPNNEKFFGTC-VKAIVE  754
K. lac.  779   GISLSDLAKRHMGKIVYSRWPFLRESKLLSLITEETVYEGVKS-GKLTKV--IERKPQDF----ERKEFRELK--MTLKS  849
S. cer.  779   NVTLEDFSKRHLNKVIYTRWPYLRESKLVSLTDGKTIYEYQES-NDKKKFGFITKPAETQ----DKKLFNSLK--NSMLR  851

H. sap.  780   HYLRRKGIIINETSAVVYAQLLTGRKYQINQNGEVRLEKQWSKQVVPFVYQTIVKDIRAFDSRFSNIKTL--DDLFPLRS  857
D. mel.  738   HFINRMGIQFANYDVLVYVRTFAGNSTEFRDKGALMVRDSWSSSVTGYPAQGVVADLTVWERMRKNFLNV--EHYFPVGS  815
M. mus.  780   QYLRRKGIIINETSAVVYAQLLTGRKYQISQNGEVRLEKQWSKQILPFVYQTIVKDIRAFDSRFSNIKTL--DDLFPPRT  857
C. qui.  755   HHSNRLAIDLGEIRQLVHVKTCVGSEY-VLKDDRYVLNKLWNQGETMYPVQAIVTDLREALRTLKPYQEV--QEMFPENC  831
K. lac.  850   NYQRTKAILLDDISALAKVVPVNG----LVRNSDGSYSKSFNETIEYYPLQLIVEDVKNKDERYIEKEPLpiNKEFPKGS  925
S. cer.  852   MYAKQKAVKIGPMEAIATVFPVTG----LVRDSDGGYIKTFSPTPDYYPLQLVVESVVNEDERYKERGPIpiEEEFPLNS  927

H. sap.  858   MVFMLGTPYYGCTGEVQDSGDVITEGRIRVIF---SIPCEPNLDALIQNQHKYSIKYNPGYVLASRLGVSGYLVSRFTGS  934
D. mel.  816   TIFLITDPYYGSEGTVQDPRLAYTNGRIQVSI---MVRPEPKVNAARQLQEERDRDYLSTFQVCNLLRISGRTLGRLSGT  892
M. mus.  858   MVFMLGTPYYGCTGEVQDSGDLITEGRIRVVF---SIPCEPNLDALIQNQHKYSIKYNPGYVLAGRLGVSGYLVSRFTGS  934
C. qui.  832   VVFLRATQWYGSMGHVVDVT--AGHKRIKTRFE---IYEEPNLDTVLKIDDEARSHYLTTYDAASSIGISANLLSRLSST  906
K. lac.  926   KVVFLGDYAYGGEATVDGYN---SETRLKLTVKkgSLRAEPNIGKVRAKLDSQALRFYPTQVFSKIARVHPLFLSKITSR  1002
S. cer.  928   KVIFLGDYAYGGETTIDGYS---SDRRLKITVEkkFLDSEPTIGKERLQMDHQAVKYYPSYIVSKNMHLHPLFLSKITSK  1004

H. sap.  935   IFIGRGSRRNPHGDH--KANVGLNLKFNKKNEEVPGYTKKVGSEWMYSSAAEQLLAEYLERAPELFSYIAKNSQE-DVFY  1011
D. mel.  893   VWVVLGPRRQ-KMENvtKHNIGLQLKYPRQNEERAGYCFRTNNQWYYSSLAVDLMRNYCQRYPDVIDFFGDSNDRaEFVF  971
M. mus.  935   IFIGRGSRRNPHGDH--KANVGLNLKFNKKNEEVPGYTKKVGNEWMYSSAAEQLLAEYIERAPELFSYIAKNSQE-DVFY  1011
C. qui.  907   IYMVTGGRRSLNVDEkgKMNIGLQLRLVSQDIETVGYTRKMAKNWMYSDKAIELVKAYYDKVPQVFEKLESFGNR-DVLF  985
K. lac.  1003  YLVNDSKKKS--------HNVGLMIKFKARNQKVLGYARCSSNKWEYSDVALGLLEQFRSTFPEFFAKLSNSKEQ-AIPS  1073
S. cer.  1005  FMITDATGKH--------INVGIPVKFEARHQKVLGYARRNPRGWEYSNLTLNLLKEYRQTFPDFFFRLSKVGND--IPV  1074

H. sap.  1012  EDDIWP---GENENGAEKVQEIITWLKGHPVSTLSRSSCDLQILDAAIVEKIEEEVEKCKQRKNNKKVRVTVK-PHLLYR  1087
D. mel.  972   EQDVFPNAvGHRRVE-----ELANWVRQQPHMKVERISCGSKTVCRETIELLIAA-VDDLRSLPVKHVKLQVK-PHLLIK  1044
M. mus.  1012  EDDIWP---GENENGAEKVQEIITWLKGHPVSTLSRSSCDLHILDAAIVEKIEEEVEKCKQRKSNKKVRVTVK-PHLLYR  1087
C. qui.  986   EDEIFGEK----REEGSGLKELVAWIKAQDHAKAEKRSCGTKILEPAAVEELVKIRAESVRQLPTMQT-MFVH-PKDLYK  1059
K. lac.  1074  ITDLFPNK--SSAEADSILKTVADWLS-EARKPFVVVSLESDSLTKASMAAVESEIIKYVSLPDSSEQKKLAKvPREAIL  1150
S. cer.  1075  LEDLFPDT--STKDAMNLLDGIKQWLK-YVSSKFIAVSLESDSLTKTSIAAVEDHIMKYAANIEGHERKQLAKvPREAVL  1151

H. sap.  1088  PLEQQHGVIpDRDAEFCLFDRVVNVRENFSVPVGLRGTIIGIKGAN    READVLFEVLFDEEFPGGLTIRCSPG---R  1160
D. mel.  1045  PNVTLPDVY-RSKRPVRLFDRVVIVRTIYMVPVGTKGTVIGIHPVT[10]HAVDTFCKVLFDSPVPNCNNIHGIAE--DR  1127
M. mus.  1088  PLEQQHGVIpDRDAEFRLFDRVVNVRESFSVPVGLRGTVIGIKGAS    READVLFEVLFDEEFPGGLTIRCSPG---R  1160
C. qui.  1060  PGMKQARSI-DYMANYELLDRVIIARETEVVPLGYRGTIIGIHLAK[10]SKEDKYFDILFDKQFPNGTHIFGIEQTrNR  1144
K. lac.  1151  NAESSYVLL--RSQRFHLGDRVMYIQDSGKVPLHSKGTVVGYTSIG    --KNVSIQVLFDNEIIAGNNFGGRLQT-RR  1221
S. cer.  1152  NPRSSFALL--RSQKFDLGDRVVYIQDSGKVPIFSKGTVVGYTTLS    --SSLSIQVLFDHEIVAGNNFGGRLRT-NR  1222
```

Appendix 2. Continued.

```
H. sap.  1161  GYRLPTSALVNLSHGSRSETGNQKLTAIVKPQPAVHQhSSSSSVSSGHLGALNHSPQSLfVPTQVPTKDDDEFCNIWQSL  1240
D. mel.  1128  VYKVPEIALVIIKTDEEGKKQNDCELPVRDPQPNQAQdEPVRATSSRYVTAAGSTSV----PITMKTQISDEFVKTR-S-  1201
M. mus.  1161  GYRLPTSALVNLSHGSRCETGNQKLTAIVKPQPSV---SHCSAAPSGHLGGLNHSPQSPfLPTQVPTKGDDEFCNIWQSL  1237
C. qui.  1145  VVRVAEGAILNISFGVADFEYKQ----VDPAQPIMLP-------AEEFCPGGLASKQ----PSTVRSV---ETIRVKPS-  1205
K. lac.  1222  GLGLDSSFLLNLSDRQL----------------------------------VYHSKASK-SADKKPKAVPNDKQVAL---  1263
S. cer.  1223  GLGLDASFLLNITNRQF----------------------------------IYHSKASK-KALEKKKQSNNRNNNTKTAH  1267

H. sap.  1241  QGSGKMQYFQPTIQEKGAVLPQEISQVNQHHKSGFNDNSVKYQQRKHDPHRKFKEECKSPKAECWS-QKMSNKQ------  1313
D. mel.  1202  DPIARTDSYKPSSEPKPVPVPEQITNWRERVSTPTN-KPQPAPNNWRINRSSSRQQGGSIF------VAPPTKTPDAAAS  1274
M. mus.  1238  QGAGKIQHLQPTVQEKGAVLPQEISQVTEGHKSGFTDHSVRHQQRKHDSQRKFKEEYKSPKAECQS-QKLSSKQTSGGSA  1316
C. qui.  1206  KPTAKSESIKKRLNERIEKNPNPMKAFVMANRKPLEENGA-------------NSQAGCDFEKVWNkLREPNQTTTTTLD  1272
K. lac.  1264  ---AKKKRVEELKKKQAHELLNHIKKDNAESNTES-----------------------------------------GSAP  1299
S. cer.  1268  KTPSKQQSEEKLRKERAHDLLNFIKKDTNEKNSESVD---------------NKSMGSQKDSKPAkKVLLKRPAQKSSE  1331

H. sap.  1314  -------------------------------PNSGIENFLASLNISKENEVQSSHHGEPPSEEHL-SPQSFAM-GTRmlK  1360
D. mel.  1275  TASTAFTAASSATLTPLDQTLALM-SVLGVGEDQSSPPLQEAVQQQRPPLLQQQRAPFPGQMPNLPKPPLFWQ------Q  1347
M. mus.  1317  RCSIKLLKRNESPGTSEAQKVVTSyPNAVHKPPSGIENFLASLNLSKENEAQLPHHGEPPDEADL-SPQSFAMkGTRmlK  1395
C. qui.  1273  ERDIKSFLANAAPAAQESAPVPTN-PLAPSSDPTDMLKKMLKISADQEPAVQTPPQLNIPMPKNLPKPPSSWRsDHK---  1348
K. lac.  1300  QIAVNTLN--------PSAANNVF------------------------NAVLNQIKPG--SQQQIQPPP-----------  1334
S. cer.  1332  NVQVDLANFEKAPLDNPTVAGSIF------------------------NAVANQYSDGIGSNLNIPTPPHPMN-------  1380

H. sap.  1361  EILKIDGSNTVDHKNEIKQIANEIPVSSNRRDEYGLPSQPKQNKKLASYMNKP----HSANEYHNVQSMDNMCWPAPSQI  1436
D. mel.  1348  EAQKQEALQQEAQQQEAQKKQQQAHAQME--PERINSQHFYRSGQTGAALNQPplgAPSKRQWHE--------WVHPRMQ  1417
M. mus.  1396  EILKIDSPDTRDSKNDMKKSDNEATVSS-RRDERGVSAHPKPSKKLTCHMNKP----HGTNEFQNVASVDSVCWPG--QM  1468
C. qui.  1349  -----SAKDTVKQQHPADKPQQKQNHQMPMPPQPFAQFQPYQLAHQQNRYQPPp-gQFLPNQYQ----------PMPRYQ  1412
K. lac.  1335  ------------------------------------------------------ANS-----LPYNFTVPPHMV-  1349
S. cer.  1381  ------------------------------------------------VVGGP---IPGANDVADVGLPYN--IPPGFMT  1407

H. sap.  1437  PPVSTP[13]PQPDFSFLRMPQTMTVCQVKLSNGLLVHGPQCHS   ENE--AKEKAALFALQQLGSLGMNFPLPSQVFA  1520
D. mel.  1418  HANAFH    AGVNNGYQMRPKKNIAAQSTFNNNVHMHLQQPYY   PNQqqQQQQQQPLQLTEINNAPPRYSTIQD---  1487
M. mus.  1469  PPVSTP[13]PQPDFSFLRTTQTMTVCQVKLSNGLLVHGPQCHS   ESE--AKERAALFALQQLGSLGVSFPLPPPIFT  1552
C. qui.  1413  PQMPMP    PQKNNNHSAYQQF---------NQHHQQLQQQLY[7]NGPqnNNNNNQHHLRQRGPNGPQNLSFNRNTPA  1483
K. lac.  1350  -PGGIP    ----------------------HPLMMQ-PPFIP   NNE------------------HIAYAAPPQ---  1377
S. cer.  1408  HPNGL-    ----------------------HPLHPH-QMPYP   NMN------------------GMSIPPPAPHGF  1438

H. sap.  1521  NYPSAVPPGTIPPAFPPPTG[6]NYA[10]SHLFGSMPWGPSVPVPGKPFHHTLYSGTMP[16]QVTKKRVANKKNFENK  1621
D. mel.  1488  ----FVPIQAYRPKKL----   NRV    -----QPAGRQDVDAT----KNPSRSPVLQ    QPTNETIDTKAS----  1535
M. mus.  1553  NYPPAVPPGAVPPVFTQPT-   ---[ 7]SHLFGSVSWRPPVPVAGNAFHYPSYPGTMP[16]QVTKKRVANRKNFENK  1640
C. qui.  1484  GTGAFVPLQAIIKSKTRPNG[2]NKS    -----NKAGSSNANSTGFAQKNAELRQKVE    QKQQENKQDFASFLGG  1549
K. lac.  1378  SQPVQNPP-------LDKEA   SRN[ 1]KNLLIRDENGRTANVE--------------    ---NKDSDDTKRSSHS  1423
S. cer.  1439  GQPISFPP-------PPPMT   N--    ----VSDQGSRIV-VN--------------    ---EKESQDLKKFING  1476

H. sap.  1622  EAQSSQATPVQTSQPDSSNIVKVSPRESSSASLKSSPIAQPASS[4]TASQGHSISHHKSTPiSSSRRKSRKLAVNFGVS  1702
D. mel.  1536  SSLPVQSAGEQVIGLMQTLEIKPAASQSESDGVSTGSANAPTAT   TSSQAVNRRKHRVPRiGAKFDLEYILPDSPHPT  1612
M. mus.  1641  EAQSSQATPLQTNKPGSSEATKMTPQESPPASSSSSQAAQPVSS[3]TASQGHVGSQPRSAP-SSSKRKSRKLAVNFSVS  1719
C. qui.  1550  AGKSVEAAAAAVVTTADEKCDKPERKKDDG-----GDGVQKTAS   TSPK---------PP----KVRQMRIAANFSQA  1608
K. lac.  1424  RGGRRGRSNRGRGASGRGGHFKNSP--------------------   ------------------KKTET----------  1453
S. cer.  1477  KQHSNGSTIGGETKNSRKGEIKPSSGTNSTECQSPKSQSNAADR   ----------------DNKKDEST---------  1528

H. sap.  1703  Kpse  1706
D. mel.        ----
M. mus.  1720  Kpse  1723
C. qui.  1609  D---  1609
K. lac.        ----
S. cer.        ----
```

Appendix 3. Fold change in RNA abundances in 293T cells infected with SINV, the sfRNA(-) KUNV, or the wild-type KUNV as determined by RNA-seq analysis.

Gene symbol, GenBank ID numbers, and fold-change in RNA abundance are indicated below.

Appendix 3A. The twenty most elevated transcripts in wild-type KUNV infected 293T cells compared to 293T cells infected with the sfRNA(-) KUNV.

Transcripts elevated in wild-type KUNV infected 293T cells relative to sfRNA(-) KUNV infected 293T cells		
Gene symbol	**ID**	**Fold change**
SPSB2	NM_032641	11.94
RIC3	NR_045405	10.61
SPATA25	NM_080608	10.61
TPPP3	NM_016140	9.29
PLIN5	NM_001013706	7.96
UCP3	NM_003356	7.30
NCAM2	NM_004540	6.63
C2orf81	NM_001145054	6.63
FILIP1L	NM_001042459	6.34
GRIP2	NM_001080423	6.19
FXYD6-FXYD2	NM_001204268	5.97
ADSSL1	NM_199165	5.31
CRLF1	NM_004750	5.31
TRIM7	NM_203297	5.31
FGF5	NM_004464	5.31
OLFM2	NM_058164	4.64
VWCE	NM_152718	4.64
SYTL5	NM_001163335	4.64
FOXB1	NM_012182	4.64
DENND2A	NM_015689	4.42

Appendix 3. Continued.

Appendix 3B. The twenty most reduced transcripts in wild-type KUNV infected 293T cells compared to 293T cells infected with the sfRNA(-) KUNV.

Transcripts reduced in wild-type KUNV infected 293T cells relative to sfRNA(-) KUNV infected 293T cells		
Gene symbol	**ID**	**Fold change**
SLC2A3	NM_006931	-12.81
FILIP1	NM_015687	-8.29
RBM24	NM_001143942	-6.03
TGFB2	NM_001135599	-6.03
PTGES	NM_004878	-5.28
ACOT11	NM_147161	-4.90
GPRC5C	NM_022036	-4.52
C10orf55	NM_001001791	-4.52
SPATA24	NM_194296	-4.52
DENND1C	NM_024898	-4.52
CEBPD	NM_005195	-4.52
FRMPD1	NM_014907	-4.15
HTR6	NM_000871	-3.77
TOX3	NM_001146188	-3.77
XKRX	NM_212559	-3.77
RBFOX3	NM_001082575	-3.77
SNCG	NM_003087	-3.77
LPPR4	NM_014839	-3.77
FAM150A	NM_207413	-3.77
ICA1	NM_004968	-3.58

Appendix 3. Continued.

Appendix 3C. The twenty most elevated transcripts in wild-type KUNV infected 293T cells relative to mock infected cells.

Transcripts elevated in wild-type KUNV infected 293T cells relative to mock infected 293T cells		
Gene symbol	**ID**	**Fold change**
IFIT2	NM_001547	54.59
FILIP1L	NM_001042459	39.13
ATF3	NM_001040619	22.02
FUT1	NM_000148	18.20
TAC1	NM_003182	15.47
OAZ3	NM_016178	13.65
SH2D3C	NM_170600	12.74
C1QTNF3	NM_181435	11.83
ANKRD1	NM_014391	11.28
SPAG4	NM_003116	10.01
PCDP1	NR_073132	10.01
TRPM6	NM_017662	9.10
DUSP8	NM_004420	7.73
CHAC1	NM_024111	7.73
HSPB8	NM_014365	7.28
IKZF2	NM_001079526	7.28
SPATA25	NM_080608	7.28
NUDT13	NM_015901	6.73
FBXL13	NM_145032	6.55
RASGRP1	NM_005739	6.37

Appendix 3. Continued.

Appendix 3D. The twenty most down-regulated transcripts in wild-type KUNV infected 293T cells relative to mock infected cells.

Transcripts reduced in wild-type KUNV infected 293T cells relative to mock infected 293T cells		
Gene symbol	**ID**	**Fold change**
UNC5A	NM_133369	-8.79
GPRC5C	NM_022036	-7.14
SLC2A3	NM_006931	-6.59
FAM43B	NM_207334	-6.59
PSD4	NM_012455	-6.04
KIAA1984	NM_001039374	-5.50
SPATA24	NM_194296	-5.50
CYP27A1	NM_000784	-5.50
S1PR1	NM_001400	-4.95
CEBPD	NM_005195	-4.95
C17orf67	NM_001085430	-4.95
JAKMIP1	NM_001099433	-4.67
FILIP1	NM_015687	-4.40
CSPG4	NM_001897	-4.40
ACOT11	NM_147161	-4.40
NECAB2	NM_019065	-4.40
FAM131C	NM_182623	-4.40
RASGEF1C	NM_175062	-4.40
RBFOX3	NM_001082575	-4.40
C8orf73	NM_001100878	-4.40

Appendix 3. Continued.

Appendix 3E. The twenty most up-regulated transcripts in sfRNA(-) KUNV infected 293T cells relative to mock infected cells.

Transcripts elevated in sfRNA(-) KUNV infected 293T cells relative to mock infected 293T cells		
Gene symbol	**ID**	**Fold change**
IFIT2	NM_001547	17.83
FUT1	NM_000148	11.66
ATF3	NM_001040619	11.08
TRPM6	NM_017662	10.97
C11orf96	NM_001145033	8.92
CD207	NM_015717	8.23
TAC1	NM_003182	8.23
PPAPDC1B	NM_001102559	7.37
ANKRD1	NM_014391	6.72
FILIP1L	NM_001042459	6.17
SH2D3C	NM_170600	6.17
SPAG4	NM_003116	6.17
AKNA	NM_030767	5.90
CHAC1	NM_024111	5.83
HSPB8	NM_014365	5.83
NUDT13	NM_015901	5.76
SNAP91	NM_001256717	5.49
OAZ3	NM_016178	5.49
ADM2	NM_024866	5.21
PTGES	NM_004878	4.80

Appendix 3. Continued.

Appendix 3F. The twenty most down-regulated transcripts in sfRNA(-) KUNV infected 293T cells relative to mock infected cells.

Transcripts reduced in sfRNA(-) KUNV infected 293T cells relative to mock infected 293T cells		
Gene symbol	**ID**	**Fold change**
C2orf81	NM_001145054	-10.21
CEL	NM_001807	-10.21
UCP3	NM_003356	-8.02
RPRML	NM_203400	-7.29
SPSB2	NM_032641	-7.29
S1PR1	NM_001400	-6.56
DMRT3	NM_021240	-6.32
VWCE	NM_152718	-5.83
CRLF1	NM_004750	-5.83
NPIPL3	NM_130464	-5.83
UNC5A	NM_133369	-5.83
PSD4	NM_012455	-5.35
ADSSL1	NM_199165	-5.10
NKX1-2	NM_001146340	-5.10
GTF2IRD2B	NM_001003795	-5.10
CTXN1	NM_206833	-5.00
KIAA1984	NM_001039374	-4.86
SEPT1	NM_052838	-4.86
RCN3	NM_020650	-4.62
MMEL1	NM_033467	-4.62

Appendix 3. Continued.

Appendix 3G. The twenty most up-regulated transcripts in SINV infected 293T cells relative to mock infected cells.

Transcripts elevated in SINV infected 293T cells relative to mock infected 293T cells		
Gene symbol	**ID**	**Fold change**
TRPM6	NM_017662	11.8
TAS2R20	NM_176889	10.3
C1QTNF3	NM_181435	7.4
FCGR2A	NM_001136219	7.4
C10orf111	NM_153244	5.9
SPAG4	NM_003116	5.9
NUPR1	NM_001042483	5.9
C11orf96	NM_001145033	5.9
HIST1H4B	NM_003544	4.4
EGFLAM	NM_001205301	4.4
OAZ3	NM_016178	4.4
COL23A1	NM_173465	4.4
PRSS27	NM_031948	4.4
SNAP91	NM_001256717	4.4
SMAGP	NM_001031628	4.0
C17orf108	NM_001076680	3.9
MTMR8	NM_017677	3.8
HEATR7A	NM_032450	3.8
CDA	NM_001785	3.7
ANP32D	NM_012404	3.7

Appendix 3. Continued.

Appendix 3H. The twenty most down-regulated transcripts in SINV infected 293T cells relative to mock infected cells.

Transcripts reduced in SINV infected 293T cells relative to mock infected 293T cells		
Gene symbol	**ID**	**Fold change**
RGS20	NM_170587	-8.8
OLFML2B	NM_015441	-6.1
C17orf67	NM_001085430	-6.1
HOMER3	NR_027297	-5.4
ZNF222	NM_001129996	-5.4
TTC39B	NM_152574	-5.4
HOPX	NM_001145460	-5.4
DMRTA2	NM_032110	-4.8
NKX1-2	NM_001146340	-4.8
GAL3ST1	NM_004861	-4.8
SUSD4	NM_017982	-4.8
ALOXE3	NM_001165960	-4.8
PAX7	NM_001135254	-4.8
DENND6B	NM_001001794	-4.8
IL6R	NM_000565	-4.4
MYLK2	NM_033118	-4.1
PLAC8L1	NM_001029869	-4.1
UBE2QL1	NM_001145161	-4.1
KCNK5	NM_003740	-3.9
DDIT3	NM_001195056	-3.8

Appendix 4. Functional annotation of stabilized RNAs in wild-type KUNV infections compared to sfRNA(-) KUNV infections.

Significantly enriched ($p \leq 0.001$) annotated functions of transcripts that were 2-fold or more increased in stability in KUNV infected cells relative to sfRNA(-) KUNV infected cells by RNA-seq were determined using the DAVID GOTERM_BP_FAT tool (Huang et al. 2009(a), Huang et al. 2009(b)) and are listed below from most to least significant.

Term	p-value
RNA processing	5.90E-15
RNA splicing	6.30E-14
ubiquitin-dependent protein catabolic process	1.60E-11
mRNA processing	1.70E-11
mRNA metabolic process	1.20E-10
mitotic cell cycle	1.20E-10
cell cycle	1.90E-10
cellular macromolecule catabolic process	3.50E-09
cell cycle process	6.10E-09
macromolecule catabolic process	1.00E-08
ncRNA metabolic process	2.20E-08
protein catabolic process	5.80E-08
proteolysis involved in cellular protein catabolic process	1.10E-07
ribonucleoprotein complex biogenesis	1.30E-07
cellular protein catabolic process	1.40E-07
anaphase-promoting complex-dependent proteasomal ubiquitin-dependent protein catabolic process	1.50E-07
modification-dependent protein catabolic process	1.80E-07
modification-dependent macromolecule catabolic process	1.80E-07
regulation of ubiquitin-protein ligase activity during mitotic cell cycle	4.80E-07
macromolecular complex subunit organization	7.40E-07
negative regulation of ubiquitin-protein ligase activity during mitotic cell cycle	1.00E-06
microtubule cytoskeleton organization	1.00E-06
macromolecular complex assembly	1.10E-06
negative regulation of ubiquitin-protein ligase activity	1.50E-06
negative regulation of ligase activity	1.50E-06
regulation of ubiquitin-protein ligase activity	1.60E-06
proteasomal protein catabolic process	1.90E-06
proteasomal ubiquitin-dependent protein catabolic process	1.90E-06
cell cycle phase	2.10E-06
regulation of ligase activity	2.50E-06
organelle fission	3.10E-06
response to DNA damage stimulus	3.60E-06
negative regulation of protein ubiquitination	4.80E-06
M phase	4.90E-06
mitosis	5.00E-06
nuclear division	5.00E-06
M phase of mitotic cell cycle	6.80E-06
regulation of protein ubiquitination	6.90E-06
nuclear mRNA splicing, via spliceosome	7.60E-06

RNA splicing, via transesterification reactions	7.60E-06
RNA splicing, via transesterification reactions with bulged adenosine as nucleophile	7.60E-06
cellular macromolecular complex subunit organization	9.80E-06
positive regulation of ubiquitin-protein ligase activity during mitotic cell cycle	1.10E-05
tRNA metabolic process	1.30E-05
chromosome segregation	1.30E-05
chromosome organization	1.40E-05
positive regulation of ubiquitin-protein ligase activity	1.40E-05
protein complex assembly	1.50E-05
protein complex biogenesis	1.50E-05
cellular macromolecular complex assembly	1.80E-05
regulation of cellular protein metabolic process	1.90E-05
positive regulation of protein ubiquitination	2.00E-05
positive regulation of ligase activity	2.20E-05
cell division	3.40E-05
microtubule-based process	5.20E-05
ribosome biogenesis	7.60E-05
DNA metabolic process	8.00E-05
protein localization	1.00E-04
ncRNA processing	1.30E-04
negative regulation of protein modification process	2.10E-04
negative regulation of cellular protein metabolic process	2.30E-04
RNA biosynthetic process	2.30E-04
ribonucleoprotein complex assembly	3.10E-04
rRNA metabolic process	3.40E-04
protein transport	3.50E-04
tRNA aminoacylation for protein translation	3.50E-04
amino acid activation	3.50E-04
tRNA aminoacylation	3.50E-04
negative regulation of protein metabolic process	3.70E-04
RNA transport	3.70E-04
establishment of RNA localization	3.70E-04
nucleic acid transport	3.70E-04
cytoskeleton organization	4.30E-04
establishment of protein localization	4.40E-04
transcription, DNA-dependent	4.60E-04
RNA localization	4.90E-04
protein folding	5.40E-04
translation	5.40E-04
cellular response to stress	7.40E-04
DNA repair	7.40E-04
positive regulation of cellular protein metabolic process	7.80E-04
rRNA processing	8.60E-04
regulation of translational initiation	9.20E-04
positive regulation of protein modification process	1.00E-03

Appendix 5. Nucleotide sequences of the 3' UTRs of sfRNA-deficient Kunjin viruses.

Below is a ClustalOmega sequencing alignment of the 3' UTRs of sequenced Kunjin virus mutants generated to assess the importance of the three-helix junction in the sfRNA in XRN1 resistance (related to Figure 29). Mutated nucleotides are in red. Abbreviations: FLSDX = wild-type Kunjin virus; all other names indicate mutated nucleotides and the position in the full-length KUNV genome.

```
FLSDX              ATAGTGTTTAGTGTGTTTAGAGTTAGAAAAATTTTAGTGAGGAAGTCAGGCCGGAAAATT
UCA10498_ACA10658  ATAGTGTTTAGTGTGTTTAGAGTTAGAAAAATTTTAGTGAGGATCACAGGCCGGAAAATT
ACA10658           ATAGTGTTTAGTGTGTTTAGAGTTAGAAAAATTTTAGTGAGGAAGTCAGGCCGGAAAATT
UCA10498           ATAGTGTTTAGTGTGTTTAGAGTTAGAAAAATTTTAGTGAGGATCACAGGCCGGAAAATT
G10519_G10680      ATAGTGTTTAGTGTGTTTAGAGTTAGAAAAATTTTAGTGAGGAAGTCAGGCCGGAAAATT
G10680             ATAGTGTTTAGTGTGTTTAGAGTTAGAAAAATTTTAGTGAGGAAGTCAGGCCGGAAAATT
G10519             ATAGTGTTTAGTGTGTTTAGAGTTAGAAAAATTTTAGTGAGGAAGTCAGGCCGGAAAATT
                   ******************************************: :**************
FLSDX              CCCGCCACCGGAAGTTGAGTAGACGGTGCTGCCTGCGACTCAACCCCAGGAGGACTGGGT
UCA10498_ACA10658  CCCGCCACCGGAAGTTGAGTAGACGGTGCTGCCTGCGACTCAACCCCAGGAGGACTGGGT
ACA10658           CCCGCCACCGGAAGTTGAGTAGACGGTGCTGCCTGCGACTCAACCCCAGGAGGACTGGGT
UCA10498           CCCGCCACCGGAAGTTGAGTAGACGGTGCTGCCTGCGACTCAACCCCAGGAGGACTGGGT
G10519_G10680      CCCGGCACCGGAAGTTGAGTAGACGGTGCTGCCTGCGACTCAACCCCAGGAGGACTGGGT
G10680             CCCGCCACCGGAAGTTGAGTAGACGGTGCTGCCTGCGACTCAACCCCAGGAGGACTGGGT
G10519             CCCGGCACCGGAAGTTGAGTAGACGGTGCTGCCTGCGACTCAACCCCAGGAGGACTGGGT
                   **** **************************************************
FLSDX              GAACAAAGCTGCGAAGTGATCCATGTAAGCCCTCAGAACCGTCTCGGAAAGAGGACCCCA
UCA10498_ACA10658  GAACAAAGCTGCGAAGTGATCCATGTAAGCCCTCAGAACCGTCTCGGAAAGAGGACCCCA
ACA10658           GAACAAAGCTGCGAAGTGATCCATGTAAGCCCTCAGAACCGTCTCGGAAAGAGGACCCCA
UCA10498           GAACAAAGCTGCGAAGTGATCCATGTAAGCCCTCAGAACCGTCTCGGAAAGAGGACCCCA
G10519_G10680      GAACAAAGCTGCGAAGTGATCCATGTAAGCCCTCAGAACCGTCTCGGAAAGAGGACCCCA
G10680             GAACAAAGCTGCGAAGTGATCCATGTAAGCCCTCAGAACCGTCTCGGAAAGAGGACCCCA
G10519             GAACAAAGCTGCGAAGTGATCCATGTAAGCCCTCAGAACCGTCTCGGAAAGAGGACCCCA
                   ************************************************************
FLSDX              CATGTTGTAGCTTCAAGGCCCAATGTCAGACCACGCCATGGCGTGCCACTCTGCGGAGAG
UCA10498_ACA10658  CATGTTGTAGCTTCAAGGCCCAAACACAGACCACGCCATGGCGTGCCACTCTGCGGAGAG
ACA10658           CATGTTGTAGCTTCAAGGCCCAAACACAGACCACGCCATGGCGTGCCACTCTGCGGAGAG
UCA10498           CATGTTGTAGCTTCAAGGCCCAATGTCAGACCACGCCATGGCGTGCCACTCTGCGGAGAG
G10519_G10680      CATGTTGTAGCTTCAAGGCCCAATGTCAGACCACGCCATGGCGTGGCACTCTGCGGAGAG
G10680             CATGTTGTAGCTTCAAGGCCCAATGTCAGACCACGCCATGGCGTGGCACTCTGCGGAGAG
G10519             CATGTTGTAGCTTCAAGGCCCAATGTCAGACCACGCCATGGCGTGCCACTCTGCGGAGAG
                   ***********************: :****************** **************
```

Appendix 6. Sindbis virus perturbs cellular mRNA stability due to sequestration of HuR.

Our findings that sfRNA formation during flavivirus infections was strongly associated with dramatic changes in cellular mRNA stability prompted us to determine if other viruses may similarly alter post-transcriptional regulation of gene expression. The Wilusz laboratory had previously demonstrated that *Alphaviruses* contained U-rich elements in their 3' UTRs that were high affinity binding sites for the host HuR protein (Sokoloski et al. 2010) as discussed in the Introduction. We therefore hypothesized that (1) the high affinity binding sites in the SINV 3' UTR could effectively act as a 'sponge' for the HuR protein, leading to the sequestration of HuR in the cytoplasm, and (2) the sequestration of the HuR protein by Sindbis virus (the prototypical *Alphavirus*) could influence post-transcriptional gene regulation in the cell as HuR was no longer available to perform its normal functions in stabilizing RNAs and influencing the nuclear processes of alternative polyadenylation and splicing. We found that transfection of GFP expression vectors or *in vitro* transcribed RNAs containing the SINV 3' UTR alone was enough to cause the re-localization of the HuR protein from the nucleus to the cytoplasm. Furthermore, we used deletion constructs to demonstrate the essential ~60nt U-rich region in the SINV 3' UTR required for this effect. To test the hypothesis that the commandeering of HuR by SINV caused changes in post-transcriptional regulation of cellular transcripts, we first analyzed the stability of several cellular mRNAs using actinomycin D transcriptional shut-off assays in 293T cells infected with SINV (or mock infected). Several transcripts were destabilized upon SINV infection, and RNA-protein co-immunoprecipitation analyses demonstrated that these mRNAs were less associated with HuR protein during SINV infection. Furthermore, we determined that alternative splicing and polyadenylation were disrupted in SINV infected cells. Major aspects of this project were reported in Michael Barnhart's thesis (towards a master's degree); however, I contributed to the publication of this work by performing all experiments necessary to address reviewer's comments for re-submission to the journal Cell Reports. I was therefore co-first

author of the manuscript published in 2013 and my contributions to this manuscript were as follows.

- Figure 1D: analysis of the region of the 3' UTR necessary for re-localization of the HuR protein from the nucleus to the cytoplasm.
- Figure 2B and 2D: analysis of the changes in mRNA stability in cells transfected with the 3' UTR of SINV compared to a control RNA.
- Figure 3B: qRT-PCR analysis of HuR-RNA co-immunoprecipitations from SINV and mock infected cells.
- Figure 4C and 4D: analysis of alternative splicing of two transcripts in SINV infected and mock infected cells; analysis of alternative polyadenylation/splicing of CALCA in cells transfected with an RNA containing the SINV 3' UTR or a control RNA.
- Finally, I also determined that the minimum amount of *in vitro* transcribed RNA containing the SINV 3' UTR that caused a re-distribution of the HuR protein from the nucleus to the cytoplasm was similar to the amount of SINV 3' UTR RNA present in the cell during an infection.

This study further contributed to our understanding of how RNA viruses can cause dramatic changes in the post-transcriptional regulation of gene expression by interacting with host RNA binding proteins during infection. Furthermore, although several studies had demonstrated that viral RNAs can sponge host microRNAs (as discussed in the Introduction), this study demonstrated that RNA binding proteins can be similarly 'sponged up' by viral RNAs. The citation for this manuscript is as follows and the article is available from Cell Reports:

Barnhart MD, Moon SL, Emch AW, Wilusz CJ, Wilusz J. Changes in cellular mRNA stability, splicing, and polyadenylation through HuR protein sequestration by a cytoplasmic RNA virus. Cell Rep. 2013 Nov 27;5(4):909-17.